
Doctoral

Science

2006-1

Aberrant Expression of Light and its Associated Receptors in Systemic Lupus Erythematosus and Coeliac Disease

Eugene Dempsey
Technological University Dublin

Follow this and additional works at: <https://arrow.tudublin.ie/sciendoc>



Part of the [Immune System Diseases Commons](#)

Recommended Citation

Dempsey, E. (2007). Aberrant Expression of Light and its Associated Receptors in Systemic Lupus Erythematosus and Coeliac Disease. Doctoral Thesis. Technological University Dublin. doi:10.21427/D7KK6M

This Theses, Ph.D is brought to you for free and open access by the Science at ARROW@TU Dublin. It has been accepted for inclusion in Doctoral by an authorized administrator of ARROW@TU Dublin. For more information, please contact arrow.admin@tudublin.ie, aisling.coyne@tudublin.ie, vera.kilshaw@tudublin.ie.

**Aberrant expression of LIGHT and its
associated receptors in systemic lupus
erythematosus and coeliac disease**



Eugene Dempsey

A thesis submitted for the award of Doctor of Philosophy

Dublin Institute of Technology

Dept of Biological Sciences

January

2006

ABSTRACT

Members of the TNF superfamily play important roles in the development and maintenance of an effective immune response. One such member of this superfamily, LIGHT, can act as a ligand for three receptors, HVEM, LT β R and DcR3. The engagement of LIGHT and HVEM, an important secondary signal for the full activation of T cells, results in a strong Th1 type response with increased production of cytokines such as INF- γ . The LIGHT-LT β R pathway plays a role in the recruitment of immune cells to sites of inflammation and can induce apoptosis in certain cells. DcR3, a soluble receptor, is speculated to function in modulating LIGHT's activity by preventing it from binding with HVEM and LT β R. Two studies published in 2001 highlighted the *in vivo* effects of constitutive expression of LIGHT on T cells in transgenic mice. The phenotype observed in these mice indicated that there was a loss of self-tolerance leading to systemic autoimmunity as characterised by the presence of multiple autoantibodies and inflammation of numerous organs.

The aim of this thesis is to investigate the expression of LIGHT and associated receptors in systemic lupus erythematosus (SLE) and coeliac disease (CD). Based on the disease manifestations seen in LIGHT transgenic mice we speculated that patients with these conditions would have altered mRNA expression patterns of LIGHT or possibly its receptors. To achieve our aim, quantitative Real-time PCR was to be employed to perform a gene expression study using a control group of healthy volunteers as well as cohorts of CD and SLE patients. A cohort of Wegener's granulomatosis (WG) patients was also included in this study.

Real-time PCR has emerged as a powerful technique for quantifying the expression of genes. However, before embarking on a logistically complex and expensive gene expression study it was felt that gaining hands-on experience in developing Real-time PCR assays for simpler studies, where the end results could be predetermined, would yield benefits in the long-term. To this end, we chose two models to study various aspects of Real-time PCR assay design.

Cystic fibrosis is the most common lethal recessive genetic disease in Caucasian populations and thus serves as a good model for developing a Real-time PCR assay for mutation detection. After identifying insufficiencies with how mutation detection is traditionally performed, we developed a novel approach on the LightCycler instrument by combining ARMS PCR with melting curve analysis. This approach allowed better design of hybridisation probes and facilitated more than one mutation to be detected per fluorescent colour channel on the LightCycler. Our optimised assays allow the detection of the five most common mutations, accounting for 90% of mutant alleles, in approximately 35 mins, which is significantly quicker than other traditional techniques.

As a model for examining the capabilities of quantitative Real-time PCR, we examined the gene dosage of peripheral myelin protein 22 (PMP22). Alterations in gene copy number of PMP22 can result in two distinct neurological diseases Charcot-Marie-Tooth disease type 1A (CMT1A) and hereditary neuropathy with liability to pressure palsies (HNPP), respectively caused by a gain or loss of a copy of the PMP22 gene. In this study, we successfully developed a quantitative multiplex Real-time PCR that can diagnose CMT1A and HNPP patients with altered PMP22 gene copy numbers. Our assay provides a rapid alternative to traditional techniques used for gene dosage quantification and could be adapted for use in the diagnosis of many genetic diseases.

Having gained knowledge in the use of Real-time PCR we proceeded to performing the gene expression study. During this study we have provided strong evidence that LIGHT and its associated receptors may play an important role in the pathogenesis of both SLE and CD and less so in WG. Our results demonstrated that LIGHT is elevated in both peripheral blood and the small intestine of patients with active CD. In SLE, there is a more profound dysregulation of LIGHT and associated receptors. Elevated levels of LIGHT and its three receptors, HVEM, LT β R and DcR3, were identified in the peripheral blood of our SLE patients. The WG and control cohorts showed similar levels of expression for LIGHT and its receptor indicating that these signalling pathways are not involved in its pathogenesis.

Studies we performed using P/I activated Jurkat cells demonstrated that there is good correlation between LIGHT mRNA upregulation and the appearance of soluble LIGHT protein in tissue culture supernatants. The analysis of soluble LIGHT levels using ELISA demonstrated that there was a significant elevation of soluble LIGHT in the SLE cohort also a large percentage of the CD patients were strongly positive. The WG patients showed a significant reduction in soluble LIGHT compared to the controls, which provides further proof that it is not involved in its pathogenesis.

Overall, our research shows that LIGHT is upregulated in both CD and SLE and given its function in promoting a strong Th1 response it is likely to contribute in the pathogenesis of both diseases. We speculate that increased LIGHT activity in SLE may promote the development of glomerulonephritis one of the more serious clinical manifestations of the disease, which can ultimately lead to renal failure and death. CD patients have a high incidence of developing secondary autoimmune disease. We hypothesize that in addition to its immediate effects in CD pathogenesis, sustained levels of soluble LIGHT may also contribute to a breakdown of self-tolerance and lead to autoimmune disease development. Further research into the expression and function of LIGHT will lead to a better understanding of the mechanisms causing these diseases. In the future, this should lead to the development of new therapies for these and related diseases.

DECLARATION

I certify that this thesis which I now submit for examination for the award of PhD, is entirely my own work and has not been taken from the work of others save and to the extent that such work has been cited and acknowledged within the text of my work.

This thesis was prepared according to the regulations for postgraduate study by research of the Dublin Institute of Technology and has not been submitted in whole or part for an award in any other Institute or University.

The work reported on in this thesis conforms to the principles and requirements of the Institute's guidelines for ethics in research. The Institute has permission to keep, to lend or to copy this thesis in whole or in part, on condition that any such use of the material of the thesis be duly acknowledged.

Signature _____ Date _____

ACKNOWLEDGEMENTS

Like any significant achievement in life, a PhD can only be completed with the generous help and support of others. Therefore, I would like to sincerely thank the following people:

Dr Fergus Ryan

Dr Sara Lynch

Dr Mohamed Abuzakouk, Prof Con Feighery,

Dr David Barton and staff at the National Centre for Medical Genetics

The crew in the lab 230: Helen, Cathal, Klaartje, Greg, Leanne, Joanne, Roslyn, Dan

The coeliac group: Stacey, Suzanne, Sharon, Bashir, Sarah, Cathal

Staff in DIT: Joe Vaughan, Derek Neylan, Jacinta Kelly, Helen Lambkin, Ursula McEvelly

Staff in SJH Immunology lab particularly Liz and Aoife

My family: Mam, Dad, Cassie and Jason

TABLE OF CONTENTS

CHAPTER 1 GENERAL INTRODUCTION

CHAPTER 1.1 LIGHT, ASSOCIATED RECEPTORS AND IMMUNE MEDIATED DISEASES

1.1.1	ACTIVATION AND CO-STIMULATION OF T CELL	001
1.1.1.1	Tumour Necrosis Factor receptor superfamily	001
1.1.1.2	TNF superfamily	002
1.1.2	LIGHT	003
1.1.2.1	Gene location and genomic organisation	003
1.1.2.2	Messenger RNA (mRNA) expression	004
1.1.2.3	Three functional forms of LIGHT	006
1.1.2.4	T cell expression of LIGHT	007
1.1.2.5	Maturation of dendritic cells by LIGHT	008
1.1.2.6	Reverse signalling via LIGHT	010
1.1.2.7	Negative selection of thymocytes	010
1.1.3	HERPES VIRUS ENTRY MEDIATOR	012
1.1.3.1	Expression of HVEM	012
1.1.3.2	Ligands for HVEM	013
1.1.3.3	B and T lymphocyte attenuator utilises HVEM as a ligand	014
1.1.3.4	Ligand and receptor interactions with HVEM	014
1.1.3.5	TRAF mediated intracellular signalling	015
1.1.3.6	HVEM and T cell responses	016
1.1.4	LYMPHOTOXIN β RECEPTOR	018
1.1.4.1	Ligands for LT β R	018
1.1.4.2	Intracellular signalling pathways	019
1.1.4.3	Secondary lymphoid organogenesis	020
1.1.4.4	Ectopic lymphoid tissues	021
1.1.4.5	IgA production	022
1.1.5	DECOY RECEPTOR 3	023
1.1.5.1	Ligands for DcR3	024
1.1.5.2	Partial proteolytic cleavage of DcR3	025
1.1.5.3	DcR3 expression in malignancy	025
1.1.6	THE IMMUNE SYSTEM AND HUMAN DISEASE	026
1.1.7	COELIAC DISEASE (CD)	027
1.1.7.1	Diagnosis of CD	027
1.1.7.1.1	Duodenal biopsy	028
1.1.7.1.2	Serological testing	029
1.1.7.2	Treatment for CD	030
1.1.7.3	Conditions associated with CD	030
1.1.7.3.1	Dermatitis herpetiformis (DH)	031

1.1.7.3.2	Malignancy and CD	032
1.1.7.3.3	Autoimmune diseases and CD	032
1.1.7.3.4	Osteoporosis and CD.....	033
1.1.7.3.5	Other conditions	033
1.1.7.4	Intraepithelial lymphocytes (IELs) in CD.....	033
1.1.7.5	Lamina propria lymphocytes (LPLs) in CD	034
1.1.7.6	Genetics of CD	035
1.1.7.6.1	HLA genes	035
1.1.7.6.2	Non-HLA genes	035
1.1.7.7	Pathogenesis of CD.....	036
1.1.7.7.1	The environmental trigger.....	037
1.1.7.7.2	Innate immune response.....	037
1.1.7.7.3	Adaptive immune response	038
1.1.8	SYSTEMIC LUPUS ERYTHEMATOSUS (SLE)	042
1.1.8.1	Diagnosis of SLE.....	042
1.1.8.2	Treatment of SLE	043
1.1.8.3	Autoantibodies in SLE.....	044
1.1.8.4	Hormonal factor involved in SLE.....	045
1.1.8.5	Genetics factors involved in SLE	045
1.1.8.5.1	Complement deficiency in SLE	045
1.1.8.5.2	HLA genes	046
1.1.8.5.3	Non-HLA genes	047
1.1.8.6	Environmental factors in SLE.....	048
1.1.8.7	Pathogenesis of SLE.....	049
1.1.8.7.1	Defects in apoptosis	049
1.1.8.7.2	T cell activation responses	050
1.1.8.7.3	B cell tolerance and maturation.....	053
1.1.8.7.4	Glomerulonephritis	054
1.1.9	WEGENER'S GRANULOMATOSIS (WG)	055
1.1.9.1	Treatment of WG.....	055
1.1.9.2	Anti-neutrophil cytoplasm antibodies (ANCA)	056
1.1.9.3	Development of ANCA	056
1.1.9.3.1	Microbial superantigens	057
1.1.9.3.2	Defective apoptosis regulation	058
1.1.9.4	Genetic factors in WG	058
1.1.9.4.1	HLA genes	059
1.1.9.4.2	Non-HLA genes	059
1.1.9.5	Pathogenesis of WG	061
1.1.9.5.1	The role of T cells	061
1.1.9.5.2	Neutrophil activation.....	062

CHAPTER 1.2 REAL-TIME PCR

1.2.1	POLYMERASE CHAIN REACTION (PCR)	065
1.2.2	REAL-TIME PCR PLATFORMS	066
1.2.2.1	The LightCycler.....	067
1.2.3	AMPLICON DETECTION	069
1.2.3.1	Non-specific dsDNA binding dyes.....	069
1.2.3.2	Specific DNA binding probes.....	071
1.2.3.3	Fluorescence Resonance Energy Transfer (FRET).....	072
1.2.3.4	Hydrolysis probes.....	072
1.2.3.5	Molecular beacons.....	074
1.2.3.6	Dual hybridisation probes.....	076
1.2.4	MUTATION DETECTION BY REAL-TIME PCR	077
1.2.4.1	Dual hybridisation probe design.....	079
1.2.4.2	Multiplex mutation detection on the LightCycler.....	081
1.2.4.3	Other detection formats for mutation detection.....	081
1.2.5	QUANTITATIVE REAL-TIME PCR	082
1.2.5.1	Dynamic range of Real-time PCR.....	084
1.2.5.2	Real-time PCR efficiency.....	084
1.2.5.3	Gene expression analysis by Real-time PCR.....	085
1.2.5.4	Relative quantification.....	086
1.2.5.5	Absolute quantification.....	087

CHAPTER 2 CHALLENGES TO REAL-TIME PCR

CHAPTER 2.1 DETECTION OF FIVE COMMON CFTR MUTATIONS BY REAL-TIME ARMS PCR

2.1.1	INTRODUCTION	089
2.1.1.1	Cystic Fibrosis (CF).....	089
2.1.1.2	Diagnosis of CF.....	089
2.1.1.3	Clinical features of CF.....	090
2.1.1.4	Treatment of CF.....	091
2.1.1.5	Cystic fibrosis transmembrane conductance regulator (CFTR).....	091
2.1.1.6	Mutations in CFTR.....	093
2.1.1.7	Pathogenesis of CF.....	095
2.1.1.8	Detection of CF mutations.....	096
2.1.1.9	Amplification Refractory Mutation System (ARMS) PCR.....	097
2.1.1.10	Aim of this chapter.....	099
2.1.2	MATERIALS AND METHODS	100
2.1.2.1	Patient DNA samples.....	100
2.1.2.2	DNA isolation.....	100

2.1.2.3	Primers.....	101
2.1.2.4	Preparation of 10% acrylamide gel for analysis of the sizing PCR products.....	101
2.1.2.5	Real-time PCR detection of the delF508 mutation.....	101
2.1.2.6	Hybridisation probe design for Real-time ARMS PCR.....	102
2.1.2.7	Multiplex set-up.....	103
2.1.2.8	Real-time PCR.....	103
2.1.2.9	Agarose gel electrophoresis.....	104
2.1.3	RESULTS	107
2.1.3.1	Comparison of Real-time and traditional PCR for the detection of delF508 mutation.....	107
2.1.3.2	Real-time multiplex PCR for detection of delF508 and R117H mutations.....	110
2.1.3.3	Real-time ARMS PCR.....	112
2.1.3.4	Blinded trial.....	118
2.1.4	DISCUSSION	120

CHAPTER 2.2

QUANTIFICATION OF THE DOSAGE SENSITIVE PMP22 GENE IN HEREDITARY PERIPHERAL NEUROPATHIES

2.2.1	INTRODUCTION	125
2.2.1.2	Charcot-Marie-Tooth (CMT) Disease.....	125
2.2.1.2	CMT classification.....	125
2.2.1.3	Clinical features of CMT1.....	127
2.2.1.4	CMT type 1A.....	127
2.2.1.5	Hereditary neuropathy with liability to pressure palsies (HNPP).....	128
2.2.1.6	Peripheral myelin protein 22 (PMP22).....	129
2.2.1.7	Schwann cell maturation.....	130
2.2.1.8	Unequal recombination at chromosome 17p11.2-12.....	131
2.2.1.9	Aim of the chapter.....	133
2.2.2	MATERIALS AND METHODS	134
2.2.2.1	Patient samples.....	134
2.2.2.2	DNA isolation.....	134
2.2.2.3	Primer and hybridisation probe design.....	134
2.2.2.4	DNA quantification.....	135
2.2.2.5	Real-time PCR.....	135
2.2.2.6	Relative quantification.....	136
2.2.3	RESULTS	138
2.2.3.1	Standard curve reproducibility and PCR efficiency.....	138
2.2.3.2	Relative quantification of PMP22 gene copy numbers.....	144
2.2.4	DISCUSSION	150

CHAPTER 3

ANALYSIS OF LIGHT MESSANGER RNA EXPRESSION BY QUANTITATIVE REAL-TIME RT-PCR IN HUMAN IMMUNE MEDIATED DISEASES

3.1 INTRODUCTION	155
3.1.1 Autoimmune diseases	155
3.1.2 LIGHT and immune-mediated diseases.....	156
3.1.3 Mitogen activation of T cells	161
3.1.4 Jurkat T cells.....	162
3.1.5 Interferon-gamma (INF- γ).....	163
3.1.6 Analysis of mRNA expression by Real-time PCR	164
3.1.7 Aim of this chapter	167
3.2 MATERIALS AND METHODS	168
3.2.1 Jurkat T cell stimulation assay	168
3.2.2 Patient samples	168
3.2.3 Total RNA isolation from cultured Jurkat T cell and peripheral blood leukocytes	169
3.3.4 Total RNA isolation from duodenal biopsies	170
3.3.5 Isolation of peripheral blood mononuclear cells (PBMCs) and granulocytes.....	170
3.3.6 Total RNA quantification	171
3.3.7 Standard curve preparation	171
3.3.8 Real-time quantitative PCR	172
3.3.9 Statistical analysis.....	174
3.3 RESULTS	176
3.3.1 Standard curve generation for absolute quantification.....	176
3.3.3 Effect of PMA concentration on the expression of LIGHT	180
3.3.4 Effect of stimulation on mRNA expression over 48hrs	181
3.3.5 Expression of mRNA in peripheral blood of test cohorts	184
3.3.6 Adjustment of mRNA expression based on lymphocyte counts.....	191
3.3.7 Identification of the cell fraction in which HVEM is being overexpressed.....	196
3.3.8 Gene expression within the coeliac intestinal lesion	198
3.4 DISCUSSION	206
3.4.1 Gene expression analysis using Real-time quantitative PCR	206
3.4.2 Gene expression in Jurkat T cells	208
3.4.3 Gene expression in peripheral blood leukocytes.....	210
3.4.4 LIGHT, associated receptors and SLE.....	211
3.4.5 LIGHT, associated receptors and CD	216
3.4.6 LIGHT, associated receptors and WG.....	222
3.3.7 Conclusion	223

CHAPTER 4

EXPRESSION OF SOLUBLE LIGHT PROTEIN IN AUTOIMMUNE/PROINFLAMMATORY DISEASES

4.1 INTRODUCTION	225
4.1.1 Soluble members of the TNF superfamily.....	225
4.1.2 Soluble LIGHT	226
4.1.3 Enzyme linked immunosorbent assay (ELISA).....	228
4.1.4 Aim of the chapter	230
4.2 MATERIALS AND METHODS	231
4.2.1 Patient samples	231
4.2.2 Jurkat T cell stimulation assay.....	231
4.2.3 ELISA for soluble LIGHT	231
4.2.4 Statistical analysis.....	232
4.3 RESULTS	233
4.3.1 Evaluation of a suitable diluent for the LIGHT ELISA standards.....	233
4.3.2 Determination of the stability of soluble LIGHT.....	235
4.3.3 Intra-assay and inter-assay variation.....	237
4.3.4 Expression of soluble LIGHT from Jurkat T cells.....	237
4.3.5 Analysis of patient samples for soluble LIGHT	239
4.4 DISCUSSION	242
4.4.1 Soluble LIGHT and CD.....	244
4.4.2 Soluble LIGHT and SLE	245
4.4.3 Soluble LIGHT and WG.....	247
4.4.4 Conclusion	249

CHAPTER 5

GENERAL DISCUSSION

5.1 Review of results.....	262
5.2 Treatment of human disease by targeting LIGHT.....	273
5.3 Future work.....	276
5.4 Conclusion	280

REFERENCES	282
-------------------------	-----

APPENDIX	310
-----------------------	-----

Publications.....	313
-------------------	-----

FIGURES

Chapter 1

Fig 1.01	The TNF/TNFR core family	005
Fig 1.02	Alternative splicing of the LIGHT gene	007
Fig 1.03	Possible mechanism of BTLA co-inhibition.....	017
Fig 1.04	Marsh classification of the coeliac lesion	029
Fig 1.05	The role of the adaptive immune response in the pathogenesis of CD	040
Fig 1.06	Development of autoimmunity in SLE	052
Fig 1.07	The role of ANCA in the pathogenesis of WG.....	064
Fig 1.08	Schematic diagram of the LightCycler Real-time PCR thermocycler	068
Fig 1.09	SYBR Green 1 detection	071
Fig 1.10	Hydrolysis probe detection	074
Fig 1.11	Molecular beacon detection.....	075
Fig 1.12	Hybridisation probe detection.....	077
Fig 1.13	Mutation detection using dual hybridisation probes	080
Fig 1.14	Quantitative Real-time PCR amplification curve	083

Chapter 2

Fig 2.01	Structure of the CFTR	093
Fig 2.02	Amplification refractory mutation system (ARMS) PCR.....	098
Fig 2.03	Three methods for detection of the delF508 mutation.....	109
Fig 2.04	Multiplex melting curve analysis for delF508 and R117H mutations	111
Fig 2.05	Orientation of hybridisation probes	113
Fig 2.06	Melting curve profiles of a delF508 heterozygote	115
Fig 2.07	Melting curve profiles of a R117H/G551D compound heterozygote	116
Fig 2.08	Melting curve profiles of a G542X heterozygote	117
Fig 2.09	Unequal crossing over between distal and proximal CMT1A repeats.....	132
Fig 2.10	Standard curves for PMP22 and β -globin quantification for 3 consecutive PCRs	139
Fig 2.11	Crossing points for 3 samples in 4 consecutive PCRs	141
Fig 2.12	Relative quantification of PMP22 gene copy number in a normal sample	146
Fig 2.13	Relative quantification of PMP22 gene copy number in a CMT1A sample.....	147
Fig 2.14	Relative quantification of PMP22 gene copy number in a HNPP sample	148
Fig 2.15	Graph showing distribution of normal, CMT1A and HNPP samples.....	149

Chapter 3

Fig 3.01	The role of LIGHT-LT β R interactions in promoting chronic intestinal inflammation.....	160
Fig 3.02	Placement of hybridisation probes to selectively detect different splice variants of LIGHT	173
Fig 3.03	Real-time standard curve for quantifying LIGHT mRNA copy numbers.....	177
Fig 3.04	Graph of crossing point verses starting copy number of LIGHT plasmid molecules	177
Fig 3.05	Total RNA extracted using Tri-reagent	179
Fig 3.06	LIGHT mRNA expression is dose dependent on PMA	180
Fig 3.07	48hr expression pattern of LIGHT and deltaLIGHT mRNA following stimulation of Jurkat T cells.....	182
Fig 3.08	48hr expression pattern of HVEM mRNA following stimulation of Jurkat T cells	183
Fig 3.09	Expression of LIGHT mRNA in PBL of the patient cohorts.....	185
Fig 3.10	Expression of deltaLIGHT mRNA in PBL of the patient cohorts	186
Fig 3.11	Expression of HVEM mRNA in PBL of the patient cohorts	187
Fig 3.12	Expression of DcR3 mRNA in PBL of the patient cohorts	188
Fig 3.13	Expression of LT β R mRNA in PBL of the patient cohorts	189
Fig 3.14	Expression of INF- γ mRNA in the PBL of the patient cohorts.....	190
Fig 3.15	Adjustment of LIGHT, deltaLIGHT, DcR3 and INF- γ mRNA expression based on lymphocyte counts	192
Fig 3.16	Positive correlation of LIGHT/deltaLIGHT with both DcR3 and INF- γ in SLE patients	193
Fig 3.17	LIGHT mRNA expression in CD patients stratified on basis of tTG serology	195
Fig 3.18	deltaLIGHT mRNA expression in CD patients stratified on basis of tTG serology.....	197
Fig 3.19	mRNA expression in PBMCs and granulocytes isolated from normal control and SLE patients.....	200
Fig 3.20	Expression of LIGHT mRNA in intestinal lamina propria.....	201
Fig 3.21	Expression of deltaLIGHT mRNA in intestinal lamina propria	202
Fig 3.22	HVEM mRNA expression in intestinal lamina propria	203
Fig 3.22	LT β R mRNA expression in intestinal lamina propria	204
Fig 3.24	INF- γ mRNA expression in intestinal lamina propria	205

Chapter 4

Fig 4.01	Format of a Sandwich ELISA	229
Fig 4.02	LIGHT ELISA standard curve using three different diluents	234
Fig 4.03	Stability of LIGHT in serum stored at room and refrigeration temperature	236
Fig 4.04	Kinetics of soluble LIGHT release from stimulated Jurkat T cells.....	238
Fig 4.05	Soluble LIGHT levels in different patient groups	241

TABLES

Chapter 1

Table 1.01	American College of Rheumatology (ACR) classification criteria for SLE	043
Table 1.02	SLE candidate genes	048

Chapter 2

Table 2.01	Sequence and concentrations of CF ARMS primers.....	105
Table 2.02	Hybridisation probes sets used to detect ARMS products in a melt-curve analysis	106
Table 2.03	Blinded trial results using optimised Real-time ARMS multiplex PCR	119
Table 2.04	Breakdown of CMT 1 subtypes	126
Table 2.05	Sequence of primers and hybridisation probes used for PMP22 dosage analysis.....	137
Table 2.06	Reproducibility of PMP22/ β -globin quantitative multiplex PCR using genomic DNA standards	140
Table 2.07	Reproducibility of PMP22/ β -globin quantitative multiplex PCR using patient samples...	142
Table 2.08	Efficiency of both PMP22 and β -globin amplification	143

Chapter 3

Table 3.01	Primers and hybridisation probes used for Real-time quantitative RT-PCR	175
Table 3.02	PCR efficiency for quantitative RT-PCR protocols.....	178

Chapter 4

Table 4.01	Percentage of patient cohort that had undetectable or strong positive soluble LIGHT levels	240
-------------------	--	-----

ABBREVIATIONS

Abbreviation	Meaning
aa	Amino acid
AGA	Anti-gliadin antibody
AP-1	Activation protein-1
APC	Antigen presenting cell
ARMS	Amplification refractory mutation system
bp	Base pair
BSA	Bovine serum albumin
BTLA	B and T lymphocyte attenuator
CD	Coeliac disease
cDNA	Complementary DNA
CF	Cystic fibrosis
CFTR	Cystic fibrosis transmembrane conductance regulator
Chr	Chromosome
CMT	Charcot-Marie-Tooth disease
Con A	Concanavalin A
Conc	Concentration
Cp	Crossing point
DAG	Diacylglycerol
DcR3	Decoy receptor 3
DH	Dermatitis herpetiformis
DMSO	Dimethylsulphoxide
DSS	Dejerine-Sottas syndrome
EATL	Enteropathy associated T cell lymphoma
EDTA	Ethylene diaminetetra-acetic acid
ELISA	Enzyme linked immunosorbent assay
EMA	Endomysial antibody
ER	Endoplasmic reticulum
FADD	FAS-associated death domain

FADD	FAS-associated death domain
FCS	Foetal calf serum
GAPDH	Glyceraldehyde-3-phosphate dehydrogenase
GFD	Gluten free diet
GVHD	Graft-versus-host-disease
HLA	Human leukocyte antigen
HNPP	Hereditary neuropathy with liability to pressure palsies
HVEM	Herpes virus entry mediator
IBD	Inflammatory bowel disease
ICAM-1	Intercellular adhesion molecule 1
ICOS	Inducible co-stimulator
IEL	Intraepithelial lymphocyte
IFN	Interferon
Ig	Immunoglobulin
IL-2	Interleukin -2
INF	Interferon
Kb	Kilobases
LIGHT	
LP	Lamina propria
LPL	Lamina propria lymphocyte
LPS	Lipopolysaccharide
LT	Lymphotoxin
LT β R	Lymphotoxin beta receptor
M	Molar
MAdCAM-1	Mucosal addressin cell adhesion molecule 1
MAP	Mitogen activated protein
Mb	Mega bases
MBP	Major basic protein
ME	2-Mercaptoethanol
MHC	Major histocompatibility complex
MIF	Migration inhibition factor
min	Minute
ml	Millilitre
mLN	Mesenteric lymph node
MMP	Matrix metalloproteinase
MPO	Myeloperoxidase
mRNA	Messenger RNA
ng	Nanogram
NK	Natural killer cell

PBL	Peripheral blood leukocytes
PBMC	Peripheral blood mononuclear cell
PCR	Polymerase chain reaction
pg	Picogram
PHA	Phytohaemagglutinin
PKA	Protein kinase A
PKC	Protein kinase C
PLC	Phospholipase C
P/I	PMA and ionomycin
PMA	Phorbol 12-myristate 13-acetate
PMP22	Peripheral myelin protein 22
PNS	Peripheral nervous system
RBC	Red blood cell
ROS	Reactive oxygen species
rRNA	Ribosomal RNA
RT	Room temperature
RT-PCR	Reverse transcription PCR
SLE	Systemic lupus erythematosus
TCR	T cell receptor
TGF- β	Transforming growth factor beta
Th	T helper cell
Tm	Melting temperature
TNF	Tumour necrosis factor
TNFRSF	TNF receptor superfamily
TNFSF	TNF superfamily
TRADD	TNF receptor-associated death domain
TRAF	TNF receptor-associated factor
tTG	Tissue transglutaminase
μ l	Microlitre
WBC	White blood cell
WG	Wegener's Granulomatosis
PBS	Phosphate buffered saline

Chapter 1

GENERAL INTRODUCTION

Chapter 1.1

LIGHT, ASSOCIATED RECEPTORS AND IMMUNE-MEDIATED DISEASES

1.1.1 Activation and co-stimulation of T cells

Naïve T cells are initially stimulated via T cell receptor (TCR) engagement with a MHC-peptide complex made available by antigen presenting cells (APC). This primary signal, while it is essential, is not on its own enough to induce a fully committed immune response. A secondary co-stimulatory signal is required and this signal determines the fate of the T cell. The two main groups of co-stimulatory receptors present on T cells are the immunoglobulin superfamily such as CD28 and inducible co-stimulator (ICOS) and the tumour necrosis factor receptor (TNFR) superfamily that includes CD27, CD30, OX40, 41BB and HVEM among others (Croft, 2003). CD28 is probably one of the best-characterised co-stimulatory receptors, which ligates with B7 present on APCs. CTLA-4 can also bind B7 to transduce inhibitory signals into T cells. The balance between stimulatory and inhibitory secondary signals helps to maintain T cell self-tolerance and prevents the induction of autoimmunity. Many members of the TNFR superfamily transduce positive co-stimulatory signals, however some members can induce apoptosis in T cells thereby regulating T cell responses by cellular elimination (Locksley, 2001).

1.1.1.1 Tumour Necrosis Factor receptor superfamily

The TNFR superfamily are all type I transmembrane proteins (C-terminus is exposed to the cytosol) (Kashii, 1999) and are characterised by the presence of 3-6 cysteine rich domains (30-40 aa) in their extracellular portion (Kwon, 1997). The cytoplasmic tails of these receptors are generally short and share very little sequence homology, as would be expected, to allow for their diverse cellular signalling. TNFR superfamily members

mediate their signals in T cells via the TNFR associated factor (TRAF) family (Chung, 2002). Ultimately the signalling cascade leads to the activation of transcription factors such as NF- κ B and AP-1 and upregulation of survival and proinflammatory genes (Beg, 1996). Members of the TNFR superfamily that can induce apoptosis such as TNFR1 and Fas have a sequence in their cytoplasmic tails called the “death domain”. Docking proteins such as TRADD (TNF receptor associated death domain) and FADD (Fas associated death domain) can bind to this domain leading to caspase activation and cell death by apoptosis (Dempsey, 2003).

1.1.1.2 TNF superfamily

Ligands for the TNFR superfamily have been categorised into the ever-growing TNF superfamily. Members of the TNF superfamily play important roles in cell activation, proliferation, differentiation, apoptosis, immunoglobulin class switching, immune evasion and immune suppression (Zhia, 1998). The majority of TNF superfamily members are clustered within the MHC on chromosome (Chr) 6 and paralogous regions on Chr 1, 9 and 19 (Collette, 2003). These ligands, with the exception of LT α , are all type II transmembrane proteins (N-terminus is exposed to the cytosol) that can also exist as soluble cytokines following cleavage by membrane metalloproteases (Chen, 2000). Most of these molecules have an intracellular N terminus, a single transmembrane-spanning domain and an extracellular C terminus. The extracellular domain folds into a β -pleated sheet “jellyroll sandwich” structure that trimerises, usually as a homotrimer (Locksley, 2001). LT α only consists of the C terminus domain and is therefore directly secreted as a homotrimer or can be membrane bound when anchored with LT β as a heterotrimer (Kashii, 1999).

1.1.2 LIGHT

LIGHT (homologous to Lymphotoxins, exhibits Inducible expression, and competes with Glycoprotein D for HVEM, a receptor expressed on T lymphocytes) also called HVEM-L or TNFSF14, is a member of the TNF superfamily (Mauri, 1998; Zhai, 1998; Harrop, 1998). LIGHT binds to three members of the TNFR superfamily (Fig 1.01), herpes virus entry mediator (HVEM), Lymphotoxin beta receptor (LT β R) (Mauri, 1998; Zhai, 1998; Harrop, 1998) and decoy receptor 3 (DcR3/TR6) (Yu, 1999) each of which will be discussed in more detail later in sections 1.1.3, 1.1.4 and 1.1.5 respectively.

1.1.2.1 Gene location and genomic organisation

The gene for LIGHT was initially located to Chr 16 using fluorescent in situ hybridisation (FISH) (Zhai, 1998), however, this was proved not to be the case, and it was subsequently shown to be located at Chr 19p13.3 (Granger, 2001). This positions LIGHT within a large genetic region paralogous to the MHC on Chr 6. The LIGHT gene is closely linked with the genes for C3, CD27L (TNFSF7) and 4-1BBL (TNFSF9). Interestingly, both CD27L and 4-1BBL play a role in T cell co-stimulation, placing the LIGHT gene within a T cell co-stimulatory locus (Granger, 2001).

The LIGHT gene spans 5.1 Kb and is comprised of four exons. The cytoplasmic tail, transmembrane domain and beginning of the extracellular stalk region are encoded by exon 1. The second and third exons, encode the remainder of the stalk region and the beginning of the trimerisation domain. Exon 4 encodes the rest of the trimerisation domain and the

receptor-binding domain and at Asp¹⁰² there is a site for N-linked glycosylation (Granger, 2001).

In 2002, Castellano and colleagues cloned the 2.1 Kb 5' region upstream from the LIGHT gene. Deletion analysis using reporter constructs showed that the – 441 bp flanking the gene was sufficient for substantial activity. Within this putative promoter region, they identified several recognition sequences for transcription factors such as NFATc/NFATp (T cell specific isoforms), which play a role in inducing LIGHT expression in activated T cell through Ca⁺⁺ signalling pathways (Castellano, 2002). They also showed that the LIGHT promoter region contained both NF-κB and AP-1 binding motifs.

1.1.2.2 LIGHT messenger RNA (mRNA) expression

The mRNA transcript of LIGHT was proposed to be 2.5 (Zhai, 1998; Mauri, 1998) – 2.7 Kb (Harrop, 1998) and is found abundantly in spleen and lymph nodes with lower expression detected in peripheral blood lymphocytes, colon, small intestine, bone marrow, thymus and lung (Harrop, 1998). Another transcript of LIGHT mRNA (3.5 Kb) was detected in the brain (Mauri, 1998) and no mRNA was detected in any tumour cell lines of nonhemopoetic/myeloid origin or fetal tissue, though LIGHT is prominently expressed on the villi of the placenta (Gill, 2002). LIGHT is also expressed on activated CD4⁺ and CD8⁺ T cells as well as immature dendritic cells (Morel, 2000).

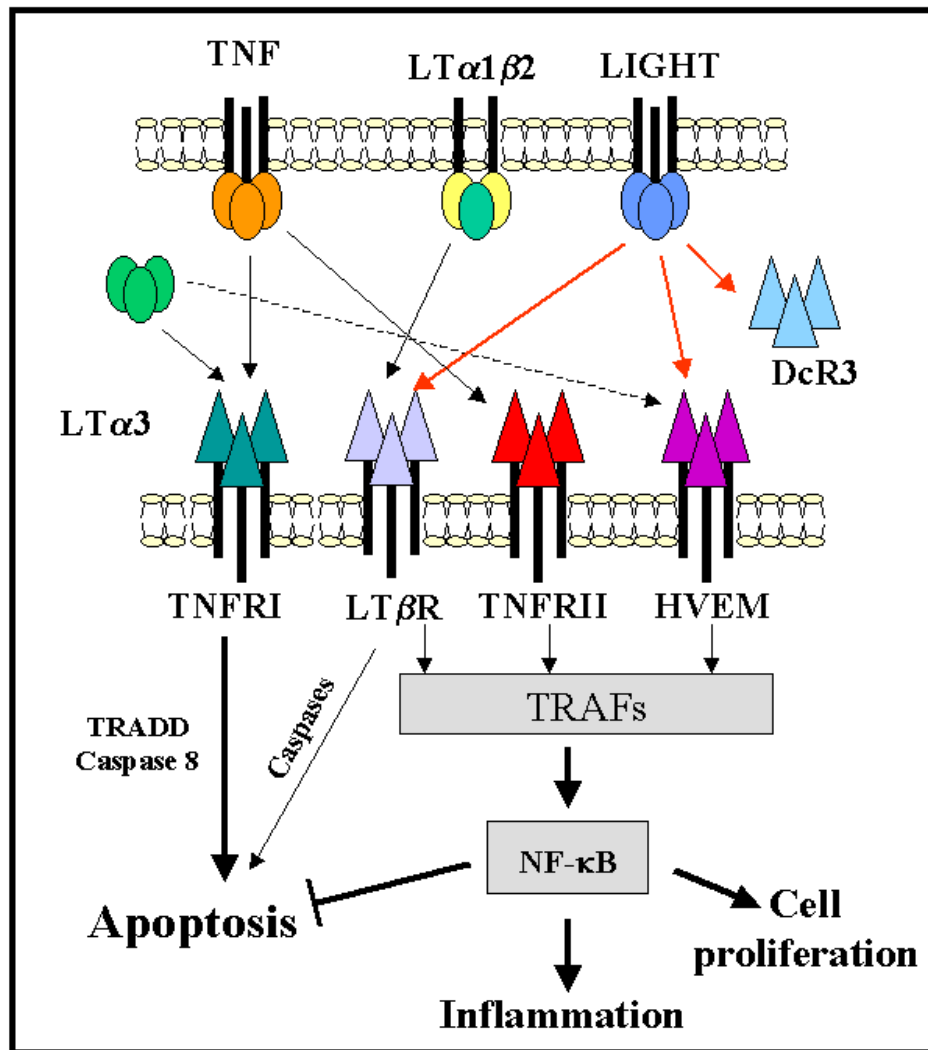


Fig 1.01 **The TNF/TNFR core family** (Adapted from Schneider, 2004; Ware, 2003; Granger, 2003). Ligand and receptor interactions are indicated with arrows. The red arrows indicate interaction directly associated with LIGHT. LT β R signalling can result in both NF- κ B activation and apoptosis.

1.1.2.3 Three functional forms of LIGHT

The full-length LIGHT mRNA transcript codes for a 29 KDa (240 aa) type II transmembrane glycoprotein (Mauri, 1998) that is expressed on the surface of activated T lymphocytes (Granger, 2001) and immature dendritic cells (Morel, 2001). There are two additional forms of the LIGHT protein, one is produced by alternative splicing (Fig 1.02), this results in translation of a 204 amino acid, non-glycosylated protein that lacks a transmembrane region and has been named deltaLIGHT (Granger, 2001). DeltaLIGHT could not be detected in cell culture supernatant but was precipitated from cell extracts indicating it is not a secreted protein but is held within the cytosol of the cell (Granger, 2001). The third form of LIGHT is soluble, approximately 25 KDa in size and is the result of LIGHT being cleaved from the cell surface by matrix metalloproteases (Granger, 2001; Morel, 2000). A metalloproteinase cleavage site that is found in FasL is also present in LIGHT (aa 81-84). Many members of the TNF superfamily such as TNF- α (Black, 1997), FasL (Kayagaki, 1995) and TRANCE (Lum, 1999) undergo cleavage from the cell surface by matrix metalloproteinases and the cleaved fragments retain biological activity. Likewise, the soluble form of LIGHT has been shown in several *in vitro* studies to retain its activity (Tamada, 2000; Zhang, 2003; Kim, 2005). As there are three different forms of LIGHT in different compartments (cell surface, intracellular and extracellular), it is thought that they may exert different biological functions.

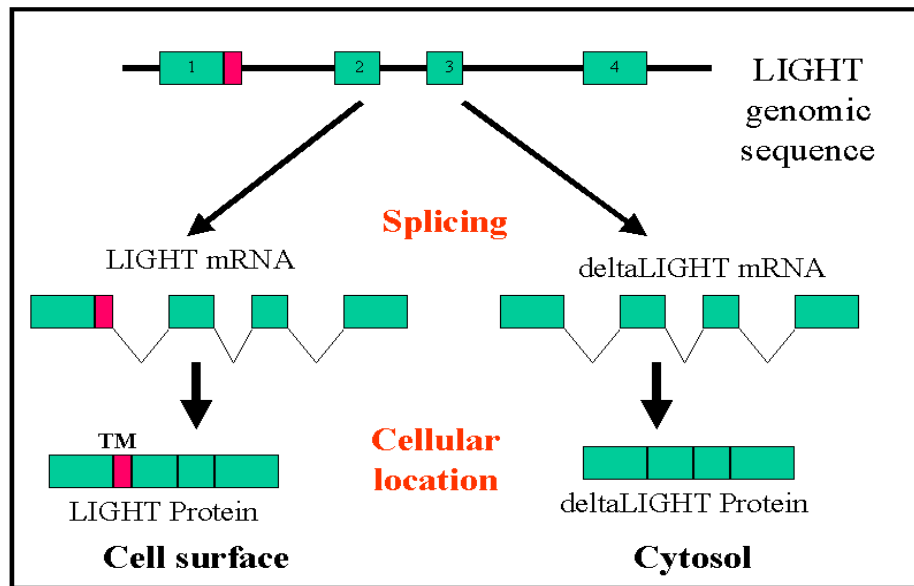


Fig 1.02 **Alternative splicing of the LIGHT gene** (Adapted from Granger, 2001)

1.1.2.4 T cell expression of LIGHT

As mentioned previously, LIGHT is transiently expressed on the surface of activated T cells (Morel, 2000). Following stimulation of peripheral blood T cells using PMA and ionomycin (P/I) the levels of LIGHT protein increase from low basal levels to peak at ~24hrs followed by a return to basal levels. The protein synthesis inhibitor cycloheximide (CHX) causes a reduction in the upregulation of cell surface LIGHT. However, this blockade is incomplete indicating that surface expression of LIGHT may be due to both re-localisation of preformed LIGHT and *de novo* protein synthesis (Morel, 2000). Stimulation of highly purified CD4⁺ and CD8⁺ T cell subsets shows that LIGHT expression is more rapidly induced and attains a much higher level of expression in CD8⁺ T cells (Morel, 2000).

The CD4⁺ T cell population can be divided into two subsets naïve and memory. The expression of CD45RA defines the naïve subset, which has never been exposed to antigen (Ag), and memory CD4⁺ T cells that have had previous exposure to Ag express CD45RO (Dutton, 1998). CD4⁺CD45RO⁺ T cells express much higher levels of LIGHT (~8-10 fold) than naïve CD4⁺ T cells (Cohavy, 2004).

The memory CD4⁺ T cell population can be further subdivided based on the expression of CCR7. CCR7 is a chemokine receptor that controls homing of T cells and dendritic cells to secondary lymphoid organs (Forster, 1999). Its expression defines two subsets of memory CD4⁺ T cells (Sallusto, 1999). The CCR7⁺ “central” memory population can recirculate through lymph nodes and can produce IL-2. The CCR7⁻ “effector” memory population can migrate to peripheral sites and can produce effector cytokines such as INF- γ and IL-4. Naïve, central and effector memory T cells have different kinetics with regard to the appearance of LIGHT on their cell surface, taking approximately 24 hrs, 4 hrs and 2 hrs respectively post stimulation (Morel, 2003). It has been demonstrated that resting CCR7⁺ and CCR7⁻ memory CD4⁺ T cells have an intracellular pool of LIGHT (Morel, 2003), however this study did not state which splice variant of LIGHT they were detecting in their system.

1.1.2.5 Maturation of dendritic cells by LIGHT

Dendritic cells (DCs) are professional antigen presenting cells (APCs) that play a vital role in the initiation of primary immune response (Bayry, 2004). Immature DCs (iDCs) are found in many tissue types where they specialise in the capture and processing of Ags.

After Ag capture DCs begin to mature and migrate from peripheral tissues to the T cell areas of lymphoid organs. Maturation of DCs results in reduced Ag uptake/processing capabilities and increased ability to stimulate T cells by upregulating the expression of co-stimulation molecules such as B7 (Banchereau, 1998). Mature dendritic cells also acquire the capacity to secrete IL-12, which promotes a Th1 type response (McDonald, 2001).

LIGHT is expressed at high levels on iDC and during maturation of DCs it is downregulated from the cell surface (Tamada, 2000). LIGHT is cleaved from the surface of DCs as they mature and it is speculated that it could play a subsequent role in T cell activation as a soluble cytokine (Tamada, 2000). LIGHT has also been shown to modulate iDC maturation in conjunction with CD154 (CD40L) (Morel, 2001). CD154 is mainly expressed on activated CD4⁺ T cells and signalling through its receptor, CD40, it is well known to induce phenotypic and functional maturation of DCs (Van Kooten, 1997). Cross-linking CD40 on DCs *in vivo* replaces the need for CD4⁺ T cell help for the induction of cytotoxic T cell (CTL) responses (Schoenberger, 1998; Bennett, 1998) When iDCs are stimulated with LIGHT they also develop a mature phenotype as characterised by the expression of CD83 and high levels of HLA class II molecules (Morel, 2001). However, LIGHT and CD154 can act in synergy to induce enhanced DC maturation, which results in significantly higher expression of IL-12, IL-6 and TNF- α , than achieved with either CD154 or LIGHT alone. In turn these LIGHT and CD154 matured DCs can enhance CTL mediated immune responses (Morel, 2001).

1.1.2.6 Reverse signalling via LIGHT

Some members of the TNF superfamily can receive stimuli from their receptors and transduce signals into cells. This process is called “reverse signalling” as the molecule, which was once a ligand, now functions as a receptor. This is a common phenomenon among TNF superfamily members with CD40L (Wiley, 1996), TRANCE (Chen, 2001), TNF- α (Eissner, 2000), CD30L (Cerutti, 2000) and FasL (Suzuki, 1998) all reported to be capable of reverse signalling. There is growing evidence that reverse signalling is possible through LIGHT (Shi, 2002; Wan, 2002). Wan et. al., concluded from their study that reverse signalling using solid-phase DcR3-Fc through LIGHT promotes Th1 but not Th2 cytokine production, enhances T cell proliferation and CTL development (Wan, 2002). A similar reverse signalling response was obtained using T cells from mice (Shi, 2002). This may indicate that not only can LIGHT⁺ T cells simulate HVEM⁺ T cells but they could also receive a signal back again.

1.1.2.7 Negative selection of thymocytes

Some members of the TNF/TNFR superfamilies, including CD40-CD40L, TNF- α -TNFRI/II and Fas-FasL (Sebzda, 1999; Kishimoto, 2000), have been identified to play a role in the negative selection of thymocytes. LIGHT has also been demonstrated to have a role in negative selection of thymocytes that have high affinity TCR (Wang, 2001; Wang, 2002). Constitutive expression of LIGHT on thymocytes leads to apoptosis of double positive (CD4⁺CD8⁺) cells and atrophy of the thymus (Shaihk, 2001). Thymocytes can be rescued from LIGHT mediated apoptosis by using a blocking soluble receptor (Wang, 2001).

Due to the wide range of effects LIGHT has within the development and maintenance of an immune response it is not surprising that great interest is being generated in its potential role in immune-mediated diseases. Studies examining the role of LIGHT in chronic inflammatory and autoimmune diseases shall be further discussed in chapter 3.

1.1.3 Herpes Virus Entry Mediator

Herpes Virus Entry Mediator (HVEM, TR2, ATAR, HveA) is a member of the TNFR superfamily. HVEM was first identified by its ability to mediate herpes simplex virus (HSV) infection into Chinese hamster ovary (CHO) cells (Montgomery, 1996). The gene encoding HVEM was located to Chr 1p36, which puts it into close proximity with several other members of the TNFR superfamily, such as CD30, OX-40, 4-1BB and TNFRII (Kwon, 1997). HVEM is a 283 aa, type I transmembrane glycoprotein that contains 3 cysteine-rich domains (CRDs) and a 50 residue cytoplasmic region that lacks a death domain (Kwon, 1997; Morel, 2000). HVEM is like other members of the TNFR superfamily and forms a homotrimeric structure that is mobilised to the surface of cells.

1.1.3.1 Expression of HVEM

HVEM is prominently expressed in lymphoid tissues such as the spleen and thymus and is moderately expressed in bone marrow and the small intestine (Harrop, 1998). It is also

expressed on various cells including CD4⁺ and CD8⁺ T cells, CD19⁺ B cells, monocytes, DCs (Harrop, 1998; Morel, 2001) and neutrophils (Kwon, 2003).

High basal levels of HVEM are expressed by resting naïve and memory T cells. Following T cell activation cell surface levels are rapidly down-regulated, a reciprocal expression pattern to that of LIGHT, and activated CD8⁺ T cells show a more pronounced down-regulation of HVEM than CD4⁺ T cells (Morel, 2001). Many members of the TNFR superfamily can undergo cleavage from the cell surface by matrix metalloproteinases (MMPs). Evidence using MMP inhibitors suggests that HVEM is not down-regulated by cleavage from the cell surface, indicating that rapid down-regulation is most likely due to internalisation of the receptor (Morel, 2001). Incubation of 48-hr activated T cells with the protein synthesis inhibitor CHX prevents the reappearance of HVEM on the cell surface suggesting that the receptor is newly synthesised and not recycled (Morel, 2001).

1.1.3.2 Ligands for HVEM

HVEM is recognised to bind to two other ligands besides LIGHT, these are LT- α 3 (Mauri, 1998), and glycoprotein D (gD) (Montgomery, 1996). LT- α 3 is a soluble cytokine and has an important role in the development of secondary lymphoid organs. It can act as a ligand for TNFR1 and TNFR2 as well as HVEM (Spahn, 2005). Little is known about the role of LT- α binding to HVEM but it is speculated that this interaction is weak (Mauri, 1998; Ware, 2005). Glycoprotein D is a structural protein found in the envelope of herpes

simplex virus (HSV). The interaction of gD with HVEM allows the virus to gain entry into the host cell (Montgomery, 1996; Whitbeck, 1997).

1.1.3.4 B and T lymphocyte attenuator utilises HVEM as a ligand

B and T lymphocyte attenuator (BTLA) a recently discovered member of the immunoglobulin superfamily (Watanabe, 2003) utilises HVEM as a ligand (Sedy, 2005; Gonzalez, 2005). Its ability to bind to HVEM is the first instance of immunoglobulin superfamily/TNFR superfamily crosstalk. BTLA signalling results in co-inhibition and suppresses T cell responses. This was confirmed using BTLA deficient cells, which show hyper-reactivity (Watanabe, 2003) and BTLA knockout mice have enhanced *in vivo* immune responses (Han, 2004).

1.1.3.5 Ligand and receptor interactions with HVEM

Mutagenesis studies have shown that LIGHT and LT- α 3 bind to distinct regions located within the CRDs 2 and 3 (Sarrias, 2001; Rooney, 2000). It has been demonstrated that BTLA binds to CRD1 (Sedy, 2005) and HSV gD also binds to CRD1 and can block HVEM ligating to both LIGHT (Mauri, 1998) and BTLA (Cheung, 2005). It has been demonstrated that LIGHT and BTLA can occupy their binding sites on HVEM at the same time *in vitro* (Gonzalez, 2005; Cheung, 2005). It remains to be ascertained whether a trimolecular HVEM-LIGHT-BTLA structure can form *in vivo*. The hierarchy of HVEM

binding to its ligands still needs to be fully elucidated. However, the binding affinity of the LIGHT-HVEM complex is an order of magnitude higher than HVEM-BTLA ligation (Cheung, 2005). As gD can inhibit binding of HVEM to both LIGHT and BTLA it is likely to have a higher affinity than LIGHT for HVEM.

1.1.3.6 TRAF mediated intracellular signalling

As mentioned previously TNFR superfamily members utilise the TRAF family of proteins to mediate signals in the cell. The TRAFs are a family of six proteins named TRAF1-6, which are characterised by a highly conserved region at the C terminus, termed the TRAF domain. They also have an N terminus ring finger domain as well as several zinc finger motifs (Dempsey, 2003). TRAFs bind directly to a TRAF interacting motif (TIM) within the cytosolic domains of TNFRs allowing transduction of signals to downstream effectors. HVEM is known to interact with TRAFs 2 and 5 (Hsu, 1997) leading to activation of the NF- κ B and AP-1 pathways resulting in cell survival, cell proliferation and proinflammatory cytokine production.

The NF- κ B family of transcription factors regulate hundreds of genes involved in the development of cells and organs involved in both the innate and adaptive immune response (Caamano, 2002; Karin, 2002; Li, 2002). The NF- κ B family comprises five members: RelA (p65), RelB, c-Rel, NF- κ B1 (p50 and its precursor p105) and NF- κ B2 (p52 and its precursor p100) (Ware, 2005). These proteins can form homodimers or a collection of heterodimers that can function as transcriptional activator or inhibitors (Ware, 2005). The

NF- κ B family are regulated by inhibitory proteins collectively termed I- κ B, which retain the transcription factors in a latent form by direct association with them (Wallach, 1999). Signal transduction pathways that lead to activation of NF- κ B must first cause phosphorylation of I- κ B, resulting in its degradation by the proteasome. The degradation of I- κ B releases an active form of NF- κ B, which is translocated to the nucleus where it can dock with its specific binding site and initiate transcription of its associated genes (Karin, 2005).

AP-1 (activating protein-1) is a collective term referring to dimeric transcription factors composed of Jun and Fos protein families (Karin, 1997). These proteins associate to form a variety of homo- and heterodimers that bind to a common site (Karin, 1995). The activation of AP-1 is involved in cellular proliferation, apoptosis, differentiation, and carcinogenesis (Shaulian, 2002). AP-1 is known to cooperate with the nuclear factor of activated T cells (NFAT) to enhance the expression of various cytokines including IL-2, IL-4, IL-8, GM-CSF, INF- γ and TNF- α (Hogan, 2003; Rao, 1997).

1.1.3.7 HVEM and T cell responses

The importance of HVEM signalling in development of an optimal T cell response was highlighted in a study where HVEM was blocked using monoclonal antibodies (Harrop, 1998). This resulted in reduced CD4⁺ T cell proliferation, sub-optimal levels of IL-2, TNF- α and INF- γ being secreted and limited the expression of several cell surface receptors such as CD25 (IL-2R α), CD71 (proliferation marker) and CD54 (ICAM-1) among others. Unexpectedly however, HVEM^{-/-} mice have an enhanced response to various T cell stimuli

and these mice were more susceptible to developing autoimmune diseases, indicating that HVEM also has the potential to inhibit T cell responses (Wang, 2005). Depending on which molecule HVEM is attached to, it has the ability to act as an on/off switch for T cell activation (Fig 1.03). BTLA-HVEM may act as a constitutive off pathway for T cells as both are expressed on resting lymphocytes (Hurchla, 2005). When T cells are activated, HVEM is down-regulated and LIGHT is upregulated. It has been demonstrated that ligation of LIGHT to HVEM is the cause of HVEM down-modulation at both the mRNA and protein level (Morel, 2001). Since LIGHT has a greater binding affinity for HVEM than BTLA, LIGHT should preferentially bind when HVEM is present at lower concentrations (Cheung, 2005). This would disrupt the BTLA-HVEM circuit, therefore releasing the T cell from this inhibitory pathway and allowing the development of a Th1 type response. This indicates that manipulation of the LIGHT-HVEM pathway could be very significant for the treatment of Th1 cytokine mediated diseases.

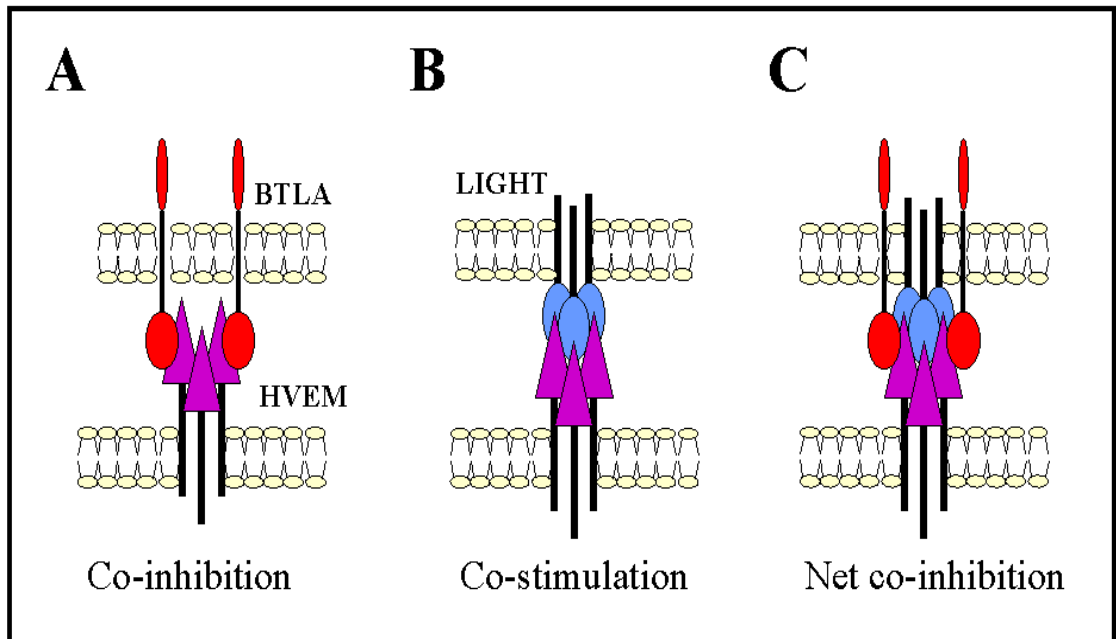


Fig 1.03 **Proposed mechanism of BTLA co-inhibition** (Adapted from Croft, 2005). A: Interaction of BTLA and HVEM results in co-inhibitory signals; B: The interaction of LIGHT-HVEM will result in co-stimulation; C: Interaction of both LIGHT and BTLA with HVEM will result in a net negative signal into the cell.

1.1.4 Lymphotoxin β receptor

Lymphotoxin β receptor (LT β R) is another member of the TNFR superfamily for which LIGHT is a ligand (Mauri, 1998; Zhai, 1998; Harrop, 1998). The LT β R gene spans 10 exons and is located at Chr 12p13.31. LT β R is expressed on most cell types including cells of the fibroblast, epithelial and myeloid lineage, but it is not expressed on T/B lymphocytes (Browning, 1997). The receptor is a 435 aa type 1 transmembrane protein of 46.7 KDa that has four CRD domains (Granger, 2003).

1.1.4.1 Ligands for LT β R

LT α can form a homotrimeric structure that lacks a transmembrane domain and is therefore released as a soluble cytokine. As mentioned previously LT α 3 acts as a ligand for TNFR1, TNFR2 and HVEM. LT α can also form a heterotrimeric structure with LT β in either LT α 1 β 2 or LT α 2 β 1 conformations (Spahn, 2004). LT α 1 β 2 is the predominant form of the heterotrimer, LT α 2 β 1 is expressed at very low concentrations and its function is not known (Ware, 2005). The association of LT α with LT β anchors it to the cell membrane where its receptor binding properties are altered allowing it to interact with LT β R. LT α 1 β 2 heterotrimer is expressed mainly on activated lymphocytes and a subset of resting B cells (Gommerman, 2004). With the expression of LIGHT and LT α 1 β 2 restricted to lymphocyte populations and LT β R expressed on most non-lymphoid cells, this pathway may act as a communication link between activated lymphocytes and surrounding cells.

1.1.4.2 Intracellular signalling pathways

LT β R has been shown to mediate its cellular signals via TRAF2, TRAF3 and TRAF5 (Nakano, 1996). It has been established that two signalling pathways stem from LT β R (VanArsdale, 1997). One pathway using TRAF2/5 leads to NF- κ B activation (Nakano, 1996; Degli-Esposti, 1997) and the other pathway mainly involving TRAF3 can lead to apoptosis of certain tumour cells (Browning, 1996; Zhia, 1998; Harrop, 1998; Rooney, 2000).

The activation of NF- κ B by LT β R leads to the up-regulation of genes involved in the proinflammatory process. These include chemokines, such as macrophage inflammatory protein 1- β (MIP-1 β) and MIP-2, as well as various integrins, such as vascular cell adhesion molecule 1 (VCAM-1) (Dejardin, 2002), intracellular adhesion molecule 1 (ICAM1) (Zhang, 2003) and mucosal addressin cellular adhesion molecule-1 (MAdCAM-1) (Wang, 2004), which can all play a role in attracting and localising leukocytes to areas of inflammation.

LT β R-LIGHT mediated cell death is dependent on TRAF3, as TRAF3 dominant negative colon adenocarcinoma cells (HT29.14) are resistant to LIGHT mediated cell death (Rooney, 2000). When LIGHT binds to LT β R, a complex of proteins is formed at the cytoplasmic tail of the receptor including TRAF3 and cellular inhibitor of apoptosis 1 (cIAP1). cIAP1 is an anti-apoptotic protein that directly interacts with caspases to inhibit their activity. The initial LIGHT-LT β R signalling also triggers the mitochondrial apoptotic pathway by an unknown mechanism, this results in the release of a protein called Smac into the cytosol which can then bind to cIAP1 (Kuai, 2003). Smac is a pro-apoptotic protein

that prevents cIAP1 from interacting with caspases and therefore releases them to eventually cause apoptosis in the cell. INF- γ may also be required to induce LT β R mediated apoptosis (Browning, 1997) to support this INF- γ has been shown to induce *de novo* synthesis of Smac (Yoshikawa, 2001). However, LT β R use of TRAF3 to mediate intracellular signalling is not as clear-cut as this. LT β R can also activate NF- κ B through TRAF3. This opposing function of LT β R-TRAF3 signalling may be explained by the fact that there are several splice variants of TRAF3, some of which are known to activate NF- κ B (van Eyndhoven, 1999).

1.1.4.3 Secondary lymphoid organogenesis

An effective immune response requires the interaction of multiple cell types. These cellular interactions are facilitated in the secondary lymphoid tissues such as the spleen, lymph nodes (LNs) and Peyer's patches (PPs). These organs have a specialised micro-architecture that positions different cell types within distinct regions; this allows optimal interactions between lymphocytes and APCs (Gommerman, 2004). PPs are specialised lymphoid organs found in the small intestinal wall that contain naïve B cells, follicular dendritic cells (FDCs) and T cell rich areas (Spahn, 2005). PPs are associated with specialised epithelial cells known as M cells. The function of M cells is to sample Ag within the lumen of the intestine and deliver it directly to APCs within the PPs.

The LT $\alpha\beta$ -LT β R pathway is essential for the formation and maintenance of these secondary lymphoid organs (Gommerman, 2003; Schneider, 2004). Knockout mice for

LT β R, LT α and LT β have demonstrated their essential role in secondary lymphoid organogenesis as these mice lack LNs and PPs and have altered splenic structure and B cell follicles (Banks, 1995; Koni, 1997; Futterer, 1998; Fu, 1999). LIGHT^{-/-} mice develop secondary lymphoid organs indicating that it may not be essential for their development. However, two studies suggest the LIGHT has a function in secondary lymphoid organ development and maintenance. Double LIGHT^{-/-} and LT β ^{-/-} mice lack mesenteric LNs (mLN), which are present in LT β ^{-/-} knockout mice indicating that LIGHT can cooperate with LT β in their formation (Scheu, 2002). LT α ^{-/-} knockout mice that overexpress LIGHT have a restored secondary lymphoid structure and function (Wang, 2002). This indicates that increased signalling by LIGHT through LT β R can compensate for the lack of LT α 1 β 2. Furthermore, overexpressing LIGHT in LT β R^{-/-} mice failed to restore secondary lymphoid organ structure (Wang, 2002). This shows that restoration of secondary lymphoid structure via LIGHT is LT β R dependent.

1.1.4.4 Ectopic lymphoid tissues

Ectopic or tertiary lymphoid tissues normally contain very few lymphoid cells but can import lymphoid cells during an inflammatory response. The LIGHT/LT-LT β R pathway also participates in the formation of tertiary lymphoid tissues (Hjelmstrom, 2000). These structures have been identified in chronically inflamed tissue and their emergence has been correlated with human disease (Gommerman, 2004). These tissues have been reported in a wide range of autoimmune conditions such as rheumatoid arthritis (Takemura, 2001),

Sjogren's syndrome (Salomonsson, 2002), Crohn's disease (Weyand, 2001) and many others.

1.1.4.5 IgA production

Immunoglobulin A (IgA) is the first line of defence against microbes entering at mucosal surfaces. This antibody prevents pathogens from colonising mucosal surface and facilitates their phagocytosis. $LT\beta R$ expression in the intestine is required for the production of IgA as $LT\beta R^{-/-}$ mice have extremely low levels of serum and fecal IgA (Kang, 2002). Transgenic (Tg) mice that overexpress LIGHT (LIGHT Tg) show a dysregulation of IgA production (Wang, 2004). These mice have reduced fecal IgA but elevated levels of serum IgA indicating a defect in IgA transportation to the lumen of the intestine, possibly due to reduced epithelial cell function (Wang, 2004). LIGHT Tg mice show an elevated level of polymeric IgA (pIgA), the intestinal source of IgA, in their serum. The ratio of pIgA to monomeric IgA (mIgA) was significantly elevated, which suggests that the elevated levels of IgA in the Tg mice originated from mucosal tissues (Wang, 2004). Polymeric IgA can very efficiently form large immune complexes (ICs) (>500 KDa) owing to its multivalent properties, these complexes can become trapped in the kidneys due to their size and their ability to bind to receptors on mesangial cells in the kidneys (Gomez-Guerrero, 1993). Deposition of ICs in the kidney results in inflammation and if not controlled leads to nephropathy. In LIGHT Tg/ $LT\beta R^{-/-}$ the elevation of serum IgA disappeared completely even in the presence of the LIGHT transgene. These mice showed no gross abnormalities or any significant T cell mediated inflammation of the intestine (Wang, 2004). This indicates that $LT\beta R$ is required for the resultant inflammation in the gut and hyperserum

IgA in LIGHT Tg mice. This links the LIGHT-LT β R pathway to intestinal inflammation and the development of IgA nephropathy, which can occur as a secondary disease in inflammatory bowel disease (IBD), coeliac disease and other chronic inflammatory diseases (Wang, 2005).

1.1.5 Decoy Receptor 3

Decoy receptor 3 (DcR3, TR6, TNFRSF6B, M68) a third receptor for LIGHT was identified by searching expressed sequence tag (EST) databases for sequences that showed homology to members of the TNFR superfamily (Pitti, 1998). Through linkage analysis the gene was located to Chr 20q13 (Pitti, 1998). Northern blotting showed that DcR3 mRNA (1.2Kb) is expressed at high levels in several normal human tissues such as the stomach, spleen, spinal cord, lymph node, lung and colon (Pitti, 1998; Bai, 2000). Its expression was reported to be weak in the thymus and undetectable in PBMCs (Zhang, 2001), however, other studies have shown that it is expressed in PBMCs (Otsuki, 2000; Wan, 2003).

The cDNA codes for a protein of 300 aa that is approximately 35 KDa in size and like other members of the TNFR superfamily DcR3 forms a homotrimeric tertiary structure. The amino terminus contains a 29-residue leader sequence, which is followed by four CRDs. Unlike most other members of the TNFR superfamily, DcR3 lacks a transmembrane domain and is therefore secreted rather than associated with the cell membrane (Pitti, 1998).

1.1.5.1 Ligands for DcR3

The binding of DcR3 to LIGHT inhibits the interaction of LIGHT with both HVEM and LT β R (Zhang, 2001; Yu, 1999). This would suggest that DcR3 dampens down co-stimulation of T cells by inhibiting LIGHT-HVEM signalling and prevents LIGHT induced apoptosis of tumour cells via LT β R.

The Fas-FasL stimulated pathway is involved in apoptosis and is important in the elimination of virus-infected cells and cancer cells by natural killer (NK) cells and CTLs. DcR3 is known to bind to FasL where it interferes with the interaction between Fas and FasL. As a result, FasL induced apoptosis of lymphocytes and tumour cells can be repressed by DcR3 (Pitti, 1998).

TL1A is the third member of the TNFSF that binds with DcR3. TL1A is mainly expressed in endothelial cells (Migone, 2002). Zhai et. al., showed that recombinant TL1A could inhibit the growth of colon carcinomas in mice, and they concluded that it functioned as an angiogenesis inhibitor (Zhai, 1999). Death receptor 3 (DR3) is expressed mainly on lymphocytes, and its interaction with TL1A can provide a co-stimulatory signal for the activation of T cells. TL1A has been shown to enhance the secretion of INF- γ and GM-CSF from T cells without affecting the production of IL-2, IL-4, IL-10 or TNF (Migone, 2002). This indicates that TL1A can promote a Th1 response and it may play a role in diseases mediated by a Th1 immune response. In fact, TL1A has been shown to be upregulated in active Crohn's disease, a Th1 mediated disease (Bamias, 2003). DcR3

strongly inhibits TL1A responses in T cells and inhibits TL1A triggered apoptosis of tumour cells (Migone, 2002).

1.1.5.2 Partial proteolytic cleavage of DcR3

There is evidence that DcR3 can be proteolytically cleaved between amino acids R218-A219 to yield a smaller (1-218) circulating DcR3 fragment. This smaller 218 amino acid fragment of DcR3 retains its ability to bind and inhibit LIGHT but loses its ability to bind and modulate FasL mediated apoptosis (Wroblewski, 2003). This processing of DcR3 may help to regulate the different co-stimulatory and apoptotic pathways induced by its ligands.

1.1.5.3 DcR3 expression in malignancy

The three ligands for DcR3, FasL (Pitti, 1998; Bai, 2000; Roth, 2001), LIGHT (Yu, 1999; Zhang, 2001) and TL1A (Migone, 2002) can all function in the initiation of apoptosis or the development of a Th1 mediated immune response. Therefore, overexpression of DcR3 could lead to gross inhibition of apoptosis and an ineffective CTL response. Pitti and colleagues speculated that certain tumours could avoid detection by the immune system, and thus Fas mediated apoptosis, by over-expressing DcR3 (Pitti, 1998). Gene amplification is a common occurrence in the development of tumours. It was shown by quantitative PCR that in many tumour cell types that DcR3 gene amplification had occurred (Pitti, 1998). Elevated levels of DcR3 mRNA and protein were also identified in these

cells. DcR3 mRNA was localised to infiltrating malignant epithelium, but absent in the surrounding stroma, indicating tumour specific expression (Pitti, 1998).

1.1.6 The immune system and human disease

The primary function of the immune system is to protect us from the constant barrage of bacteria, viruses and other parasites that invade our bodies. For this the immune system needs to be quite flexible so that it can recognise an almost endless array of foreign invaders. However, on occasion the through a number of mechanisms it may turn its powerful array of cells, cytokines and proteases against us leading to autoimmune diseases.

As described above LIGHT plays role in the activation of T cell and maturation of DC. Over-expression of LIGHT in transgenic mice can cause severe intestinal inflammation (see chapter 3) and symptoms of systemic autoimmunity (Wang, 2001; Shaikh, 2001). One of the aims of this thesis is to analyse the gene expression of LIGHT and associated receptors in human immune-mediated disease using Real-time PCR. The diseases chosen for this study include coeliac disease, systemic lupus erythematosus and Wegener's granulomatosis, a brief description of each disease follows in sections 1.17, 1.18 and 1.1.9 respectively.

1.1.7 Coeliac disease (CD)

Coeliac disease (CD) is a chronic inflammatory disease of the upper small intestine that is the result of gluten ingestion by genetically susceptible individuals. The disease was once thought to be quite rare, but in recent years, it has been reported to have a prevalence of 1 in 120 to 300 individuals in both Europe and North America (Farrel, 2003). However, the true prevalence of CD is difficult to determine. Some patients may have atypical symptoms and be incorrectly diagnosed or have silent CD, which can remain undiagnosed, as the patients show no symptoms (Visakorpi, 1997). CD is more often associated with a female population (2:1 ratio) and presentation with the disease may occur at all ages (Oxentenko, 2003).

1.1.7.1 Diagnosis of CD

Patients with CD present with a wide range of symptoms including diarrhoea, malabsorption (anaemia, osteoporosis) abdominal distension, failure to thrive (children), weight loss and neuropsychiatric symptoms (anxiety, depression) among many others (Collin, 2005; Duggan, 2003) and it is this broad range of symptoms that can make CD difficult to diagnose.

1.1.7.1.1 Duodenal biopsy

The gold standard for CD diagnosis is a duodenal biopsy, which is used to look for the characteristic lesion in the gut including: villous atrophy, crypt hyperplasia and elevated levels of intraepithelial lymphocytes (IELs) and lamina propria lymphocytes (LPLs). The lesion is graded according to the Marsh classification system (Fig 1.04) (Marsh, 1992). Type 0 is not seen that often in CD but more so in the related gluten induced condition called dermatitis herpetiformis (DH). It has been demonstrated that these patients have IgA and IgM anti-gliadin antibodies in their intestinal secretions (O'Mahony, 1990). A Marsh Type I (infiltrative) lesion shows normal villous structure with lymphocyte infiltration into the villous epithelial layer. It is generally accepted that more than 30-40 lymphocytes per 100 enterocytes is a significant increase (Marsh, 1992). A Marsh II (hyperplastic) lesion in conjunction to lymphocyte infiltration there is also evidence of crypt hyperplasia. The villous height /crypt depth ratio is generally below the normal value of 3-5. Villous atrophy is the hallmark of Marsh class III (destructive) lesions. This class is further subdivided based on the level to which the villous is damaged. Class IIIA show partial villous atrophy with villous height /crypt depth ratio of less than one. Class IIIB describes subtotal villous destruction where individual villi are still recognisable. Marsh Class IIIC biopsies show total destruction of the villi. Type IV (hypoplastic) lesions are rare and specific to CD. These are characterised by chronic unresponsiveness to the removal of gluten from the diet, resulting in irreversible destruction of the mucosal surface.

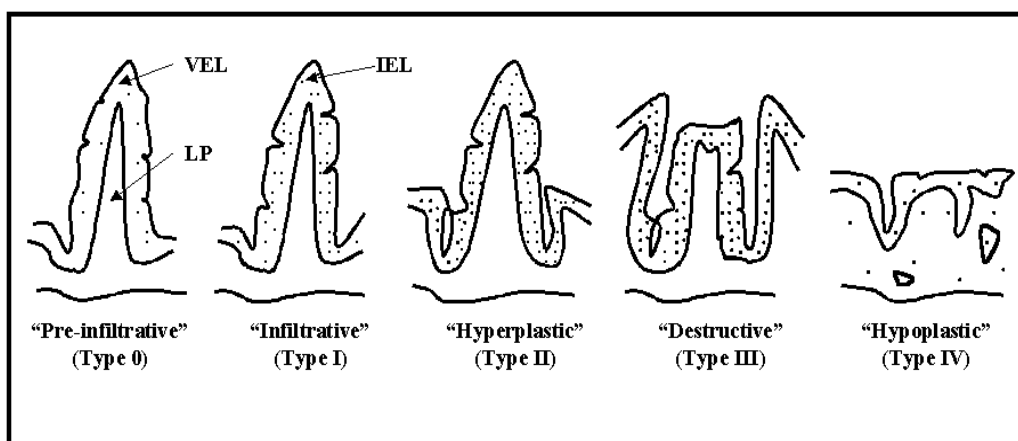


Fig 1.04 **Marsh classification of the coeliac lesion** (Adapted from Marsh, 1992). Villous epithelial layer (VEL); Lamina propria (LP); Intraepithelial lymphocyte (IEL).

1.1.7.1.2 Serological testing in CD

Serological tests for CD are now commonly used to assist in diagnosis and monitoring the adherence to a gluten free diet (GFD) by the patient. These serological assays include testing for endomysial antibodies (EMA), anti-gliadin antibodies (AGA) and anti-tissue transglutaminase (tTG) antibodies. The presence of antibodies against endomysium is nearly 100% specific in the diagnosis of CD (Hill, 2005; Farrel, 2002; Feighery, 1998). Detection of anti-tTG autoantibodies in CD stems from the discovery that tTG is the main antigen to which anti-EMA are directed (Dieterich, 1997). These serology tests usually detect IgA autoantibodies. As selective IgA deficiency occurs in 1.7 – 2.6 % of CD patients (Cataldo, 1998) serology results may be falsely negative; therefore, a total serum IgA test is also performed in conjunction with the other Ab tests. In cases where IgA deficiency is diagnosed it is necessary to test for IgG antibodies to EMA, AGA and tTG.

1.1.7.2 Treatment for CD

The treatment for CD is the life-long removal of gluten from the diet including all sources of wheat, barley and rye. This can be a challenge for the patient, as many processed foods contain gluten, so close consultation with a dietician is important in the management of the disease. Oats have been reported to be non-toxic to CD patients (Janatuinen, 2002; Kilmartin, 2003). Patients may also require replenishment of vitamins and minerals with supplements as deficiencies in iron, folate, calcium and vitamin D are found in untreated CD patients (Farrel, 2002). Once gluten is removed from the diet, the majority of patients show a clinical improvement within a few weeks. Histological improvement in the small intestine can take longer, from months to years (Feighery, 1999). Some patients fail to respond to a GFD or initially respond and then relapse again; these patients can be diagnosed with refractory CD. Patients with refractory CD may require immunosuppressive treatments with corticosteroids azathioprine or cyclosporine (Rolny, 1999; Vaidya, 1999).

1.1.7.3 Conditions associated with CD

Many conditions have been associated with the presence of CD (Collin, 1994). It is likely that some of these associations are due to the malnourished status endemic in the CD population and should improve with a GFD. However, more complex disease associations such as malignancy and autoimmunity could be due to dysregulation of common immune effector pathways. Nevertheless, as the true prevalence of CD is not known, there is also the possibility that some of these associations are coincidental (Feighery, 1999).

1.1.7.3.1 Dermatitis herpetiformis (DH)

DH affects 10-20% of CD patients (Reunula, 2001; Fry, 2002) and presents as a pruritic bullous rash, classically on the extensor surfaces of the body, which may leave pigmentation and scarring (Oxentenko, 2003). As in CD, DH patients suffer from gluten sensitivity and are seropositive for AGA and anti-tTG antibodies, although at lower levels (Porter, 1999). Gastrointestinal symptoms are usually absent and this may be explained by the fact that there are generally only mild histological changes in the small intestine. Diagnosis is normally made by finding granular deposits of IgA in the papillary dermis, with increased numbers of activated T cells. The disease may occur due to molecular mimicry between tissue transglutaminase found in the gut and epidermal transglutaminase (TG3) found in the skin (Sardy, 2002). Treatment for the disease includes adherence to a GFD and the rash can be treated with a suppressive medication such as dapsone (diaminodiphenylsulfone). Dapsone suppresses the inflammation in the skin but has no effect on the intestinal abnormality (Zone, 2005). As there are usually no severe gastrointestinal symptoms associated with DH, many patients neglect a GFD choosing to contain the rash with medication instead.

1.1.7.3.2 Malignancy and CD

CD has been linked to development of malignancies such as small bowel adenocarcinoma, oesophageal and oropharyngeal squamous carcinoma and non-Hodgkin lymphoma (NHL) (Catassi, 2002). The incidence of small bowel adenocarcinoma in CD is ~80 fold higher

than in the general population (Green, 2001). Enteropathy associated T cell lymphoma (EATL), a rare high grade T cell NHL of the upper small intestine, is specific to CD (O'Farrelly, 1986). Some investigators have suggested that EATL is the last stage of refractory CD (Catassi, 2005). EATL does not respond well to chemotherapy and the patients health often rapidly declines (Green, 2005).

1.1.7.3.3 Autoimmune diseases and CD

Autoimmune disorders are ten times more frequent in CD patients than the general population (Green, 2003). Associated autoimmune conditions include type 1 diabetes (Cronin, 1997; Lampasona, 1999), autoimmune thyroid disorders (Mainardi, 2002), autoimmune myocarditis (Frustaci, 2002), autoimmune hepatitis (Volta, 1998), rheumatoid arthritis, systemic lupus erythematosus (Collin, 1994) and Sjogren's syndrome (Iltanen, 1999). Some reports indicate that autoimmune disease association with CD is dependent on the length of gluten exposure, as children diagnosed under the age of two have no increased risk of developing a secondary autoimmune disease (Ventura, 1999). There is also a strong association with both IgA nephropathy (Farrel, 2002) and IgA deficiency (Duggan, 2004) and CD.

1.1.7.3.4 Osteoporosis and CD

Osteoporosis is another associated complication with CD (Walters, 1995), probably because of malabsorption of minerals, circulating inflammatory cytokines and failure to

attain maximum bone density during childhood (Green, 2003). Adherence to a GFD results in mineral bone density improving but it may not return to within a normal range (Meyer, 2001).

1.1.7.3.5 Other conditions associated with CD

CD has also been statistically associated with many other medical conditions such as Down's syndrome (Gale, 1997), cystic fibrosis (Farrel, 2002), male/female infertility (Sher, 1994) and depression (Holmes, 1996). Very little is known about how these conditions are associated with CD.

1.1.7.4 Intraepithelial lymphocytes (IELs) in CD

Two distinct populations of IELs are expanded in CD, $\text{TCR}\alpha\beta^+\text{CD8}^+$ and $\text{TCR}\gamma\delta^+\text{CD8}^-\text{CD4}^-$ (Cerf-Bensussan, 1997). It has been shown that when patients are put on a GFD the $\text{TCR}\alpha\beta^+\text{CD8}^+$ cells return to normal levels but the $\text{TCR}\gamma\delta^+\text{CD8}^-\text{CD4}^-$ population remains expanded (Spencer, 1991; Kutlu, 1993). Activated IELs produce several cytokines including $\text{INF-}\gamma$, IL-2, IL-8 and $\text{TNF-}\alpha$ (Lundqvist, 1996). A percentage of IELs are also positive for granzyme B and TiA indicating that they have a cytotoxic T cell phenotype (Oberhuber, 1996).

Refractory CD patients have a large proportion of IELs with an abnormal phenotype of TCR⁻, CD4⁻, CD8⁻ and CD3⁻ (Patey-Mariaud, 2000; De Serre, 2000). These IELs have also been demonstrated to have a monoclonal TCR γ gene rearrangement (Cellier, 1998).

1.1.7.5 Lamina propria lymphocytes (LPLs) in CD

There is a significant infiltration of CD4⁺TCR $\alpha\beta$ ⁺ T cells in to the lamina propria during active disease (Sollid, 2000). Most of these T cells have a memory phenotype as characterised by the expression of CD45RO⁺ (Halastensen, 1990). There is also a significant percentage of T cells positive for CD25 (IL-2R α), indicating that they have an activated phenotype. These cells however fail to express the proliferation marker Ki-67 (Halastensen, 1993), indicating gluten induces non-proliferative activation of CD4⁺ lamina propria T cells. Studies examining mRNA levels of cytokines expressed by active CD4⁺ T cells show that there is a significant increase in INF- γ in untreated CD (Nilsen, 1998). There is also a smaller increase in the levels of IL-2, IL-4, IL-6 and TNF- α (Nilsen, 1998).

Plasma cells also increased in number during active CD and these cells decline in number when the patient undertakes a GFD (Scott, 1984). These plasma cells produce IgA, IgM and IgG antibodies that are directed towards gliadin (Falchuk, 1974) and endomysium (Picarelli, 1996).

1.1.7.6 Genetics of CD

There is a strong genetic association with CD with the risk of disease occurrence in first-degree relatives 20-30 times higher than the general population and the concordance rate between monozygotic twins is 75% (Greco, 2002).

1.1.7.6.1 HLA genes in CD

CD is primarily associated with specific HLA class II molecules, DQ ($\alpha 1^*0501$, β^*02) known as DQ2 and DQ ($\alpha 1^*03$, β^*0302) which can be abbreviated to DQ8. HLA DQ2 is found in the majority of CD patients (95%) and DQ8 in the remainder (Alaedini, 2005). DQ2 is present in the general population at approximately 20-30% (Sollid, 1993). The genetic contribution of HLA genes in CD has been estimated at approximately 40%, (Bevan, 1999) indicating that non-HLA genes have a major role in determining susceptibility to CD.

1.1.7.6.2 Non-HLA genes in CD

A non-HLA locus that has been reproducibly shown to be associated with CD is the CTLA-4/CD28 gene region on chr 2q33, which has been separately demonstrated in Swedish (Naluai, 2000), Finnish (Holopainen, 1999), French (Dijilali-Saiah, 1998) and UK (King, 2002) populations. CTLA-4 has an important role in maintaining tolerance to self-antigens; studies have shown that CTLA-4 knockout mice develop severe autoimmune disease (Waterhouse, 1995).

Several genome wide studies have been performed using CD patients in order to identify non-HLA risk factors. There is however very little consensus between these studies which may indicate that each non-HLA gene has only a small impact on the disease (Sollid, 2002). Some of the chromosomal regions where there is evidence of association with CD include 5q (Greco, 2001; Naluai, 2001), 11q (Holopainen, 2001; Naluai, 2001), 6q21-23 and 19p13.1 (Van Belzen, 2003). These regions contain many possible candidate genes some of which have been implicated in other immune-mediated diseases. Interestingly, the 19p13.1-19p13.3 region is a paralog of the MHC found on Chr 6, and is one of four locations thought to have arisen by chromosomal duplication, along with Chr 1q21-q25/p11-p32 and Chr 9q33-q34 (Kasahara, 1999; Abi Rached, 1999). The LIGHT gene is situated in this region along with CD27L and 4-1BBL within a T cell co-stimulatory locus (Granger, 2001).

1.1.7.7 Pathogenesis of CD

The mechanisms behind the development of CD have not been fully elucidated. However, the most popular hypothesis is based on a T cell driven intolerance to gluten in genetically susceptible individuals.

1.1.7.7.1 The environmental trigger

Wheat gluten is a mixture of a number of different proteins that have been grouped into the gliadin and glutenin fractions according to their solubility. Gliadins are alcohol soluble and have unusually high content of proline (15%) and glutamine (35%) residues (Dewar, 2003). Based on their amino acid sequence gliadins can be subdivided into α , γ and ω gliadins. Of

these, the subtypes α and γ -gliadins are partially resistant to digestion by pancreatic and brush-border proteases (Hausch, 2002; Shan, 2002). This gives rise to a number of antigenic peptides that may cross into the lamina propria via the paracellular or transcellular routes. Movement by the paracellular route is facilitated by the increased permeability of tight junctions within the epithelial layer. This is the result of an elevation in zonulin (controls tight junctions in the small intestine) expression within the coeliac lesion in response to gliadin (Fasano, 2000; Clemente, 2003). The gliadin peptides can move via the transcellular route using enterocytic vesicles where they can then gain access to the lamina propria (Zimmer, 1998). These antigenic peptides have been proposed to activate both an innate (Schuppan, 2003) and the adaptive immune response (Schuppan, 2000).

1.1.7.7.2 Innate Immune response

Little is known about how gliadin derived peptides initiate a response from the innate arm of the immune system. Interleukin-15 (IL-15) a cytokine typical of the innate immune system (Fehniger, 2001) has been proposed to play a major role in causing damage to the intestinal mucosa in CD (Maiuri, 2001; Maiuri, 2000). Specific toxic gliadin peptides have been shown to induce the expression of IL-15, cyclo-oxygenase-2 (COX-2) and activation markers (CD25 and CD83) by lamina propria mononuclear cells (LPMCs) whilst, not causing activation of CD4⁺ T cells (Maiuri, 2003). Intestinal epithelial cells can also produce IL-15 (Reinecker, 1996), which is a potent stimulator of IELs (Ebert, 1998). Epithelial cells in conditions of stress or inflammation increase their expression of molecules such as MICA and the MHC class I molecule HLA-E. Gliadin can directly cause overexpression of MICA on enterocytes in CD (Martin-Pagola, 2004). Both MICA

and HLA-E are recognised by natural killer (NK) receptors, NKGD2 and CD94, present on IELs (Braud, 1998; Jabri, 2000). The expression of these NK receptors can be regulated by IL-15 (Robert, 2001). Enterocytes that express MICA and HLA-E can be targeted by NK receptor expressing IELs, whereupon the enterocyte is killed by apoptosis. Therefore, gliadin peptides can directly (MICA upregulation) and indirectly (IL-15 upregulation) cause IELs to induce the apoptosis of enterocytes. Uncontrolled activation of these pathways could lead to extensive enterocyte damage and villous atrophy.

1.1.7.7.3 Adaptive Immune response

Tissue transglutaminase (tTG) is a Ca^{++} dependent enzyme that can perform two types of reactions *in vivo*, transamidation and deamidation. The transamidation reaction facilitates the cross-linking of proteins through the amino acids glutamine and lysine. Deamidation involves the conversion of glutamine to glutamic acid in the presence of H_2O . At pH 7.3, the transamidation reaction takes preference, however a drop in pH switches the balance in favour of the deamidation reaction. The enzyme is ubiquitously expressed in the body; in the small intestine, it is expressed just below the epithelial layer (Molberg, 1998). The enzyme can be present intracellularly or extracellularly. As an extracellular enzyme it functions in extracellular matrix assembly, cell adhesion and wound healing (Aeschlimann, 1994).

The deamidation activity of tTG is significant in the development of an adaptive immune response in CD. The peptide-binding grooves of the MHC class II molecules DQ2 and DQ8 prefer negatively charged amino acids at key anchor positions (Sollid, 2000). Optimal binding of gliadin-derived peptides to these MHC molecules is facilitated by tTG converting key glutamine residues within the peptides to glutamic acid (negative charge) (Quarsten, 1999; Molberg, 2001). The binding affinity of deamidated gliadin peptides to DQ2 is 25 times higher than the native gliadin peptide (Kim, 2004).

Once the toxic peptides gain entry into the lamina propria, they can be deamidated by tTG, taken up by APC and when presented in the context of DQ2/DQ8 to CD4⁺ T cells it initiates their activation. Gluten specific CD4⁺ T cells isolated from the small intestine of patients with active CD produce large quantities of INF- γ (Nilsen, 1995; Nilsen, 1998). INF- γ can have a wide range of potent effects on various cells within the lamina propria and on the enterocytes themselves. INF- γ can induce macrophages to produce TNF- α . These two cytokines can work synergistically to have a direct cytotoxic effect on intestinal epithelial cells (Deem, 1991). IFN- γ sensitises enterocytes to apoptosis via FAS by upregulating its expression on these cells (Martin, 2002; Ruemmele, 1999). INF- γ can also induce fibroblasts and other cells in the lamina propria to release matrix metalloproteinases (MMPs) which when not controlled can cause death to surrounding cells and destruction of the mucosal matrix (Pender, 1997). In particular, MMP1 and MMP3 are overexpressed in the coeliac lesion (Daum, 1999).

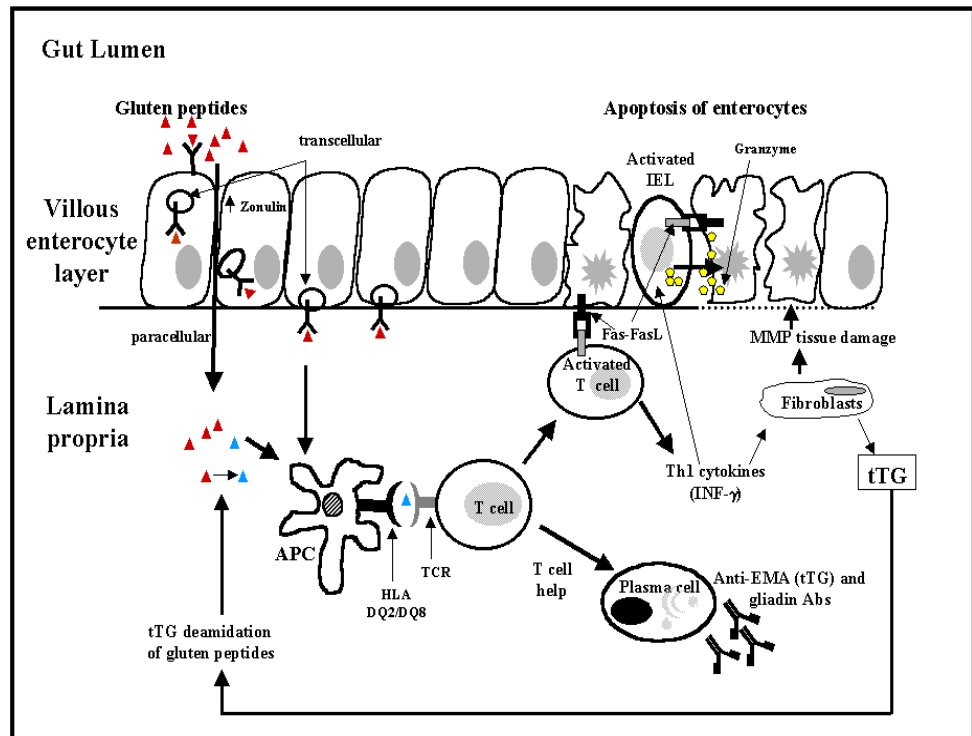


Fig 1.05 The role of the adaptive immune response in the pathogenesis of CD (adapted from Cicciocioppo, 2005; Kagnoff, 2005). tTG, tissue transglutaminase; APC, antigen presenting cell; Ab, antibody; MMP, matrix metalloproteinases; IEL, intraepithelial lymphocyte, EMA endomysial antibody; INF, interferon; G, granzyme.

The expression of tTG is also elevated in the small intestine of active CD patients (Molberg, 1998; Bruce, 1985), which would serve to deamidate further gliadin molecules and thus sustain the inflammatory process (Fig 1.05). The situation is made more complex by the fact that CD patients have autoantibodies to tTG, which is now recognised as the major autoantigen for the disease (Dieterich, 1997). How these antibodies occur may be explained by the fact that as part of its normal function tTG can cross-link proteins through its transamidation reaction. It is thought that it may be possible for tTG to cross-link itself to gliadin-derived peptides by autocatalysis (Molberg, 1998). This new tTG-gliadin complex could then be internalised by B cells via specific surface immunoglobulins. Portions of the gliadin fragments may then be presented by DQ2 or DQ8 to gliadin-specific T cells, which would in turn then provide help for B cell maturation, isotype switching and antibody production. This model is supported by the fact that anti-tTG antibodies disappear once a patient complies with a GFD, as the T cell help needed for antibody production is eliminated (Sulkanen, 1998).

It is not known to date whether the tTG-autoantibodies contribute to the development of gut lesion. However, anti-tTG antibodies have also been characterised from patients, which inhibit the bioactivity of tTG in the coeliac intestine (Esposito, 2002). One of the many functions that tTG can perform is the activation of transforming growth factor (TGF) β (Nunes, 1997). TGF- β can effect the differentiation of intestinal epithelium, stimulate extracellular matrix formation and regulate many immune cells within the gut (Halttunen, 1996; Dignass, 1996). Therefore, anti-tTG antibodies could have an indirect effect on TGF- β activation and in doing so contribute to the formation of the lesion.

1.1.8 Systemic Lupus Erythematosus (SLE)

SLE is an autoimmune disease of unknown aetiology, which is characterised by the production of various autoantibodies, directed against several cytoplasmic, nuclear and cell surface molecules and immune complex (IC) formation. Deposition of ICs in tissues can lead to inflammation and cause damage to multiple organs. SLE patients can suffer from a wide range of symptoms including glomerulonephritis, dermatitis, thrombosis, vasculitis, seizures and arthritis (Hochberg, 1997). The prevalence rate has been reported to be 40 and 200 per 100000 in Caucasian and Afro-Caribbean populations respectively (Johnson, 1995). The disease predominantly affects women, with a female to male ratio of 8:1 (Tsao, 2003).

1.1.8.1 Diagnosis of SLE

Diagnosis of SLE is made when a patient fulfils at least four of the eleven, American college of rheumatology (ACR) criteria, which were revised in 1997 (Table 1.01) (Tan, 1982; Hochberg, 1997).

Symptoms leading to positive diagnosis of SLE

- 1 Malar rash
- 2 Discoid rash
- 3 Photosensitivity
- 4 Oral ulcers
- 5 Arthritis: (non-erosive)
- 6 Serositis: Pleurisy/pericarditis
- 7 Renal: proteinuria >0.5g/24 hours
- 8 Neurological: seizures or psychosis
- 9 Haematological: haemolysis/leucopenia/lymphopenia/thrombocytopenia
- 10 Immunological: anti-DNA/anti-Sm/antiphospholipid antibodies
- 11 Positive ANA

Four or more criteria: 96% sensitive; 96% specific for SLE

Table 1.01 **American college of Rheumatology (ACR) classification criteria for SLE.**

(Modified from Maddison, 2002).

1.1.8.2 Treatment of SLE

Treatment for SLE involves the use of immunosuppressive drugs such as cyclophosphamide and corticosteroids, these cause non-specific immune suppression and are used in high doses during acute phases of the disease. Due to cyclophosphamide's many side effects such as cytopenia, infections and the possibility of malignancy (Eiser, 1994), new therapies are being investigated including mycophenolate mofetil (T and B cell suppressor) (Karim, 2002), B cell depletion using Rituximab, (monoclonal CD20 antibody) (Anolik, 2003), autologous stem cell transplantation (Jayne, 2004) and blocking co-stimulatory molecules such as CD40-CD40L (Quezada, 2003). With effective intervention,

the prognosis for patients with SLE has significantly improved, with a ten-year survival rate of approximately 90% (Goldblatt, 2005).

1.1.8.3 Autoantibodies in SLE

SLE patients have a set of characteristic antibodies directed against several components of cells. Recently it has been shown that these autoantibodies may be present for several years preceding the onset of clinical symptoms (Arbuckle, 2003). Antinuclear antibodies (ANA) are present in 98% of SLE patients (Maddison, 2003). Nonetheless, ANA antibodies are not specific for SLE as they are found in a wide range of systemic rheumatic diseases such as 80% of Sjogren's syndrome patients, and organ specific autoimmune diseases including 70% of autoimmune hepatitis cases (Maddison, 2003). Anti-double stranded DNA (dsDNA) antibodies are present in 70% of SLE patients (Mok, 2003). Anti-DNA antibody titres tend to fluctuate over time and with disease activity and are associated with the development of glomerulonephritis in SLE (Mok, 2003). Antibodies against four groups of RNA-binding proteins (Sm, UIRNP, Ro and La) are also commonly found in SLE (Reichlin, 1988). Anti-Sm antibodies are the most specific to SLE and they react to the core protein group of small nuclear ribonucleoproteins (snRNPs). There is however a wide ethnic variation in the presence of anti-Sm antibodies, they are found more commonly in Afro-American and Afro-Caribbean than Caucasian populations (Arnett, 1988)

1.1.8.4 Hormonal factor involved in SLE

The strong association of the disease with the female population would suggest that there is a hormonal influence on the development of SLE. In animal model studies, using lupus prone mice (MLR-lpr/lpr mice) oestrogen can act to accelerate disease progression (Carlsten, 1990). There is also evidence from mouse models that androgens may have a protective role and this hypothesis has been tested in human trials for the treatment of SLE (Chang, 2002).

1.1.8.5 Genetics factors involved in SLE

SLE shows a strong familial association and the concordance rate between monozygotic twins is approximately 25-58% and drops to 5% for dizygotic twins (Piesesky, 1997). SLE is seen as a polygenetic disease with many genetic loci identified as being associated with disease susceptibility. Murine studies have shown that more than 40 genes can induce lupus-like syndrome (Raman, 2003). Despite this rather large number of genes most can be classified into one of three functional groups: molecules that effect the clearance of apoptotic cells, molecules involved in the apoptosis of lymphocytes and molecules that can amplify or modulate lymphocyte signalling and expansion (Raman, 2003).

1.1.8.5.1 Complement deficiency in SLE

In the majority of SLE patients, multiple susceptibility genes are required with estimates of up to four susceptibility genes required for the development of this complex disease (Schur, 1995). However, in a small proportion of SLE patients (<5%) a single gene may be involved (Mok, 2003). These include homozygous deficiency in the early complement proteins C1 (C1q, C1r and C1s), C2 and C4 (Carrol, 2004; Nath, 2004). Deficiency in C1q is a particularly strong susceptibility gene as greater than 90% of these patients develop SLE (Tsao, 2003). The complement system has an important role to play in the uptake and clearance of apoptotic blebs. It has been proposed that defects in this pathway could lead to open presentation of self-antigens, which subsequently leads to the development of high affinity IgG autoantibodies (Botto, 1998). However, there is a concern with this hypothesis as individuals deficient in the complement protein C3 have a reduced risk of developing SLE (Carrol, 2004). Another hypothesis suggests that the early complement proteins have a role in inducing B cell tolerance. Complement coated self-antigens are bound to developing B cells through the complement receptor 1 (CR1) and CR2 and this enhances negative selection. The loss of early complement components would result in defective elimination of autoreactive B cells (Carrol, 2004).

1.1.8.5.2 HLA genes

Population studies have extensively looked at the contribution of major histocompatibility complex (MHC) genes to human autoimmune disease. The HLA-DR2 and HLA-DR3 class II genes have been consistently associated with SLE in several studies using Caucasian populations with a two-fold relative risk conferred by each allele (Tsao, 2002). Conversely, there is less consistent evidence for HLA association in non-Caucasian populations.

1.1.8.5.3 Non-HLA genes

Linkage analysis studies using SLE families have also located several other susceptibility regions outside of the MHC region. Chromosomal regions that show significant linkage to SLE include 1q23 (Moser, 1998; Edberg, 2002), 1q41-42 (Edberg, 2002; Shai, 1999; Tsao, 1997), 2q35-37 (Lindqvist, 2000), 4p16-15.2 (Gray-Mcguire, 2000) and 16q12 (Gaffney, 2000; Nath, 2004). Each of these chromosome regions contains many possible SLE susceptibility genes (Table 1.02).

A study involving just Caucasian subjects showed linkage between Chr 19p13.2 (Lindqvist, 2000) and SLE. In a separate study, stratification of patients based on their major manifestations of SLE showed that the development of anti-DNA antibodies was linked to this chromosomal region (Namjou, 2002). This region is in close proximity to the LIGHT co-stimulation locus (Granger, 2001).

Candidate genes for SLE

Gene	Chromosome region	Associated allele	Reference
FCγRIIa	1q22-23	R131	Salmon, 1996
FCγRIIIa	1q22-23	F176	Wu, 1997
IL-10	1q31-32	Multiple alleles	Mehrain, 1998
CTLA-4	2q33	+49G	Ahmed, 2001
PDCD-1	2q37	PD-1.3A	Prokunia, 2002
TNF-α	6p21	TNF2	Wilson, 1994
LTα	6p21	-----	Kim, 1996
MBL	10q11.2-q21	230A	Davies, 1995
FasL	1q23	-844C	Wu, 2003
Fas	10q24	297C/416G	Horiuchi, 1999
Bcl-2	18q21	Multiple alleles	Mehrain, 1998

Table 1.02 SLE candidate genes (Adapted from Nath, 2004).

1.1.8.6 Environmental factors in SLE

The concordance rate between monozygotic twins would indicate that environmental factors might play an important role in the development of SLE. UV light, particularly UVB, has been shown to be an important trigger for the disease (Mok, 2003). UV light can induce apoptosis in keratinocytes, resulting in the formation of apoptotic blebs on the surface of the dying cell that contain nuclear and cytoplasmic antigens (Casciola-Rosen, 1996), thus exposing them to the immune system which can provoke autoimmunity. Exposure to environmental oestrogens such as those used in hormone replacement therapy

(HRT) (Sanchez-Guerrero, 1995; Meier, 1998) and oral contraception (Sanchez-Guerrero, 1997) also have been shown to cause a small increase in the risk of SLE development. Dietary factors such as the ingestion of L-canavanine, found in alfalfa sprouts, has been reported to cause lupus-like symptoms in some individuals (Prete, 1985).

1.1.8.7 Pathogenesis of SLE

SLE is seen predominantly as an overactive B cell disorder due to the presence of pathogenic antibodies (Lipsky, 2001). Nonetheless, the development and survival of these pathogenic B cells is dependent upon T cell help (Manson, 2003). ANA producing B cells show evidence of having undergone T cell driven Ig class switching and affinity maturation, as the autoantibodies are of the IgG isotype (Hoffman, 2004).

1.1.8.7.1 Defects in apoptosis

Central tolerance removes self-reactive lymphocytes from the immune repertoire, however, this process is incomplete and low affinity self-reactive B and T cells can escape and become part of the normal peripheral immune system (Shlomchik, 2001). Autoantigens may be presented to low affinity self-reactive T cells in the periphery. In normal individuals, tolerance to these self-antigens is induced or the T cell is eliminated via activation induced cell death (AICD). AICD is a process whereby lymphocytes are deleted after encountering soluble antigen or after persistent activation and proliferation (von

Herrath, 2003). T cells from SLE patients show defects in AICD, these cells resist anergy or AICD by upregulating and sustaining cyclooxygenase-2 (COX-2) expression (Lu, 2004). In SLE, excessive self-antigens are made available due to abnormal apoptosis of cells and the subsequent failure to remove these apoptotic bodies by phagocytosis. Prolonged exposure to apoptotic cells could be an important factor for breaking T cell tolerance in genetically susceptible individuals. All autoantigen targets in SLE can be identified within apoptotic blebs found on the surface of dying cells (Casciola-Rosen, 1994). Clearance of apoptotic cells by macrophages is facilitated by several receptors including complement receptors, scavenger receptors and LPS receptors (CD14) (Berden, 2003). As mentioned earlier, defects in complement receptors or early complement proteins C1, C2 and C4 are particularly strong SLE susceptibility genes.

1.1.8.7.2 T cell activation responses in SLE

T cells isolated from SLE patients have an elevated and greatly extended intracellular Ca^{++} flux compared to control T cells when stimulated *in vitro* (Vassilopoulos, 1995). The sustained increase in intracellular Ca^{++} maintains enzymes such as calcineurin and protein kinase C (PKC) in an activated state and they in turn can activate a wide range of transcription factors such as NFAT, AP1 and NF- κ B. As mentioned previously, activation of these transcription factors promotes cell survival and upregulation of proinflammatory cytokines. It has also been reported that there is a reduction in the level of mRNA and enzyme activity of PKA isoenzymes in SLE T cells (Laxminarayana, 1999). PKA isoenzymes mediate negative regulatory effects on signalling events and defects within this pathway could lead to abnormally high T cell responses (Tsokos, 2000).

Regulatory T cells (CD4⁺CD25⁺) are reduced in the periphery of SLE patients during times of disease activity and during remission the numbers of these cells return to that of normal individuals (Crispin, 2004; Liu, 2004). There is also impairment in CD8⁺ suppressor function in human SLE, which can strongly inhibit B cell maturation (Filaci, 2001). Natural killer T (NKT) cells, which express the NK receptor and invariant TCR, are also reduced in number in active SLE patients (Oishi, 2001). NK T cells have been reported to inhibit autoreactive B cells (Singh, 2004). Activation of NK T cells using α -galactosylceramide in murine models of SLE, suppresses lupus dermatitis (Yang, 2003) and lupus nephritis (Singh, 2004), whereas the loss of NK T cells exacerbates the symptoms of lupus in these animal models.

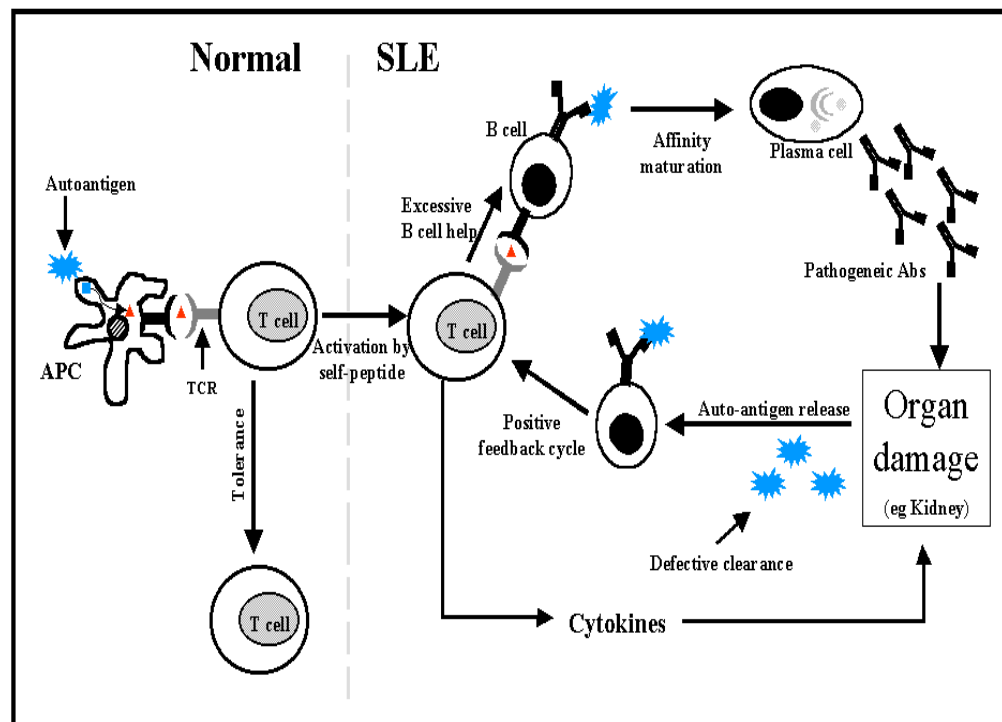


Fig 1.06 **Development of autoimmunity in SLE.** (Adapted from Shlomchik, 2001). In normal individuals, tolerance is induced in T cell when presented with self-antigen. Due to many genetic and environmental factors, peripheral tolerance is lost in SLE patients, which subsequently leads to the development of pathogenic antibodies and organ damage.

1.1.8.7.3 B cell tolerance and maturation

The early complement proteins such as C1q are speculated to have a role in the generation of B cell tolerance (Carrol, 2004). Failure to induce tolerance in these low affinity self-reactive B cells, in SLE patients, means that they are now available to mature in a T cell dependent manner. Elevated levels of B lymphocyte stimulator (BlyS) a member of the TNFSF has been reported in active human lupus (Zhang, 2001). Continued stimulation of

B cells by BlyS leads to the generation of plasma cells in a T cell dependent manner (Schiemann, 2001), which can then produce large quantities of autoantibodies. Animal studies have also shown that there is excessive co-stimulation between T cell-B cell-APC via the CD40-CD40L and CD28-B7 pathways in SLE (Hoffman, 2004).

The maturation process leads to the generation of high affinity B cells from the low affinity precursors (Sholmchik, 2001). The resulting pathogenic autoantibodies can form ICs with soluble antigen. Links between polymorphisms in the FC γ RIIa (CD32) and FC γ RIIIa (CD16) genes and increased risk of developing SLE have also been made (Salmon, 1996; Edberg, 2002). These receptors are involved in the phagocytosis of IgG2 and IgG3, the main IgG isotypes found in IC deposits. The FC γ RIIa allele R131 (Salmon, 1996) and FC γ RIIIa allele (F176) (Wu, 1997) can cause a decrease in the receptors binding affinity for IgG2 or IgG3 antibodies. The defective clearance of ICs, allows them to deposit within various organs such as the kidneys where they can induce local inflammation and tissue damage. This organ damage results in further self-antigens being released to the immune system, thereby sustaining the inflammatory process. T cells themselves may also cause tissue damage due to the release of potent cytokines such as TNF- α and INF- γ (Hoffman, 2004).

1.1.8.7.4 Glomerulonephritis in SLE

The kidney is particularly at risk of being damaged in SLE as the autoantibody-antigen ICs are targeted to the glomerular basement membrane (GBM). The GBM is naturally anionic,

due to the presence of large amounts of heparan sulphate and components of the major autoantigens in SLE are strongly cationic, this combination facilitates their attachment to the GBM (Berden, 2003). The IC deposition triggers the infiltration of immune cells resulting in local inflammation (Ravetch, 2001). Th1-type cytokines, including INF- γ , play a pivotal role in the resulting glomerular inflammation (Calvani, 2005). Sustained lupus nephritis can result in glomerulosclerosis or renal fibrosis followed by end-stage renal disease and death (Singh, 2005).

1.1.9 Wegener's granulomatosis (WG)

Wegener's granulomatosis (WG) is a systemic autoimmune disease that is characterised by necrotising granulomatous inflammation of the upper and lower respiratory tract and vasculitis of small and medium sized blood vessels (Langford, 1999). The disease is also associated with the presence of anti-neutrophil cytoplasmic antibodies (ANCA) in patient sera and the development of glomerulonephritis (van der Woude, 1985; Fauci, 1983). WG is a rare disease, 2-3 cases per 100000 (Mahr, 2004), that has a higher prevalence in Caucasian populations, with a male to female ratio of 1:1 (Cotch, 1996). As a disease, WG can be divided into two categories: localised disease and generalised/systemic disease. Localised WG starts in the upper respiratory tract with granuloma formation. This can precede generalised WG, characterised by the presence of systemic vasculitis, for a long period of time (Mueller, 2000).

1.1.9.1 Treatment of WG

The prognosis for WG is quite poor, with a median survival time of five months if left untreated (Langford, 1999). Combination immunosuppressive therapy using cyclophosphamide and glucocorticoid is the most effective treatment for active disease. With this treatment, 75% of patients achieve remission (Yi, 2001) and the 5-year survival rate is 80% (Savage, 1997). However, the use of this aggressive immunotherapy can lead to other complications such as malignancy (carcinoma of the bladder) and infection (Talar-Williams, 1996).

1.1.9.2 Anti-neutrophil cytoplasm antibodies (ANCA)

ANCA are circulating antibodies directed mainly towards components of neutrophil granules and monocyte lysosomes (van der Woude, 1985). ANCA are associated with a heterogeneous group of diseases called the primary systemic vasculitides (PSV) (Falk, 1988). WG, microscopic polyangiitis (MPA) and Churg-Strauss syndrome (CSS) are the most common ANCA-associated PSV. ANCA are pathogenic and correlate well with disease activity (Pall, 1994). ANCA are divided into two groups based on their immunofluorescent staining pattern. Cytoplasmic staining patterns are designated c-ANCA and peri-nuclear staining patterns are named p-ANCA. The major antigens of p-ANCA and c-ANCA are myeloperoxidase (MPO) (Falk, 1988) and proteinase-3 (PR3, PRTN3) (Jenne, 1990) respectively. MPO is located exclusively in the azurophil granules, but PR3 is located in the secretory vesicles as well as the granules. PR3 is a member of the serine protease family and is an antibiotic protein. The presence of c-ANCA is associated with WG and is found in ~80% of patients with active disease, p-ANCA antibodies are found in a minority (~15%) of WG patients (Wiik, 2000).

1.1.9.3 Development of ANCA

Although the development of ANCA antibodies in WG is not completely understood, two main hypotheses have emerged: the microbial superantigen hypothesis and the defective apoptosis regulation hypothesis (Reumaux, 2004).

1.1.9.3.1 Microbial Superantigens

Superantigens (SAGs) are components of bacteria, viruses etc. that can act as powerful stimulators of the immune system. T cell SAGs bind to MHC class II molecules outside of the peptide-binding groove and to conserved regions of specific families of T cell receptor V-beta chains (TCR V β), regardless of the Ag specificity of the T cell. This allows SAGs to stimulate the non-specific proliferation of all T cells that express TCR V β . Staphylococcal protein A (SpA), a cell wall component found in most clinical strains of *Staphylococcus aureus*, has been identified as a B cell SAG (Sasso, 1989). SpA can bind to membrane immunoglobulin heavy chains encoded by the V_{H3} family genes and induce a polyclonal antibody response (Popa, 2002). Therefore, SAGs have the potential to activate autoreactive B cells in a T cell dependent and independent manner.

Evidence to support the possible role of SAGs in ANCA development in WG patients comes from the finding that 60-70% are chronic nasal carriers of *Staphylococcus aureus* (Reumaux, 2004) and carriers experience relapse nearly 8 times more frequently than non-carriers (Stegeman, 1994). A higher risk of relapse was associated with the staphylococcal SAG, toxic-shock-syndrome toxin 1 (TSST-1) (Popa, 2002). It has also been reported that in WG there is a skewing of the TCR V β repertoire in peripheral T cells (Giscombe, 1995). It has also been reported that WG patients have ANCA antibodies with a V_{H3} encoded heavy chain, which indicates that they have a potential to bind SpA (Sibilia, 1997).

1.1.9.3.2 Defective apoptosis regulation

Defects in apoptosis or the clearance of apoptotic cells may lead to the exposure of self-antigens that are normally sequestered from the immune system leading to a response. Apoptosis of neutrophils is an important mechanism in maintaining control of the early inflammatory response and limits tissue damage (Reumaux, 2003). Furthermore, ANCA have been identified to interact with components on the surface of apoptotic neutrophils (Gilligan, 1996). The proteolytic events that take place during apoptosis may modify self-antigens to reveal novel epitopes that by-pass normal tolerance, or they could become complexed to macromolecules from infectious agents to produce novel epitopes that elicit a sustained immune response (Utz, 1998).

1.1.9.4 Genetic factors in WG

There have been reports of WG developing in members of the same family (Harper, 2000; Huang, 2001) and there seems to be a Caucasian population bias for development of the disease (Hoffman, 1992). This would indicate that there are genetic factors that predispose to the development of WG. WG is likely to be a complex genetic disease with many loci involved to give rise to disease susceptibility.

1.1.9.4.1 HLA genes

In a recent study using 202 microsatellite markers in more than 150 WG patients, a significant increase was seen in the frequency of the HLA DPB1*0401 allele and a decrease in DPB1*0301 allele (Jagiello, 2004). Other studies have shown associations with other HLA alleles such as DR1-DQw1 (Papiha, 1992), DR2 (Elkon, 1983) and B50 (Cotch, 1995). Nevertheless, there is no consistent associations identified with particular HLA alleles and this may indicate that they make only a small contribution to the development of WG.

1.1.9.4.2 Non-HLA genes

The constitutive expression of PR3 on resting neutrophils in circulation is genetically determined (Schreiber, 2003). Higher constitutive expression of PR3 on neutrophils is a risk factor for WG (Witko-Sarsat, 1999). The (A-564G) polymorphism in the PR3 promoter region that is located within a putative Sp-1 transcription-factor binding site shows association with WG (Gencik, 2000). This polymorphism potentially leads to increased PR3 expression (Jagiello, 2005). Alpha 1-antitrypsin (α_1 -AT) is a natural inhibitor of PR3, and decreased levels of functional α_1 -AT have been found in WG patients (Esnault, 1997). A deficiency in α_1 -AT in WG has been associated with a poor prognosis, greater organ involvement and increased mortality (Spegalmark, 1995).

Polymorphisms within Fc receptor (Fc γ R) genes also seem to play a role in the manifestation of WG (Dijstelbloem, 1999). There are three subgroups of these receptors:

Fc γ RI (CD64), Fc γ RII (CD32) and Fc γ RIII (CD16). Neutrophils typically express Fc γ RIIa and Fc γ RIIIb whereas monocytes/macrophages express Fc γ RIa, Fc γ RII and Fc γ RIIIa. These receptors bind the Fc portion of antibodies. They have a wide range of functions and are involved in leukocyte degranulation, cytokine and chemokine production, generation of oxidative burst, activation of complement receptor-mediated phagocytosis and antibody-dependent cellular cytotoxicity (ADCC) (Huang, 2001). One particular polymorphism in the Fc γ RIIa gene, R131H, alters the ability of the receptor to bind IgG2 (Salmon, 1992; Parren, 1992). Analysis of WG patients showed that those homozygous for the R131H polymorphism had a greater incidence of disease relapse (Edberg, 1997). Two common allelic forms of Fc γ RIIIb exist, NA1 and NA2. It has been reported that these have quite different effects on cell activation; NA1 induces a greater Fc γ R-mediated phagocytic response (Salmon, 1995). The NA1 allele has been found at a higher frequency in WG patients that also suffered from kidney disease.

TNF- α , LT- α , IL1- α , IL1- β and INF- γ are well-characterised proinflammatory cytokines and have been demonstrated to be critical in granuloma formation (Huang, 2001). Polymorphism within the TNF- α promoter region (-238G/A allele) and the INF- γ intron 1 polymorphism (+874 T/T allele) have also been linked with susceptibility to WG (Spriewald, 2005). The -238G/A allele in the TNF- α promoter has been associated with the production of higher levels of the cytokine (Reich, 2002). The INF- γ T/T allele is linked with a high expressor phenotype (Pravica, 2000).

Other genes that have polymorphisms associated with WG are IL-10 (Zhou, 2000), CTLA-4 (Giscombe, 2002) and IL-1 β (Huang, 2000).

1.1.9.5 Pathogenesis of WG

WG is a complex disease requiring environmental factors as well as a genetically susceptible background for it to develop. Many cell types from both the innate and adaptive immune response are involved in the development of WG.

1.1.9.5.1 The role of T cells in WG

Infiltrates of activated CD4⁺ and CD8⁺ T cells are found in granulomatous lesions and the periphery of WG patients (Schlesier, 1995; Mueller, 2000). T cells (CD4⁺, HLA DR⁺) isolated from active WG patients show increase proliferation, TNF- α and INF- γ production in response to non-specific stimulation (anti-CD3) when compared with healthy controls (Ludviksson, 1998). This and other studies (Mueller, 2000) support the fact that Th1 cytokines are dominant in WG. INF- γ causes endothelial cells (EC) to increase expression of MHC class II molecules and causes the upregulation of adhesion molecules such as ICAM-1 and VCAM-1 (Huang, 2001). This upregulation of adhesion molecules allows for further accumulation of immune cells within vasculitic lesions.

T cells isolated from the peripheral blood of WG patients show responsiveness to isolated PR3 (Van der Woude, 1990; Brouwer, 1994). Antigen-specific T cells can provide help to B cells and induce affinity maturation and the production of high affinity antibodies. In WG, there is evidence that ANCAs are high affinity antibodies of the IgG subclass indicating that both affinity maturation and Ig class switching have taken place (Jayne, 1991; Mulder, 1994). Antigen-specific T cells have also been found to remain present in

the periphery of patients during remission (King, 1998). These T cells may have an important role in the tendency of patients to suffer from disease relapse.

1.1.9.5.2 Neutrophil activation

TNF- α released from activated T cells and macrophages can stimulate the translocation of PR3 from the cytosol to the surface of neutrophils (Fig 1.07). Subsequently, ANCA-IgG binds with the Fab regions to PR3 and the Fc region can bind with Fc γ R either on the same cell, known as the Kurlander phenomenon, or on neighbouring neutrophils (Reumaux, 2004). This in turn, enhances the activation of the neutrophil and causes the release of reactive oxygen species (ROS) such as hydrogen peroxide (H₂O₂), hypochlorous acid (HOCl) and hydroxyl radicals (OH). PR3, MPO and elastase are also released. All of these molecules are capable of causing apoptosis in endothelial cells (Varani, 1989; Yang, 1996). In addition, due to PR3 and MPO cationic nature these enzymes can non-covalently bind to the anionic surface of endothelial cells (EC). This facilitates the binding of ANCA and the triggering of EC damage through ADCC (Savage, 1993; Varaganam, 1992). Activated neutrophils also release cytokines and chemokines that attract more cells to infiltrate the site of inflammation, thereby sustaining the disease process.

In normal circumstances following activation of neutrophils, they undergo apoptosis and are cleared by macrophages (Zimmerman, 1992; Savill, 1992). In WG, there is evidence of dysregulated and accelerated apoptosis of neutrophils that are initially primed with TNF- α and then incubated with ANCAs (Harper, 2000). These apoptotic neutrophils show no expression of surface phosphatidylserine, an important 'eat-me' signal to scavenging

phagocytes. Failure to clear these apoptotic neutrophils may lead to secondary necrosis and further tissue damage. Apoptotic neutrophils that are opsonised by IgG stimulate the production of TNF- α by phagocytosing macrophages (Manfredi, 1998). As PR3 is expressed on the surface of neutrophils (Csernok, 1994), the opsonisation of these cells by ANCA may increase the production of proinflammatory cytokines to be released from macrophages, thus producing further tissue damage.

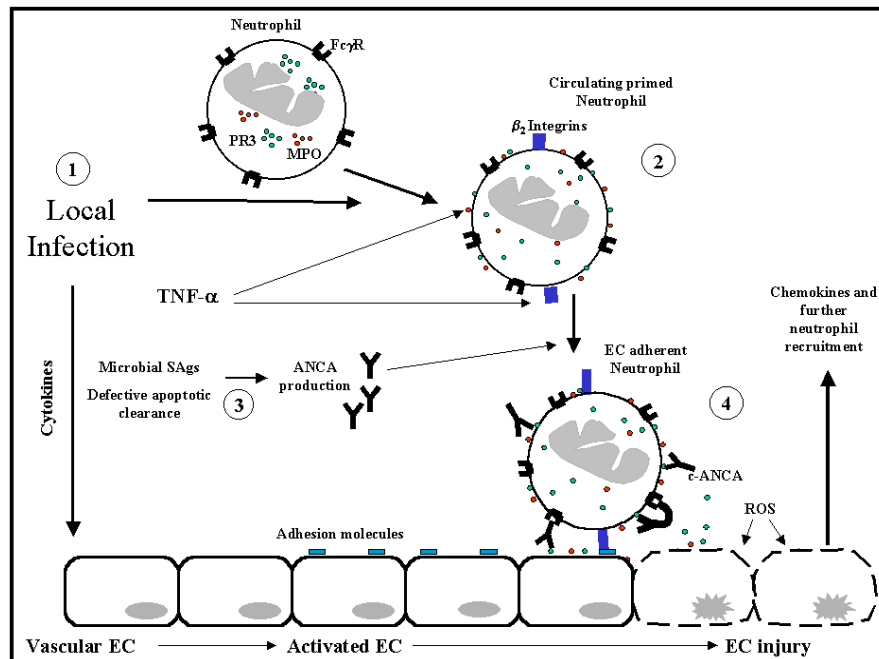


Fig 1.07 **The role of ANCA in the pathogenesis of WG** (Adapted from Reumaux, 2004; Langford, 1999). (1) Local infection can cause the release of cytokines from T cells allowing activation of endothelial cells (EC) and priming of circulating neutrophils. (2) TNF- α has a potent effect on neutrophils causing relocalisation of MPO and PR3 from intracellular stores to the cell surface and the upregulation of integrins. (3) Individuals who may have a polyclonal T and B cell response to SAGs or defects in apoptotic cell clearance may be susceptible to the production of ANCA. (4) Binding of ANCAs to neutrophils causes further activation and results in degranulation and the release of PR3, MPO and ROS. Following release PR3 may bind to the surface of EC, causing ANCA to also bind to the surface of ECs leading to enhanced adhesion molecule and cytokine expression resulting in increased neutrophil recruitment. The culmination of these processes is the development of a self-propagating immune response that damages to the ECs.

Chapter 1.2

REAL-TIME PCR

1.2.1 Polymerase chain reaction (PCR)

The idea of producing millions of copies of a specific DNA sequence was first proposed in 1971 (Kleppe, 1971). However, it took until 1985 (Saiki, 1985) for the first polymerase chain reaction (PCR) to be developed for β -globin. At this time, there were no thermostable DNA polymerases available; therefore, fresh enzyme needed to be added before each extension step. Water baths were used to cycle through the different reaction temperatures, as automated thermocyclers were not available. In 1988, the first use of a thermostable DNA polymerase in PCR was reported (Saiki, 1988), and soon thereafter automated thermocyclers were developed. Both of these innovations had a major impact on the practicality and cost of performing PCR

The most recent advance in PCR technology was the development of Real-time PCR or kinetic PCR (Higuchi, 1992; Higuchi, 1993). Work carried out by Higuchi et al laid the foundations for Real-time PCR, however it is only in recent years that this technology has become mainstream. Real-time PCR is the monitoring of amplicon accumulation during the exponential phase of PCR using a fluorescent reporter. Detection of a fluorescent signal, the point at which fluorescence starts to rise above the background noise is called the crossing point (Cp) and can often be referred to as the cycle threshold (Ct). The Cp is proportional to the initial starting copy number of the target sequence (Higuchi, 1993). Due to this relationship between the Cp and initial starting concentration Real-time PCR can be used to accurately quantify target sequences, which has a wide range of applications. Advantages of using Real-time PCR include rapid cycling times (~30 mins for 35 cycles), low risk of cross-contamination because of a closed tube system, no post-PCR

manipulation, high sensitivity (~3 pg genomic DNA (gDNA)), amplicon detection across a wide range ($10\text{-}10^{10}$ copies) and accurate quantification (Logan, 2004). Some of the current disadvantages are the high cost of equipment, a high level of technical skill is necessary and there is limited capacity for performing multiplex PCR (Logan, 2004).

1.2.2 Real-time PCR platforms

In the late 1990's, the first commercial Real-time PCR machines became available. The first of these was the ABI Prism 7700 sequence detection system (Applied Biosystems), which was closely followed by the LightCycler (Roche Diagnostics) (Wittwer, 1997). Both companies have released newer, improved versions of these machines and several other companies have entered into the Real-time PCR market with their own instruments such as the Mx4000 (Stratagene), iCycler (BioRad) and the DNA engine opticon2 (MJ Research) among others. While there are some major differences in how each machine operates, they all consist of a thermocycler, optics for fluorescence excitation and emission acquisition and a computer with software for data analysis.

1.2.2.1 The LightCycler

The LightCycler instrument was the first machine to allow ultra-rapid thermocycling (Wittwer, 1997). This was achieved through two methods. Firstly, the LightCycler system dispensed with the use of a thermal heating block to cycle through temperatures during

PCR, instead the machine uses air to heat and cool the PCR reaction components. The air is warmed by passing it through a heating coil in a thermal chamber, which allows for very rapid temperature transitions rates of up to 20°C/second (Fig 1.08). Secondly, the PCR occurs in a specially designed borosilicate glass capillary that has a maximum volume of 20 µl. The capillaries provide a large surface-to-volume ratio that allows rapid equilibrium between the air in the thermal chamber and the PCR components. The combination of these two innovations allows for a 30-40 cycle PCR to be performed in 20-30 mins. The LightCycler also has an inbuilt optical unit comprising of a light emitting diode (LED) and 3 photodetection diodes. The photodetection diodes are set to 3 different wavelengths: 530 nm (F1 channel), 640 nm (F2 channel) and 710 nm (F3 channel). These different wavelength channels can be used to detect fluorescence from different fluorescent dyes used during Real-time PCR. The LightCycler is compatible with all the major fluorescent chemistries used to detect amplicon accumulation during Real-time PCR as discussed below.

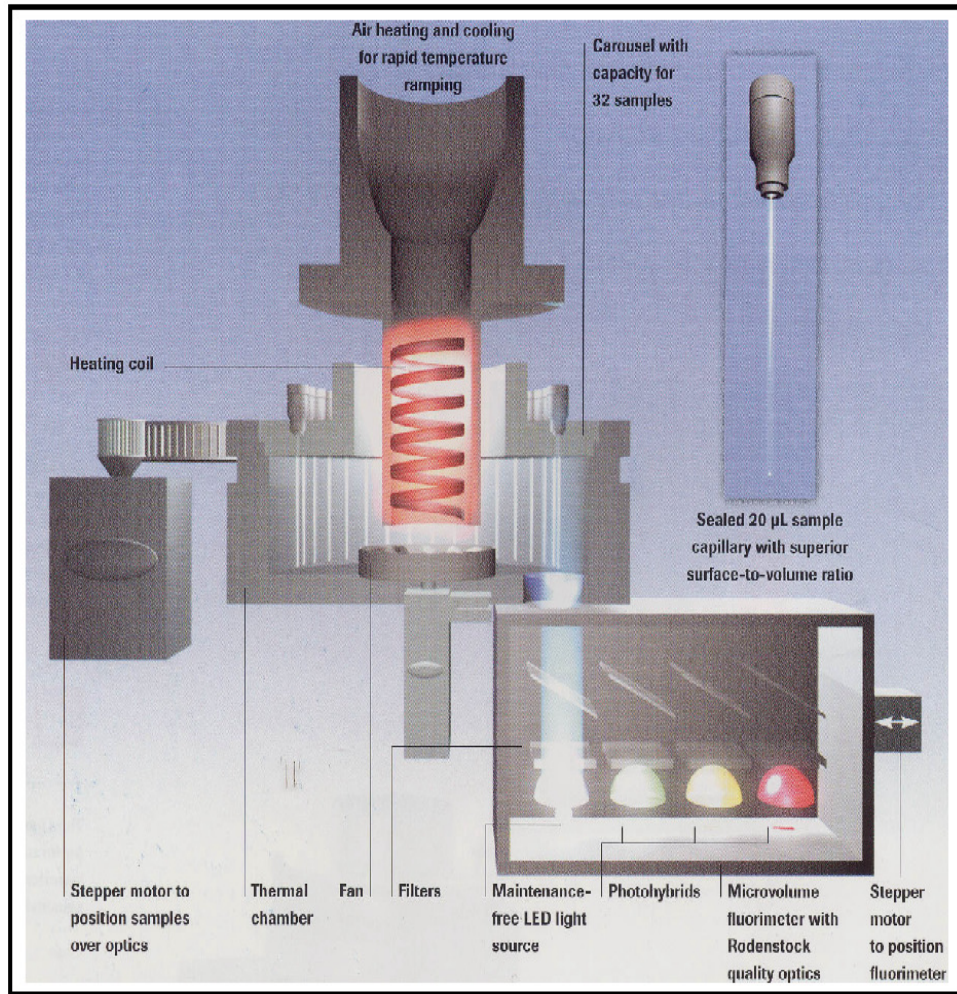


Fig 1.08 Schematic diagram of the LightCycler Real-time PCR thermocycler (LightCycler brochure, 2001).

1.2.3 Amplicon detection

As mentioned previously Real-time PCR is based on the ability to monitor the amplification of PCR product as it is being generated by the polymerase enzyme. To do this a fluorescent reporter system is incorporated into the PCR reaction. There are many different reporter systems on the market, nonetheless they all fall into one of two categories, non-specific double stranded (ds) DNA binding dyes or fluorescent-labelled sequence specific probes (Lee, 2004).

1.2.3.1 Non-specific dsDNA binding dyes

Ethidium bromide (EtBr) is the most common nucleic acid binding dye used in molecular biology, with its conventional use being to stain agarose gels used during traditional PCR product analysis. In 1992, Higuchi et al reported the use of EtBr to monitor the amplification of PCR product in a closed tube format (Higuchi, 1992). In 1993, Higuchi et al coined the term “kinetic PCR” after they demonstrated that fluorescence intensity during thermocycling was proportional to the starting copy numbers of the target sequence (Higuchi, 1993). In recent years, the minor groove binding dye SYBR Green 1 (Morrison, 1997) has clearly become the favourite of the non-specific dsDNA binding dyes with many publications reporting its use (Vandenbroucke, 2001; Gundry, 2002). The SYBR dyes typically increase in fluorescence by 20 to 100 fold when bound to dsDNA and have a similar emission spectrum to that of fluorescein (approx 520 nm) (Lee, 2004). Fluorescence is usually monitored at the end of the extension phase in a typical SYBR

Green 1 Real-time PCR experiment, as it is at this point that there is the maximum amount of dsDNA present for that cycle number (Fig 1.09).

The use of non-specific binding dyes can be favoured by many researchers as they are widely available, cheap and very little optimisation is required to transfer an efficient traditional PCR over to a Real-time format. Whilst generic dyes can be used for quantitative Real-time PCR, there are some limitations due to their non-specific DNA binding action. Any PCR artefact formed, such as primer-dimers, when performing Sybr Green 1 quantitative Real-time PCR will also be detected due to the non-specific nature of the dye. This could lead to misinterpretation of the data. However, there are further optimisation strategies that can be employed to help avoid this, such as performing a touchdown PCR, which will help reduce the production of non-specific amplicons in the early stages of the PCR. Another method to improve the use of SYBR Green 1 for quantification is to establish the T_m of both the specific amplicon and PCR artefacts using melting-curve analysis. If the T_m of the artefact is significantly lower than that of the specific amplicon then fluorescence readings can be acquired at a temperature above that of the T_m for the artefact. Therefore, any increase in fluorescence is now specific to the amplicon of interest (Ball, 2003; Morrison, 1998). Multiplexed quantification is not possible as there is no way to differentiate the two products from each other, as fluorescence from both will be detected in the same channel.

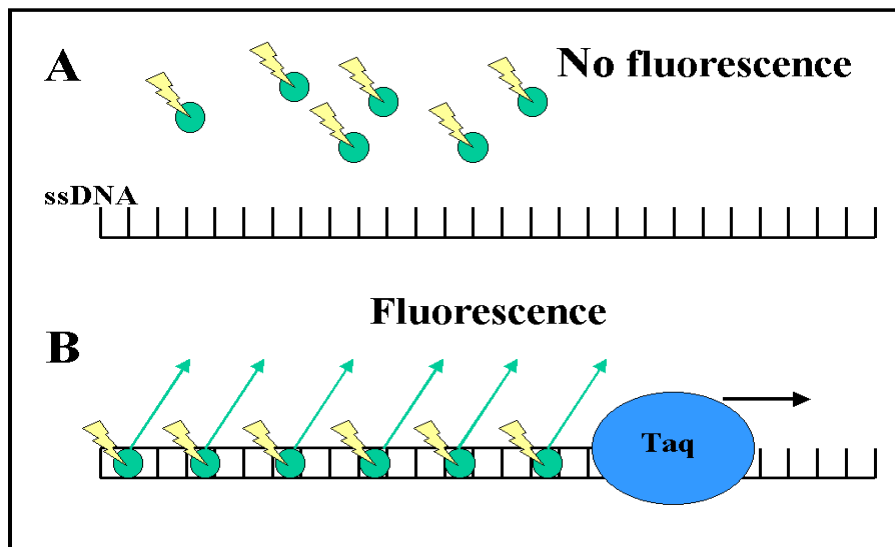


Fig 1.09 **SYBR Green 1 detection**. SYBR Green 1 cannot bind to ssDNA (A) but as Taq polymerase extends the primer, SYBR Green 1 can bind to the minor groove of the duplex and its fluorescence emission is enhanced (B).

1.2.3.2 Specific DNA binding probes

There are many different probe chemistries available on the market today, each with a slight variation of a common theme: an oligo-nucleotide that is coupled to a fluorophore. When the probe/probes bind to their complementary target sequence a fluorescent event can be monitored which is directly related to the amount of amplicon present at that cycle. There are three commonly used probe types; hydrolysis probes (Fig1.10), molecular beacons (Fig 1.11) and dual hybridisation probes (Fig1.12). As probes are sequence specific they avoid the problems of non-specific detection of PCR artefacts associated with

the use of Sybr Green 1. Nevertheless, the use of probes increases the cost of each test and each probe must be carefully designed otherwise it may not work efficiently.

1.2.3.3 Fluorescence Resonance Energy Transfer (FRET)

Fluorescence resonance energy transfer (FRET) is a spectroscopic process where energy is passed between two molecules up to 10-100 Å apart which have overlapping emission and absorption spectra (Clegg, 1992). The mode of action of the commonly used probes is based on the principles of FRET. For some probe types such as the 5' hydrolysis probes and molecular beacons, FRET occurs between a fluorogenic label and a dark or 'black-hole' non-fluorescent quencher, which dissipates the energy as heat rather than fluorescence (Ginzinger, 2002). Other probes, such as hybridisation probes, use FRET to transfer the energy from one fluorogenic dye to another which then releases a longer wavelength of light that is then detected by the instrument (Wittwer, 1997).

1.2.3.4 Hydrolysis probes

The hydrolysis probes are often more commonly named TaqMan probes, and while they work with many Real-time platforms, these probes seem to have found their home on the ABI Prism 7700 sequence detection system (Applied Biosystems). These probes utilise the fact that Taq (or several other polymerase enzymes) have 5' → 3' exonuclease activity (Gelfand, 1989). The 5' end of the probe is labelled with a reporter dye (FAM, TET, JOE,

HEX or VIC) and the 3' end has a covalently linked quencher (TAMRA, DABCYL). The proximity of both molecules to each other when attached to the probe allows FRET to occur, however the energy is dissipated as heat rather than fluorescence by the quencher. When the probe binds to the target sequence at the annealing phase, Taq can now cleave the 5' reporter dye from the probe, which now releases it from the effects of the quencher and fluorescence, can be emitted and recorded by the instrument (Fig 1.10). A drawback when using this type of probe is that in order for the probe to remain annealed to its specific sequence the extension temperature must be adjusted. Therefore it is common to have a combined annealing and extension step at 60-62°C, this ensures that the probe remains hybridised so it can be cleaved by the 5'-3' exonuclease activity of Taq and Tth polymerases. However, the sub-optimal extension temperature affects the enzymes processivity and is therefore not suitable for longer amplicons (Bustin, 2000). These probes have been used for a wide range of applications such as gene copy number quantification (Aarskog, 2000), virus quantification (Quinlivan, 2005; Kawai, 1999), quantification of cytokine mRNA expressed in Hodgkin's lymphoma (Malec, 2004) and analysis of DNA and RNA extracted from archival material (Lehmann, 2001; Godfrey 2000) to name but a few.

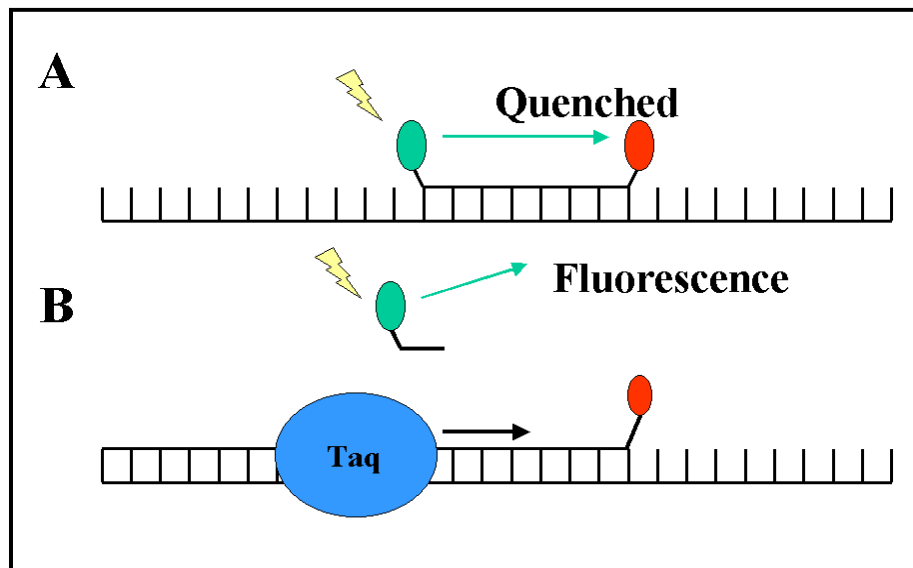


Fig 1.10 **Hydrolysis probe detection.** When the probe is intact the fluorophore is quenched (A), the 5'-3' exonuclease activity of Taq cleaves the probe releasing the reporter dye into solution where it is no longer quenched (B).

1.2.3.5 Molecular beacons

The molecular beacons (Livak, 1995) mode of action is based on a conformational change, from hairpin loop to linear structure, when it is bound to its specific sequence. The linearisation of the probe causes a reporter and quencher dye to be separated from each other so that fluorescence can be emitted from the reporter (Tyagi, 1996) (Fig 1.11). The major drawback in using molecular beacons is that the probes are complex to design. If the stem region is not optimal, the probe may form alternative conformations, which may not place the fluorophore and quencher in close proximity to each other. This can result in a proportion of the free probe not being quenched, which leads to a high background signal

(Bustin, 2000). If the stem region has too high of a binding affinity then this may interfere with hybridisation of the probe to its target sequence resulting in inefficient detection of the amplicon.

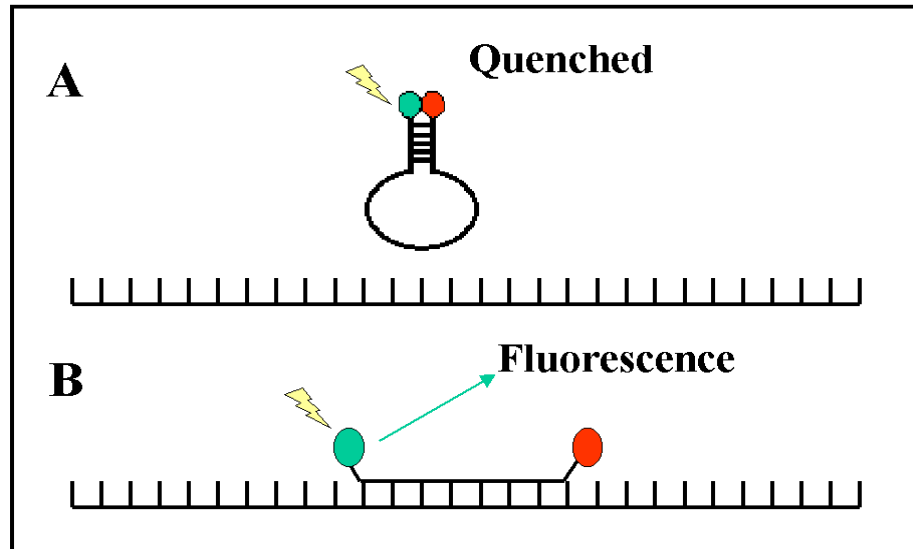


Fig 1.11 **Molecular beacon detection.** When the probe is not hybridised to its specific sequence it forms a stem-loop conformation that causes the fluorophore to be quenched (A), binding of the probe causes a conformational change that separates the fluorophore and quencher and allows emission of fluorescence (B).

1.2.3.6 Dual hybridisation probes

This method utilises two independent probes, which maximises the assays specificity (Wittwer, 1997). One probe is labelled on its 3' end with a donor dye (anchor probe), and the second probe is labelled with an acceptor dye at its 5' end (detector probe) (Fig 1.12). Using this arrangement, as the anchor and detector probes anneal to their specific sequence the two dyes are brought into close proximity to each other allowing FRET to occur. The detector probes 3' end is usually blocked with a phosphate group to prevent it from being extended by Taq polymerase (Landt, 2001). These probes have few draw backs as they are easy to design, relatively easy to multiplex and as the probe is not hydrolysed they can be used for melt curve analysis, which is particularly applicable to mutation detection. However, one of the drawbacks of using these probes is that amplicons must be bigger than if only a single probe system is used. This can limit their use in applications that involves fragmented nucleic acids, such as that which has been extracted from archival tissue samples, as shorter amplicons work much more efficiently in these circumstances (Lehmann, 2001).

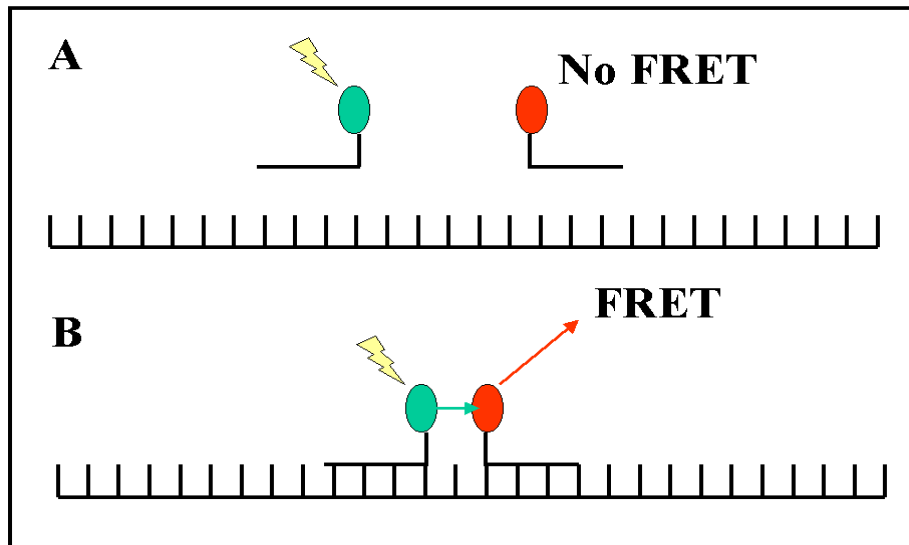


Fig 1.12 **Hybridisation probe detection.** When both probes are free in solution FRET cannot occur as the two dyes are apart (A), when both probes hybridise to there target sequence the dyes are brought into close proximity that allows FRET to occur (B).

1.2.4 Mutation detection by Real-Time PCR

Mutations can be large rearrangements of genetic material such as gene insertions/deletions or small variations such as small insertions/deletions (a couple of base pairs (bp) or point mutations. Small genetic variations are usually referred to as single nucleotide polymorphisms (SNPs) and are the most common type of mutation, occurring approximately every 1000 nucleotides (Sachidanandam, 2001; Venter, 2001). The majority of these are found in the non-coding regions of the genome and are thought to be of no significance, but can be used as genomic markers in population genetics. A SNP in the

coding region of a gene may result in an altered protein and detection of these is important in many monogenetic diseases such as cystic fibrosis (Kerem, 1989).

DNA sequencing will remain the gold standard for characterisation of unknown sequences/mutations however its use for rapid mutation detection is quite poor. Since the development of PCR (Mullis, 1987; Saiki, 1985), many variations such as restriction fragment length polymorphism (RFLP) PCR and amplification refractory mutation system (ARMS) PCR (Newton, 1989) have been developed for use in mutation detection. The majority of these techniques are laborious, slow and expensive. Real-time PCR provides an improvement on all of the conventional techniques in terms of throughput, flexibility and ease of analysis.

The LightCycler when used in conjunction with hybridisation probes allows for mutation detection by performing melting curve analysis directly after the amplification step (Wittwer, 1997). During melting curve analysis fluorescence is continuously monitored as the temperature is slowly increased (0.1 °C/sec). At a specific temperature, the detector probe will begin to dissociate (“melt”) from its target sequence. The melt temperature (T_m) is the temperature at which 50% of the probe is dissociated from the target sequence. As the temperature approaches the T_m of the detector probe a decrease in the level of FRET will be observed as a melting curve. When a mutation occurs in the target sequence, this has a destabilising effect on the detector probe and it has a lower T_m than that of the perfectly matched probe (Fig 1.13 A, B). The LightCycler software displays the melting curves as melting peaks by plotting the negative derivative of fluorescence ($-dF$) against the

negative derivative of temperature ($-dT$) (Fig 1.13 C) and this allows easy discrimination of wildtype, mutant and heterozygote genotypes (Lay, 1997).

1.2.4.1 Dual hybridisation probe design

The detector probe is designed to span the site of the possible mutation and is typically 15-30 bases in length. The anchor probe should have a T_m 5-10°C higher than the detector probe this ensures that the detector probe “melts” first (Landt, 2001). Consequently, the drop in FRET is due to the detector probe, which allows the presence or absence of a mutation to be determined. If the detector probe is designed so that the mutation is approximately at the centre of the probe this has the greatest destabilising effect on the probe than if it is at either end (Landt, 2001). A larger destabilising effect on the probes T_m means the melting curve peaks are further apart, allowing the identification of wildtype and mutant genotypes to be made easier (Bernard, 2001).

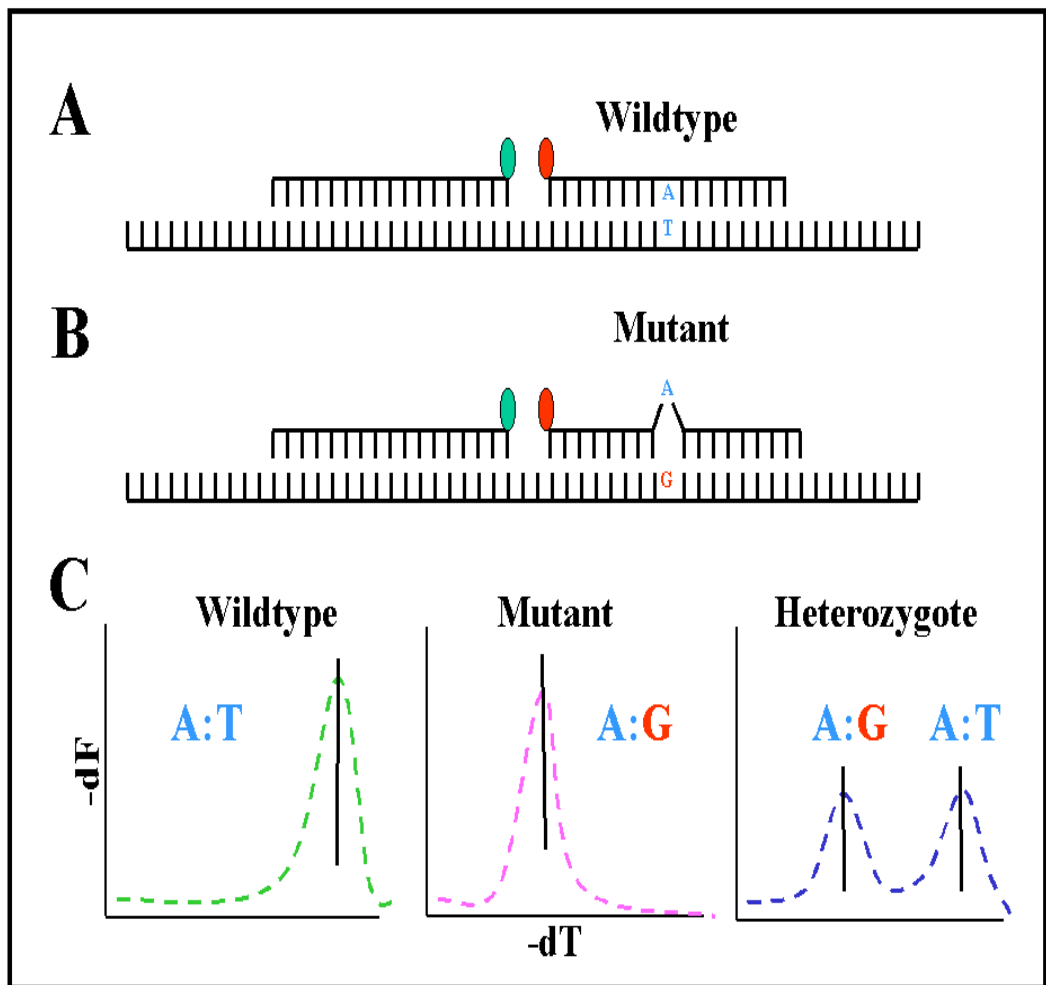


Fig 1.13 **Mutation detection using dual hybridisation probes.** Absence of a point mutation allows for perfect hybridisation of the detector probe (A), presence of a mutation causes incomplete hybridisation of the detector probe (B). The matched probe (A:T) requires a higher melting temperature than mismatched (A:G) probe (C). Negative derivative of fluorescence (-dF), Negative derivative of temperature (-dT).

1.2.4.2 Multiplex mutation detection on the LightCycler

Multiplex PCR is the process of generating more than one amplicon at a time. This increases the information obtained from a single PCR and helps to reduce the cost of analysis. Multiplex mutation detection can be performed on the LightCycler by using two of the instruments detection channels. The F2 and F3 channels can be used to detect fluorescence from the LCRed640 and LCRed705 dyes respectively. Using two different set of hybridisation probes each specific for a single mutation and labelled with one of the two LightCycler dyes it is possible to type at least two different mutations per sample (Aslanidis, 1999; Bernard, 1998).

1.2.4.3 Other detection formats for mutation detection

The other common detection systems can all be used for mutation analysis. Mutation detection can be performed using Sybr Green 1 (Wittwer, 1997; Ririe, 1997). However the use of Sybr green 1 is a low-resolution method, as a single bp change will have only a small impact on the T_m of amplicon that maybe a couple of hundred bp in length. A newer dye called LCGreen 1 has been specifically developed for use in mutation detection (Wittwer, 2003). The one advantage of using the intercalating dyes is that any mutation within the amplicon can be detected and therefore used for mutation scanning (Wittwer, 2003). By using high-resolution melting techniques with customised equipment, it is possible to detect single-base heterozygotes in products up to 1000 base pairs in length (Wittwer, 2004).

Hydrolysis probes, because of their mode of action, cannot be used to perform melting curve analysis as the probe is consumed during the amplification stages. Therefore, to use this system for mutation detection it is necessary to design two probes, one that will bind to the wildtype and another for the mutated sequence, each of which is labelled with a different reporter dye (Edwards, 2004). Mismatches between the probe and target sequence reduce the efficiency of binding and as a result Taq does not cleave the probe and no reporter dye is released. Genotypes can be assessed based on which reporter dye is released during amplification. Molecular beacons have also been adapted to SNP detection assays (Tyagi, 1998).

1.2.5 Quantitative Real-Time PCR

Quantification of nucleic acids has many applications such as in monitoring gene amplification in tumours, viral quantification and gene expression analysis between normal and disease states. Since its inception PCR would seem to have been the best method for quantitative analysis as it has a sensitivity 5 orders of magnitude greater than the best blotting techniques (Rasmussen, 2001). However, the exponential amplification of the target sequence is not ideally suited to quantification, as small differences in amplification efficiency from sample to sample can result in huge differences after 35-40 PCR cycles. Additionally, reagent limitations or the production of pyrophosphate molecules leads to a decrease in amplicon synthesis and the PCR enters the “plateau phase” (Fig 1.14). In the plateau phase, the PCR is no longer generating product at an exponential rate, and some

reactions will enter this stage earlier than others and therefore generate less amplicon. It is this reason, which makes end-point quantification so unreliable (Ginzinger, 2002).

Since Higuchi et al (1992) showed that it was possible to measure the kinetics of a PCR by monitoring product accumulation from cycle to cycle in Real-time, allowing truly quantitative PCR to be performed. From the simple addition of ethidium bromide to a PCR mix to the use of more complex and specific probe technologies Real-time quantitative PCR has become a fast growing field with many applications in biotechnology and molecular medicine.

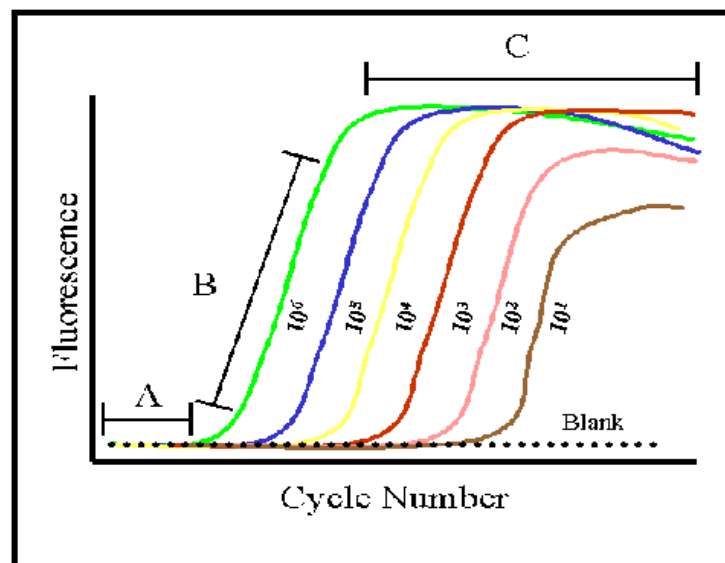


Fig 1.14 **Quantitative Real-time PCR amplification curve.** During amplification there is an initial lag phase (A) followed by the exponential phase (B) and lastly the plateau phase (C).

1.2.5.1 Dynamic range of Real-time PCR

The dynamic range of a Real-time quantitative PCR is between 10 and 10^{10} copies of initial template (Saunders, 2004). The upper limit is set by the need to establish a base-line level of fluorescence before amplicon accumulation is detected, since after this point it is not possible to accurately determine the C_p (Saunders, 2004). The lower limit for accurate quantification is determined by the sensitivity of the PCR, which is often influenced by the reaction components, so careful optimisation can enhance the sensitivity of the PCR. Pre-amplification of the target sequence using external primers, nested PCR, has been used by some investigators to enhance the sensitivity of the assay (Brechtbuehl, 2001). However, the use of nested PCR cancels out many of the benefits of Real-time particularly the avoidance of possible cross-contamination, as PCR tubes must be opened.

1.2.5.2 Real-time PCR efficiency

One of the most crucial factors in carrying out quantification is that the efficiency of the reaction is similar between control/standards and the actual test samples. The efficiency of PCR can be estimated from the slope of the C_p plotted against log of concentration. The slope reflects the number of cycles it takes to increase the amplicon number by 1 log value (Saunders, 2004). This relationship should be linear with a slope of approximately -3.33. Efficiency can be calculated from the following equation: $E = 10^{-1/\text{slope}}$ (Rasmussen, 2001). A reaction that is 100% efficient (perfect doubling of amplicon per cycle) will give a value of 2 from this equation (Bernard, 2002). Therefore, values less than 2 indicate that the

reaction is not operating at 100% efficiency. Efficiency can be improved by careful optimisation of the PCR parameters such as primer concentration, annealing temperature, amplicon length and so on. PCRs with low efficiency ($E = 1.5$) can be used for quantification, however, this can have an effect on the dynamic range of detection and samples with low copy numbers may be missed (Saunders, 2004).

1.2.5.3 Gene expression analysis by Real-time PCR

The messenger RNA (mRNA) content of a cell is a good indicator of the genes that a cell is expressing at that particular time. In response to environmental changes, a cell may adjust the mRNA copy numbers as part of a complex regulation mechanism. This has particular significance with many different diseases, as they are often associated with changes at the mRNA level. There are five common methods for detecting and quantifying mRNA transcripts: northern blotting, in situ hybridisation, RNase protection assay (Hod, 1992), micro-array analysis and reverse transcription (RT) PCR (Simpson, 1988; Vrieling, 1988). The first three methods are quite labour intensive and have a comparatively low sensitivity. Micro-array analysis is still prohibitively expensive for routine gene expression analysis such as in monitoring a patient's response to chemotherapy. RT-PCR is the most sensitive and flexible of the quantification methods (Wang, 1999) and is suitable for routine analysis. As RNA cannot directly act as a template for PCR, it is first necessary to generate a cDNA copy of the RNA that can then be amplified using PCR. Until the arrival of Real-time PCR, there has been a problem with the quantification of mRNA transcripts, as end-point PCR does not reflect the initial starting copy number of the target sequence. A real-time

approach to RT-PCR avoids many of the problems associated with conventional quantitative protocols and its sensitivity, specificity and wide dynamic range has made it the method of choice when quantifying steady-state mRNA levels (Bustin, 2000).

1.2.5.4 Relative quantification

Relative quantification determines the changes in steady-state mRNA levels of a gene in comparison to an internal control/reference RNA (Fink, 1998). The reference is usually described to as a housekeeping gene. Housekeeping genes are genes that should remain at a constant level within a cell regardless of environmental/experimental factors. Amplification of the housekeeping gene can occur in the same reaction as the target sequence (multiplex) or in a separate tube, either way all samples are expressed as an X-fold difference relative to the housekeeping gene. This form of quantification is independent of RNA/DNA concentration added to the RT-PCR/PCR. Nonetheless, there are some problems associated with this type of quantification. The major problem is due to the difficulty in finding a suitable reference gene whose expression remains constant under experimental conditions (Bustin, 2004). It has been recommended that the expression of at least 10 reference genes should be analysed along with target gene mRNA in order to get accurate relative quantification data (Vandesompele, 2002). If cohort samples sizes are even of a modest size this then becomes quite a large and demanding task. Some common reference genes are glyceraldehyde 3-phosphate dehydrogenase (GAPDH), TATA-box binding protein (TBP), hypoxanthine-guanine phosphoribosyltransferase (HPRT), β -2 microglobulin (β 2M), phosphoribosyl deaminase (PBGD), and 18S/28S ribosomal RNAs

to name but a few. Incidentally, while GAPDH has been a widely used reference gene for many years, its suitability as a reference gene is questionable. There is an overwhelming amount of evidence indicating that GAPDH is an unsuitable reference gene. GAPDH mRNA concentrations can vary, between individuals (up to 5 orders of magnitude) (Bustin, 1999), during pregnancy (Cale, 1997), during the cell cycle (Mansur, 1993) and it is upregulated in certain cancers (Ripple, 1995). GAPDH transcription can also be induced by hypoxia (Zhong, 1999), calcium ionophore A23187 (Chao, 1990), insulin (Barroso, 1999) and apoptosis (Ishitani, 1997). Therefore the use of GAPDH as an internal control for Real-time quantitative should be discouraged (Bustin, 2000).

1.2.5.5 Absolute quantification

The other option for Real-time quantification is absolute quantification, which involves the determination of the exact copy number of target sequences within a quantity of sample. It provides a more accurate and reliable, albeit more labour intensive method for quantification of nucleic acids (Ke, 2000). A series of standards are generated and a plot of C_p versus log concentration allows the C_p of the unknown samples to be compared to the standards. Standard curves can be generated in a number of ways. Purified PCR product or synthetic oligonucleotides can be used to generate standard curves. Sometimes there can be problems with reamplification and this approach may only be suitable for the quantification of short amplicons (Pfaffl, 2005). Recombinant DNA can also be used to generate standard curves; these are very stable and produce very reproducible results (Pfaffl, 2001). The one drawback is, when used for mRNA quantification this type of standard is not subjected to

the RT phase of the assay, therefore differences in RT efficiency will not be reflected in the standard curve. A third method for generating standards is to use recombinant RNA; these standards will reflect all stages of an RT-PCR reaction. Nevertheless they are difficult to produce and purify, are very labile and the resulting PCR is less efficient (Pfaffl, 2001). The results are usually then expressed as copy number per denominator, which could be per mg tissue or per μg total RNA and so on.

Real-time PCR is an adaptable, sensitive and rapid technique for the quantification of nucleic acids. It also provides a platform for rapid SNP detection using post-PCR melting curve analysis. In the last couple of years the technology has become an integral part of many diagnostic and research laboratories, which should serve to drive the technology forward, by improving the instruments, the detection chemistries and reduce the cost of analysis.

Chapter 2

CHALLENGES TO REAL-TIME PCR

Chapter 2.1

**DETECTION OF FIVE COMMON CFTR
MUTATIONS BY REAL-TIME ARMS PCR**

2.1.1 INTRODUCTION

2.1.1.1 Cystic Fibrosis (CF)

Cystic fibrosis (CF) is the most common recessively inherited lethal genetic disease of Caucasians, with a prevalence of 1 in 2500 (Collins, 1992; Mateu, 2002). The disease also has an astounding carrier frequency of 1 in 25 (worldwide) (Hutchison, 2001) and in Ireland, the carrier frequency has been reported to be as high as 1 in 19 (McQuaid, 2000).

2.1.1.2 Diagnosis of CF

In 1953, it was demonstrated that children with CF had excessive salt in their sweat (DiSant' Agnese, 1953). This led to the measuring of sodium (Na^+) and chloride (Cl^-) levels in the sweat as a diagnostic standard for the disease (Gibson, 1959). The normal levels of NaCl in sweat is approximately 15-40 mM, people with CF may have NaCl levels >100 mM (Wine, 2001). With the advent of molecular techniques and the identification of the gene (CFTR) involved in CF, the combination of two CFTR mutations and an abnormal concentration of sweat electrolytes is generally accepted as sufficient for diagnosis (Stern, 1997)

2.1.1.3 Clinical features of CF

The main pathological hallmark of CF is the build up of thick viscous mucus in the airways (Wine, 1995), which is very significant, as the usual cause (>90%) of death in CF is respiratory failure (Davies, 1998). The build up of the mucus in the lungs helps to initiate a cycle of chronic infection and inflammation. The lungs become infected in early childhood and eventually become damaged and scarred. Colonisation of the lungs generally follows a similar pattern, beginning with *Staphylococcus aureus* and *Haemophilus influenzae* in early childhood and ends with *Pseudomonas aeruginosa* in adolescence (Hutchison, 1999). *Pseudomonas aeruginosa* can be isolated from 80-90% of adult CF lungs (Hutchison, 1999). Individuals that have avoided colonisation, with the opportunistic pathogen, have survival rate twice that of patients who have been colonised (Hutchison, 1999). The main cause of damage occurs when recruited neutrophils, whose number may be a million fold higher than in normal lungs, die and release a protease called elastase (Bradbury, 2001). The elastase destroys elastic fibres in the lung, which over time reduces the lungs air capacity ultimately leading to respiratory failure.

The gastrointestinal tract is also involved in most patients; approximately 85% (Collins, 1992) show pancreatic insufficiency caused by obstructed pancreatic ducts resulting in destruction of the pancreas. Nearly 10% of newborns with CF suffer with intestinal obstruction (*meconium ileus*), which can be fatal if left untreated (Rowe, 2005). Men with CF are often infertile due to obstruction of the vas deferens *in utero* leading to a condition known as congenital bilateral absence of the vas deferens (CBAVD). There is also a significant increase in the incidence of liver disease and overt cirrhosis in patients with CF

who also carry a homozygous or compound heterozygous mutation in the protein mannose-binding lectin (Gabolde, 2001). An increased risk of digestive tract cancers has also been reported in CF patients (Neglia, 1995).

2.1.1.4 Treatment of CF

The treatment of CF includes chest percussion to help clear mucus build-up in the lungs, antibiotics to control bacterial infection, pancreatic enzyme supplements to compensate for the damage caused to the pancreas and dietary supplements to help patients meet their nutritional requirements. This combination of therapy has greatly improved the life expectancy of an individual diagnosed with CF from approximately 1 year in 1930 to 30-32 years today (Geddes, 1998; Bradbury, 2001). Lung transplantation is also now becoming a common treatment for suitable patients with severe damage to the airways. Other experimental treatments include delivery of elastase inhibitors (either recombinant or synthetic forms) to the lungs, which may help to reduce damage caused to the lungs during inflammation (Bradbury, 2001).

2.1.1.5 Cystic fibrosis transmembrane conductance regulator (CFTR)

In 1989 the CF gene was identified, it was first mapped to chromosome 7q31 using linkage analysis (Riordan, 1989). Then by using chromosome-walking techniques, a candidate gene was identified (Rommens, 1989). The CF gene itself is quite large at 250,000 bp

(Kerem, 1989) and contains 27 exons. The CF gene's protein product was named the cystic fibrosis transmembrane conductance regulator (CFTR) (Riordan, 1989). The CFTR is an integral membrane protein, 1480 amino acids in length that contains a glycosylation site. The CFTR is a member of the ABC (ATP-Binding Cassette) superfamily of transporters that transports chloride ions (Cl⁻) across the plasma membrane (Riordan, 1989). As the movement of water is linked osmotically to the transport of ions, Cl⁻ secretions maybe one method of hydrating the mucosal surface of the respiratory and intestinal tracts (Geddes, 1998).

The CFTR protein has two hydrophobic domains that incorporate themselves into the plasma membrane. Each of the domains has six loops that span the plasma membrane. There are also two nucleotide-binding domains called NBD1 and NBD2. The regulatory domain controls the status of the channel. The CFTR is regulated by protein kinase A (PKA) and ATP (Collins, 1992). Activation of the channel first involves a rise in the cells cyclic AMP (adenosine 3'5'-monophosphate) concentration, which in turn activates protein kinase A (PKA). Once activated, PKA phosphorylates four serine residues in the regulatory domain (Collins, 1992). This causes a conformational change in the CFTR structure and ATP can now bind to the two NBDs. Cleavage of the ATP at NBD1 causes the channel to open and Cl⁻ ions can pass through. Binding of ATP to NBD2 is thought to stabilise the open conformation of the protein. When NBD2 hydrolyses the ATP the channel closes and requires another ATP to bind to open again (Jenstch, 1996). Deactivation of the channel is carried out by protein phosphatases (Akabas, 2000), mainly protein phosphatase 2C, which has been shown to be closely associated with CFTR through immunoprecipitation studies (Zhu, 1999).

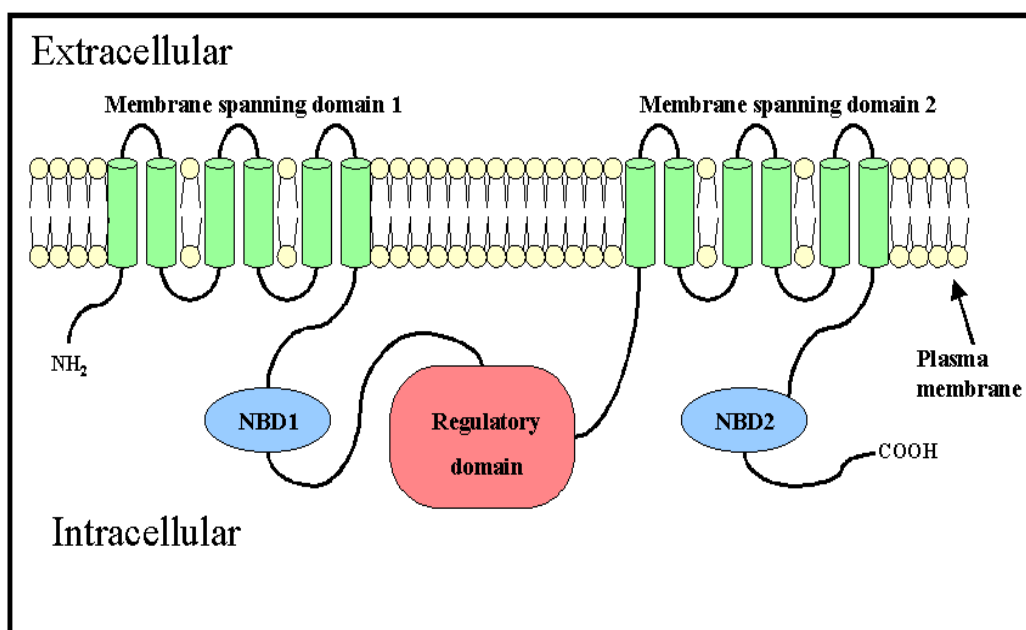


Fig 2.1 **Structure of the CFTR.** The protein has 5 distinct domains consisting of: 2 membrane spanning domains which form the channel across the plasma membrane, 2 nucleotide binding domains (NBD) and a regulatory domain (Adapted from Riordan, 1989; Rowe, 2005).

2.1.1.6 Mutations in the CFTR

To date more than 1000 mutations have been described in this gene, however the majority of these are rare (Tsui, 2003). CFTR mutations can be classified into groups (I-VI) based on how they are believed to cause CF. Class I mutations result in no protein being synthesised, class II mutations block correct processing of the protein, class III mutations result in disordered regulation of the protein, class IV mutations result in altered conductance through the channel, class V mutations cause a reduced number of CFTR transcripts due to promoter or splicing abnormalities and class VI mutation result in an

accelerated turnover of the protein from the cell surface (Rowe, 2005). Classes I-III tend to cause a severe CF phenotype and classes IV-VI resulting in a milder phenotype.

By focusing on five common mutations it is possible to detect the disease causing mutation in approximately 90% of Irish patients (Scotet, 2003) and ~71% in the worldwide population (Tsui, 2003). The five mutations are delF508 (77.4%, 66.0%), G551D (7.1%, 1.6%), R117H (2.7%, 0.3%), 621+1 G>T (1.4%, 0.7%) and G542X (0.5%, 2.4%) figures are for the Irish population (Scotet, 2003) and worldwide (Tsui, 2003) respectively.

The delF508 mutation is a class II mutation, which is found in exon 10 of the CF gene that codes for the NBD1 domain (Naruse, 1999). It involves a 3 bp (CTT) deletion, which results in the loss of a phenylalanine (F) at codon 508. The delF508 mutation results in a protein-processing defect, which traps the delF508 CFTR in the endoplasmic reticulum (Devidas, 1997) and prevents it from being transported to the apical plasma membrane. Of the other mutations G542X is a class I mutation (Rowe, 2005) it is found in exon 11 (Karem, 1990) and results in the introduction of a premature stop codon. G551D is a class 3 mutation (Rowe, 2005) also found in exon 11 (Cutting, 1990). The protein is processed and targeted correctly to the plasma membrane but lack responsiveness to stimulation by cAMP. The 621+1G→T is a class V mutation is located in intron 4 and results in the mRNA being incorrectly spliced. R117H is class IV mutation and results in altered conductance through the CFTR channel (Sheppard, 1993).

2.1.1.7 Pathogenesis of CF

How lung disease develops in the CF lung has been a difficult problem to explain. Healthy lungs are sterile below the first bronchial division (Wine, 1999) despite a constant influx of bacteria and viruses from the air we breathe. Lung sterility is maintained by a wide range of methods, such as mucociliary clearance, which cleans the airways mechanically. The airway surface liquid (ASL), which is thin film of liquid that coats the surface of the lungs, contains a wide range of proteases, antimicrobial peptides and antibodies that inactivate or destroy pathogens without causing collateral damage to the cells of the lungs.

There are currently two proposed hypotheses of how disease is initiated. These are the high salt hypothesis (Smith, 1996; Zabner, 1998) and the low volume hypothesis (Matsui, 1998). The high salt model is based mainly on the CFTR function as an anion channel. Non-functional CFTR results in reduced transepithelial Cl^- transport, the resulting elevated levels of NaCl in the ASL would be enough to inactivate antimicrobial peptides and therefore predispose patients to colonisation by opportunistic pathogens such as *Pseudomonas aeruginosa*.

The low volume model is based on CFTR ability to regulate other channels particularly epithelium sodium channels (ENaC) (Reddy, 1999). The absence of CFTR leads to over activity of Na^+ absorption through the ENaC, it is thought then that the transepithelial imbalance in Na^+ and Cl^- ions leads to the absorption of Cl^- via other non-CFTR channels. The result of this is there is an increase in absorption of Na^+ , Cl^- and water causing the dehydration of the airway surfaces and defective mucociliary clearance.

Explanations for the cause of pulmonary defects in CF are unlikely to explain the damage sustained to other organs. In the pancreas there is no evidence of overactive Na^+ absorption, also in the intestine there is no evidence of increased susceptibility to infection by altered immune responses as occurs in the lung (Rowe, 2005). However, in glandular tissues of CF patients there is a defect in Cl^- and fluid secretions. When secretin binds its receptor on pancreatic duct cells, resulting in elevated intracellular levels of cAMP normal CFTR function is initiated. In the pancreas, this results in the efflux of Cl^- , Na^+ and water into the lumen of the pancreatic ducts (Naruse, 1999). In the absence of functional CFTR, the deficiencies in fluid secretions results in the blockage of ducts leading to organ damage. Similar mechanisms are proposed to cause damage to the vas deferens, liver and other glands in cystic fibrosis.

2.1.1.8 Detection of CF mutations

Many mutation detection systems have been utilised to detect common CF mutations, including single stranded conformation polymorphism (SSCP) (Ravik-Glavac, 1994), restriction fragment length polymorphism (RFLP) (Shrimpton, 1991), Amplification Refractory Mutation System (ARMS) PCR (Ferrie, 1992) and reverse dot-blot (Cuppens, 1992). These techniques rely on PCR amplification of the target region, which is then followed by extensive post-amplification analysis. In recent years improvements in technologies has led emergence of homogeneous methods, where both the amplification and detection occur in a single “closed-tube” reaction (Foy, 2001). Current homogeneous techniques include Real-time PCR (Wittwer, 1997), ligase chain reaction (LCR) (Austina,

1997) and strand displacement amplification (Little, 1999). The advantage of closed-tube systems is the reduced risk of cross contamination and improved speed with no post-amplification processing.

2.1.1.9 Amplification Refractory Mutation System (ARMS) PCR

ARMS PCR is a technique that allows a specific allele to be PCR amplified (Newton, 1989; Wu, 1989; Sommer, 1989; Okayama, 1989). It is also referred to as allele specific amplification (ASA). The technique makes use of the fact that DNA polymerase enzymes such as Taq polymerase require the ultimate 3' end base of the primer to be complementary to the template sequence for amplification to occur. If the 3' end base matches with the base on the target DNA, then amplification takes place. However, if a mismatch occurs, the 3' end will not be fully hybridised and Taq polymerase will be unable to initiate amplification (Fig 2.2). Thus, by designing primers complementary to the wildtype and mutant sequences and using them in two separate PCRs, both homozygous and heterozygous samples can be genotyped. For ARMS to work it is important that a DNA polymerase without proof-reading capabilities is used, as a proof-reading enzyme could correct the mismatch and discrimination between alleles would be lost (McPherson, 2000). The amplicons are separated on agarose gels, and presence or absence of a particular band implies the genotype of the sample. Extensive optimisation of the amplification conditions is generally essential for proper ARMS analysis (Kwok, 1990; Sommer, 1992).

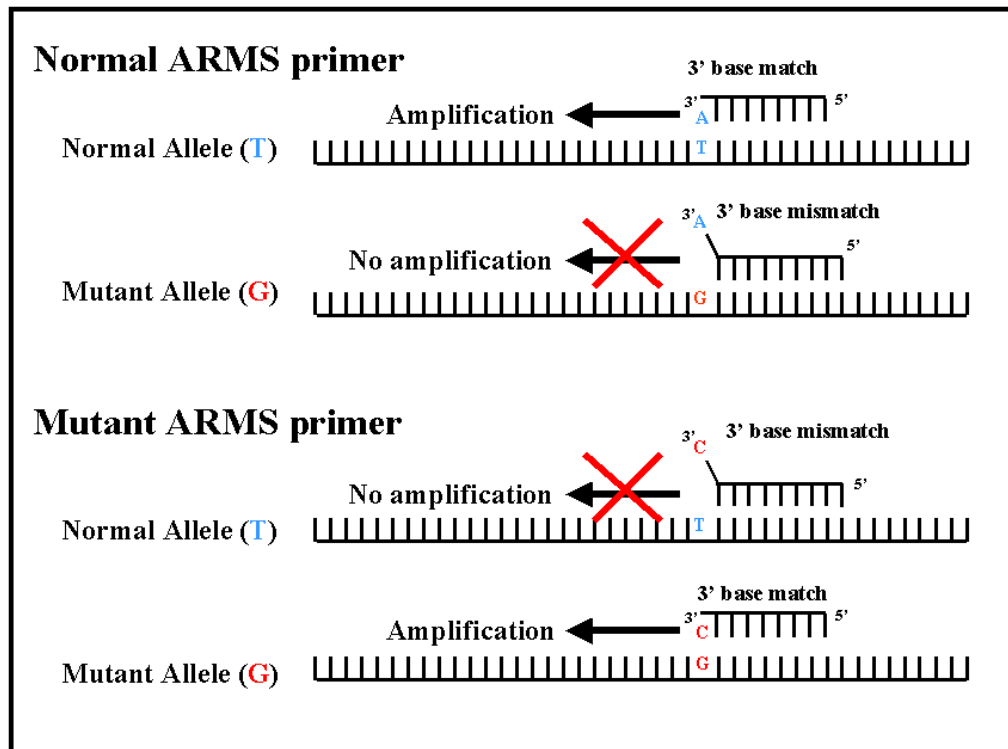


Fig 2.2 **Amplification refractory mutation system (ARMS) PCR.** The normal ARMS primer (3' A) will successfully bind to the normal allele and allow the initiation of PCR amplification. The normal ARMS primer will not allow amplification of the mutant allele due to the 3' mismatch. The mutant ARMS primer (3' C) will only match with the mutant allele and will not amplify the normal allele.

2.1.1.10 Aim of this chapter

The aim of this chapter is to examine the use of Real-time PCR for mutation detection in cystic fibrosis. Current methods for carrying out mutation detection do not make full use of melting curve analysis, meaning that at most two mutations can be looked at in a single PCR (1 per colour channel). The work outlined here seeks to make an improvement on this by combining ARMS and Real-time PCR for use in the diagnosis of cystic fibrosis with particular emphasis put on mutations pertinent to the Irish population.

2.1.2 MATERIALS AND METHODS

2.1.2.1 Patient DNA samples

Both control DNA samples for protocol optimisation and 21 test DNA samples used in the blinded study were obtained from Dr David Barton at the National Centre for Medical Genetics, Our Lady's Hospital for Sick Children, Crumlin, Dublin 12.

2.1.2.2 DNA isolation

Where DNA needed to be extracted, EDTA blood was used with the following protocol: firstly red blood cells (RBCs) were lysed by incubating 3 ml of whole blood in 9 ml of RBC lysis solution (155 mM Ammonium chloride, 10 mM Potassium hydrogen carbonate, 1 mM EDTA) at room temperature for 10 mins. Followed by a centrifugation step at 3000 rpm for 10 mins. After decanting the supernatant the resulting white blood cell (WBC) pellet was suspended in 3 ml of WBC lysis solution (25 mM EDTA, 2% SDS). Then 1 ml of protein precipitation solution (10 M ammonium acetate) was added, followed by a 10 second vortex. The resulting solution was centrifuged at 3000 rpm for 10 mins. The supernatant was then subjected to an isopropanol (0.5 ml) precipitation step, followed by centrifugation at 3000 rpm for 5 mins the resulting DNA pellet was washed in 1ml of ice cold 70% ethanol and then resuspended in Tris-EDTA at pH 8.0.

2.1.2.3 Primers

The sizing primers for detection of the delF508 mutation are CF10-B (GTTTTCTGGAT TATGCCTGGGCAC) and CF10-D (GTTGGCATGCTTTGATGACGCTTC).

The ARMS PCR primers used in this study were previously published primer sets (Ferrie, 1992), the name and sequence of each primer and the concentration used in the final reaction is outlined in Table 2.1. All primers were synthesised by Proligo, France.

2.1.2.4 Preparation of 10% Acrylamide gel for analysis of the sizing PCR products

See appendix 1

2.1.2.5 Real-time PCR detection of the delF508 mutation

Real-time PCR detection of the delF508 mutation was performed using previously published primer and hybridisation probes (Gundry, 2001). Primers used were CF-245F (GGAGGCAAGTGAATCCTGAG) and CF-500R (CCTCTTCTAGTTGGCATGCT). The hybridisation probe sequences were as follows delF508 ANCHOR (TTTTCTGGATTATGCCTGGCACCTTAA-F) and delF508 DETECTOR (705-GAAAATATCATCTTTGGTGTTC-P). Primers and hybridisation probes were synthesised by Proligo, France. Real-time PCR was performed on a LightCycler instrument (Roche Diagnostics). The total reaction volume was 10µL, containing: 1µL of 10X LightCycler DNA Master Hybridisation enzyme mix (Roche Diagnostics), 4 mM

MgCl₂, 0.1µM hybridisation probes and 0.5 µM primers. PCR conditions were 95°C for 6 mins, followed by 40 cycles at 95°C for 0 secs, 60°C for 10 secs and 72°C for 10 secs. Melting curve analysis was performed directly post PCR and the condition were 95°C for 0 secs, 40°C for 10 secs followed by heating back to 70°C while continuously monitoring the fluorescence in each capillary.

2.1.2.6 Hybridisation probe design for Real-time ARMS PCR

Using sequences downloaded from the National Centre of Biotechnology Information (NCBI) website hybridisation probes were design as per the usual guidelines for primer design. The sequences used were CFTR exon 4 (Genbank accession no.M55109.1), CFTR exon 10 (Genbank accession no.M55115.1) and CFTR exon 11 (Genbank accession no. M55116.1). Once suitable locations were identified for the probe sets within these sequences the predicted melt-temperatures of the detector probes were calculated using MeltCalc software (www.meltcalc.com). The probes were modified to give the most suitable T_m to give the best melt-curve profile. The name, sequence, concentration used in the final reaction and T_m of the probes as well as the mutation they can be used to detect is outline in Table 2.2. All probes were synthesised by Proligo, France.

2.1.2.7 Multiplex set-up

Two multiplex PCR reactions were optimised using previously published ARMS primers (Ferrie, 1992). The first reaction detects the G551D, R117H and F508del mutations. The F508del ARMS primers (CF-DFjN and CF-DFwM) are specific for this mutation and are not influenced by the benign I506V and F508C. As the CF-DFwM primer is complementary to the sequence distal to the delF508, the presence of the delI507 mutation is not recognised (Ferrie, 1992). The second reaction detects the 621+1 G→T and G542X mutations. A PCR product should be formed in both the A and B ARMS reactions regardless of the sample genotype.

2.1.2.8 Real-time PCR

Real-time ARMS PCR was carried out on a LightCycler (Roche Diagnostics). The total reaction volume was 10µL, containing: 1µL of 10X LightCycler DNA Master Hybridisation enzyme mix (Roche Diagnostics), 3 mM MgCl₂, 0.1µM hybridisation probes and ARMS primers concentrations as outlined in Table 2.1. ARMS PCR and subsequent melting curve analysis was carried out as follows: Initial denaturation was 7.5 min at 95°C followed by 40 cycles of 95°C for 1s, 64°C for 20s and 72°C for 20s. A touchdown PCR was carried out with the annealing temperature starting at 70°C and dropping to 64°C at 1°C/cycle. Fluorescence was measured at the end of the annealing step. The PCR stage was followed by a melting curve analysis, 95°C for 10s, 40°C for 30s and heating back up to 70°C at 0.1°C/sec with continuous monitoring of fluorescence. The touchdown PCR

conditions used allowed specific amplification of wildtype or mutated sequences as detected by standard agarose electrophoresis and melting curve analysis.

2.1.2.9 Agarose Gel electrophoresis

Agarose gel electrophoresis was carried on samples tested using the Real-time ARMS PCR to confirm the presence of the bands. In order to retrieve the PCR mix back from the LightCycler capillary the cap was removed and inverted into a 0.5 ml eppendorf and centrifuged at 3000 rpm for 5-10 secs. ARMS PCR products were then separated on a 2.5% agarose gel run at 100 V for 1 hour.

ARMS primer name and seq (5' to 3')*	Multiplex rxn	Primer conc
delF508		
DF-C: ACTTCACTTCTAATGATGATTATGGGAGA	1A/B	100 ng
DF-j-N: TATCTATATTCATCATAGGAAACACCACA	1A	100 ng
DF-w-M: TATCTATATTCATCATAGGAAACACCATT	1B	100 ng
G551D		
11-C: TAAAATCAGCAATGTTGTTTTGACCT	1A/B	150 ng
GD-j-N: GCTAAAGAAATTCTTGCTCGTTGCC	1B	150 ng
GD-j-M: AGCTAAAGAAATTCTTGCTCGTTGCT	1A	150 ng
R117H		
RH-C: CACATATGGTATGACCCTCTACATAAACTC	1A/B	120 ng
RH-d-N: CCTCTGCCTAGATAAAATCGCGATAGAAC	1A	120 ng
RH-d-M: CCTCTGCCTAGATAAAATCGCGATAGAAT	1B	120 ng
621+1 G→T		
621-C: TCACATATGGTATGACCCTCTATATAAACT	2A/B	200 ng
621-j-N: TGCCATGGGGCCTGTGCAAGGAAGTATTCC	2A	200 ng
621-j-M: TGCCATGGGGCCTGTGCAAGGAAGTATTCC	2B	200 ng
G542X		
11-C: TAAAATCAGCAATGTTGTTTTGACCT	2A/B	40 ng
GX-e-N: ACTCAGTGTGATTCCACCTTCTAC	2B	40 ng
GX-e-M: CACTCAGTGTGATTCCACCTTCTCA	2A	40 ng

Table 2.01 **Sequence and concentrations of CF ARMS primers.** Primer with a “C” in their name indicates that it is a common primer and is present in both the wildtype and mutant reactions. The names of the wildtype specific primers end in a “N” and mutant specific primer names end in a “M”. * ARMS primer sequence taken from Ferrie, 1992.

Real-time PCR probe seq (5' to 3')	Conc	Tm
Detection of wildtype and mutant R117H and 621+1 G>T		
CF4ARMS-A: CCTTTTGTAGGAAGTCACCAAAGCAGTAC-f	0.1µM	
CF4ARMS-D: 640-GCCTCTCTTACTGGGAAGAATCA-p	0.1µM	62°C
Detection of wildtype and mutant delF508		
CF10ARMS-A: GCACAGTGGAAGAATTTTCATTCTGTTCTCAG-f	0.1µM	
CF10ARMS-D: 640-TTCCTTGGATTATGCCT-p	0.1µM	51°C
Detection of wildtype and mutant G542X and G551D		
CF11ARMSA: TATGATTACATTAGAAGGAAGATGTGCCTTT-f	0.1µM	
CF11ARMS-D: 705-AATTCAGATTGAGCATACT-p	0.1µM	55°C

Table 2.02 **Sequence of Real-time PCR probes sets used to detect ARMS products in a melt-curve analysis.** Anchor probe (A), Detector probe (D), (Fluorescein (f), Phosphate (p), LC Red 640 dye (640, detected in the F2 channel), LC Red 705 dye (705, detected in the F3 channel).

2.1.3 RESULTS

2.1.3.1 Comparison of Real-time and traditional PCR for the detection of delF508 mutation

In the first part of this study, we compared the detection of the delF508 mutation in CF by Real-time PCR and two other traditional PCR based methods. The two traditional approaches were a sizing PCR and ARMS PCR. The sizing PCR is based on the fact the delF508 mutation is the result of a 3 bp deletion. Primers amplify a region, which includes the possible mutation site, the PCR products are then analysed using a 10% acrylamide gel. In a wildtype sample the resultant PCR product will be 97 base pairs (bp) in length, an individual who is homozygous mutant will have a PCR amplicon of 94 bp and a heterozygote will display a band at the two different product sizes (Fig 2.3, Panel A). The ARMS PCR analysis for the delF508 was performed using the ARMS primers detailed in Table 2.1. In ARMS PCR each sample is tested in two separate PCRs, one specific for the wildtype allele and the other for the mutant allele. An internal control set of primers was also included in both PCR to ensure that a PCR product is formed in each reaction as a quality control step. The PCR products were then separated on a 2% agarose gel and diagnosis can be made on the resulting band patterns observed (Fig 2.3, Panel B). These two techniques were compared to a set of published primers and hybridisation probes, which were used to perform Real-time melting curve analysis for the detection of the delF508 mutation. During melting curve analysis, a temperature will be reached which causes FRET activity to decrease as the detector probe is disassociated from its complementary sequence adjacent to the anchor probe. The first derivative of the melting

curve is determined by the LightCycler analysis software (Roche) that allows the drop in fluorescence to be seen as a peak. If there is no mutation present, the probe requires more energy (higher temperature) to destabilise it, in this case resulting in a melt curve peak at 61°C (Fig 2.3, Panel C, blue line). If the mutation is present then the detector probe will become destabilised at a lower temperature, in this case 51°C (Fig 2.3, Panel C, red line). A heterozygote will show a peak at both temperatures (Fig 2.3, Panel C, green line). When all three protocols were successfully optimised in our hands, we performed a small, blinded study using a mix of samples that were wildtype, heterozygous and homozygous mutant for the delF508 mutation using each of the three methods. All samples were correctly identified using the three different PCR based methods. However, the time required to perform the Real-time PCR based method was considerably shorter (35 mins) than the other two techniques (ARMS, 5 hrs; sizing PCR, 6 hrs).

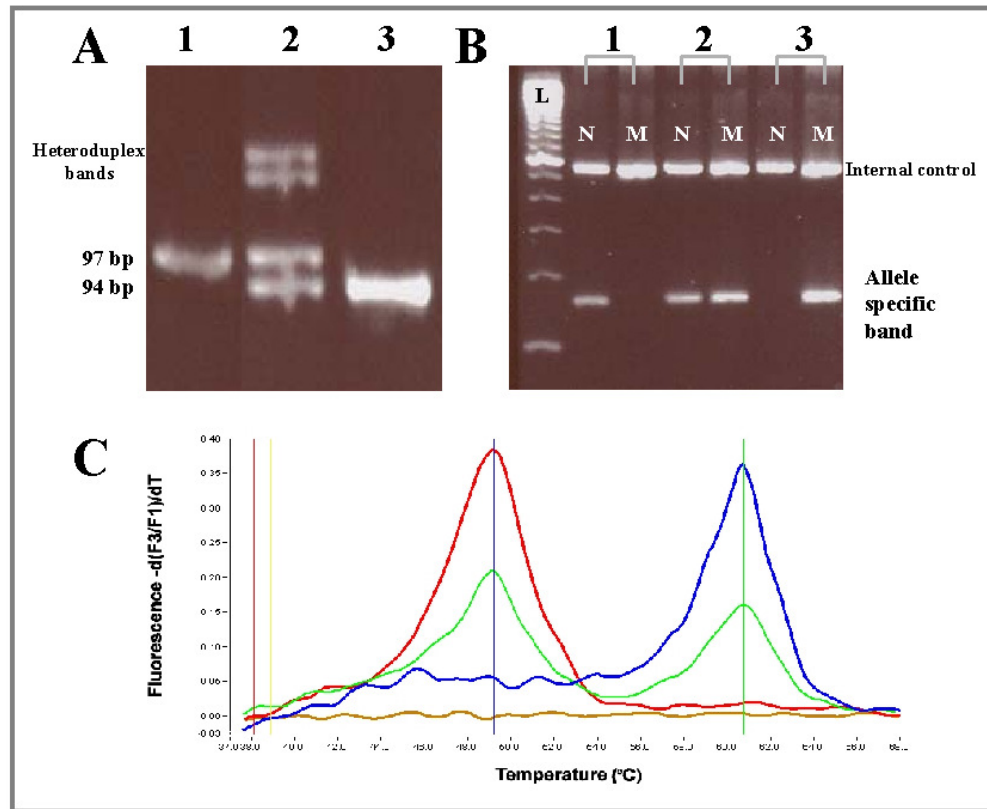


Fig 2.3 **Three methods for detection of the delF508 mutation.** Panel A: Standard sizing PCR; Lane 1 197 bp band (normal), Lane 2 97 and 94 bp band (heterozygote) Lane 3 94 bp band (homozygous mutant). Panel B: ARMS PCR; 100 bp sizing ladder (L), normal ARMS (N), mutant ARMS (M). An internal control is present in each reaction to ensure that the PCR is working. Sample 1 Wildtype, Sample 2 heterozygote, Sample 3 homozygous mutant. Panel C: Real-time PCR melting curve analysis; Blue curve (normal), Green curve (heterozygote), Red curve (homozygous mutant).

2.1.3.2 Real-time multiplex PCR for detection of delF508 and R117H mutations

After we had shown that Real-time PCR was a suitable method for mutation detection, we set about designing a multiplex PCR to detect more than one mutation at a time. This would have the advantage of saving time and cutting cost of performing the test. The LightCycler has two colour channels that can be used to detect fluorescence from two different reporter dyes (LCRed640, F2 channel; LCRed705, F3 channel). We aimed to develop a multiplex Real-time PCR that would allow two mutations to be detected per colour channel ie four mutations in total. We firstly designed a set of primers and hybridisation probes that would be detected in the same channel as the delF508 hybridisation probes from the previous experiment. However, despite careful design of the R117H hybridisation probes, under melting curve analysis the R117H and delF508 wildtype peaks merged with each other (Fig 2.4) not allowing the genotype to be clearly identified. Therefore, we realised that if we were to detect more than one mutation per colour channel on the LightCycler, we would need to take a novel approach to designing hybridisation probes for mutation detection on the LightCycler instrument.

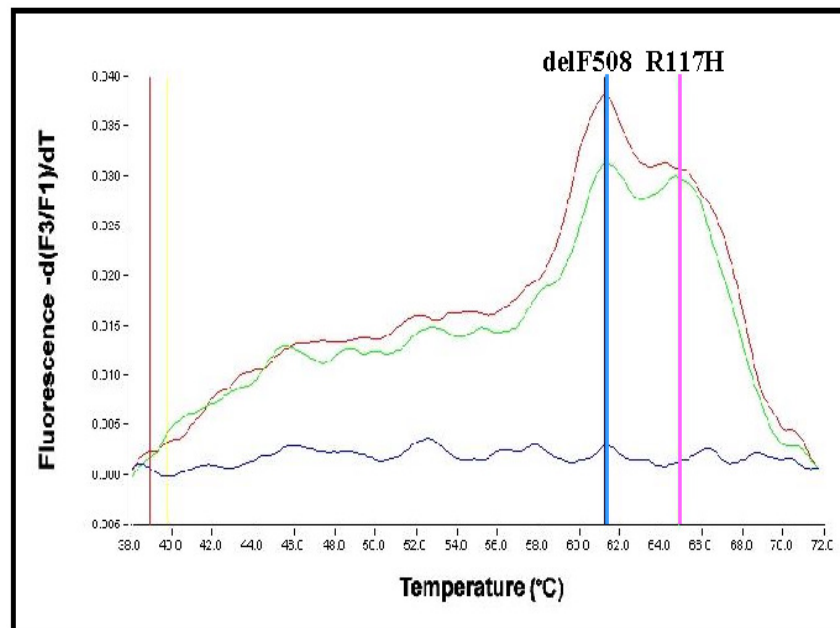


Fig 2.4 Multiplex melting curve analysis for delF508 and R117H mutations. Green and red melting curves are of wildtype samples for both mutations. The delF508 peak is at 61°C and the R117H peak is at 65°C, however peaks are not clearly distinguishable from each other.

2.1.3.3 Real-time ARMS PCR

Traditionally during the design of hybridisation probes for mutation detection, the detector probe is positioned over the site of the mutation (Fig 2.5, Panel A). Preferably, with the possible mutation site as close to the centre of the probe to cause the biggest destabilisation effect when a mutant allele is present. However, we showed in the previous experiment that even with careful design of the detector probe, it is difficult to be sure of the T_m at which it will disassociate during melting curve analysis. Hence we took an approach that allowed us to design hybridisation probes that would melt at the temperature which we desired, and which could be positioned anywhere along the length to the amplicon. For this we combined traditional ARMS PCR with Real-time PCR. The ARMS primers will detect the genotype of the sample and a set of hybridisation probes that will have a predefined T_m will be used to detect the presence or absence of a PCR product. With this approach the hybridisation probes can be placed anywhere along the length of the amplicon (Fig 2.5, Panel B). One of the advantages of this is it allows us to design better working hybridisation probes. The ARMS primers used were previously published primer sets (Ferrie, 1992) and are outlined in Table 2.1 (Methods). Using a combination of the LightCycler hybridisation probe design software version 1.1 (Roche) and the melt-calc software package (Schütz, 1999), hybridisation probes were designed to detect the PCR amplicons produced by the ARMS primers (Table 2.2, Methods)

The CF4ARMS-A/D probes detect both the R117H and 621+1 G→T mutations and produce a peak at 62°C during a melting curve analysis. CF10ARMS-A/D probes detect the delF508 mutation and melt at 51°C. CF11ARMS-A/D produces a T_m peak at 55°C and detects both the G551D and G542X mutations.

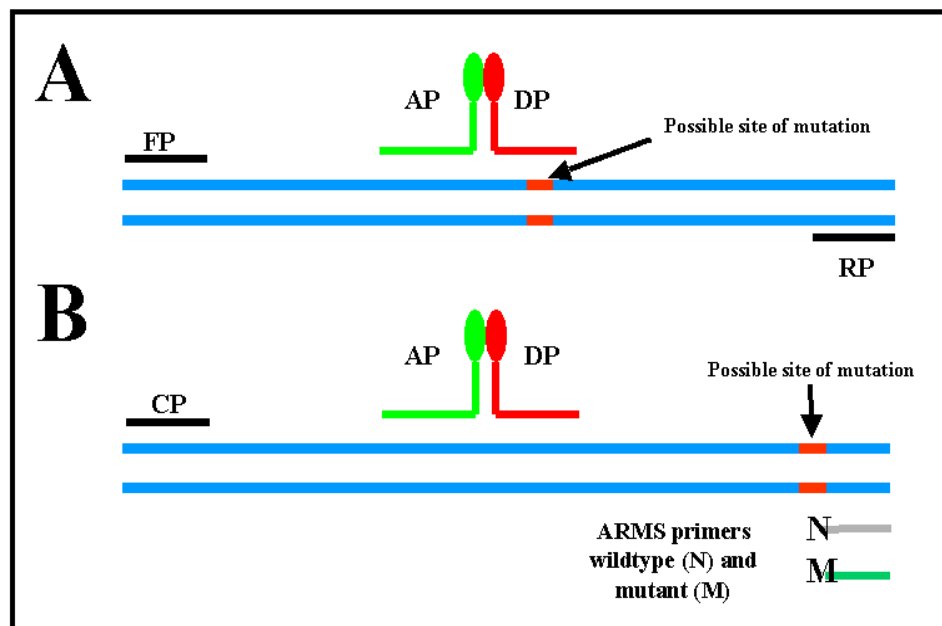


Fig 2.5 **Orientation of hybridisation probes for Real-time ARMS PCR.** Panel A: shows the traditional position that Hybridisation would be located with respect to the possible site of the mutation. Panel B: shows the position of the hybridisation probes in our system with respect to the mutation site. AP, Anchor probe (AP), Detector probe (DP), Forward primer (FP), Reverse primer (RP), Common primer (CP), Normal ARMS primer (N), Mutant ARMS primer (M).

The optimisation of the ARMS Real-time PCR reactions was performed in the usual manner, magnesium ions were titrated, primer concentrations varied and adjustment of the annealing temperature were all carried out until a reproducible assay was developed. Following the optimisation procedure, samples with a variety of mutation combinations were tested with the assay, some examples of the resulting melting curve profiles are outlined in Fig 2.06, Fig 2.07 and Fig 2.08. As can be seen peaks are now clearly distinguishable from each other and the genotype of each sample can be clearly identified. This protocol was very rapid taking approximately 45 mins.

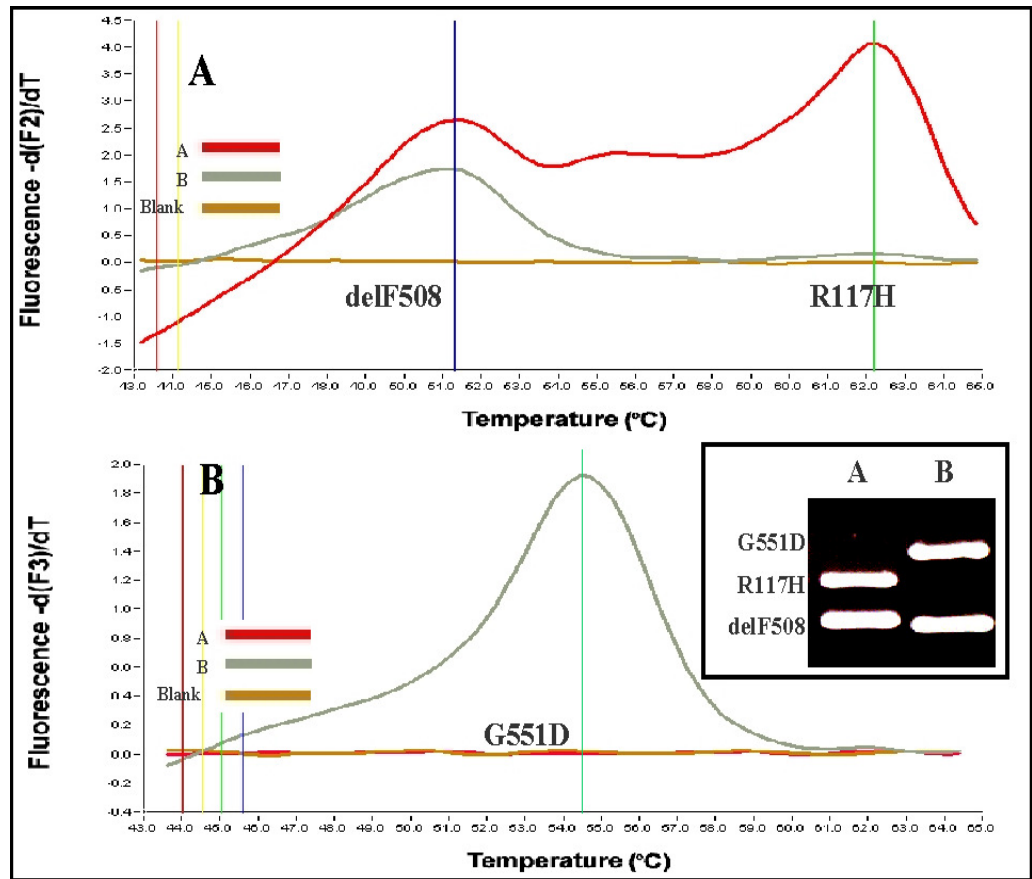


Fig 2.06 **Melting curve profiles of a delF508 heterozygote.** The A reaction (red line) detects wildtype delF508 and R117H (F2 channel) and mutant G551D (F3 channel), the B reaction (grey line) detects mutant delF508 and R117H and wildtype G551D. As can be seen from the upper graph a product is detected in both the wildtype and mutant reactions for the delF508 indicating the carrier status of this sample. The agarose gel (inset) also shows the presence of two bands for delF508 in this sample.

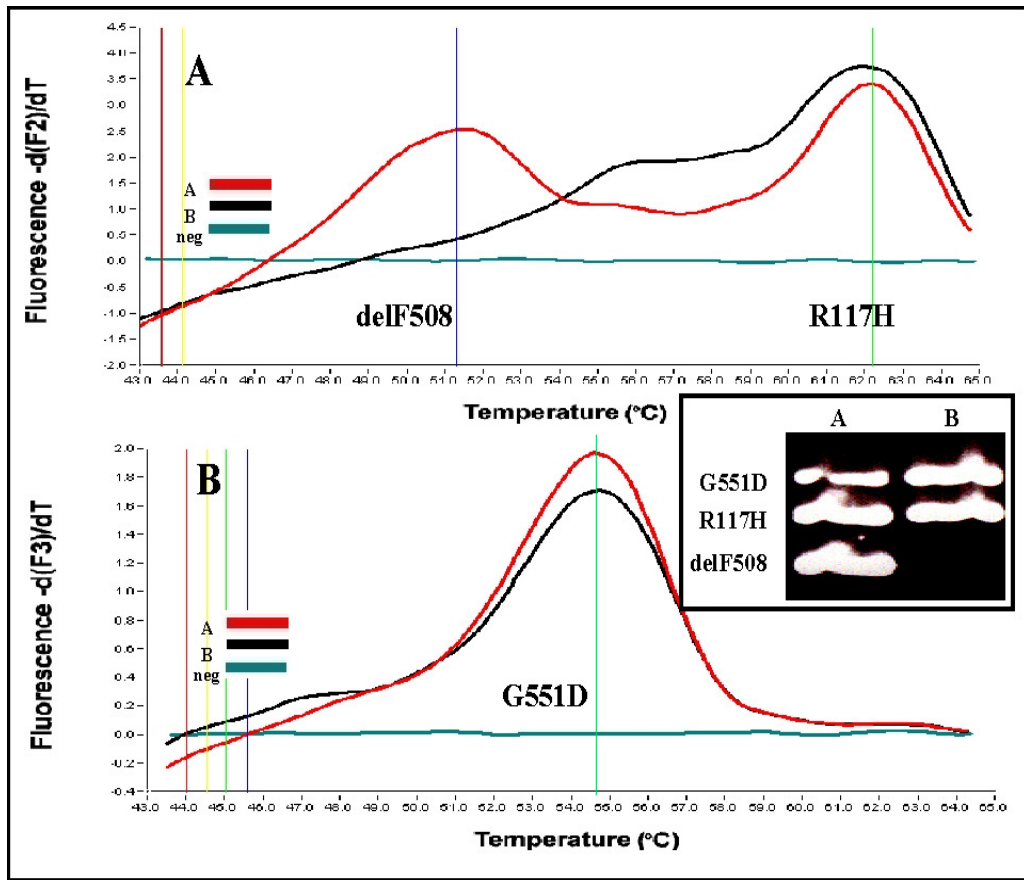


Fig 2.07 **Melting curve profiles of a R117H/G551D compound heterozygote.** The A reaction (red line) detects wildtype delF508 and R117H (F2 channel) and mutant G551D (F3 channel), the B reaction (black line) detects mutant delF508 and R117H and wildtype G551D. As can be seen from the upper graph (F2) a product is detected in both the wildtype and mutant reactions for the R117H. The lower graph (F3) also shows 2 peaks for G551D indicating that the sample is a compound heterozygote and would be affected with CF. The agarose gel (inset) confirms the genotype of the sample.

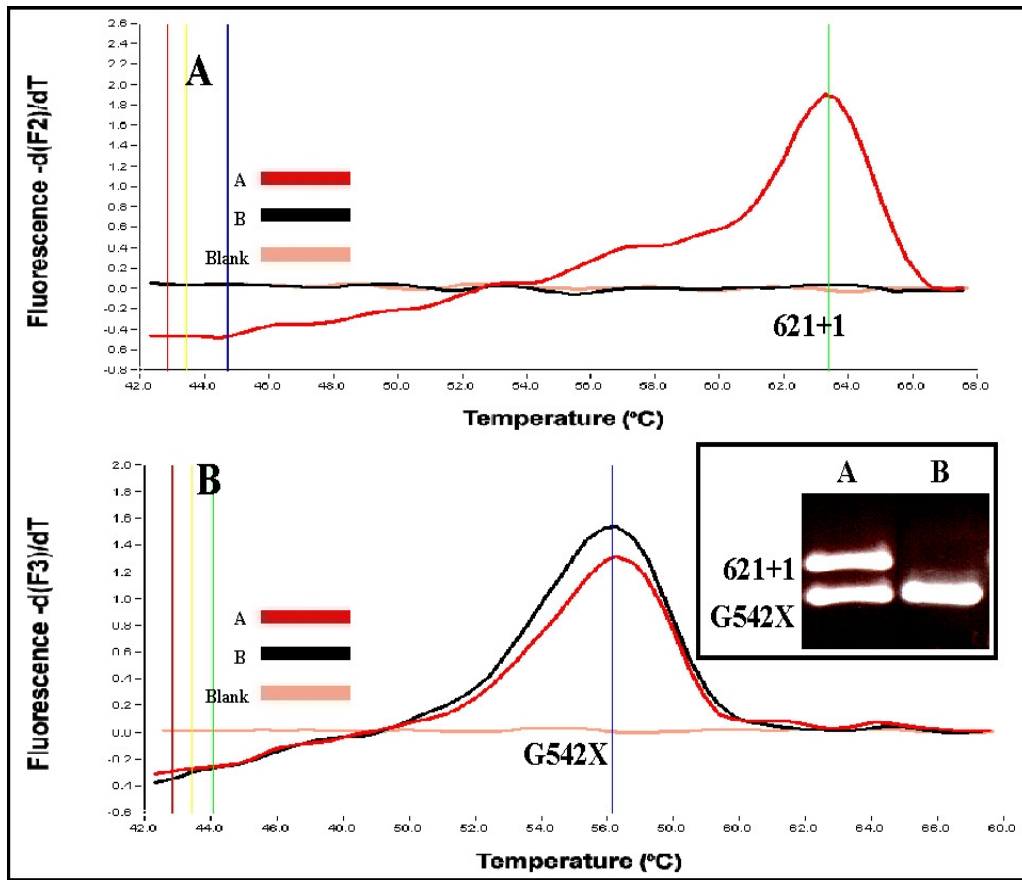


Fig 2.08 **Melting curve profiles of a G542X heterozygote.** The A reaction (red line) detects wildtype 621+1 G>T (F2 channel) and mutant G542X (F3 channel), the B reaction (black line) detects mutant 621+1 G>T and wildtype G542X. As can be seen from the lower graph (F3) a product is detected in both the wildtype and mutant reactions for the G542X indicating the carrier status of this sample. The agarose gel (inset) confirms the presence of two bands for G542X in this sample.

2.1.3.4 Blinded Trial

Using the optimised protocol as outlined in the methods, a panel of patient samples containing combinations of the five mutations (delF508, G551D, R117H, G542X and 621+1G→T) were tested blind. All of the patient samples provided were correctly identified and correlated with previous genotyping carried out in the National Centre for Medical Genetics, Our Lady's Hospital for Sick Children, Crumlin, Dublin 12. The results are presented in Table 2.3.

Sample No	delF508	R117H	G551D	621+1	G542X	Genotype
Sample 1	W	C	C	W	W	R117H/G551D
Sample 2	C	W	W	C	W	delF508/621+1
Sample 3	C	W	C	W	W	delF508/G551D
Sample 4	C	W	C	W	W	delF508/G551D
Sample 5	C	W	W	W	W	delF508/N
Sample 6	C	W	W	W	W	delF508/N
Sample 7	C	W	W	C	W	delF508/621+1
Sample 8	C	W	W	W	W	delF508/N
Sample 9	W	W	C	W	W	G551D/N
Sample 10	W	W	W	W	W	N/N
Sample 11	M	W	W	W	W	delF508/delF508
Sample 12	W	W	W	W	W	N/N
Sample 13	W	W	W	W	W	N/N
Sample 14	C	W	W	W	W	delF508/N
Sample 15	C	W	W	W	W	delF508/N
Sample 16	W	M	W	W	W	R117H/R117H
Sample 17	M	W	W	W	W	delF508/delF508
Sample 18	W	W	W	W	W	N/N
Sample 19	C	W	W	W	W	delF508/N
Sample 20	W	W	W	C	W	621+1/N
Sample 21	C	W	C	W	W	delF508/G551D

Table 2.03 **Blinded trial results using optimised Real-time ARMS multiplex PCR.**

Wildtype, W; Heterozygote, C; homozygous mutant, M.

2.1.4 DISCUSSION

Cystic fibrosis is the most common genetic disease in people of a European descent (Mateu, 2002). The disease is monogenic disorder caused by insufficiencies in the CFTR protein. In the last 10-20 years, a better understanding of the mechanisms behind the development of CF has led to better clinical management of the disease and ultimately improved the life span of patients. However, the first step in treatment of a disease is a definitive diagnosis.

Real-time PCR has provided a dynamic platform for the molecular diagnosis of hereditary diseases. Many of the detection chemistries used for Real-time PCR and melting curve analysis have already been applied to the diagnosis of CF, such as Sybr Green 1, (Kleinle, 2002; Wittwer, 2003) scorpion probe (Thelwell, 2000) and dual hybridisation probe (Burggraf, 2002; Gundry, 1999) based detection systems. Each detection system has its advantages and disadvantages. Sybr Green 1 is a non-specific dye and by this very fact, it is cheap and quick to develop a real-time PCR assay. However, it has the downfall of detecting non-specific products making it difficult to perform multiplex PCR. Scorpion probes have the benefit of incorporating a forward primer and detector probe in one oligonucleotide, but are expensive and complex to design. Hybridisation probes offer the highest specificity of all the detection chemistries (Wittwer, 1997). Nevertheless, due to their dual probe system, they are required to be longer than the other probe types and the design of an efficient probe pair can be limited by the nature of the sequence around the site of a mutation.

The work in this chapter aimed to improve multiplexing capabilities of Real-time PCR in its use for mutation detection. In the first part of the study, we demonstrated that Real-time PCR was a feasible approach to mutation detection in CF by comparing it to two other traditional methods for detecting the delF508 mutation (Fig 2.3). The Real-time PCR technique proved to be as accurate in genotyping the patient samples as the two traditional methods (sizing PCR and ARMS PCR). Melting curve peaks for wildtype and mutant alleles were clearly distinguishable from each other (Fig 2.3, Panel C) and the test was very rapid (~ 35 mins).

The next stage was to start multiplexing the most common mutations in Ireland (Scotet, 2003) into one Real-time PCR assay. To begin with, a set of primers and probes were designed for the R117H mutation, and would be detected in the same colour channel as the delF508 primers and probes. However, it was soon realised that this approach would prove to be very difficult. When the hybridisation probes were designed for the R117H mutation we tried to generate a detector probe that would have a T_m above that of the delF508 detector probe ie greater than 61°C (Fig 2.3C). This was to ensure that melting curve analysis peaks would be distinguishable from each other therefore making genotyping of the sample a straightforward process. Despite trying to keep the peaks separated from one another, during melting curve analysis the wildtype peaks for both delF508 and R117H merged with each other, not allowing a clear genotype to be identified (Fig 2.4). The problem arose from the use of a traditional approach to hybridisation probe design, where the detector probe is positioned over the site of the mutation (Bernard, 1998; Bernard, 2001). This places limits on designing effective hybridisation probe pairs. The DNA sequence around the mutation site may not always be the best suited for the task. The DNA

sequence may have a very high G:C content, which would result in a very stable detector probe even when a mutation is present. This would cause the wildtype peak and mutant peak to be poorly differentiated from each other. Another problem with this approach is that it is very difficult to determine how much a particular mutation will destabilise the detector probe during a melting curve analysis. In the case of the delF508 mutation, 3 bp are deleted which has a large destabilisation effect on the detector probe, hence the 10°C difference between the T_m of the wildtype peak and mutant peak (Fig 2.3). However, with single bp substitutions as in the case of the R117H mutation the destabilisation effect will be much smaller. Therefore, it was decided to take a novel approach to performing multiplex mutation detection on the LightCycler instrument. We would need a technique that would allow us more freedom to design effective hybridisation probes by not being restricted to placing the hybridisation probe over the mutation site.

To this end, Amplification Refractory Mutation System (ARMS) PCR primers were used to selectively amplify the wildtype or mutant alleles in separate reactions. Subsequent detection of PCR products is carried out using a common set of hybridisation probes. The advantage of this system is it increases the flexibility of the hybridisation probe design allowing probes with precise T_m s to be generated. In this way, melting curve peaks can be at a predetermined T_m for a particular PCR product, which allows for easier multiplexing of Real-time PCR. Similar ARMS based techniques have been developed for the ABI prism 7700 sequence detector from PE Applied Biosystems using TaqMan® probes (Glaab, 1999). These protocols depend on the detection of an amplification curve and are limited to the detection of one mutation per colour channel. Our protocol detects melting curve peaks, post amplification and allows multiple mutations to be detected per colour channel.

Optimisation of the annealing temperature was particularly crucial, as at the incorrect annealing temperature a certain amount of mispriming occurred, the mutant primers were producing a product in a wildtype sample. This problem occurred mainly due to the sensitivity of the LightCycler instrument, often when a misprimed peak occurred the band was very faint on the corresponding agarose gel. The problem of the mispriming was solved by careful optimisation of the annealing conditions, primer concentrations and the addition of a “touch-down” segment to the start of the amplification stage. The “touch-down” PCR provides more stringent annealing conditions in the initial cycles of the amplification process and in doing so eliminated the mispriming event.

The main advantage of the LightCycler system is its speed; the optimised protocol takes approximately 45 minutes to complete, which is a significant improvement over standard ARMS followed by gel electrophoresis, which can take approximately 5 hours to perform. Genotyping on the LightCycler system, using standard multiplex hybridisation probes that overlie the mutation site can be technically challenging and have some limitations. Even with careful design of the hybridisation probes, wildtype and mutant alleles may not necessarily be discriminated from each other (Bernard, 1998). Our system allows hybridisation probes to bind to any region of the amplicon therefore providing scope for better probe design. The number of mutations that can be detected in a single reaction is dependent on the number of melting peaks that can be clearly differentiated from each other (Von Ahsen, 1999). This usually leads to development of multiplex reactions where a single mutation is detected per colour channel (Gundry, 2001, Bestmann, 2002). Here we have demonstrated a method, which makes it quite possible to detect more than one mutation in a single channel. Using the nearest neighbour formula in the MeltCalc

software package (Schütz, 1999), detector probes can be carefully designed that produce a peak within 1-2°C of the predicted T_m . This allows T_m peaks, which indicate the presence or absence of a PCR product, to be strategically placed within the normal melting curve range of 45-70°C for hybridisation probes. Over this melting curve range, we feel it should be possible to clearly distinguish three peaks in a single channel. This potentially makes it possible to multiplex six mutations into two capillaries when using both fluorescent channels. This enhances the capabilities of the LightCycler for mutation detection; similar strategies could also be employed for other Real-time systems.

To conclude, the results presented here demonstrate the ability to carry out multiplex mutation detection using a combination of ARMS PCR and Real-time melting curve analysis. This method provides an improvement over current techniques for performing multiplex mutation detection on the LightCycler instrument. Any laboratory currently using ARMS PCR in a diagnostic setting can quite easily convert their standard ARMS PCR to a Real-time ARMS PCR. This will have a significant advantage in time saving, prevent any possible of cross contamination and reduce the handling of the potential carcinogen ethidium bromide.

Chapter 2.2

QUANTIFICATION OF THE DOSAGE SENSITIVE PMP22 GENE IN HEREDITARY PERIPHERAL NEUROPATHIES

2.2.1 INTRODUCTION

2.2.1.1 Charcot-Marie-Tooth (CMT) disease

In 1886 Drs Charcot and Marie in France and Dr Tooth in England separately described patients suffering from an inherited form of peroneal muscular atrophy (Charcot and Marie, 1886; Tooth, 1886). Charcot-Marie-Tooth (CMT) disease is now used to describe a clinically and genetically heterogeneous group of disorders that can be characterised by a chronic motor and sensory polyneuropathy. CMT is the most common inherited disease of the peripheral nervous system (PNS) with a prevalence rate of 1 in 2500 (Boerkoel, 2002).

2.2.1.2 CMT classification

CMT can be subdivided into five major groups: CMT1, CMT2, CMT3 (usually referred to as Dejerine-Sottas syndrome, DSS), CMT4 and CMTX and there are several subtypes within each group (Vance, 2000). Groupings are based on mode of inheritance (autosomal dominant (CMT1 and CMT2), autosomal recessive (CMT4), X-linked (CMTX)) and the chromosomal locus involved. The autosomal dominant forms are divided based on nerve conduction velocities (NCVs). Normal NCVs are typically >40-45 meters/second (m/s), and patients with CMT1 have significantly reduced NCVs usually between 10-30 m/s (Hoogendijk, 1994; Birouk, 1997; Thomas, 1997; Krawjewski, 2000). In CMT2 NCVs are usually within the normal range though they can fall within the low normal or mildly abnormal range (35-50 m/s) (Dyck, 1993; Saito, 1997). CMT1 is the most common type

(Kamholz, 2000) and has been further divided into 4 subtypes (Table 2.04). CMT1 subtypes are clinically indistinguishable from each other and identification is based on the chromosomal locus involved (Bird, 2004).

CMT1 subtype	Genetic mechanism	Locus	% of cases
CMT 1A	Duplication of PMP22 Point mutations in PMP22	17p11	70-80%
CMT 1B	Point mutations in MPZ (P0)	1q22-q23	5-15%
CMT 1C	?	16q*	10-15%
CMT 1D	Point mutation in EGR2	10q21	<5%

Table 2.04 **Breakdown of CMT 1 subtypes.** PMP22, peripheral myelin protein 22; MPZ, myelin protein zero (P0); EGR2, early growth response 2. * No gene has been identified for CMT1C however using linkage analysis it has been mapped to Chr 16q (Street, 2002).

2.2.1.3 Clinical features of CMT1

The clinical symptoms of CMT1 usually appear in patients during the first or second decades of life (Carter, 1995; Garcia, 1999). The disease is characterised by slowly progressive atrophy of the distal muscles, predominantly those innervated by the peroneal nerve (Dyck, 1992; Lupski, 1991). Patients usually present with muscle weakness in the legs and feet, 20-30% of these experience pain particularly in the feet (Carter, 1998). *Pes cavus* (highly arched foot) is not seen during the early stages of disease but generally develops as the patient gets older, and results from imbalances between the extrinsic and intrinsic muscles of the feet (Garcia, 1999). Other symptoms that develop with age are claw-hands, stork-leg appearance (due to atrophy of the leg muscles), enlarged nerves (the greater auricular nerve may be visible at the surface of the neck) and 40% of patients develop hand tremor by their mid-30s (Caradoso, 1993). Histological findings in CMT1 are segmental demyelination and Schwann cell proliferation forming concentric arrays, often referred to as “onion bulb” formations, around demyelinated or partially remyelinating axons (Dyck, 1993; Ionasescu, 1995).

2.2.1.4 CMT type 1A

CMT1A accounts for 70-80% of CMT1 patients and has an estimated prevalence of 1:10000 (Nelis, 1996). In 1989, CMT1A was linked to the short arm of chromosome 17 (Raeymaekers, 1989; Vance, 1989). During 1991, two independent reports described a large segmental duplication (~ 1.5 Mb of DNA) to associate with CMT1A patients within

band 17p11.2 (Lupski, 1991; Raeymaekers, 1991). This duplicated region was subsequently shown to contain the gene for peripheral myelin protein 22 (PMP22) (Matsunami, 1992; Patel, 1992; Timmerman, 1992; Valentijn, 1992a). A gene dosage effect was hypothesised to be the molecular pathogenic cause of the disease; further evidence to support this was shown when a patient who had 4 copies of the PMP22 gene had a more severe phenotype (Lupski, 1992). The dosage hypothesis was given even more strength by the generation of transgenic mice and rats that carried additional copies of the PMP22 gene (Huxley, 1996; Huxley, 1998; Magyar, 1996; Sereda, 1996; Vallat, 1996; Perea, 2001). Point mutations within the PMP22 gene have also been identified in CMT1A patients where a duplication could not be found (Fabrizi, 1999; Roa, 1993; Valentijn, 1992b). CMT1A due to point mutations in the PMP22 gene often presents as a more severe disease phenotype than duplication positive patients (Tyson, 1997).

2.2.1.5 Hereditary neuropathy with liability to pressure palsies (HNPP)

Hereditary neuropathy with liability to pressure palsies (HNPP) is an autosomal dominant disorder, that is characterised by recurrent peripheral motor/sensory nerve palsies which occur due to minor compression trauma (Verhagen, 1993). NCVs are significantly reduced at compression sites within the peripheral nerves (Verhagen, 1993). The disease is sometimes referred to as “tomaculous neuropathy” due to the presence of sausage shaped swellings in the myelin sheath (Latin: sausage = tomaculum). These tomaculum can occur in both the sensory and motor neurons (Oda, 1990). Patients also have variable degrees of segmental demyelination and axonal loss (Lenssen, 1998).

The underlying genetic defect in 84% (Sutton, 2004) of HNPP families is a 1.5-Mb deletion on chromosome 17p11.2, which contains the gene for PMP22 (Chance, 1993). However, in a minority of HNPP families no deletion could be detected (Marimam, 1994; Harding, 1995). Point mutations within the PMP22 gene have also been associated with HNPP (Lenssen, 1998; Bort, 1997; Young, 1997).

2.2.1.5 Peripheral myelin protein 22 (PMP22)

PMP22 is an 18 KDa polypeptide that undergoes post-translational modification to form a mature 22 KDa glycoprotein. The protein is 160 aa in length and has 4 distinct hydrophobic domains and 2 extracellular domains (D'Urso, 1997) that are highly conserved among different species (Agostoni, 1999; Wulf, 1999). The cDNA for PMP22 was first identified by screening for genes that were repressed in peripheral nerves following nerve damage (Welcher, 1991). The gene for PMP22 was mapped to 17p11.2-p12 using Southern analysis of somatic cell hybrids (Patel, 1992) and by fluorescent in situ hybridisation (FISH) (Takahashi, 1992). Cloned Human PMP22 was shown to have 87% and 86% homology to rat and mouse PMP22 respectively (Patel, 1992). The PMP22 gene has 2 promoter regions that regulate the expression of 2 alternatively utilised 5' noncoding exons, termed exons 1a and 1b (Suter, 1994).

The protein is highly expressed in myelinating Schwann cells, mRNA transcripts were found to be upregulated 200-fold during myelination (Snipes, 1992) and at lower levels in several non-neural tissues (Spreyer, 1991; Welcher, 1991; Baechner, 1995). PMP22 is

mainly localised within the compact portion of the myelin sheath it is not found in non-compact myelin (Snipes, 1992; Haney 1996) and is estimated to comprise 2-5% of total myelin protein (Pareek, 1993).

PMP22 like any other integral membrane protein is processed through the secretory pathway, involving synthesis in the rough endoplasmic reticulum (RER), maturation in the Golgi and targeting to the plasma membrane. It has been shown that the majority of newly synthesised PMP22 is retained in the ER and degraded (Pareek, 1993; Pareek 1997; Notterpek, 1999). The small percentage of PMP22 that leaves the ER for the Golgi and undergoes glycosylation making it more stable (Pareek, 1997).

The function of PMP22 is not fully characterised but seems to have an important role in the formation and maintenance of myelin (Snipes, 1992; Li, 2004). PMP22 has also been implicated in the formation of the intracellular junction of epithelial cells (Notterpek, 2001) as well as the regulation of cell proliferation and apoptosis (Fabbretti, 1995; Karlsson, 1999; Zoidl, 1995; Zoidl, 1997).

2.2.1.6 Schwann cell maturation

During development of the PNS, Schwann cell precursors arise from the neural crest; these precursors then migrate and make contact with developing peripheral axons (Le Douarin, 1993). These immature Schwann cells then invade and ensheath bundles of axons, where they then differentiate further into non-myelinating or pro-myelinating Schwann cells (Webster, 1993). Pro-myelinating cells develop a one to one association with an axon; these cells can then differentiate into mature myelinating Schwann cells. Mature myelinating Schwann cells turn on genes that code for the major myelin proteins and turn off previously expressed genes (Scherer, 1997). The mRNA for PMP22, MPZ, myelin basic protein (MBP), and myelin-associated glycoprotein (MAG) are rapidly upregulated. Once myelination of the axon is complete, maintenance of the sheath depends on continued Schwann cell-axon interactions (Kamholtz, 2000).

2.2.1.7 Unequal recombination at chromosome 17p11.2-12

The CMT1A and HNPP disease phenotypes seem to result from gene dosage sensitivity (Lupski, 1992; Chance, 1993), which Gabriel and colleagues provided more evidence for, through immunohistochemistry on CMT1A and HNPP nerve biopsy samples (Gabriel, 1997). Mapping of the 1.5 Mb segment that can be duplicated or deleted showed that located on either side of the region are two almost identical (>98%) 24 Kb repeats, that have been termed CMT1A-REPs (Pentao, 1992; Chance, 1994; Kiyosawa, 1995). The unequal recombination event occurs between a flanking proximal CMT1A-REP on one

homolog and a misaligned distal CMT1A-REP on the other homolog (Han, 2000). It has been shown that recombination events do not happen equally across the entire 24 Kbs of the repeats. There is a 3.2 Kb “hot-spot” region most (75-80%) recombination events can be located to (Lopes, 1998; Reiter, 1997) and a further 9.2 Kb region that contains the majority of the remaining rearrangements (Kiyosawa, 1995; Lopes, 1998). Most *de novo* cases of CMT1A and HNPP are of paternal origin (Bort, 1997; Palau, 1993; Lopes, 1997) arising from interchromosomal recombination during spermatogenesis. Duplication and deletions that are of maternal origin seem to be the result of an intrachromosomal process, either unequal sister chromatid exchange (Lopes, 1998) or, in the case of deletions, by excision of an intrachromatidial loop (LeGuern, 1996).

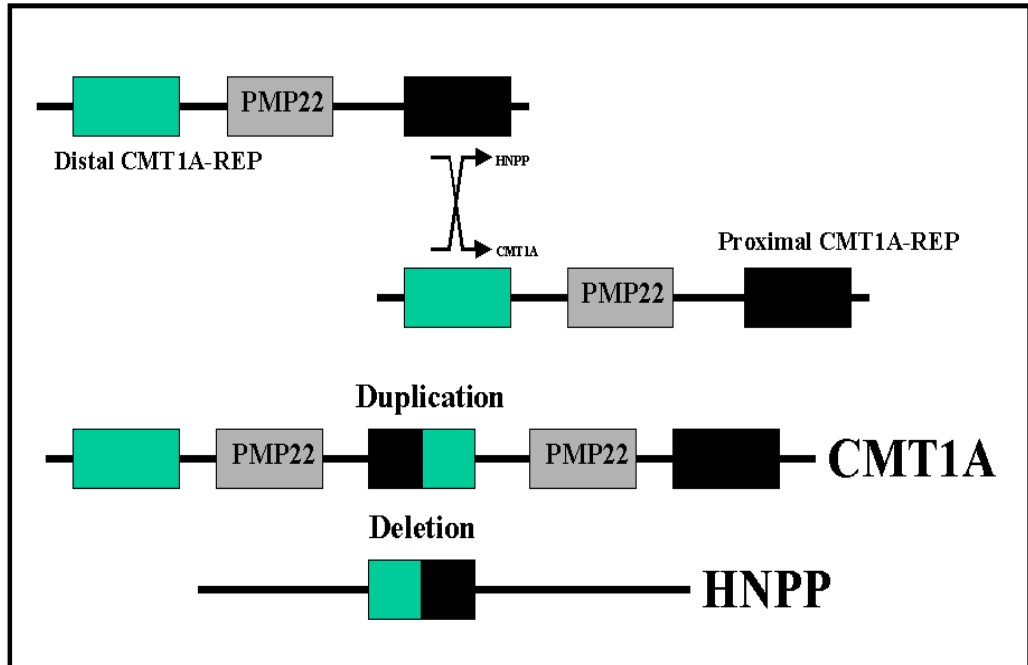


Fig 2.9 Unequal crossing over between distal and proximal CMT1A repeats (adapted from Lopes, 1999).

2.2.1.8 Aim of the chapter

The aim of this study is to successfully develop a quantitative Real-time multiplex PCR that will be capable of detecting changes in PMP22 gene copy number. This will push Real-time PCR to the limits of its capabilities, as any changes in PMP22 gene copy number will be very subtle. Multiplexing both the reference and target gene into the same reaction and detecting them using different coloured hybridisation probes is an important aspect of this study. By having both amplicons form in the same PCR, under the same conditions, this should help to reduce variability in the assay. β -globin will be used as a reference gene and the final results will be presented as a relative ratio of PMP22 to β -globin gene copy numbers.

2.2.2 MATERIALS AND METHODS

2.2.2.1 Patient samples

CMT1A and HNPP samples used in this study were kindly provided by Dr David Barton, from the National Centre for Medical Genetics. Normal control samples were obtained from within the Department of Biological Sciences, Dublin Institute of Technology, these samples would have consisted of staff and student volunteers who had given informed consent.

2.2.2.2 DNA isolation

DNA was isolated as previously described (Materials and methods chapter 2.1.2.2).

2.2.2.3 Primer and hybridisation probe design

Primers and hybridisation probes were designed for β -globin (NCBI accession no: NG_000007.3) and the exon 1a portion of the PMP22 gene (NCBI accession no: U08049) with the aid of the LightCycler probe design software version 1.0. The name and sequence of each primer and hybridisation probe is outlined in Table 2.05 as well as the concentration used in the final reaction.

2.2.2.4 DNA quantification

DNA was quantified using Hoechst quantification reagent (Molecular probes). The assay was carried out as per the manufacturer's instructions and measurements were taken on a VersaFluor™ Fluorimeter (BioRad). The DNA concentration of each sample was quantified in this manner and then samples were diluted in nuclease free water to a working concentration of 25 ng/μl, which was determined to be sufficient for Real-time PCR analysis.

2.2.2.5 Real-time PCR

Real-time quantitative PCR was carried out on a LightCycler instrument (Roche Diagnostics). The total reaction volume was 10 μl, containing: 1 μl of 10X LightCycler DNA master hybridisation enzyme mix (Roche Diagnostics), 4 mM MgCl₂, 0.1 μM hybridisation probes and primer concentrations were at 1 μM. PCR conditions were carried out as follows: initial denaturation was 5 min at 95°C followed by 40 cycles of 95°C for 0s, 55°C for 20s and 72°C for 20s. A touchdown PCR was carried out with the annealing temperature starting at 55°C and dropping to 50°C at 1°C/cycle. Fluorescence was measured at the end of each annealing step. Data analysis was carried out using the second derivative maximum analysis method in the LightCycler software version 3.5.

2.2.2.6 Relative quantification

Relative quantification was performed with the aid of the LightCycler relative quantification software version 1.1 (Roche). To carry out relative quantification, efficiency correction files were generated by analysing a dilution series of control DNA with the optimised β -globin/PMP22 multiplex. Standard curve files were exported from the LightCycler software into the relative quantification software so that an efficiency correction file could be generated. This is an important step as it compensates for any difference in the amplification efficiency between β -globin and PMP22 amplicons. Not correcting for efficiency could result in an over/under-estimation of PMP22 copies relative to β -globin copies and thus giving a false positive or negative result. Sample data was then analysed using the relative quantification (Roche) software as per the manufacturers instructions.

Primer/hybridisation probe seq (5' to 3')	Conc
β-globin primer	
bGCMTF: CATTGCTTCTGACACAAC	1.0 μM
bGCMTR: CTGGGTCCAAGGGTAG	1.0 μM
β-Globin hybridisation probes	
bGCMT-p1: GAAGTCTGCCGTTACTGCCC-f	0.2 μM
bGCMT-p2: 640-TGGGGCAAGGTGAACGT-p	0.2 μM
PMP22Ex1a primers	
PMP22Ex1aF: GGCCTCTTGGGATTAT	1.0 μM
PMP22Ex1aR: GCTCCCCGAGATGTTC	1.0 μM
PMP22Ex1a hybridisation probes	
PMP22-p1: CCAGCATTGGACCAGCCC-f	0.2 μM
PMP22-p2: 705-GAATAAACTGGAAAGACGCCTGG-p	0.2 μM

Table 2.05 **Sequence of primers and hybridisation probes used for PMP22 dosage analysis.** Fluorescein (f), Phosphate (p), LC Red 640 dye (640, detected in the F2 channel), LC Red 705 dye (705, detected in the F3 channel). The final concentration (conc) of each primer/probe in the multiplex PCR is also indicated.

2.2.3 RESULTS

2.2.3.1 Standard curve reproducibility and PCR efficiency

The exponential nature of PCR amplification and the small quantities of target molecules used at the start, mean that even small variations in the reaction component can affect the reproducibility of PCR (Wu, 1991). The first part of this study involved careful design of both PCR primers and hybridisation probes for both PMP22 and β -globin. β -globin will act as a reference gene to which PMP22 gene copy numbers will be represented as a ratio of. Extensive optimisation was then required to ensure the multiplex was reproducible and that each amplicon had a similar efficiency.

When we had successfully optimised the multiplex PCR, we tested both genomic DNA standards and patient samples to show that the results were reproducible from assay to assay. The Cps were reproducible for the quantitative multiplex when using the same set of prepared genomic DNA standards in consecutive PCRs (Fig 2.10) as indicated by the low coefficient of variation (CV) (Table 2.06). Crossing points for test samples were also reproducible, 3 samples tested over 4 separate PCRs and showed very little variation in Cp values (Fig 2.11) the CV was also low (Table 2.07).

It is also important that the efficiency of each amplicon in the multiplex is similar. If the efficiency for one amplicon varied much from the other amplicon within the multiplex PCR this could lead to over/under estimation of the copy number, potentially leading to misdiagnosis of the sample. The efficiency is calculated from the slope of Cp against log

concentration using the following equation: Efficiency (E) = $10^{-1/\text{slope}}$ (Rasmussen, 2001). As mentioned previously a slope of -3.33 , indicates that the PCR is 100% efficient. When we calculated the efficiency for amplification of both PMP22 and β -globin amplicons were 109% and 108% respectively (Table 2.08). This shows that there is only a marginal difference in efficiency between amplification of PMP22 and β -globin in our optimised multiplex PCR.

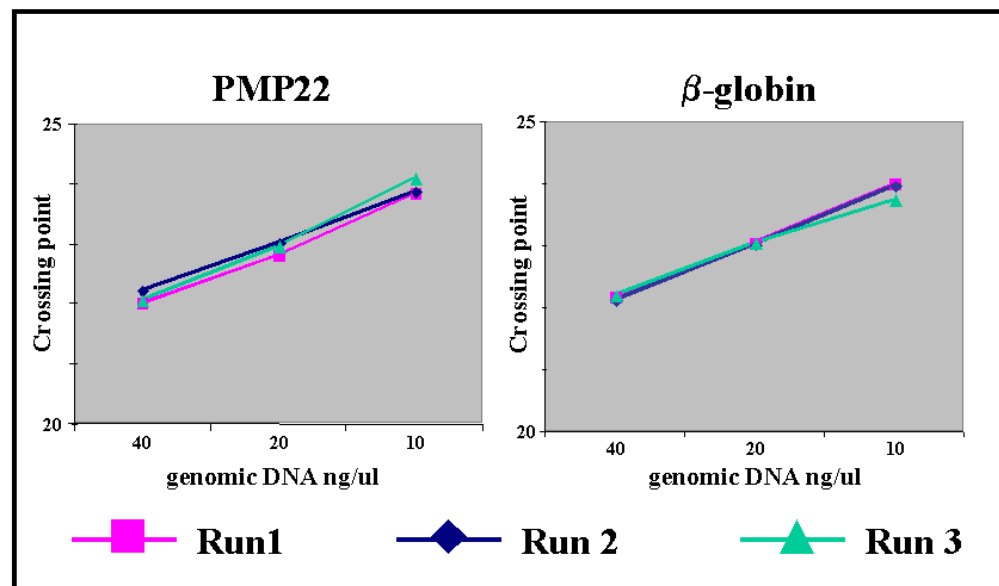


Fig 2.10 Standard curves for PMP22 and β -globin quantification for 3 consecutive PCRs.

Cp reproducibility for genomic DNA standards

Genomic DNA standards

	40 ng/ul	20 ng/ul	10 ng/ul
PMP22			
Mean Cp	22.09	22.93	23.94
Range	(22.01-22.22)	(22.80-23.02)	(23.84-24.01)
Std dev	0.112	0.114	0.142
CV %	0.50	0.49	0.59
β-globin			
Mean Cp	22.17	23.05	23.91
Range	(22.13-22.21)	(23.02-23.06)	(23.74-24.01)
Std dev	0.04	0.023	0.146
CV %	0.18	0.10	0.60

Table 2.06 **Reproducibility of PMP22/β-globin quantitative multiplex PCR using genomic DNA standards.**

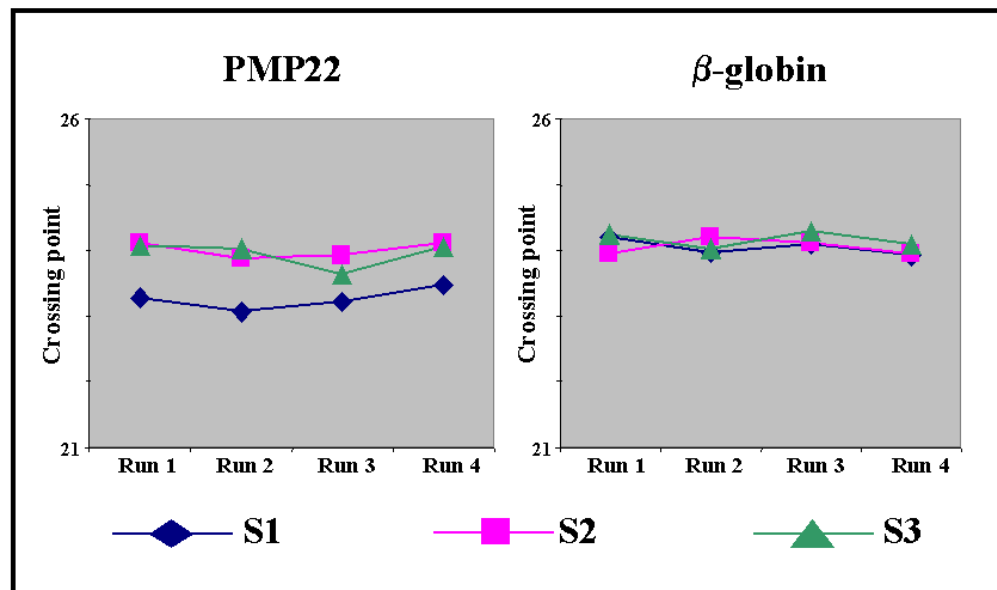


Fig 2.11 **Crossing points for 3 samples in 4 consecutive PCRs.** Sample 1 (S1) is a CMT1A positive sample hence the lower Cps in the PMP22 graph when compared with the β -globin graph.

Cp reproducibility for patient samples

	Sample 1	Sample 2	Sample 3
PMP22			
Mean Cp	23.25	24.01	23.95
Range	(23.07-23.46)	(23.87-24.12)	(23.65-24.07)
Std dev	0.163	0.134	0.198
CV %	0.70	0.56	0.83
β-globin			
Mean Cp	24.04	24.06	24.16
Range	(23.92-24.19)	(23.95-24.20)	(24.02-24.29)
Std dev	0.121	0.126	0.141
CV %	0.51	0.52	0.59

Table 2.07 **Reproducibility of PMP22/β-globin quantitative multiplex PCR using patient samples.** Efficiency (E), Standard deviation (Std dev), coefficient of variation (CV).

PCR efficiency calculations

	Slope	$E = 10^{-1/\text{slope}}$	% E
PMP22			
Mean	-2.943	2.187	109.34
Std dev	0.171	0.11	5.25
CV %	5.8	4.8	4.8
β-globin			
Mean	-2.985	2.163	108.14
Std dev	0.135	0.07	3.93
CV %	4.5	3.6	3.6

Table 2.08 **Efficiency of both PMP22 and β -globin amplification.** Efficiency (E), Standard deviation (Std dev), coefficient of variation (CV).

2.2.3.2 Relative quantification of PMP22 gene copy numbers

Relative quantification involves expressing the target amplicon as a ratio of a control amplicon that should remain constant in a test sample. A separate relative quantification software package is available for the LightCycler instrument that determines the relative concentration of an unknown sample by normalising it to a calibrator sample. In this study, the calibrator is a genomic DNA sample that is known to have neither a duplication/deletion of the PMP22 gene. This calibrator sample is included in each run and it is used by the software to establish a normal ratio. The software calculates a relative ratio based on the comparative threshold cycle method (Livak, 1997). Firstly, the $\Delta\Delta C_p$ ($\Delta\Delta C_p$) is calculated as follow:

$$\Delta\Delta C_p = [\Delta C_p \beta\text{-globin (calibrator sample)} - \Delta C_p \text{PMP22 (calibrator sample)}] - [\Delta C_p \beta\text{-globin (patient sample)} - \Delta C_p \text{PMP22 (patient sample)}].$$

After the $\Delta\Delta C_p$ is calculated the relative gene copy number of unknown to calibrator sample can be calculated using the expression: $2^{-\Delta\Delta C_p}$. Using this method, the expected results for a normal individual would be a ratio of ~ 1:1, 1.5:1 for CMT1A and 0.5:1 for HNPP. Use of the LightCycler relative quantification software avoids the need to manually calculate ratio values. The software also allows efficiency correction files to be generated, which can be used to normalise ratio values if there is a difference in efficiency between the calibrator and target amplification.

Following optimisation of the PMP22/ β -globin quantitative multiplex, we tested a number of samples for PMP22 duplication or deletions. A typical example of an amplification curve for a normal sample is seen in Fig 2.12. As we can see, the difference between the Cps for the calibrator and test sample is similar for both β -globin (Fig 2.12, Panel A) and PMP22 (Fig 2.12, Panel B). A CMT1A sample shows a larger difference between the Cps of the calibrator and test sample for β -globin than for PMP22 (Fig 2.13). This indicates that in that sample there are more copies of the PMP22 gene than β -globin. The reverse is seen when a HNPP sample is tested (Fig 2.14).

The relative ratios of PMP22 to β -globin gene copy numbers of all samples tested are shown in Fig 2.15. The mean ratio of PMP22 to β -globin for the control, CMT1A and HNPP groups were 1.03 (range: 0.83-1.2; standard deviation: 0.110; CV: 10.7%), 1.70 (range: 1.47-2.2; standard deviation: 0.281; CV: 16.5%) and 0.44 respectively. These figures are within the expected theoretical values for the different relative ratios. From these results we can see that a ratio of >1.4 is indicative of CMT1A. The diagnosis of HNPP can be made with samples that have a relative ratio of <0.55 . There was no overlap of copy number between the CMT1A or HNPP patients and the controls.

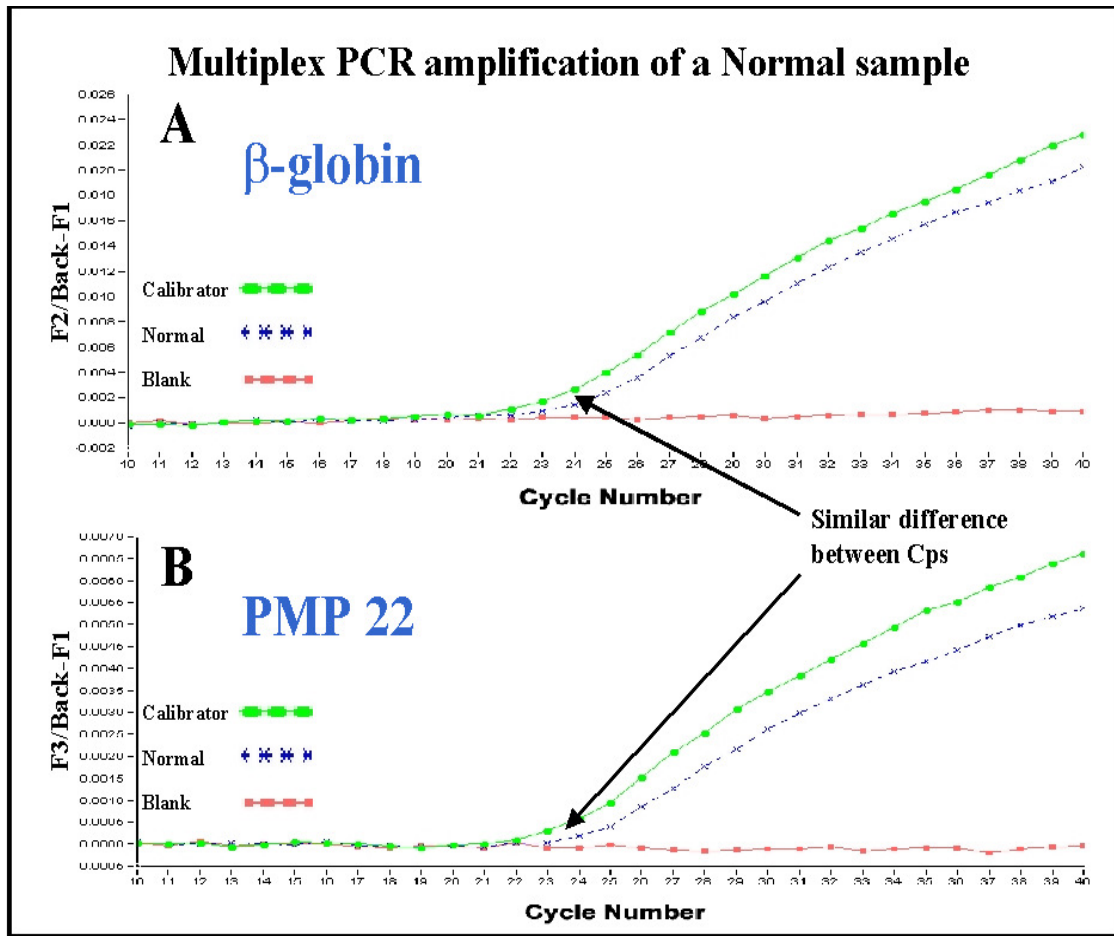


Fig 2.12 **Relative quantification of PMP22 gene copy number in a normal sample.** The calibrator is labelled in green, the unknown sample in blue and the negative control in red. As can be seen there is no major difference between the delta Cp for the calibrator and test sample for either β -globin (panel A) or PMP22 (panel B).

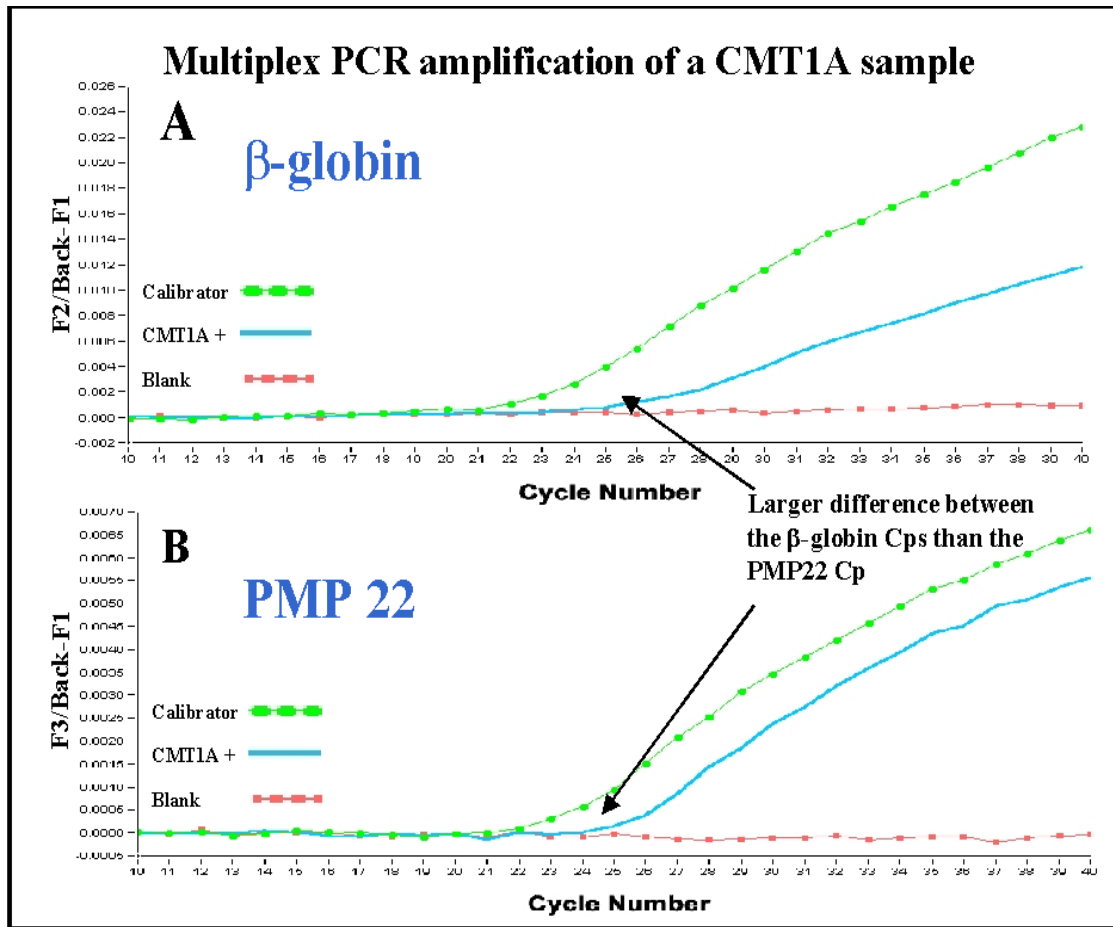


Fig 2.13 **Relative quantification of PMP22 gene copy number in a CMT1A patient.** The calibrator is labelled in green, the sample is in blue and the negative control is in red. As can be seen in this example the delta Cp between the calibrator and sample for β -globin (panel A) is greater than the delta Cp between the calibrator and sample for PMP22 (panel B) indicating that there is an increased amount of PMP22 genes in this sample.

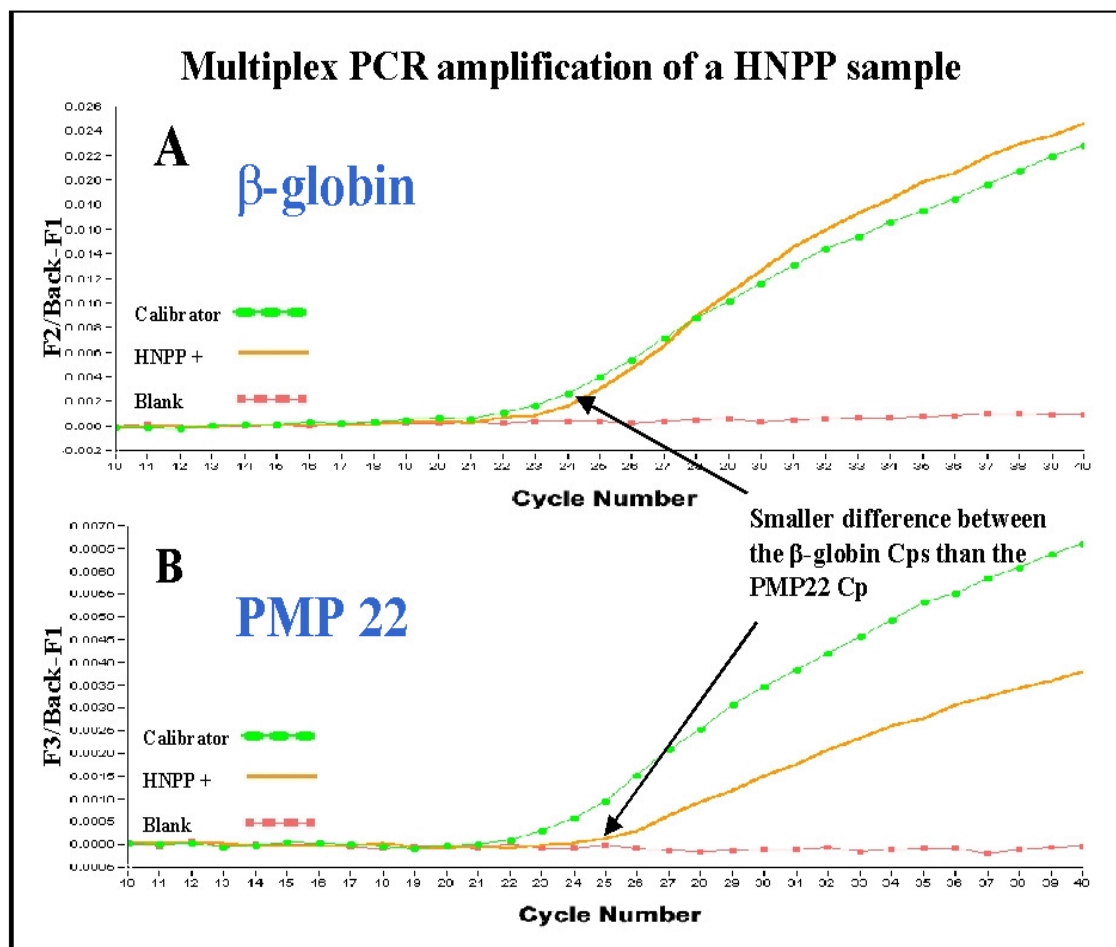


Fig 2.14 **Relative quantification of PMP22 gene copy number in a HNPP sample.** The calibrator is labelled in green, the sample is in orange and the negative control is in red. As can be seen in this example the delta Cp between the calibrator and sample for β -globin (panel A) is smaller than the delta Cp between the calibrator and sample for PMP22 (panel B) indicating that there is a decreased amount of PMP22 genes in this sample.

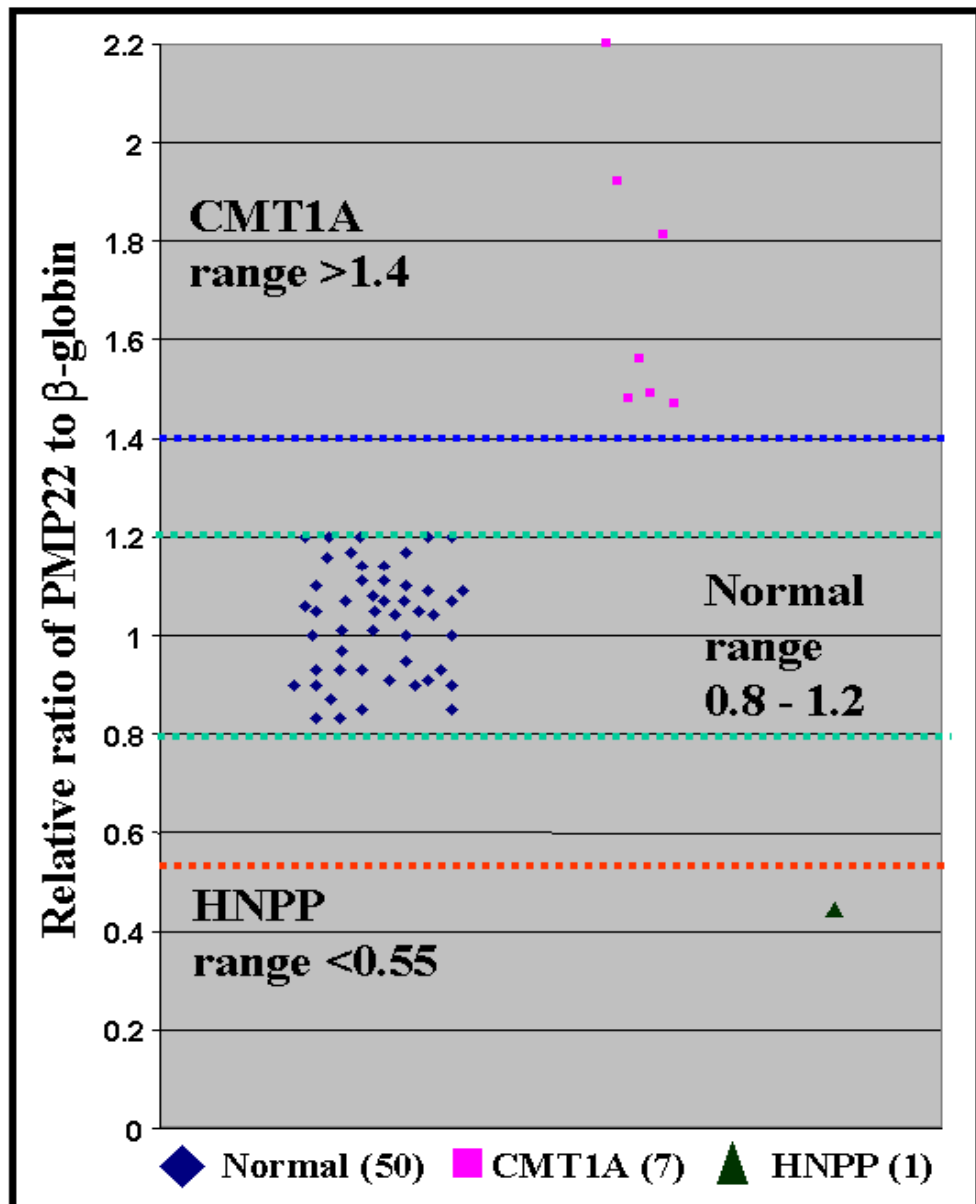


Fig 2.15 **Distribution of normal, CMT1A and HNPP samples.** The number of samples in each group is indicated in brackets. Samples falling on or between the green lines are within the normal range (0.8-1.2). Samples above the blue line indicate that duplication is present and are therefore CMT1A positive. A sample below the red line indicates that there is a loss of a copy of the PMP22 gene and are therefore HNPP positive.

2.2.4 DISCUSSION

The major cause of CMT1A is the duplication of a 1.5Mb region on chromosome 17p11.2 (Lupski, 1991; Raeymaekers; 1991), which was shown to contain the gene for peripheral myelin protein 22 (PMP22) (Matsunami 1992; Patel, 1992; Timmerman, 1992; Valentijn, 1992). Hereditary neuropathy with liability to pressure palsies (HNPP) has been associated with a reciprocal deletion of the same 1.5 Mb region (Chance, 1993). A gene dosage effect was hypothesised to be the molecular pathogenic cause of the diseases (Lupski, 1992). Overexpression of PMP22 leads to the CMT1A disease phenotype and underexpression of PMP22 leads to the HNPP phenotype. This hypothesis has been lent more weight with the use of transgenic mouse models for both diseases (Huxley, 1996; Huxley, 1998; Magyar, 1996; Sereda, 1996; Vallat, 1996; Perea, 2001).

Many molecular techniques have been applied to the diagnosis of these two neuropathies. Southern blotting was used in conjunction with densitometric measurements to detect differences in gene dosage (Lupski, 1991). Pulsed field gel electrophoresis (PFGE) has been used to detect recombination specific junction fragments (Chance, 1994). Interphase fluorescence in situ hybridisation (FISH) methodologies have also been developed to detect the gain or loss of the PMP22 gene (Shaffer, 1997; Kaskork, 1999). Other techniques include repeat-PCR (REP-PCR) (Stronach, 1999), short tandem repeat (STR) PCR (Haupt, 1997; Badano, 2001) and endpoint quantitative PCR (Poroppat, 1998; Young, 1998). However, many of these techniques have several drawbacks. The hybridisation techniques are very time consuming and large amounts of high-grade DNA are required. Endpoint PCR is only semi-quantitative at best due to PCR reaching a plateau in latter

cycles and requires a considerable amount of post-PCR processing followed by densitometric analysis.

Real-time PCR a recent advancement of the PCR technology has led to development of a truly quantitative technique. Quantification is based on the principle that the C_p is proportional to the starting copy number of the target sequence (Higuchi, 1993). One of the advantages of using Real-time PCR for the diagnosis of hereditary diseases is that the detection systems used are very sensitive, requiring only small amounts of DNA making them suitable for neo-natal screening.

In this chapter, we aimed to determine how sensitive Real-time PCR is for quantification of subtle changes in gene copy number. It is clear that Real-time PCR can easily detect log fold changes in the target amplicon but would it be able to measure changes as small as a 1.5 fold increase? To achieve this we developed a Real-time multiplex PCR to quantify the duplication or deletion of the gene for PMP22. Recently other groups have taken Real-time PCR approaches for gene dosage analysis in CMT1A. These have included a competitive gene dosage assay, where the area under a melting curve peak for an intronic polymorphic markers are compared between a PCR competitor and a test sample (Ruiz-Ponte, 2000). Other approaches have included Sybr Green 1 based relative quantification of PMP22 gene dosage using either β -globin (Choi, 2005) or albumin (Kim, 2003) as a reference gene. The inability to perform multiplex PCR is a major disadvantage of using Sybr Green 1 for quantification, this means both the target and the reference gene have to be amplified in separate reactions. Any pipetting errors made when loading the test sample into 2 separate PCRs could result in a false positive/negative result. The optimum approach is to develop a

multiplex reaction whereby both the target and a reference gene are amplified in the same reaction. In this system, any sample loading variations will not alter the result. Other advantages include the saving of time and reagents, as only a single PCR is needed to assess both amplicons. This approach to the quantification of PMP22 gene dosage was taken by a group using TaqMan probes and albumin was used as a reference gene (Thiel, 2003).

We used the multiplex PCR approach to co-amplify portions of exon 1a of the PMP22 gene and β -globin gene simultaneously. Using hybridisation probes labelled with different dyes meant that each amplicon could be detected in a different colour channel on the LightCycler. A relative quantification strategy was employed, meaning that PMP22 copy number would be expressed as a ratio of β -globin copy number. Careful optimisation of the PCR parameters was required, as the efficiency at which both amplicons were being produced had to be similar. PCR efficiency calculations were made by running serial dilutions of a standard, in this case a commercial preparation of gDNA at a known concentration, in the multiplex. The slope of the resulting standard curves could then be put into the following equation: $E = 10^{-1/\text{slope}}$, the average efficiency of both reactions was very similar differing by only 1% (Table 2.08). Calculation of the Cp values for both the calibrator and test samples was performed using the second derivative maximum algorithm in the LightCycler data analysis software. This approach was taken, as it is a more automated way of obtaining Cp data. Cp values were reproducible from day to day for both standards (Table 2.06 and Fig 2.10) and patient samples (Table 2.07 and Fig 2.11).

Relative quantification was performed by exporting the Cp data for each sample into the LightCycler relative quantification software. Use of this software serves two purposes, firstly efficiency files can be generated from the standards, this allows for correction of efficiency if differences occur between the two amplicons. Secondly, it is a more automated way of obtaining ratio values. Automation of any aspect of a diagnostic test can eliminate/reduce human error when interpreting the results.

The mean ratio of PMP22 to β -globin for the different groups, controls, CMT1A and HNPP are 1.03, 1.70 and 0.44 respectively, which is similar to previously published data (Choi, 2005; Aarskog, 2001; Ruiz-Ponte, 2000; Thiel, 2003). There is a clear gap between the gene copy number ratios between each group (Fig 2.15) with no overlapping results. The control and CMT1A cohort numbers are similar or better than other studies. The single HNPP sample is a limitation of this study, nonetheless, it is clearly discernible from the normal cohort and falls within the ratio range of other studies (Choi, 2005; Aarskog, 2001).

To conclude, the Real-time multiplex PCR assay that we have developed allows the rapid differentiation of gene deletions and duplications and allows for the diagnosis of CMT1A and HNPP patients. The assay is quick (~ 45 mins), requires very little DNA (~25 ng/ μ l) and data interpretation is automated which facilitates high-throughput. As this work has also shown that Real-time PCR techniques are sensitive enough to detect subtle changes in gene copy numbers, similar approaches could be employed for a wide range of genetic diseases such as Down's syndrome caused by trisomy 21 (Zimmermann, 2000). Many cancer cells undergo amplification of certain genes that help them avoid the immune system resulting in a more aggressive tumour such as decoy receptor 3 in gastrointestinal

tumours (Pitti, 1998; Bai, 2000) and Her2/neu in breast cancer (Slamon, 1987). These events could also be monitored with an approach similar to the one used in this study.

CHAPTER 3

ANALYSIS OF LIGHT MESSENGER RNA EXPRESSION BY QUANTITATIVE REAL- TIME RT-PCR IN HUMAN IMMUNE- MEDIATED DISEASES

3.1 INTRODUCTION

3.1.1 Autoimmune diseases

Autoimmune diseases are individually rare but when taken together they affect approximately 5 % of the population in the western world with a disproportionately skewed effect on women (McKay, 2004; O'Shea, 2001). The consensus is that these diseases occur due to abnormal lymphocyte activation, however, other cells types can make a significant contribution to disease pathogenesis, particularly APCs such as DCs (Bayry, 2004). The development of autoimmune conditions is a complex process involving genetic predisposition as well as environmental triggers such as pathogen exposure and diet (Rioux, 2005).

Autoimmune diseases are often categorised into organ/tissue-specific as in the case of insulin dependent diabetes mellitus (IDDM), multiple sclerosis (MS) and thyroiditis or systemic diseases such as rheumatoid arthritis (RA) and SLE in which multiple organs can be affected. Despite these differences, there are many common elements between the various clinical diseases. Genome-wide linkage analysis shows that many autoimmune diseases share common susceptibility loci (Maas, 2002). Different clinical diseases may also over-lap within families or individuals. This would possibly indicate that common groups of genes could contribute to the development of different autoimmune diseases.

3.1.2 LIGHT and immune-mediated diseases

As mentioned previously, LIGHT plays important roles in a variety of different aspects of the immune system including T cell co-stimulation (Harrop, 1998; Tamada, 2000), DC maturation (Morel, 2001), mLN organogenesis (Wang, 2002) and negative selection of thymocytes (Wang, 2002; Wang 2001). With such a diverse effect on the immune system, LIGHT is a good candidate gene to have a role in the development of immune-mediated diseases.

In 2001, two papers were published that identified the *in vivo* effects of T cells overexpressing LIGHT using transgenic mice (Shiakh, 2001; Wang, 2001). Both groups constitutively overexpressed LIGHT on T lymphocytes using lineage specific promoters. These LIGHT-Tg mice developed a lymphoproliferative disorder with gross enlargement of the spleen and LNs caused by the expansion of the T cell compartments. Haematoxylin and Eosin (H&E) staining of the small intestine showed signs of chronic inflammation with substantial infiltration of mononuclear cells, loss of goblet cells, distortion and hyperplasia of the crypts and villus atrophy (Shiakh, 2001). Following *in vitro* activation of T cells there was a significantly increased number of INF- γ , IL-4 and Granulocyte-monocyte colony stimulating factor (GM-CSF) producing cells in LIGHT-Tg mice than in the WT mice (Wang, 2001). GM-CSF leads to the preferential increase in GM lineages and activation of mature macrophages and granulocytes. Granulocytes and monocytes/macrophages are major effector cells of the immune response; elevated levels of these cells in conjunction with high levels of activated T cells may cause the destruction of peripheral tissue and ultimately lead to autoimmunity.

In addition to severe intestinal inflammation, the LIGHT-Tg mice also developed glomerulonephritis, involving 80% of the glomeruli and strong IgG deposits were observed in the glomeruli of Tg mice (Wang, 2001). These manifestations resemble those seen in MRL-lpr/lpr mice, which is an established mouse model for SLE. The LIGHT-Tg mice were also shown to have an 8-fold increase in anti-DNA autoantibodies, with there being only a slight increase in total IgG levels when compared with WT mice (Wang, 2001).

These studies showed that while LIGHT could trigger symptoms of systemic autoimmunity, overexpression of LIGHT had a particularly profound effect on the intestine. Only memory and activated T cells have the ability to effectively migrate to peripheral tissues (Masopust, 2001), while naïve T cells migrate to secondary lymphoid organs (Butcher, 1999; von Andrian, 2001). Migration of T cells to effector sites such as the lamina propria is facilitated by interaction with tissue-specific integrins and chemokine gradients. Mucosal addressin cell adhesion molecule 1 (MAdCAM-1), which is expressed at constitutively low levels in the intestine specifically promotes $\alpha 4\beta 7$ integrin bearing T cells to migrate to intestinal effector sites (Berlin, 1993). LIGHT-Tg mice showed increased *in vivo* expression of MAdCAM-1 on endothelial cells (Wang, 2004) and recombinant LIGHT has been demonstrated to increase the expression of MAdCAM-1 (Wang, 2005). Peyer's patches (PP) derived DC have the ability to induce high expression of $\alpha 4\beta 7$ integrin on T cells, as LIGHT plays a role in DC maturation, excessive LIGHT could lead to increased PP DC maturation ultimately leading to increased numbers of T cells with a predilection for the gut. Activation of LT β R on LP stromal cells by LIGHT expressed on activated T cells leads to the creation of microenvironments that are conducive to increased recruitment of cells to the LP (Fig 3.01) (Chin, 2003).

To further prove that LIGHT-expressing T cells preferentially home to the gut an adoptive transfer study was performed. The mLN cells were transferred from LIGHT-Tg mice into recombination activating gene-1 knockout (RAG-1^{-/-}) mice (Wang, 2005). The LIGHT-Tg mLN cells caused severe intestinal inflammation in the recipient, whereas the transfer of wildtype mLN cells into the RAG-1^{-/-} model did not cause intestinal inflammation.

LIGHT knockout (LIGHT^{-/-}) mice have also been generated, and their T cells show decreased proliferation and release of cytokines in response to *in vitro* stimulation (Scheu, 2002). This indicates the importance of LIGHT signalling via HVEM to allow full activation of T cells. CD 8⁺ T cell responses in particular are sub-optimal in these LIGHT knockout animals. Blocking LIGHT binding to its receptors using either HVEM-Ig or LTβR-Ig recombinant fusion proteins has been shown to alleviate T cell-mediated autoimmune diseases. Insulin dependent diabetes mellitus (IDDM) is an autoimmune disease caused by T cell-mediated destruction of insulin producing β cells of the pancreatic islets of Langerhans (Bach, 1994). The non-obese diabetic (NOD) mouse, a well-established model for IDDM was used to test the role of LIGHT in T cell-mediated disease. Treatment of the mice with HVEM-Ig significantly reduced the development of IDDM by blocking LIGHT-signalling pathways (Wang, 2001).

LIGHT expression by T cells has been linked to a wide range of immune-mediated diseases such as rheumatoid arthritis (Kim, 2005), Crohn's disease (Wang, 2005; Cohavy, 2005), ulcerative colitis (UC) (Mao-Mao, 2005) atherosclerosis (Lee, 2004) chronic heart disease (Yndestad, 2002) autoimmune hepatitis (Anand, 2006) as well as graft versus host disease (GVHD) (Tamada, 2000). The evidence overall, from both animal and human studies

suggests that the overproliferation and hyperactivation of T cells caused by T cell derived LIGHT can lead to the breakdown of self-tolerance. This implies that dysregulation of LIGHT expression could be an important factor in the induction of both T and B cell autoimmunity and in the pathogenesis of autoimmune diseases.

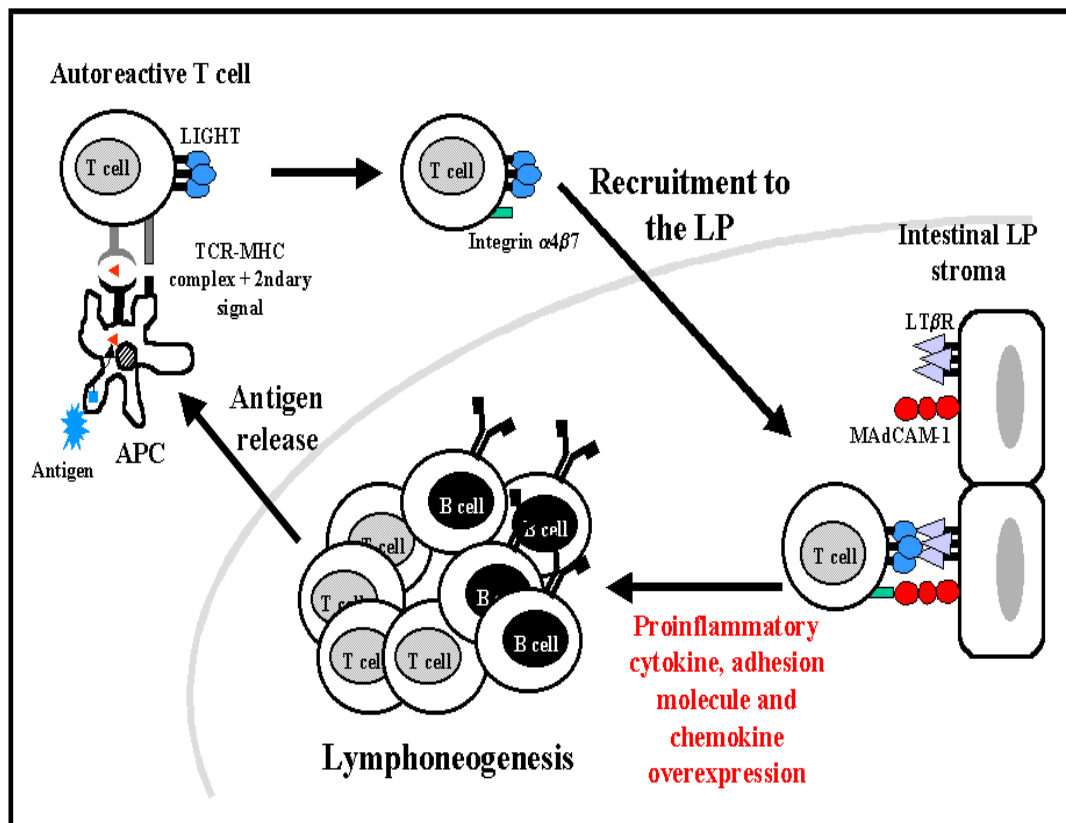


Fig 3.01 **The role of LIGHT-LT β R interactions in promoting chronic intestinal inflammation** (Adapted from Chin, 2003). Activated autoreactive T cells can migrate to the lamina propria via upregulation of the integrin $\alpha4\beta7$ which can bind to MAdCAM-1 which is constitutively expressed in the intestine. Activation of LT β R on LP stroma by LIGHT on autoreactive T cells leads to increased expression of adhesion molecules, chemokines and proinflammatory cytokines. This leads to increased migration of inflammatory cells to the LP in a positive feedback loop, leading to chronic inflammation and tissue destruction. TCR, T cell receptor; MHC, major histocompatibility complex; APC, antigen presenting cell.

3.1.3 Mitogen activation of T cells

The first stage in the activation of T cells is the engagement of the T cell receptor (TCR) with a MHC-peptide complex. Intracellular signalling through the TCR results in the recruitment of a large number of proteins to its cytoplasmic domain and the activation of enzymes such as phospholipase C (PLC). PLC can convert phosphatidylinositol 4, 5 phosphate (PIP₂) to inositol 1, 4, 5 triphosphate (IP₃) and diacylglycerol (DAG) two important second messengers within cells. Increases in intracellular levels of IP₃, result in the generation of a Ca⁺⁺ flux within cells and the activation of Ca⁺⁺ dependent phosphatases such as calcineurin. This in turn can cause the activation and translocation of transcription factors such as NF-AT and AP-1 to the nucleus. DAG has a role in the activation of protein kinase C (PKC). To date there have been nine isoenzymes of PKC identified, some are ubiquitously expressed while others are tissue-specific. PKC isoenzymes generally require both an increase in Ca⁺⁺ and DAG to become activated. However, PKC θ a T cell, monocyte and platelet specific isoform can be activated by DAG alone (Newton, 1997). PKC θ is rapidly recruited to the site of TCR clustering upon stimulation (Monks, 1997) and deletion of the gene in knockout mice results in defective T cell activation (Sun, 2000).

Activation of T cells via the TCR can be mimicked in a number of ways; by using monoclonal anti-CD3 antibodies, by the use of T cell specific lectins such as Concanavalin A (ConA) or Phytohaemagglutinin (PHA) or by using a combination of a phorbol ester such as phorbol 12-myristate 13-acetate (PMA) and a calcium ionophore such as ionomycin. PMA is an analog of DAG and thus it can directly bind and activate PKC isoenzymes. Ionomycin is a polyether antibiotic produced by *Streptomyces conglobatus* (Liu, 1978).

Ionomycin is capable of binding to divalent ions such as Ca^{++} and Mg^{++} in a 1:1 stoichiometry (Lui, 1978). The calcium salt of ionomycin is a very effective mobile carrier of Ca^{++} , leading to a flux of Ca^{++} within cells. In T cells, this results in the expression of activation markers such as CD7 (Ware, 1991), or the hydrolysis of phosphoinositides and the activation of PKC (Chatila, 1989). PMA and ionomycin can work in synergy to bypass the TCR signalling and directly activate down-stream signal transduction pathways that ultimately lead to activation of the T cell.

3.1.4 Jurkat T cells

The Jurkat T cell line was originally derived from peripheral blood of a 14-year-old boy suffering from acute lymphoblastic leukaemia (ALL) (Schneider, 1977). The original line was designated JM, but was heavily infected with mycoplasma. A bid to clear the cell line of the infection yielded the Jurkat E6-1 clone, which has become the standard Jurkat cell line used today (Abraham, 2004). The Jurkat cell has been used over the last 25 years by T cell immunologists to identify many of the events following on from TCR stimulation that leads to activation of the cell and the initiation of an immune response (Abraham, 2004). Incubation of Jurkat cells in the presence of PMA and ionomycin induces a strong activation response, as measured by the increased expression of IL-2 (Abraham, 2004).

3.1.5 Interferon-gamma (INF- γ)

The outcomes of an antigen driven T cell response is tightly regulated by cytokines, which play a key role in dictating which T helper (Th) cell pathway is induced. The Th1 pathway or cell-mediated immune response is characterised by the presence of IL-12, IL-2 and INF- γ , whereas the Th2 pathway or humoral response is defined primarily by the production of IL-4 and IL-10 (Mossman, 1989). These two pathways tend to be antagonistic of each other, Th1 cytokines downregulate Th2 responses and vice versa. The majority of autoimmune diseases in both human and animal studies that are associated with specific MHC class II allotypes have been characterised as being mediated by the Th1 pathway (Rosloniec, 2002). INF- γ is the cytokine that defines Th1 differentiation (O'Shea, 2001) and its role in autoimmunity has been extensively investigated. The INF- γ gene is located on Chr 12q14 (Zimonjic, 1995) that codes for a mature protein of 146 amino acids. It is expressed by activated Th1, NK and cytotoxic T cells and it has a wide range of proinflammatory effects on various cells of the cell-mediated immune response. INF- γ has been shown to enhance the activity of macrophages, induce proliferating B cells to switch to IgG2a antibody production, increasing the expression of both MHC class I and II molecules on various cells and inhibiting the proliferation of Th2 cells. SLE patients have been shown to have elevated levels of both INF- γ mRNA and soluble protein in their peripheral blood (Csiszár, 2000). CD patients have also been demonstrated to show increased expression of INF- γ in duodenal biopsies (Nilsen, 1998).

3.1.6 Analysis of mRNA expression by Real-time PCR

Many cellular decisions such as differentiation, survival and growth are linked to altered patterns of gene expression within the cell. The ability to quantify transcription levels of specific genes has become a central part of research into their function and how they may be altered during disease processes. Reverse transcription (RT) PCR remains the most sensitive method for the detection of mRNA and coupled to a Real-time quantitative system it has become the method of choice when assessing steady state mRNA levels (Bustin, 2000). The design of a quantitative RT-PCR has to take into consideration many factors that may have an effect on the result.

The first decision is whether to use mRNA or total RNA as a target for the RT-PCR. The use of mRNA has been reported to give better sensitivity (Burchill, 1999). However, extra steps are needed to isolate it from the total RNA, which can result in loss of transcripts and not all mRNA molecules have poly A tails (essential for enrichment of mRNA from total RNA). Therefore, for most assays, the use of total RNA is advisable (Bustin, 2004).

The next decision to make is which type of primer will be used to generate cDNA from mRNA during the RT phase. The RT step can be primed using oligo-dT, random hexamer/nonomers and target specific primers. Oligo-dT primers initiate RT by binding to the poly A tail of mRNA molecules, therefore it cannot prime RNAs that lack a poly A tail eg histone or viral RNAs (Bustin, 2004). Random primers initiate RT from multiple points along the transcript. They yield the most amount of cDNA and can be useful for transcripts that contain large amounts of secondary structure. Nonetheless, it has been reported that

their use can lead to an overestimation of mRNA by ~19 fold when compared to target-specific primers (Zhang, 1999). Target specific primers synthesize the most specific cDNA and are probably the most sensitive option for quantification (Lekanne, 2002). A drawback of using target specific primers is that separate priming reactions are necessary for each individual target that is analysed, whereas the use of random/oligo-dT primers yields a stock of cDNA which can be used to amplify multiple targets.

The last major factor to be considered is whether a one-step or two-step RT-PCR will be required and the choice of RT enzyme. A one-step RT-PCR involves both the RT and PCR phases being performed in the same reaction tube (Goblet, 1989; Mallet, 1995). In a two-step RT-PCR the RT step is performed in a separate reaction and then an aliquot of this is added to the PCR for amplification of the specific target sequence. Each approach has its advantages and disadvantages. The one-step is less time-consuming and the possibility of cross-contamination is reduced. Nevertheless, this requires more RNA than a two-step RT-PCR when analysing multiple mRNA targets, this only becomes a factor when samples are very small and RNA is limited. The two-step allows multiple target mRNA to be PCR-amplified from a single RT reaction.

There are several RNA dependent DNA polymerases on the market that can be used for RT. The most common two are avian myeloblastosis virus reverse transcriptase (AMV-RT) and Moloney murine leukaemia virus reverse transcriptase (MMLV-RT). AMV-RT is a more robust enzyme and has a greater processivity than MMLV-RT (Brooks, 1995). Both enzymes work optimally in the region of 37-42°C, which makes them susceptible to problems during first strand synthesis if there is a high degree of secondary structure

present. There are enzymes on the market, which to some extent can avoid problems with RNA secondary structure such as Tth polymerase. Tth polymerase is derived from the thermostable bacteria *Thermus thermophilus* (Myers, 1991). The enzyme in the presence of Mn^{++} ions (Chiocchia, 1997) has both PCR and RT activities allowing a “single-enzyme” one-step RT-PCR to be performed. Unlike AMV-RT and MMLV-RT, Tth polymerase is a truly thermostable enzyme allowing the RT reaction to be carried out at a higher temperature (61°C). Only the primer T_m limits the temperature at which the RT reaction can be carried out. Carrying out RT reactions at a higher temperature (61°C instead of 45°C) has the advantage of relaxing secondary structure within the mRNA, which can affect the ability of the RT enzyme to generate transcripts (Bustin, 2000). The co-purification of RT-PCR inhibitors during RNA extraction can present as a serious problem to accurate and reproducible quantification of mRNA levels (Cone, 1992). Common PCR inhibitors include heavy metals (Wilson, 1997), residual presence of heparin (anti-coagulant) (Beutler, 1990) and haem compounds like haemoglobin (Akane, 1994) and myoglobin (Belec, 1998). Tth polymerase has been shown to be very resistant to the inhibitory effects of K^+ and Na^+ (Al Soud, 1998) and biological sample contaminants (Poddar, 1998). The sensitivity of target mRNA detection using Tth polymerase has also been reported to be very high, with detection of low abundance mRNA from a single cell being possible (Chiocchia, 1997). Therefore, Tth polymerase displays many properties that make it suitable for one-step, specifically primed, quantitative RT-PCR.

3.1.7 Aim of this chapter

The TNF superfamily is an ever-growing group of powerful immunomodulatory molecules. Each member has a complex role to play in the initiation or inhibition of an immune response. As the family grows, the interactions of each of the members and their receptors form an even more complex web of interacting effector pathways. Many lines of evidence in both animal model and human studies indicate an association of aberrant LIGHT expression with the development and maintenance of immune-mediated diseases. The aim of this chapter is to examine the mRNA expression of LIGHT and its associated receptors (HVEM, LT β R and DcR3) in CD and SLE. CD is characterised by profound inflammation in the small intestine and SLE is associated with anti-DNA autoantibodies and glomerulonephritis and these manifestations have been clearly identified in LIGHT-Tg mice. We speculate that increase expression of LIGHT may contribute to the strong Th1 response associated with both conditions. A cohort of WG patients was also included in the study, as the disease is characterised by the presence of autoantibodies and glomerulonephritis.

3.2 MATERIALS AND METHODS

3.2.1 Jurkat T cell stimulation

Jurkat cells were grown in RPMI 1640 (Sigma) supplemented with 10% fetal calf serum (FCS) (Sigma), 2mM glutamine (Sigma) and penicillin/streptomycin solution (Sigma) and incubated at 37°C in 5% CO₂. For the stimulation time-course assay, cells were grown in 6 well tissue culture plates (Greiner) at 1x10⁶ per ml. At time zero, cells were stimulated using a combination of 10 ng/ml PMA (Sigma) and 1 µg/ml ionomycin (Sigma), unless otherwise stated. Cells were harvested for RNA extraction over a period of 48 hrs.

3.2.2 Patient Samples

Whole blood samples (3 ml) were collected into sterile EDTA Vacutainer tubes from 35 healthy controls, 27 CD, 15 WG and 14 SLE patients. Consent was obtained from all patients in accordance with both the Dublin Institute of Technology's ethics review board and St James's hospital ethics review board.

As samples for medical based research are becoming more difficult to obtain, we decided to use existing intestinal tissue that had been collected as part of a wider study investigating the molecular mechanisms involved in the destruction of epithelial cells in CD patients. For that study the epithelial layer was striped from the duodenal biopsy using an enzymatic

digestion protocol, samples were then frozen and transported on dry ice before being processed for RNA extraction. The samples collected included 9 patients with untreated or active disease, 2 treated patients that were on a GFD and 4 disease controls. Intestinal biopsies were collected from CD patients undergoing routine diagnosis at St James's hospital and all patients had given informed consent.

3.2.3 Total RNA isolation from cultured Jurkat T cell and peripheral blood leukocytes

Erythrocytes were lysed in red blood cell (RBC) lysis solution (155mM ammonium acetate, 10mM Potassium Hydrogen Carbonate, 1mM EDTA). PBL were pelleted at 3000 rpm for 5 minutes at room temperature. The PBL pellet was then briefly washed in RBC lysis solution, before being homogenised in 1 ml of Tri reagent (Invitrogen) using a sterile 23g needle and syringe. Tri reagent combines phenol and guanidine thiocyanate in a monophasic solution to facilitate the immediate and most effective inhibition of RNase activity. Total cellular RNA was extracted as per the manufacturer's instructions; RNA pellets were resuspended in RNase free water and samples were stored at -80°C pending further analysis. Cell lines were spun at 3000 rpm for 5 mins to remove cell culture media, RNA was then extracted from these in the same manner as WBCs.

3.2.4 Total RNA isolation from duodenal biopsies

Biopsy material was transported on dry ice and stored at -80°C before processing for RNA isolation. Three biopsies were used for each patient, firstly the biopsies were teased apart in $100\mu\text{l}$ of Tri reagent (Invitrogen) on a sterile microscope slide which had been pre-treated with RNazap (Sigma). The crudely broken down sample was then transferred to a 1.5 ml eppendorf where an additional $100\mu\text{l}$ of Tri-reagent was added, the sample was then further broken down using a motorised pellet pestle (Sigma). Finally, a further $800\mu\text{l}$ of tri-reagent was added to the eppendorf and passed through a 23g needle several times. This processing ensured full homogenisation of the sample. Total RNA was then isolated as per the manufacturers instructions.

3.2.5 Isolation of peripheral blood mononuclear cells (PBMCs) and granulocytes

PBMCs were isolated using Histopaque-1077 (Sigma). Histopaque-1077 is a solution of polysucrose and sodiumdiatrizoate, adjusted to a density of 1.077 g/ml . During centrifugation, erythrocytes and granulocytes are aggregated by the polysucrose and rapidly sediment. Lymphocytes and other mononuclear cells remain at the plasma/histopaque-1077 interface. PBMC were isolated as per the manufacturer's instructions. The resulting PBMC pellet was processed for total RNA isolation using Tri-reagent. The granulocytes were retrieved from the sedimented pellet following histopaque-1077 separation from the

PBMCs. The pellet contains a mix of granulocytes and erythrocytes. Erythrocytes were lysed using RBC lysis buffer and following centrifugation the resulting granulocyte pellet was processed for total RNA isolation using Tri-reagent.

3.2.6 Total RNA quantification

Total RNA from the cell lines, peripheral blood and duodenal biopsies was quantified using RiboGreen quantitation reagent (Molecular probes). Ribogreen is an ultra sensitive fluorescent stain for quantifying RNA in solution. The assay was carried out as per the manufacturer's instructions and measurements were taken on a VersaFluor™ Fluorimeter (BioRad). The total RNA concentration of each sample was quantified in this manner and then samples were diluted in nuclease-free water (Gibco) to a working concentration of 50 ng/μl, which was determined to be sufficient for Real-time PCR analysis.

3.2.7 Standard curve preparation for quantitative Real-time PCR

In order to carry out absolute quantification a series of standards were produced. This was done by cloning the PCR product of interest into the multiple cloning site of a pCR TOPO 2.1 vector (Invitrogen) as stated in the manufacturer's instructions. White positive transformed bacterial colonies were selected and isolation of the recombinant plasmid was

carried out using a Wizard® Plus SV miniprep DNA purification system (Promega). Purified plasmid was quantified using a Fluorescent DNA quantitation kit (BioRad) and fluorescent measurements were taken on a VersaFluor™ Fluorimeter (BioRad). This allowed the exact number of plasmid molecules per µl of plasmid miniprep to be calculated as follows (Whelan, 2003):

Weight in Daltons (g/mol) = (bp size of ds product)(330 Daltons X 2nt/bp)

Hence: (g/mol)/Avogadro's number = g/molecule = copy number

(Where: bp = base pair, ds = double stranded, nt = nucleotide, Avogadro's number = 6.023×10^{23})

Each plasmid contains a single copy of our sequence of interest. These could then be used to generate accurate standards for quantitative Real-time PCR over the range of 1×10^7 to 1×10^2 copies.

3.2.8 Real-time quantitative PCR

One-step quantitative RT-PCRs were performed on a LightCycler (Roche) using a LightCycler RNA master hybridisation probes RT-PCR kit (Roche). This kit utilises the ability of Tth polymerase to carry out both RT and PCR activities in the presence of Mn^{++} ions. Primers and hybridisation probes (Table 3.01) used in this study were designed using the LightCycler probe design software (Roche). Primers were designed so they spanned

exon-intron boundaries so that they would not amplify sequences from genomic DNA. In the case of quantifying LIGHT and the splice variant deltaLIGHT the same primers are used but the LIGHT hybridisation probes bind to the region that is spliced out in the alternative transcript and therefore detect only the full-length message (Fig 3.02). The deltaLIGHT hybridisation probes span across the splice site and can therefore only cause fluorescent resonance energy transfer (FRET) when bound to the spliced message. In this way, we can track changes in the levels of the two different spliced variants of LIGHT. The one-step quantitative RT-PCR thermocycling conditions were as follows 61°C for 20 mins, 95°C for 2 mins followed by 45 cycles of 95°C for 0s, 55 °C for 12s and 72°C for 14s.

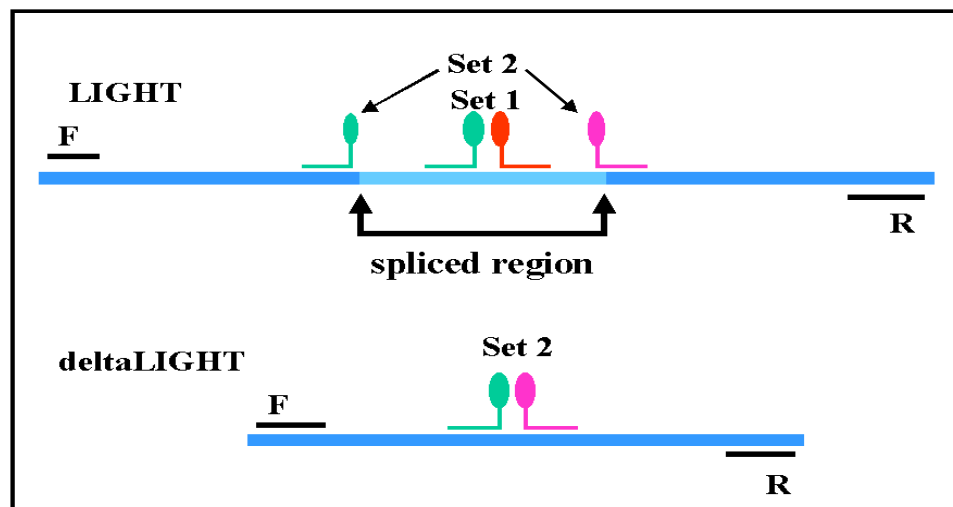


Fig 3.02 Placement of hybridisation probes to selectively detect different splice variants of LIGHT. The first set of hybridisation probes (set 1), bind to a sequence within the spliced region, which is only present in the full-length mRNA transcript. The second set of hybridisation probes (set2) span the splice junction site and are therefore separated in the full-length transcript. In the alternative transcript, they can bind in close

proximity to each other allowing FRET to occur. The advantage of this system is that only one set of primers is used to amplify both transcripts, this will ensure that the efficiency of both PCRs will be similar allowing levels to be directly compared.

3.2.9 Statistical analysis

A non-parametric Mann-Whitney U-test was performed to compare the median mRNA expression of two sample populations for statistical differences. P values were two-sided and statistical significance was considered when $P \leq 0.05$. Correlations between the expression of different mRNAs within a sample group were measured using Spearman's rank order correlation coefficient. Results were deemed to be statistically significant when $P \leq 0.05$. A students T test was performed to compare the mean mRNA expression values from the different cell populations in the control and SLE patients. P values were two-sided and statistical significance was considered when $P \leq 0.05$.

	Primer/hybridisation probe seq (5' to 3')	Conc (µM)
LIGHT		
Forward	GACAGACCGACATCCCATT	1.0
Reverse	TGCTGGGTTGACCTCGT	1.0
Probe 1	GCTGCACTGGCGTCTAGGAGAGA-f	0.2
Probe 2	x-CGTCACCCGCTGCCTGACG-p	0.2
deltaLIGHT		
Probe 1	ACCGGAGACAGTGGTGCAGTGTGG-f	1.0
Probe 2	x-CCGGGACGGACCTGCAGG-p	1.0
HVEM		
Forward	ATGTAGTCAAGGTGATCGT	0.2
Reverse	GTATCTCTGGCGTCGG	0.2
Probe 1	GGTGGCCGTGGAGGAGACAATACCCTCATTACAG-f	0.2
Probe 2	x-CGAGGAGCCCAAACCACTGACCCA CAGACTCT-p	0.2
DcR3		
Forward	TTTCTGCTTGGAGCAC	1.0
Reverse	CCTCTTGATGGAGATGT	1.0
Probe 1	CACCTTCTCAGCCAGCAGCTCCAGCTCAG-f	0.2
Probe 2	x-CAGTGCCAGCCCCACCGCAACT-p	0.2
LTβR		
Forward	GCAAAAATCCATTAGAGC	1.0
Reverse	GGAAGTATGGATGGGC	1.0
Probe 1	GAAACTGGGATCGCTGCTCAAGAGGC-f	0.2
Probe 2	x-CCGCAGGGAGAGGGACCC-p	0.2
INF-γ		
Forward	CAAAAGAGTGTGGAGACC	1.0
Reverse	TCGACCTTGAAACAGCA	1.0
Probe 1	CCAACGCAAAGCAATACATGAACTCATCCAAGTGATG GC-f	0.2
Probe 2	x-CAACTGTCCGAGCAGCTAAAACAGGGAAGCG-p	0.2

Table 3.01 **Primers and hybridisation probes used for Real-time quantitative RT-PCR.**

Fluorescein (f); phosphate (p); LCRed 640/705 dye (x).

3.3 RESULTS

3.3.1 Standard curve generation for absolute quantification

To perform absolute quantitative Real-time PCR a series of standards were produced for each of the mRNAs being analysed in this study. To do this the PCR products generated using the primers in Table 3.01 for each of the mRNA species and were cloned into a pCR 2.1 TOPO vector. Positive recombinant plasmids could then be grown in bacterial culture from which stocks of the plasmids could be purified and the copy number calculated. Once the copy number was calculated, standard curves could be generated by serially diluting the recombinant plasmid over the range of 1×10^7 to 1×10^2 , an example of a typical result is seen in Fig 3.03. Using this method to generate standard curves, from which unknown samples could be measured, proved to be very reproducible from assay to assay (Fig 3.04). Using the slope of each standard curve the efficiency of each PCR could be established. As can be seen from Table 3.02 each of the quantitative PCRs has a very high efficiency (~100%) indicating that the RT-PCR protocols have been successfully optimised.

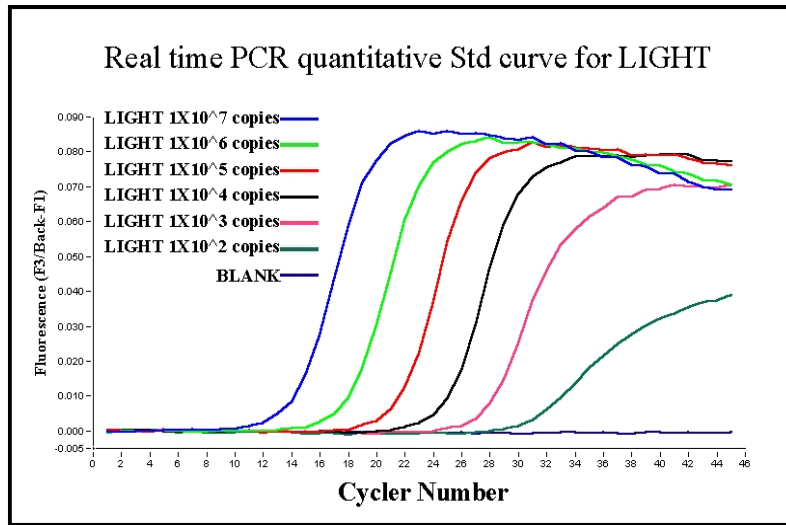


Fig 3.03 Real-time standard curve for quantifying LIGHT mRNA copy numbers. This curve has a wide dynamic range of 6 orders of magnitude.

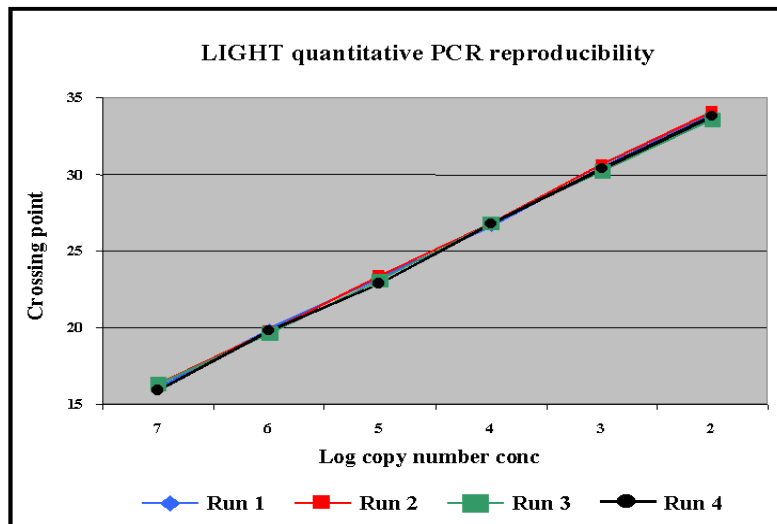


Fig 3.04 Reproducibility of crossing point verses starting copy number of LIGHT plasmid molecules.

Real-time PCR efficiency calculations

	Slope	E = 10 ^{-1/slope}	% E
LIGHT	-3.324	1.999	99.96
deltaLIGHT	-3.254	2.029	101.46
HVEM	-2.908	2.207	110.37
LTβR	-3.503	1.930	96.48
INF-γ	-3.063	2.121	106.03
DcR3	-3.808	1.831	91.53

Table 3.02 **PCR efficiency for quantitative RT-PCR protocols.** Efficiency (E) is calculated for the slope of the standard curve. E = 2 is equivalent to E = 100%, indicating that there is optimal amplification of the amplicon during the PCR phase.

3.3.2 Total RNA extraction

The extraction of high quality RNA is essential in any gene expression study. We used a commercial RNA extraction solution called Tri-reagent to perform total RNA isolation from the cells and tissue used in this study. This protocol is quick and allows the extraction of high quantity RNA as indicated by a strong 28S and 18S ribosomal bands. Fig 3.05 shows 4 total RNA samples as a representative of the high quality RNA isolated using this method, each lane contains approximately 1 μ g of total RNA.

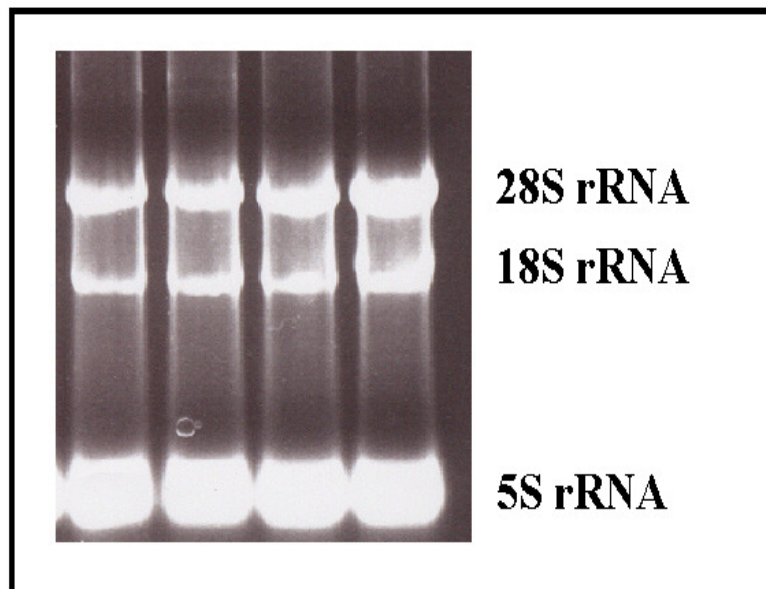


Fig 3.05 Total RNA extracted using Tri-reagent.

3.3.3 Effect of PMA concentration on the expression of LIGHT

In order to ensure that we could measure changes in mRNA expression using our RT-PCR protocol we used the Jurkat T cell line as an in vitro model. In the first experiment using Jurkat cells, we tested the effect that 24 hr stimulation using PMA and ionomycin (P/I) would have on the expression of LIGHT mRNA. This demonstrated that the stimulation of LIGHT message is dependent on PMA, (Fig.3.06) ionomycin alone is insufficient to induce expression. From this experiment it was decided that 10ng/ml PMA and 1µg/ml ionomycin was sufficient to induce an upregulation of LIGHT mRNA in Jurkat T cells and these concentrations were used in further experiments.

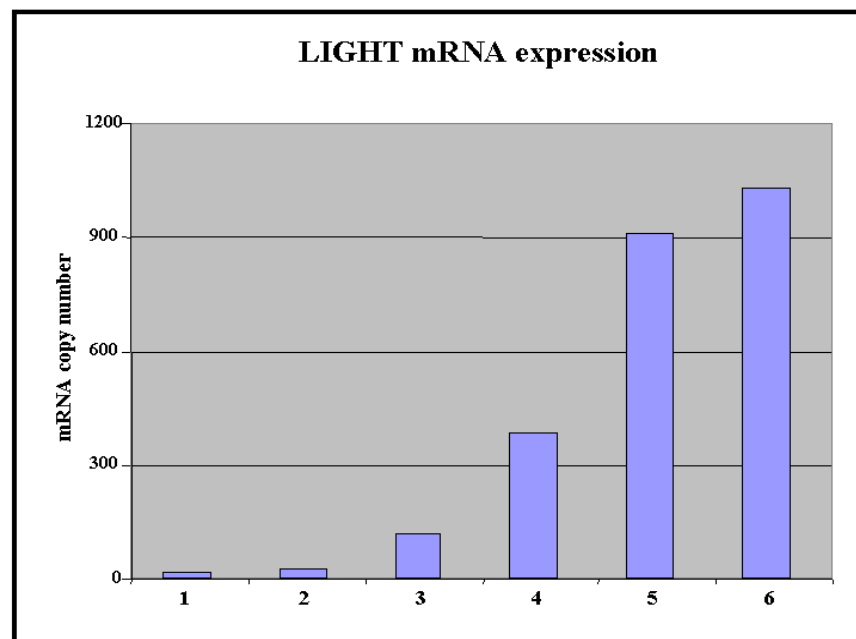


Fig 3.06 LIGHT mRNA expression is dose dependent on PMA. 1: RPMI control; 2: 1µg/ml ionomycin; 3: 10ng/ml PMA; 4: 1ng/ml PMA and 1µg/ml ionomycin; 5: 10ng/ml PMA and 1µg/ml ionomycin; 6: 100ng/ml PMA and 1µg/ml ionomycin

3.3.4 Effect of stimulation on mRNA expression over 48hrs

While the kinetics of LIGHT and HVEM expression have been previously established (Granger, 2001) the quantification of their mRNA changes over a 48 hr period would provide a good test for our Real-time RT-PCR protocol. Jurkat cells were cultured for 48 hrs in the presence or absence of P/I, cells were harvested at various time-points and the expression of LIGHT, deltaLIGHT and HVEM mRNA were analysed. Visible changes in the levels of LIGHT mRNA expressed occur after ~ 8 hrs and steadily increased and by 24 hrs there was approximately an 8-fold increase in LIGHT expression (Fig 3.07) when compared with the RPMI control. By 48 hrs the level of LIGHT mRNA has completely diminished back to low basal levels. The expression of deltaLIGHT shows a similar pattern of expression to LIGHT following stimulation, mRNA levels peak at 28 hrs with an approximate 7 fold increase in message levels (Fig 3.07). At the 48 hr time point the expression of deltaLIGHT mRNA remains ~ 2.5 fold higher than the RPMI control. In contrast to LIGHT, HVEM mRNA levels undergo a rapid downregulation with changes seen as early as 4 hrs. After 24 hrs there is approximately a 3.5 fold decrease in the total amount of HVEM mRNA expressed, and by 48 hrs expression starts to return to normal basal levels (Fig 3.08).

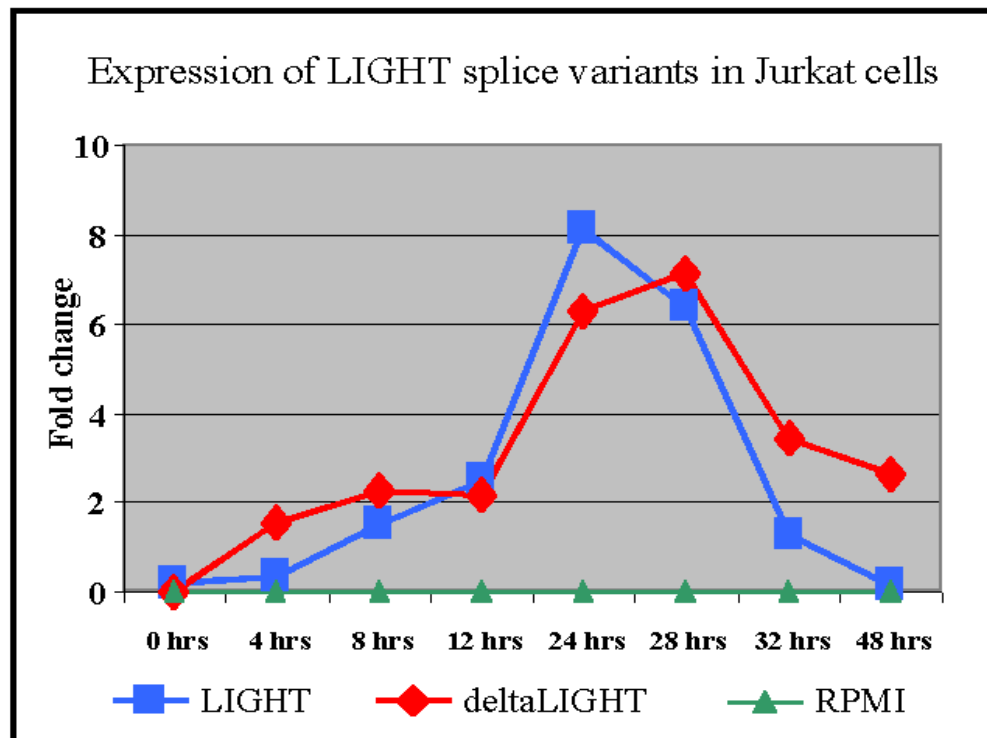


Fig 3.07 48hr expression pattern of LIGHT and deltaLIGHT mRNA following stimulation of Jurkat T cells. Stimulation was carried out using PMA (10ng/ml) and ionomycin (1µg/ml). The results are expressed as fold change of the RPMI control at each time point.

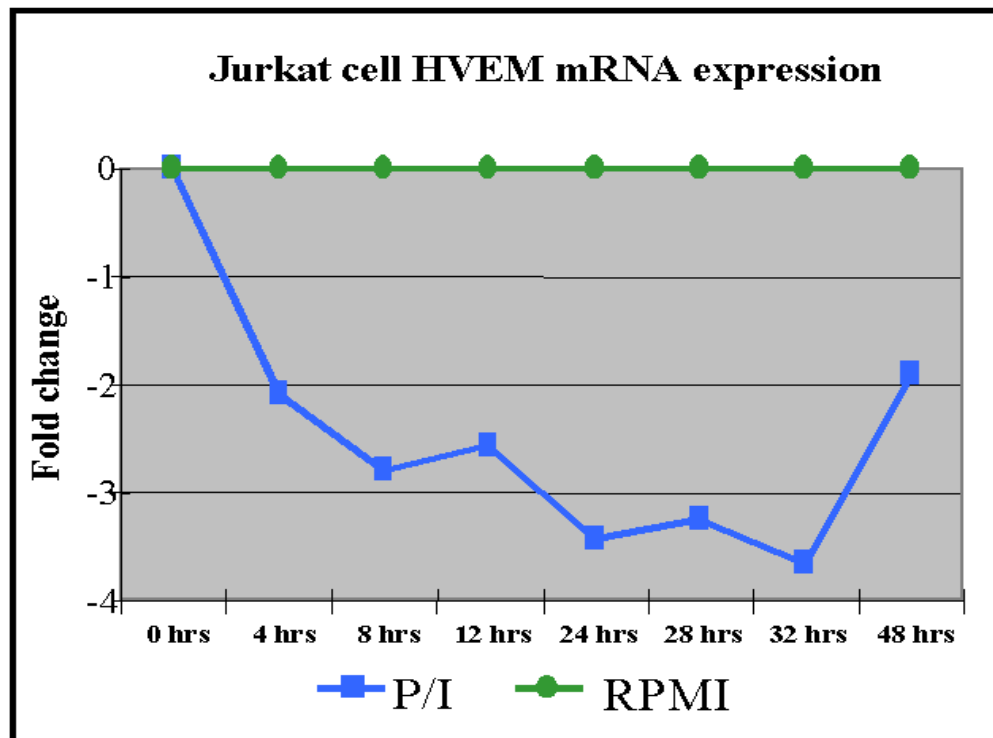


Fig 3.08 48hr expression pattern of HVEM mRNA following stimulation of Jurkat T cells. P/I: PMA (10 ng/ml) and ionomycin (1 μ g/ml). The results are expressed as fold change of the RPMI control at each time point.

3.3.5 Expression of mRNA in peripheral blood of test cohorts

Once we established that our Real-time PCR protocol was suitable for detecting changes in the level of mRNA using the Jurkat T cells, we proceeded to quantify the levels of mRNA expressed in the periphery of a normal control (NC) cohort (35 samples) and of patients with CD (27 samples), WG (15 samples) and SLE (14 samples). The expression of LIGHT, deltaLIGHT, HVEM, DcR3, LT β R and INF- γ mRNA were analysed for all the groups (Fig 3.09 – 3.14). When the CD cohort was compared to the control group, no statistical differences were seen between the two groups for any of the mRNA species with the exception of INF- γ (P = 0.008). The WG cohort showed lower expression of LIGHT (P = <0.0001) and deltaLIGHT (P = 0.002) than the control group. Whereas the levels of HVEM, LT β R, DcR3 and INF- γ mRNA expression in the periphery were not statistically different from that of the control cohort. The SLE patients showed a lower expression of LIGHT (P = 0.002), no change was seen in the levels of DcR3 and elevated levels of deltaLIGHT (P = 0.05), HVEM (P = <0.0001), INF- γ (P = <0.0001) and LT β R (P = 0.024) were seen when compared to the control cohort.

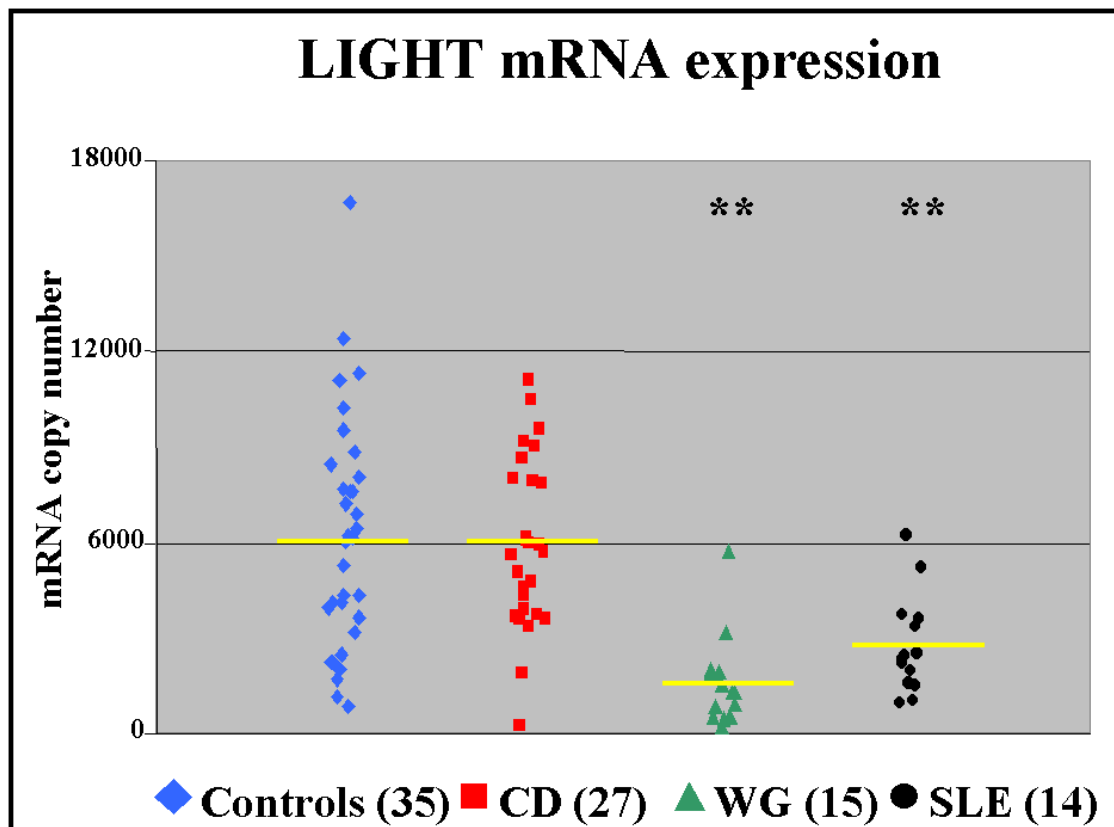


Fig 3.09 Expression of LIGHT mRNA in PBL of the patient cohorts. The number in brackets indicates the number of patients within the test group and the yellow line marks the mean of the group. ** Indicates a group that is significantly different from the controls. No difference was seen between the controls and the CD patients ($P = 0.831$). However, a statistically significant lower expression of LIGHT mRNA was seen in the WG ($P < 0.0001$) and SLE patients ($P = 0.002$).

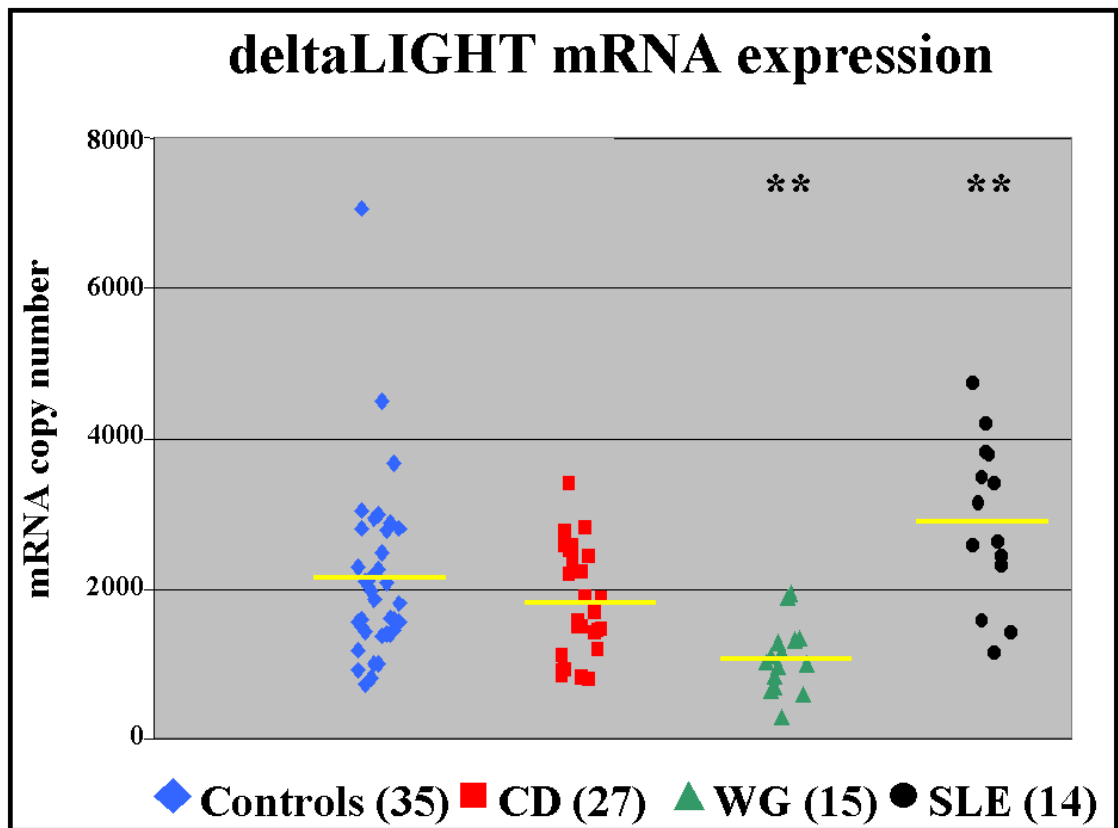


Fig 3.10 Expression of deltaLIGHT mRNA in PBL of the patient cohorts. The number in brackets indicates the number of patients within the test group and the yellow line marks the mean of the group. ** Indicates a group that is significantly different from the controls. No difference was seen between the controls and the coeliac (CD) patients ($P = 0.345$). A statistically significant lower expression of deltaLIGHT mRNA was seen in the WG group ($P < 0.0001$). The SLE patients showed a statistically significant higher expression of deltaLIGHT mRNA than the normal controls ($P = 0.017$).

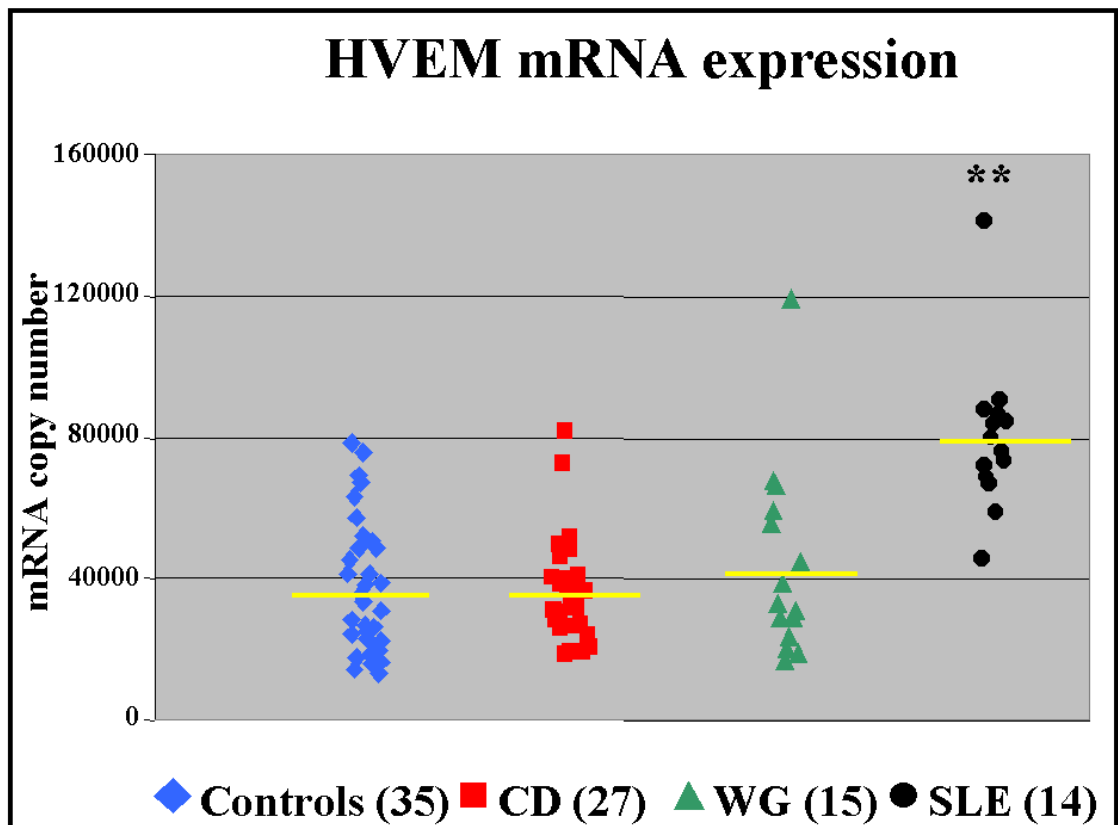


Fig 3.11 Expression of HVEM mRNA in PBL of the patient cohorts. The number in brackets indicates the number of patients within the test group and the yellow line marks the mean of the group. ** Indicates a group that is significantly different from the controls. No difference was seen between the controls and either the CD patients ($P = 0.798$) or the WG patients ($P = 0.484$). The SLE patients showed a statistically significant higher expression of HVEM mRNA than the control group ($P = < 0.0001$).

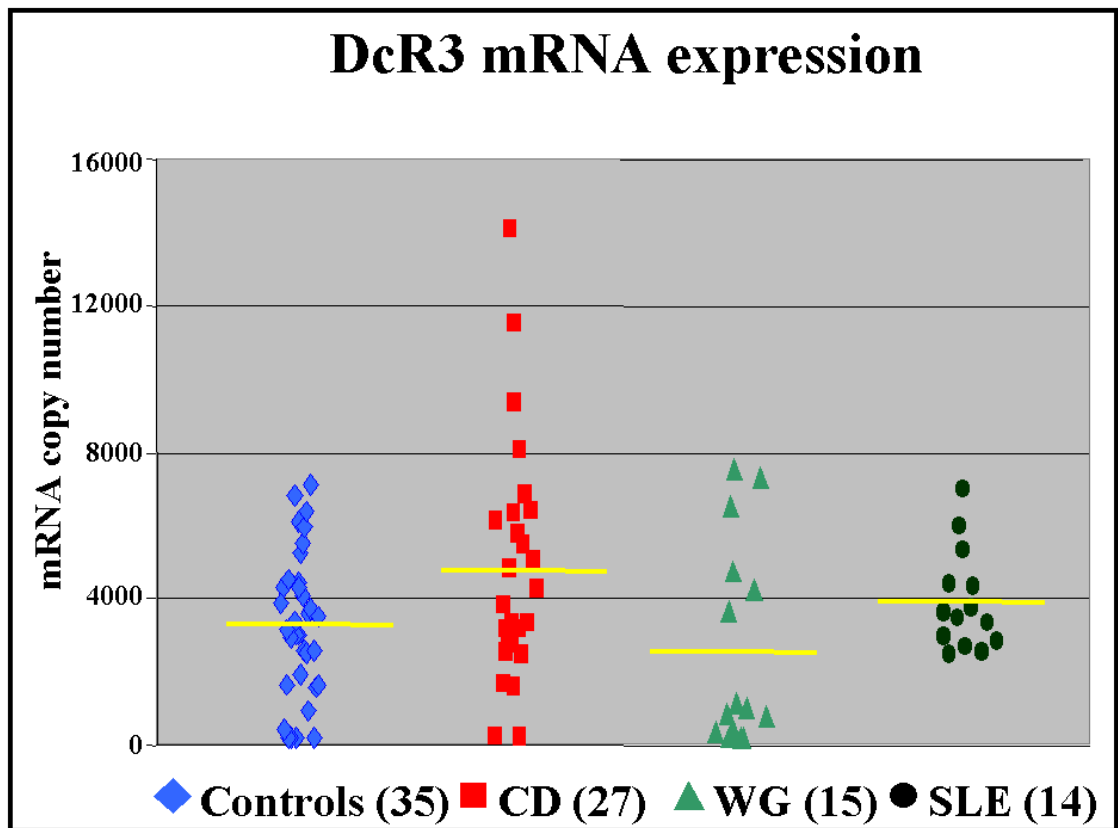


Fig 3.12 Expression of DcR3 mRNA in PBL of the patient cohorts. The number in brackets indicates the number of patients within the test group and the yellow line marks the mean of the group. No difference was seen between the controls and either the CD patients ($P = 0.232$), the WG patients ($P = 0.596$), or the SLE patients ($P = 0.521$).

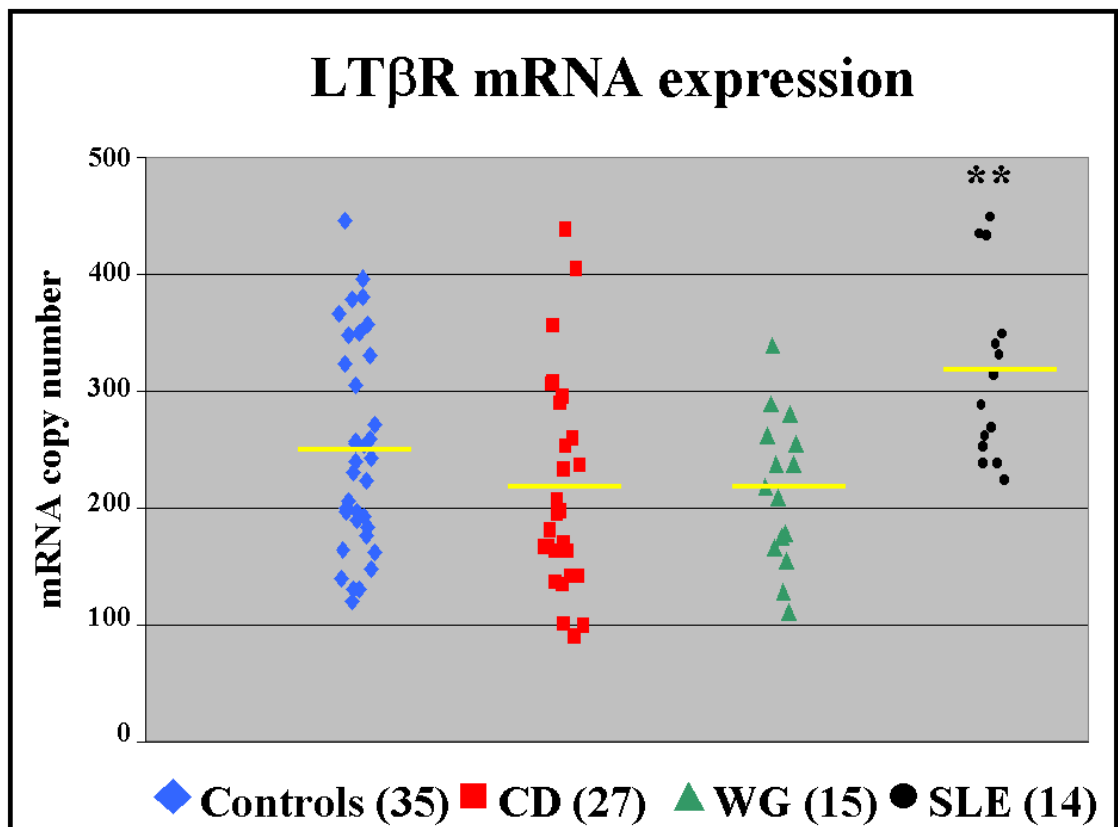


Fig 3.13 **Expression of LTβR mRNA in PBL of the patient cohorts.** The number in brackets indicates the number of patients within the test group and the yellow line marks the mean of the group. ** Indicates a group that is significantly different from the controls. No difference was seen between the controls and the CD patients ($P = 0.118$) or the WG ($P = 0.275$). A statistically significant higher expression of LTβR mRNA was seen in the SLE group ($P = 0.024$).

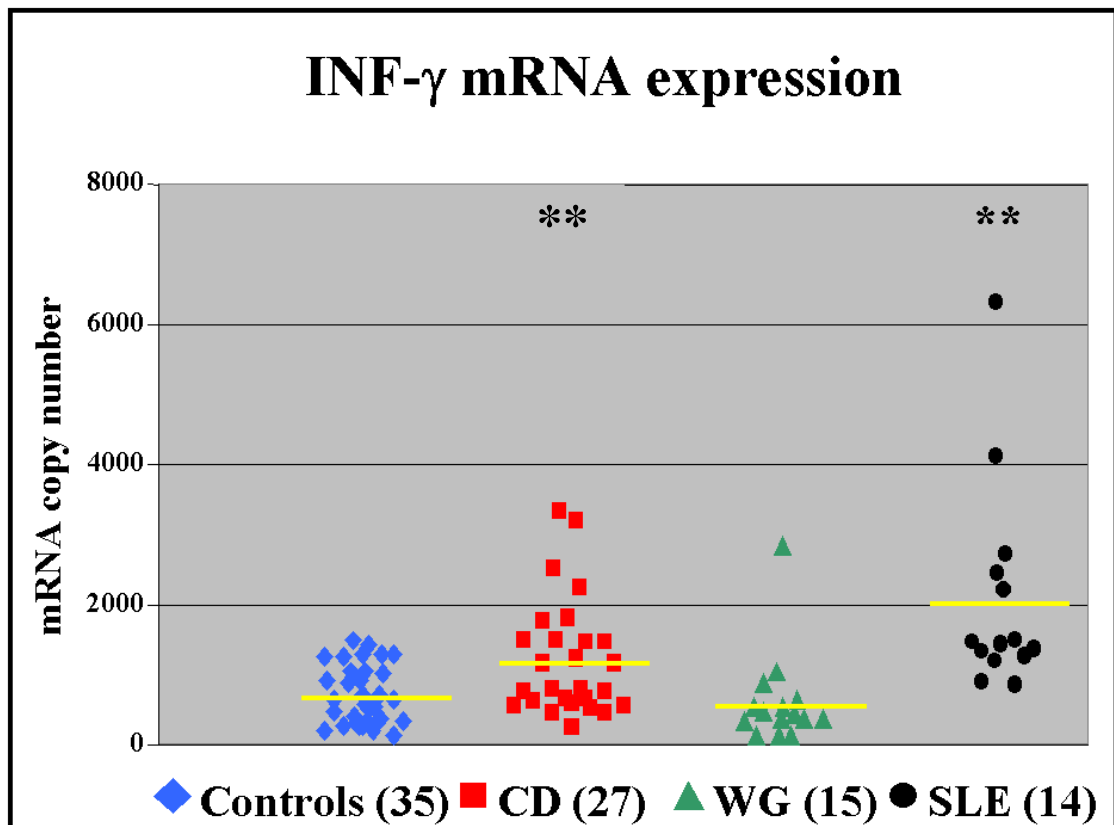


Fig 3.14 Expression of INF- γ mRNA in the PBL of the patient cohorts. The number in brackets indicates the number of patients within the test group and the yellow line marks the mean of the group. ** Indicates a group that is significantly different from the controls. No difference was seen between the controls and the WG patients ($P = 0.589$). A statistically significant higher expression of INF- γ mRNA was seen in the CD ($P = 0.008$) and SLE ($P < 0.0001$) patient groups.

3.3.6 Adjustment of mRNA expression based on lymphocytes counts

Lymphocyte counts were obtained for all patients included in the study with the exception of 2 CD and 1 SLE patient. Lymphocyte counts were only available for 6 samples of the control group at the time that blood was donated for the study. Re-adjustments were made to the Real-time quantitative RT-PCR data based on these lymphocyte counts. As we had speculated the expression of LIGHT in both SLE and WG was no longer significantly reduced when the data was analysed in this manner (Fig 3.15). The mRNA expression of deltaLIGHT, DcR3 and INF- γ was identified to be significantly elevated in the SLE cohort ($P < 0.05$). The levels of LIGHT mRNA were identified as being elevated in the CD cohort (< 0.05). The WG cohort showed very similar levels of expression for LIGHT, deltaLIGHT, DcR3 and INF- γ as the control group. Correlations between LIGHT or deltaLIGHT and DcR3 and INF- γ mRNA expression were made for the SLE cohort (Fig 3.16). LIGHT mRNA expression correlates strongly with both DcR3 ($R_s = 0.643$; $P < 0.05$) and INF- γ ($R_s = 0.687$; $P < 0.05$) mRNA levels in the SLE patients. DeltaLIGHT mRNA expression also positively correlated with DcR3 ($R_s = 0.676$; $P < 0.05$) and INF- γ ($R_s = 0.775$; $P < 0.05$) levels of mRNA.

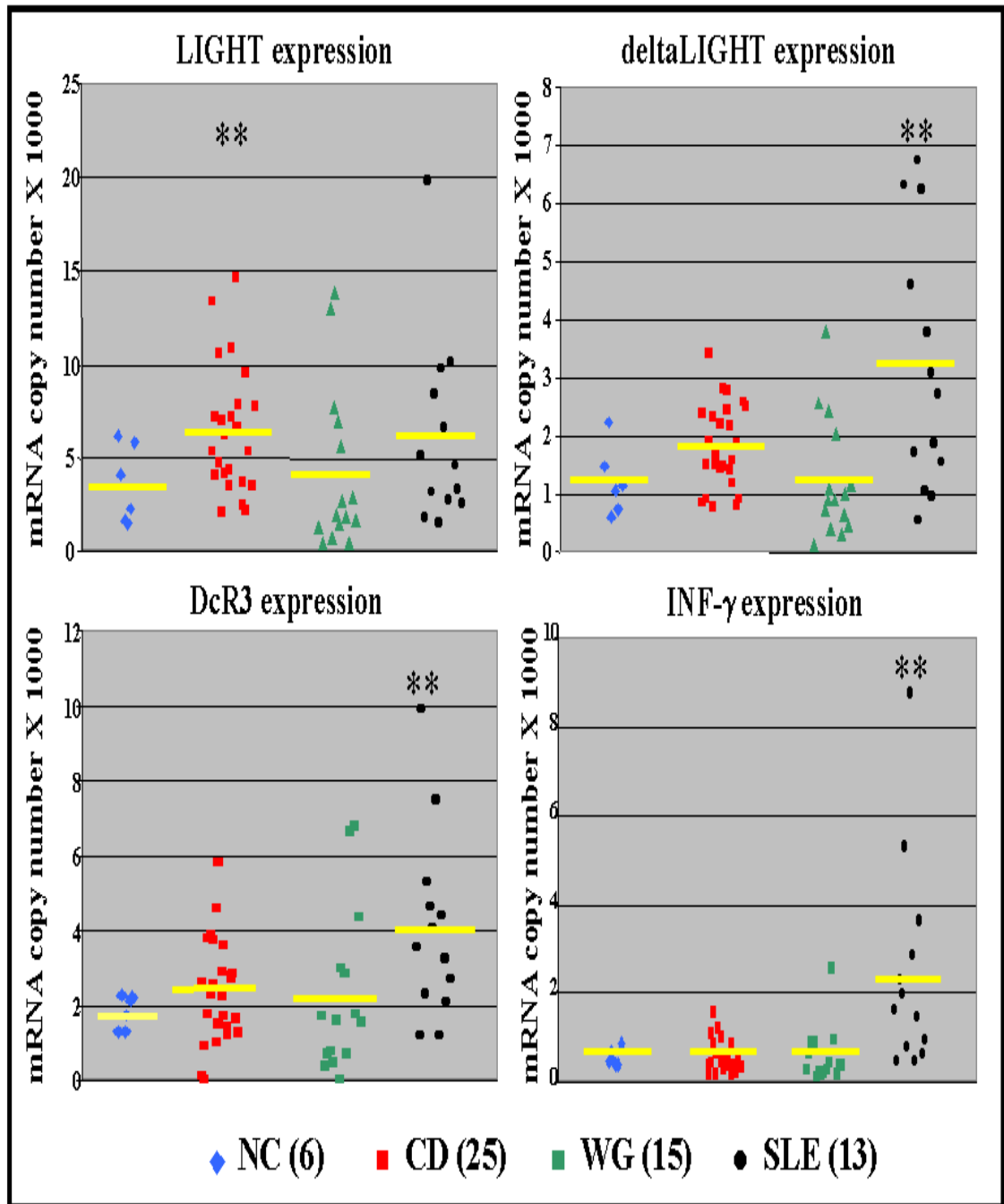


Fig 3.15 Adjustment of LIGHT, deltaLIGHT, DcR3 and INF-γ mRNA expression based on lymphocyte counts. The yellow line indicates the mean of each group, ** indicates a cohort that was significantly different from the control group (NC) i.e. $P \leq 0.05$.

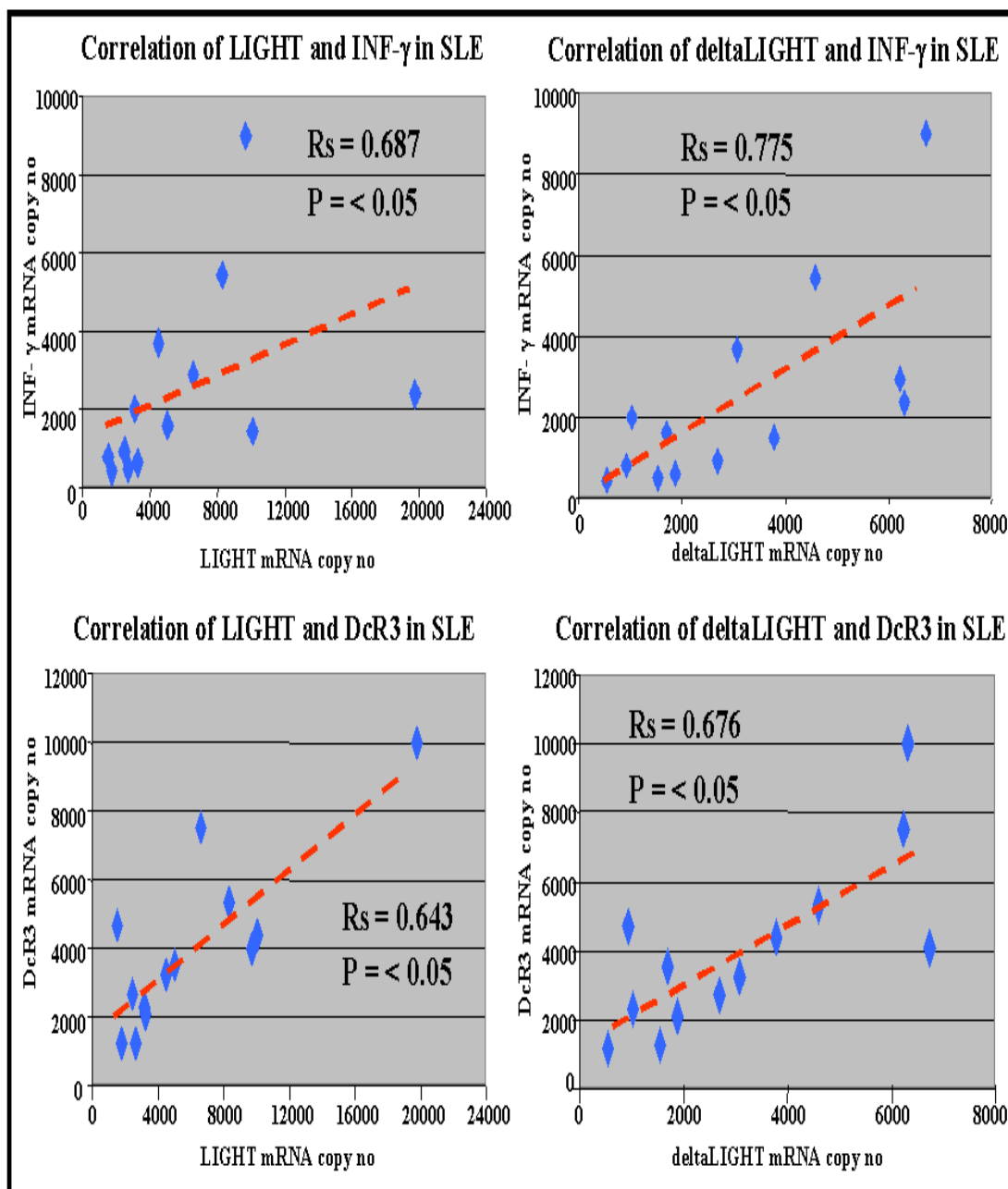


Fig 3.16 **Positive correlation of LIGHT/deltaLIGHT with both DcR3 and INF- γ in SLE patients.** Correlations were tested using the Spearman's rank correlation test. Spearman's correlation rank coefficient (R_s) and P value are included with each separate graph.

3.3.7 Stratification of CD patients based on tTG serology

For further analysis of the CD cohort we divided the samples into 2 groups based on whether they were positive or negative for anti-tissue transglutaminase autoantibodies (anti-tTG) at the time of sample collection (Fig 3.17 A). Based on this subdivision of the samples the anti-tTG positive CD patients show a higher expression of LIGHT mRNA than the normal controls ($P = 0.018$). The tTG negative CD samples fall in between the positive tTG patients and the NC cohort, not being significantly different from either group. The expression of deltaLIGHT mRNA follows a similar trend to that of LIGHT, with the highest expression in the tTG positive patients, the negative tTG patients in the middle and the NC showing the lowest expression of deltaLIGHT (Fig 3.17 B), however the results were not deemed to be statistically significant. The HVEM mRNA data was also stratified based on the tTG serology and these results were reciprocal to that of LIGHT (Fig 3.17 C). The highest levels of expression were found in the NC cohort. The tTG positive patients showed a significant reduction in HVEM compared with the NC group ($P = 0.025$). The tTG negative patients, in a similar manner to LIGHT and deltaLIGHT expression, are situated between the NC and tTG positive cohort.

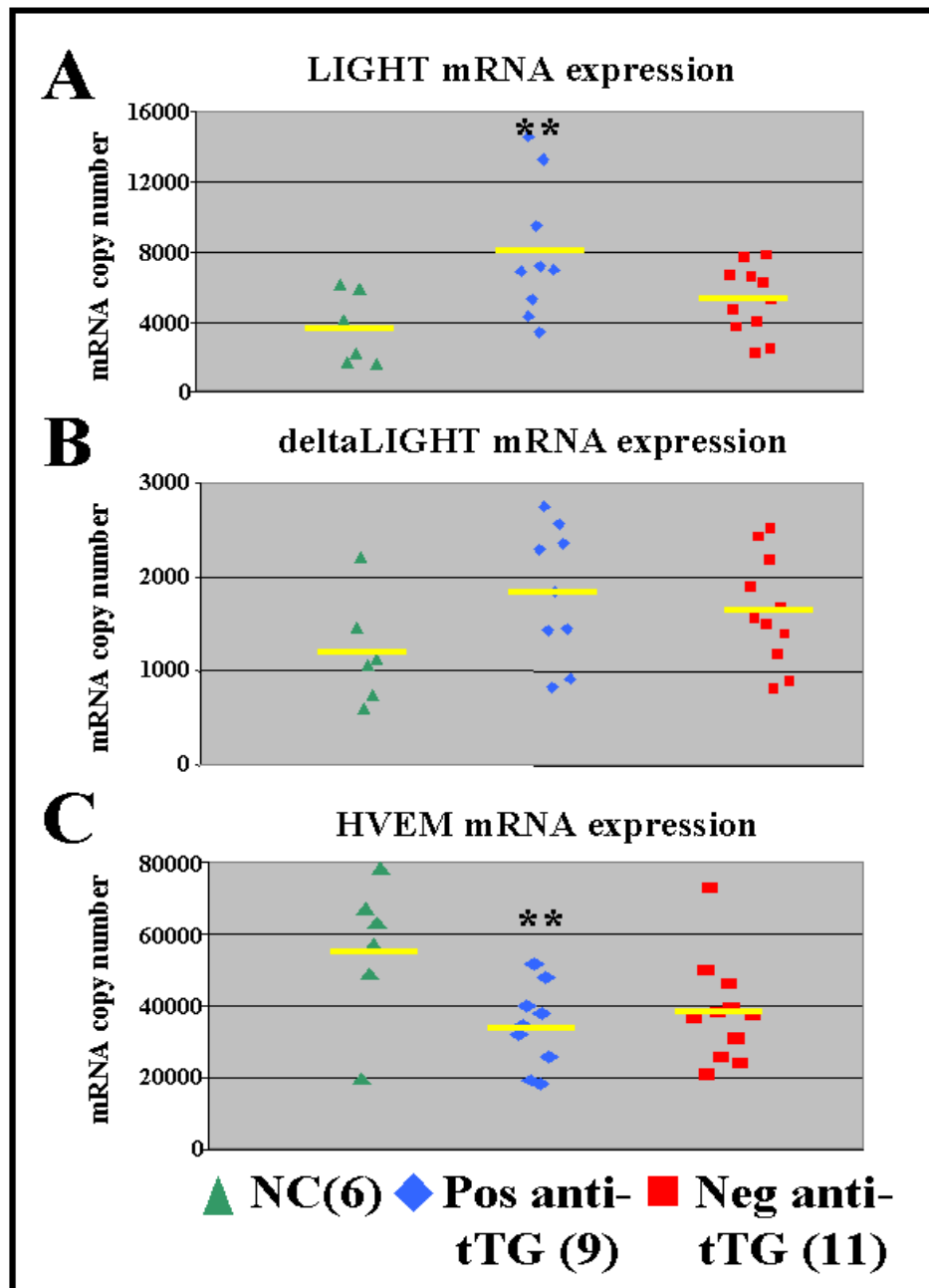


Fig 3.17 Gene expression in CD patients stratified on basis of tTG serology.

** Indicates that groups are significantly different ($P < 0.05$) from the NC group.

3.3.8 Upregulation of HVEM mRNA in granulocytes

PBMCs and granulocytes were isolated from two control and two SLE samples to test the hypothesis that HVEM was being overexpressed on cells other than lymphocytes. The results of this experiment showed that there was a statistically significant decrease in HVEM mRNA expression in PBMCs isolated from SLE samples when compared with controls ($P = 0.025$). However, there was a very significant increase in HVEM mRNA expression in the granulocyte cells isolated from SLE samples when compared with controls ($P = 0.031$). Both LIGHT and deltaLIGHT mRNAs were significantly increased in the PBMC isolated from SLE patients with very little mRNA for both variants being detected in the granulocyte cell population (Fig 3.18).

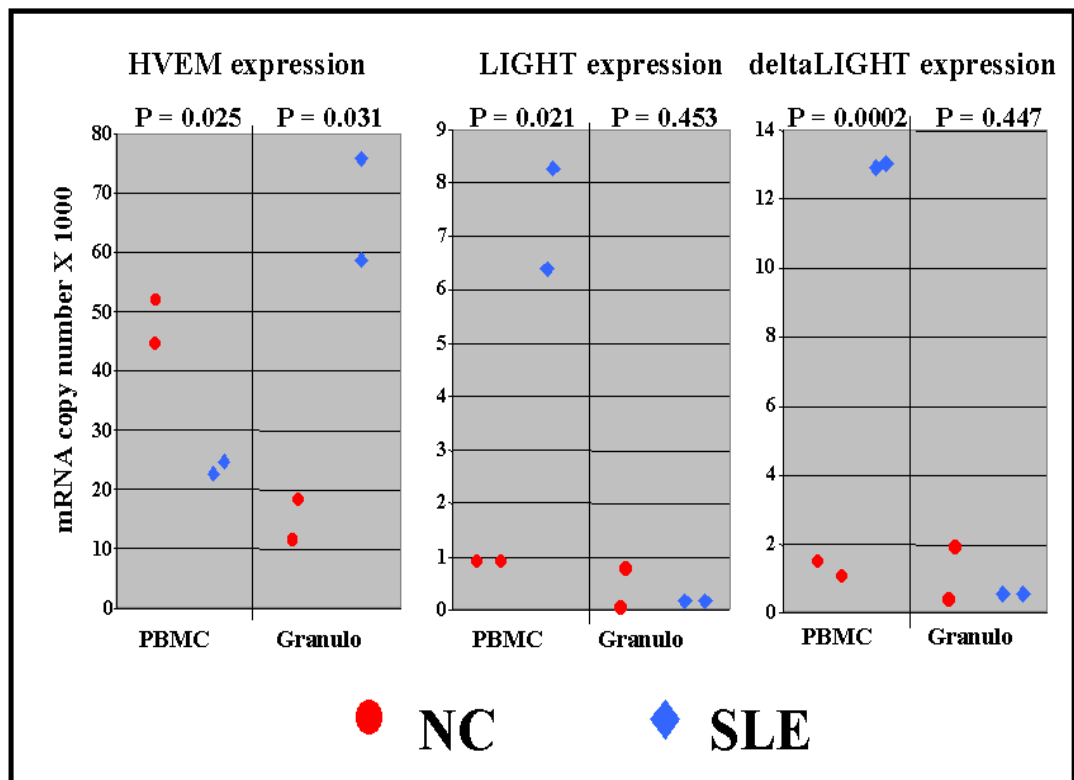


Fig 3.18 mRNA expression in PBMCs and granulocytes isolated from normal control (NC) and SLE patients. P values are indicated above each group, P <0.05 was taken to be statistically significant.

3.3.9 Gene expression within the coeliac intestinal lesion

As LIGHT overexpression has a predilection to cause intestinal inflammation, we analysed the expression of LIGHT, deltaLIGHT, HVEM, LT β R and INF- γ in the lamina propria of untreated CD (9 samples), treated CD (2 samples) and non-CD (4 samples) patients. LIGHT mRNA is significantly increased in untreated CD patients when compared with the non-CD group ($P = 0.05$). LIGHT mRNA also remained elevated in the treated CD patients however statistical significance was not achieved due to the small number of samples in this group (Fig 3.19). The expression of deltaLIGHT did not reach statistical significance difference between the untreated CD and control samples, however a general expression pattern similar to that of LIGHT was identified (Fig 3.20). The expression of HVEM mRNA in the different groups was reciprocal to that of LIGHT. The untreated CD patients had a significant decrease in mRNA expression when compared with both the non-CD ($P = 0.032$) and treated CD ($P = 0.0003$). HVEM levels in the treated CD were comparable to that of the non-CD cohort (Fig 3.21). LT β R expression patterns were similar in all three tested groups (Fig 3.22). As to be expected, the expression of INF- γ mRNA was significantly elevated in the lamina propria of the untreated CD patients when compared with the non-CD patients ($P = 0.05$). As was the case with HVEM, the levels of INF- γ mRNA in the treated CD were comparable with non-CD patients (Fig 3.23).

In addition to the expression of the above mRNA species, we also examined the levels of IL-2, LT- β and BTLA mRNA in the intestinal biopsy samples. IL-2 a Th1 cytokine that promotes the expansion of T cells has been previously reported to be elevated in CD (Lahat, 1999). Therefore, like INF- γ it acts as a positive control as it should be elevated in

the untreated CD patients. As expected, there is a significant difference ($P < 0.05$) between the untreated CD and control cohorts (Fig 3.24 A). As $LT\alpha 1\beta 2$ can also act as a ligand for $LT\beta R$, the mRNA expression of the $LT\beta$ subunit was also quantified. Our quantitative analysis shows that $LT\beta$ is not regulated at least at the mRNA level in the CD lesion (Fig 3.24 B). BTLA a recently discovered ligand for HVEM (Sedy, 2005; Gonzalez, 2005) can suppress T cell responses. In our cohort of untreated CD patients, there is a significant reduction in the level of BTLA expressed in the lamina propria when compared to the control group (Fig 3.24 C). The expression of BTLA in the treated CD patients was similar to that of the controls and was significantly higher than the untreated patients ($P < 0.05$).

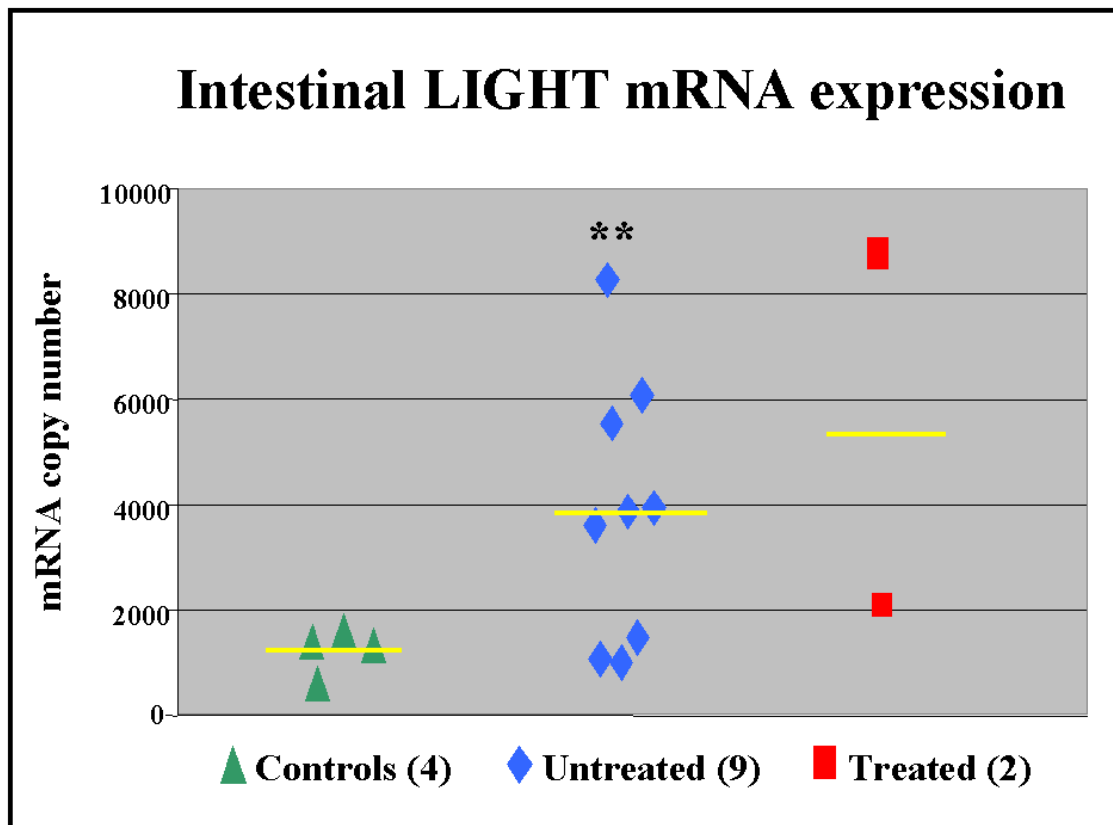


Fig 3.19 Expression of LIGHT mRNA in intestinal lamina propria. Controls, green; Untreated CD, blue; treated CD, red. The yellow line indicates the mean of each group. A significant increase in mRNA expression was seen between the control and untreated CD groups ($P = 0.05$). No statistically significant difference was seen between the control and treated ($P = 0.111$) and the untreated and treated ($P = 0.495$) groups.

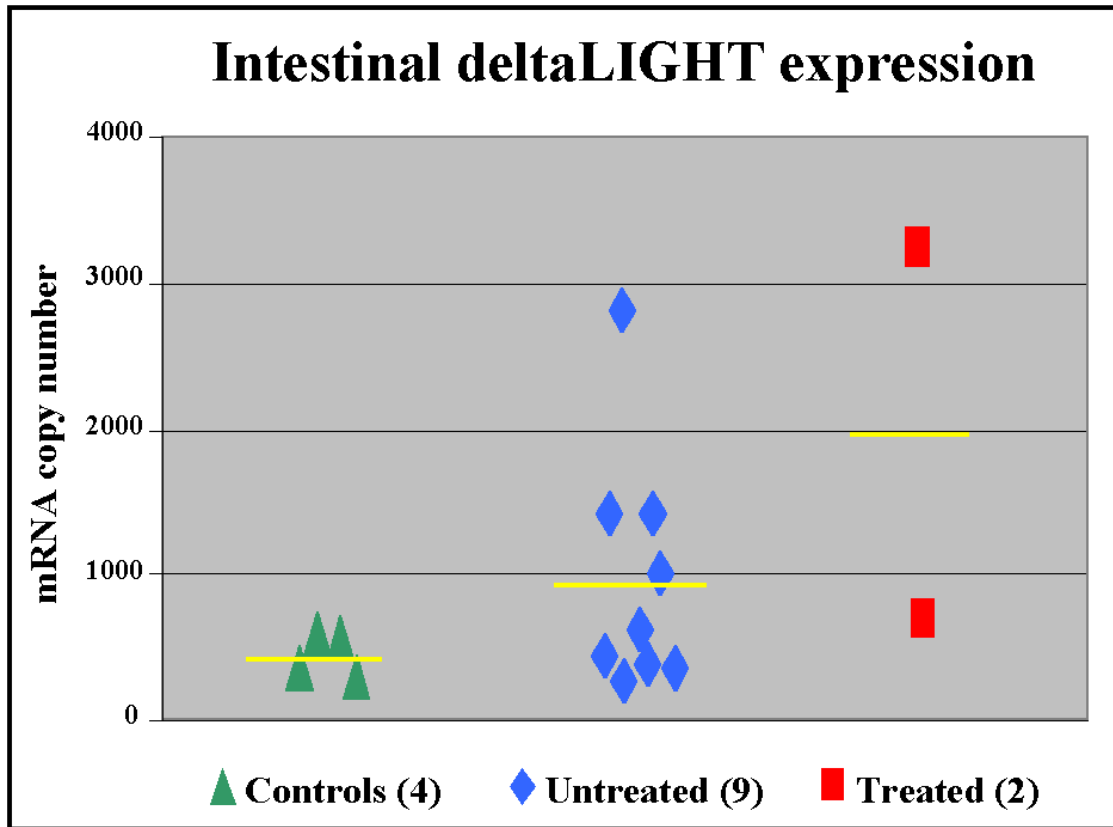


Fig 3.20 **Expression of deltaLIGHT mRNA in intestinal lamina propria.** Controls, green; Untreated CD, blue; treated CD, red. The yellow line indicates the mean of each group.

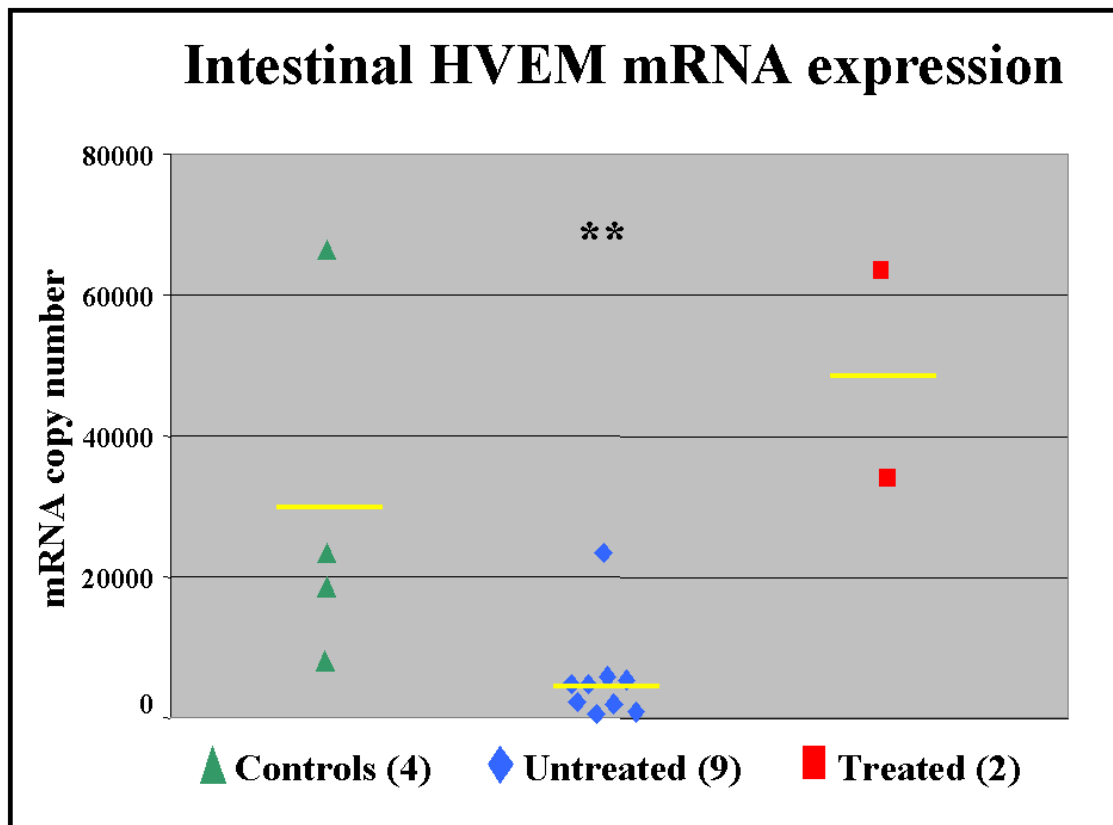


Fig 3.21 HVEM mRNA expression in intestinal lamina propria. Controls, green; Untreated CD, blue; treated CD, red. The yellow line indicates the mean of each group. No significant change was seen between the control and treated CD groups ($P = 0.404$). A statistically significant difference was seen between the control and untreated ($P = 0.032$) and the untreated and treated ($P = 0.0003$) groups.

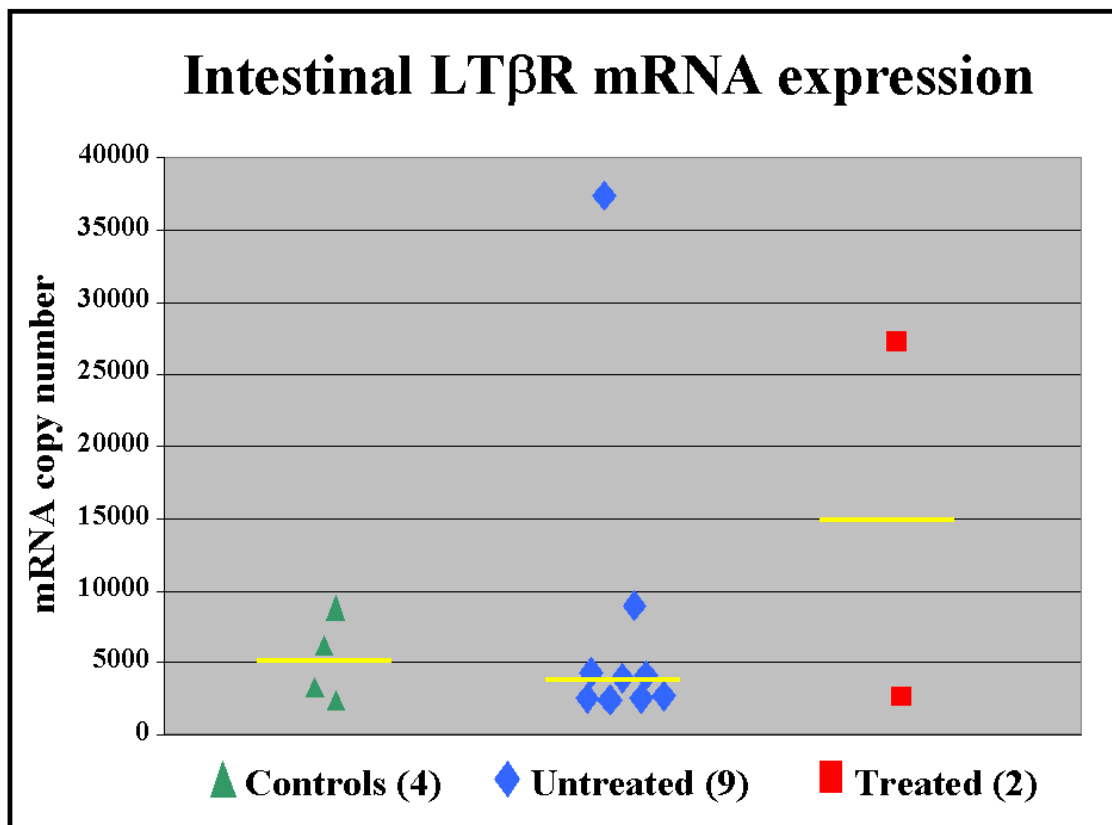


Fig 3.22 **LT β R mRNA expression in intestinal lamina propria.** Controls, green; Untreated CD, blue; treated CD, red. The yellow line indicates the mean of each group. No significant change was seen between the control and treated CD patients ($P = 0.283$) and the untreated cohort ($P = 0.722$).

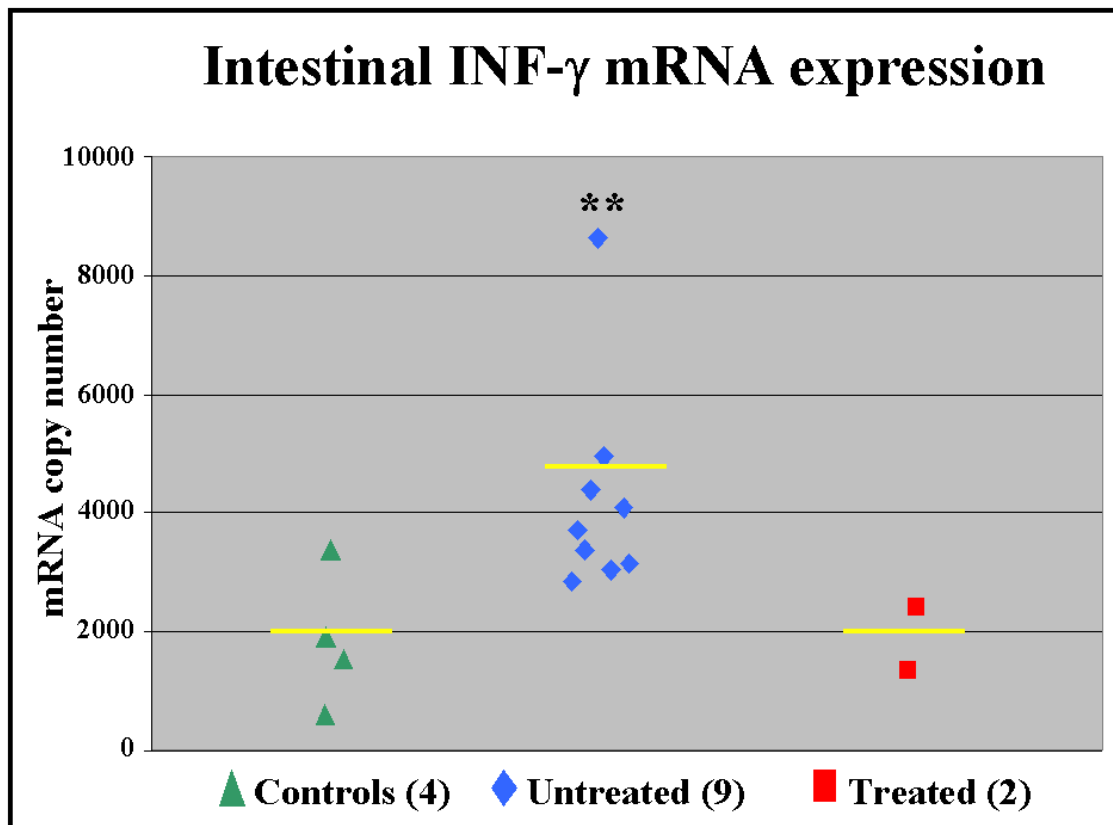


Fig 3.23 **INF- γ mRNA expression in intestinal lamina propria.** Controls, green; Untreated CD, blue; treated CD, red. The yellow line indicates the mean of each group. No significant change was seen between the control and treated CD groups ($P = 0.991$). A statistically significant difference was seen between the controls and untreated ($P = 0.034$). The change seen between the untreated and treated groups did not reach statistical significance ($P = 0.108$).

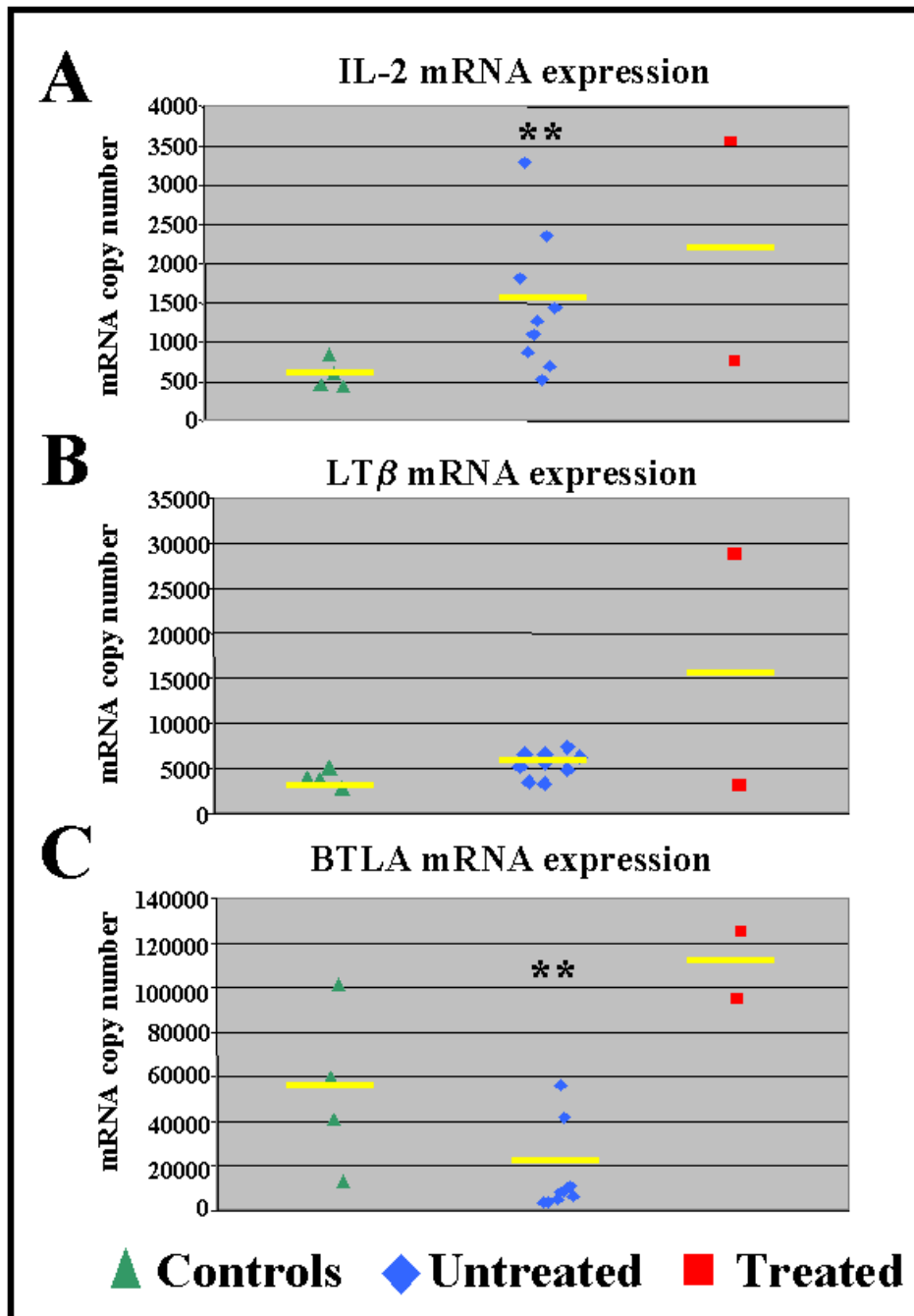


Fig 3.24 Expression of IL-2, LT β and BTLA in the lamina propria. Controls, green; Untreated CD, blue; treated CD, red. **Indicates a groups that is significantly different from the control samples (P<0.05)

3.4 DISCUSSION

3.4.1 Gene expression analysis using Real-time quantitative PCR

Cells have the ability to alter their mRNA copy numbers; this is a crucial element in the regulation of gene expression in response to a wide range of endogenous and exogenous stimuli. Many disease processes are also associated with alterations in gene expression patterns within cells. In recent years, quantitative Real-time RT-PCR has become the gold standard technique for quantifying alterations in gene expression (Bustin, 2004). This technique has a wide dynamic range ($10\text{-}10^{10}$ copies) (Saunders, 2004), is highly sensitive and specific for the amplicon of interest when specific probes are used.

In this study, the aim was to develop a quantitative Real-time RT-PCR to measure the levels of LIGHT, its splice variant deltaLIGHT and associated receptors (HVEM, LT β R and DcR3). INF- γ was also included in the study as its role in Th1 mediated diseases is well documented. In designing the RT-PCR protocol, we decided on a one-step RT-PCR approach, due to the ease of RT-PCR set up, which helps to reduce pipetting steps, and hence possible errors. There is also be a reduced risk of cross-contamination of samples with this approach. Of the various enzymes on the market, Tth polymerase was selected for use in this study. This enzyme, as mentioned previously, is capable of performing both RT and PCR stages when Mn⁺⁺ ions are present. This allows the use of one enzyme to perform both stages rather than having to employ separate RT and PCR compatible enzymes such as AMV-RT and Taq polymerase. Tth also works optimally at a specific concentration of Mn⁺⁺ ions (3.25 mM), thereby reducing the need to optimise this parameter, as would be

the case when using Mg^{++} ions with Taq polymerase. Tth is also a thermostable enzyme and works optimally at 61°C. This has the advantage of relaxing secondary structure that forms within mRNA molecules, which can prevent them from being efficiently reverse transcribed (Bustin, 2000).

We initially approached this study with the idea of performing relative quantification by expressing our target mRNA as a ratio of a housekeeping gene. Housekeeping or reference genes are those whose expression should remain at a constant level within a cell. At the outset of this study, the levels of six commonly used housekeeping genes (HPRT, ALAS, beta-globin, beta-2-microglobulin, G6PDH and PBGD) were measured in 11 normal control samples (data not shown). It was found that the expression varied from sample to sample, by up to 2 log fold for some of the genes tested. These results indicated that none of these housekeeping genes were suitable for performing relative quantification. Hence, we switched to performing absolute quantification instead.

Absolute quantification provides a more accurate and reliable, albeit more labour intensive method for the quantification of nucleic acids (Ke, 2000). A series of standards are generated and a plot of C_p versus log concentration allows the C_p of the unknown samples to be compared to the standards. Using this method, our standard curves were highly reproducible (Fig 3.04) from assay to assay, allowing accurate quantification data to be obtained. Normalisation of the data was done by quantifying the total RNA in each sample using Ribogreen fluorescent dye and copy number of each mRNA molecule was expressed per 50 ng of total RNA. The use of Ribogreen is a proven method for normalisation of samples for quantitative RT-PCR (Hashimoto, 2004).

3.4.2 Gene expression in Jurkat T cells

Once the quantitative Real-time RT-PCR assays were optimised, the next stage was to ensure that changes in mRNA copy numbers could be measured with our system. Consequently, it was decided to use the Jurkat T cell line stimulated with PMA and ionomycin as an *in vitro* model of T cell activation. In the first experiment using the Jurkat cell line, we showed that the optimal induction of LIGHT mRNA in these cells requires the synergistic stimulation by both PMA and ionomycin. Cells that were incubated with both PMA and ionomycin showed a marked increase in LIGHT mRNA expression, which was dose-dependent on PMA concentration (Fig 3.06). This result is similar to previously reported findings (Granger, 2001).

Following on from the initial Jurkat results, we performed a time-course experiment to show the kinetics of LIGHT mRNA expression over a 48-hour period post stimulation with PMA and ionomycin. From a previous study, it had been demonstrated that there is a reciprocal expression of HVEM and LIGHT upon activation of primary T cells (Morel, 2000). This study used a combination of FACS analysis and semi-quantitative PCR to demonstrate that there was a reciprocal expression pattern of HVEM and LIGHT in activated T cells. Our results from the Jurkat T cell time course experiments also demonstrated this.

Resting T cells, in this case Jurkat cells at time zero, express little or no LIGHT mRNA whereas HVEM mRNA is at maximum levels. Following activation, as LIGHT levels begin to increase, HVEM mRNA is downregulated as seen in Figs 3.07 and 3.08

respectively. We also demonstrated that deltaLIGHT mRNA transcripts follow a similar pattern to that of the full-length variant of LIGHT. By 48 hrs HVEM mRNA levels are starting to return to high basal levels and the level of LIGHT mRNA expressed has been downregulated to that of non-stimulated cells. Conversely, deltaLIGHT mRNA, remained approximately 2.5 fold higher than the RPMI control at the 48 hr time-point. This may indicate that either downregulation, post activation, of deltaLIGHT mRNA transcription takes longer than that of LIGHT or that once activated, T cells continue to express deltaLIGHT transcripts even as the cell returns to a resting state. Evidence to support the latter option comes from a study where memory T cells from the periphery were isolated and it was demonstrated that these cells had an intracellular pool of LIGHT (Morel, 2003). This study did not identify which variant of LIGHT protein was detected in their system. The deltaLIGHT protein is retained in the cytosol as it loses its transmembrane domain as part of the splicing process (Granger, 2001). Therefore it is possible that this intracellular store of LIGHT in resting central and effector memory CD4⁺ T cells is actually deltaLIGHT, hence the increased level of expression of deltaLIGHT in our Jurkat cells even after LIGHT has returned to low basal levels.

3.4.3 Gene expression in peripheral blood leukocytes

Once we had established that we could measure changes in mRNA expression using our Real-time RT-PCR protocol we set about collecting patient samples. The diseases chosen to be included in the study were SLE, CD and WG, diseases whose symptoms were related to autoimmune manifestations seen in LIGHT-Tg mice (Shiakh, 200; Wang, 2001).

LIGHT-Tg mice as mentioned previously, have high levels of autoantibodies such as anti-DNA antibodies, a hallmark of SLE (Hochberg, 1997), they also have chronic inflammation in the small intestine with villous atrophy and crypt hyperplasia which are symptoms strongly associated with CD (Marsh, 1992). WG was included in the study as it is also characterised by the production of autoantibodies and glomerulonephritis (van der Woude, 1985; Fauci, 1983).

We initially measured the mRNA expressed in PBLs from each of the cohorts. The mRNA copy numbers were expressed per 50 ng of total RNA added to the quantitative RT-PCR. This did have some advantages; most notably, it allowed us to see that the HVEM expression was possibly elevated in cells other than lymphocytes in the SLE cohort. However, by relating the expression back to total RNA we inadvertently skewed the results because the SLE and WG had lower lymphocyte counts compared to the other two groups. Consequently, the true expression levels of LIGHT, deltaLIGHT, DcR3 and INF- γ mRNA were masked due to the presence of RNA from many cells that were not expressing these molecules. We readjusted the way in which mRNA copy numbers were expressed so that they were based on lymphocyte counts at the time of blood sampling. This proved to be another advantage of using absolute quantification, as once the mRNA copy numbers are obtained the denominator (ie per μg total RNA or cell number etc) can be altered to be more reflective of the circumstances.

3.4.4 LIGHT, associated receptors and SLE

SLE is a prototypical autoimmune disease that is genetically complex and characterised by the presence of many different autoantibodies, formation of immune complexes (ICs) and inflammation in multiple organs, including the skin, blood vessels, kidneys and central nervous system (Rönblom, 2002; Bennett, 2003). The major pathogenic antibodies are directed against nuclear components such as dsDNA, nucleosomes and snRNP (Mok, 2003). Overexpression of LIGHT in Tg mice induced the development of anti-DNA antibodies and lupus-like glomerulonephritis (Wang, 2001). This indicated that LIGHT might be a good candidate gene to play a contributing role in the pathogenesis of human SLE.

When the expression of LIGHT mRNA in PBLs of our control and SLE cohorts were analysed (Fig 3.09) a significant reduction in LIGHT mRNA was identified in the SLE cohort. A lymphocytopenia is common in SLE, we speculated that the reduction in LIGHT was artifactual, due to the lower number of lymphocytes (the primary cells expressing LIGHT) within these samples compared to the controls. Therefore, as mentioned the results were adjusted to reflect the amount of lymphocyte mRNA contained in each sample (Fig 3.15). This showed there was no reduction in LIGHT mRNA expression in SLE, and some patients had in fact higher amounts of LIGHT mRNA than the controls. To further prove that the actual levels of LIGHT mRNA were being masked PBMCs were isolated from SLE patients. Subsequent Real-time PCR analysis established that the levels of LIGHT mRNA in SLE PBMCs was elevated by approximately 6-8 fold over that of normal control PBMCs (Fig 3.18). This is similar to the fold increase in expression that we

demonstrated in P/I stimulated Jurkat T cells (Fig 3.07). A recent genome wide gene profiling study on CD4⁺ T cells from a patient with severe SLE before and after chemotherapy showed that LIGHT was upregulated on these cells during active SLE (Deng, 2005), thus confirming our data.

The SLE cohort showed elevated levels of deltaLIGHT mRNA when compared to the control cohort (Fig 3.10 and Fig 3.15). PBMCs isolated from SLE patients also demonstrated a significant increase in deltaLIGHT mRNA of approximately 6-7 fold (Fig 3.18). Little is known about the expression of deltaLIGHT protein in cells other than it is held intracellularly (Granger, 2001). To date there have been no reports indicating the function of this splice variant, making it very difficult to speculate as to its role in the pathogenesis of SLE. Nevertheless, it is likely to function in the activation/proliferation of T cells, as it is rapidly expressed by Jurkat T cells following stimulation with P/I (Fig 3.07).

Elevated levels of LIGHT in SLE would strongly promote a Th1 response and the release of cytokines such as INF- γ (Shiakh, 2001; Wang, 2001; Cohavy, 2004; Brown, 2005). INF- γ has been reported to be elevated in both murine models of SLE (Peng, 1997) and in human subjects (Csiszár, 2000). We too in this study have also confirmed that there is elevated levels of INF- γ mRNA in the periphery of SLE patients (Fig 3.14). It has also recognised that there is a significant correlation with the amount of INF- γ secreted by PBMCs and the severity of SLE (Ferry, 1997; Viillard, 1999). In particular, elevated levels of INF- γ are known to contribute to the development of glomerulonephritis (Uhm, 2003; Kikawada, 2003; Masutani, 2001). In this study, there is significant correlation between mRNA levels of INF- γ and both LIGHT and deltaLIGHT in our SLE cohort (Fig 3.16).

The SLE patients who participated in this study show a significant increase in HVEM mRNA expressed in their PBLs when compared to the control cohort (Fig 3.11). This too was a surprising result, as we know from the Jurkat experiments that there is a downregulation of HVEM in activated T cells (Fig 3.08). This result indicated that HVEM was either not regulated as normal (Morel, 2001) in SLE or that it was upregulated on another cell type. We speculated that in SLE patients that there was aberrant expression of HVEM mRNA in cells other than lymphocytes as it is expressed on a wide variety of cells (Harrop, 1998; Morel, 2001; Kwon, 2003). To narrow down the possible cell type that HVEM is overexpressed in, PBMCs were separated from granulocytes using standard density centrifugation techniques. This experiment showed that the level of HVEM mRNA expression in the PBMC population was actually significantly lower than the control samples (Fig 3.18). This demonstrates that the reciprocal expression of LIGHT/deltaLIGHT and HVEM is conserved within the lymphocyte cell population of SLE patients. The majority of HVEM overexpression seems to occur in granulocytic cells (Fig 3.19). Admittedly, the number of samples in this experiment is small. Nevertheless, the result does clearly indicate that HVEM mRNA is overexpressed in SLE and this is most likely due to altered expression in cells other than T cells.

HVEM is constitutively expressed by neutrophils (Kwon, 2003; Heo, 2006), which have been associated with kidney disease and vasculitis in SLE patients (Hotta 1996; Qasim, 1996). A recent report has demonstrated the significance of the LIGHT/HVEM interaction on neutrophils (Heo, 2006). *In vitro* addition of soluble LIGHT to neutrophils enhances their ability to secrete IL-8, TNF- α , nitric oxide (NO) and reactive oxygen species (ROS)

(Heo, 2006). IL-8 acts as a strong chemoattractant for neutrophils that has been implicated in the pathogenesis of renal inflammation and glomerulonephritis (Rovin, 2002). NO, whilst an important innate defence mechanism (Nathan, 1997), in excessive amounts it can promote tissue injury and contribute to the development of several human diseases (Abramson, 2001) including SLE (Belmont, 1997). Administration of inhibitors of NO production to the MRL-lpr/lpr murine model of lupus suppresses the development of glomerulonephritis (Weinberg, 1994). The pathogenic anti-DNA antibodies found in SLE have a greater capacity to bind DNA that has been modified by ROS (Blount, 1994). The resulting immune complexes deposit in the kidneys resulting in inflammation. TNF- α has also been found deposited in the kidneys of patients with lupus nephritis (Aringer, 2003). This would indicate that the dysregulated expression of HVEM in SLE could be a major contributing factor to the development of glomerulonephritis. Whether the overexpression of HVEM in granulocytes is constitutive in SLE or is an effect of cell activation would need to be addressed. A recent report examining the expression of HVEM protein on granulocytes from peripheral blood and synovial fluid in RA indicated that HVEM expression was not upregulated following activation of granulocytes as indicated by increased CD11b expression (Kim, 2005). This may indicate that the increased expression of HVEM mRNA in SLE is constitutive. This finding warrants further investigation.

In a previous study, which used semi-quantitative RT-PCR it was shown that DcR3 mRNA levels were elevated in PBMCs from SLE patients (Otsuki, 2000). This study, which uses a better quantification technique, also demonstrates that DcR3 is overexpressed in the periphery of our SLE cohort (Fig 3.15). DcR3 is secreted from activated PBMCs (Wan, 2003), which is supported by our data as its mRNA levels significantly correlate with the

expression of both LIGHT and deltaLIGHT (Fig 3.16). DcR3 as its name suggests functions as a decoy receptor that is capable of neutralising both FasL- and LIGHT- (Yu, 1999) induced apoptosis. Besides its inhibitory effects, DcR3 has also been reported to play a role in modulating DC differentiation and maturation (Hsu, 2002). DCs incubated with recombinant DcR3 show alterations in the surface expression of the B7 family of T cell co-stimulatory molecules (Hsu, 2002). DcR3 induces B7.1 (CD80) downregulation with the simultaneous upregulation of B7.2 (CD86) (Hsu, 2002). It has been shown that while both B7.1 and B7.2 equivalently stimulate IL-2 and INF- γ production, B7.2 can induce more IL-4 production than B7.1 (Kuchroo, 1995; Freeman, 1995). This would indicate that DcR3 could cause a shift from Th1 to Th2 cytokine production, as IL-4 is an integral cytokine in the Th2 pathway. The cytokine profile in SLE is quite complex, as both Th1 and Th2 cytokines have been reported to be elevated (Singh, 2005).

SLE patients also showed elevated levels of LT β R mRNA expressed in peripheral blood leukocytes (Fig 3.13). Increased apoptosis is thought to be an important trigger for the development of SLE (Casicicola-Rosen, 1994). LT β R is also known to induce caspase activation and ultimately apoptosis of cells by interacting with LIGHT. It has been reported that INF- γ may sensitise cells to LT β R mediated apoptosis (Browning, 1997). We have shown in this study that SLE patients express elevated mRNA levels for all three molecules indicating that this pathway could contribute to the increase in apoptosis seen in SLE (Berden, 2003; Tsokos, 2001).

3.4.5 LIGHT, associated receptor and CD

Coeliac disease is characterised by chronic inflammation of the small intestine due to an abnormal immune response to dietary gluten in genetically susceptible individuals (Sollid, 2000). The chronic inflammation results in destruction of the villi in the small intestine (Marsh, 1992). While many aspects of how the disease develops remain to be determined, CD is unique from the respect that the environmental trigger (gluten), the major genetic susceptibility locus (DQ2) and the autoantigen (tTG) are all known. While LIGHT-Tg mice show symptoms of systemic autoimmunity the main site of inflammation is the gut. Following histological analysis villous atrophy, crypt hyperplasia and infiltration of immune cells into the lamina propria was identified in these Tg mice (Wang, 2001; Shiakh, 2001). These are all features of the gut lesion seen in CD, indicating that LIGHT may play a role in its pathogenesis.

It has been previously reported that there is a relationship between cytokine mRNA levels expressed in the intestine and peripheral blood of CD (Lahat, 1999). This indicates that there is a continuous recirculation of activated immune cells between the inflamed small intestine and the periphery (Lahat, 1999; Nilsen, 1996; Kertula, 1995). Hence, we initially examined the mRNA expression of LIGHT and associated receptors in the peripheral blood of a cohort of CD patients. The initial analysis of mRNA expression in PBL isolated from CD patients showed no significant differences from that of the normal control cohort for LIGHT (Fig 3.09), deltaLIGHT (Fig 3.10), HVEM (Fig 3.11), DcR3 (Fig 3.12) and LT β R (Fig 3.13).

When the data was re-examined based on lymphocyte counts, there was a significant elevation in LIGHT mRNA in PBLs isolated from coeliac patients (Fig 3.15). The CD patients were then stratified based on their anti-tTG serology results at the time blood samples were collected for this study. Detection of anti-tTG antibodies has become standard practice to assist in the diagnosis of CD. Their levels give an indication to disease activity, as they become undetectable during a GFD (Dewar, 2004). Our results show that the expression of LIGHT mRNA is elevated in the periphery of CD patients with positive anti-tTG autoantibodies when compared to a control cohort (Fig 3.17 A). The expression of deltaLIGHT mRNA also follows a similar trend to that of LIGHT (Fig 3.17 B). HVEM mRNA levels in PBLs are lower during active CD than in normal control cohort (Fig 3.17 C). Indicating, that the reciprocal expression of LIGHT and HVEM mRNA (Morel, 2001) is maintained in CD. This result indicates that active CD patients have higher levels of LIGHT-expressing activated T cells in their circulation than normal controls. The LIGHT-Tg mice have shown that increased LIGHT on peripheral T cells can lead to the breakdown of peripheral tolerance leading to the development of autoimmunity (Wang, 2001). The rate of autoimmune diseases in CD is 10 times that of the general population (Green, 2003). Long term exposure to gluten could expand the number of T cells that express LIGHT in the periphery and then in a similar manner to that of the LIGHT-Tg mice self-tolerance could breakdown and symptoms of autoimmune disease could occur.

As mentioned earlier, LIGHT-Tg mice have profound inflammation in the small intestine (Shiakh, 2001; Wang, 2001) and more recently it has been shown that there is increased expression of LIGHT in the intestine of patients with active Crohn's disease (Cohavy, 2005; Cohavy, 2004, Wang, 2004). CD4⁺ T cells within the lamina propria are speculated

to play a central role in the pathogenesis of CD (Sollid, 2000). Using our established Real-time RT-PCR protocols to measure mRNA expression in PBLs, we aimed to identify if there was also dysregulation of LIGHT expression in the small intestine of CD patients.

Duodenal biopsies (15) were collected from 9 untreated CD, 2 treated CD and 4 controls that had neither CD or IBD. Total RNA was extracted and subsequent quantitative Real-time RT-PCR analysis was performed. Our results indicate, in a manner similar to that seen in Crohn's disease (Cohavy, 2005, Wang, 2005), that the levels of LIGHT mRNA are increased in CD patients with active disease (Fig 3.18). The expression of HVEM mRNA in the coeliac lesion is normally regulated, as during active disease it is downregulated (Fig 3.20). Hence, the regulatory mechanisms that control HVEM expression in the periphery are conserved within the intestinal compartment.

LIGHT signalling via HVEM is costimulatory and augments proinflammatory cytokine expression and T cell proliferation (Harrop, 1998). CD is characterised by a predominance of the Th1 profile and our results are consistent with this as the mRNA copy numbers for INF- γ (Fig 3.23) and IL-2 (Fig 3.24 A) are elevated in our untreated patients. The increased expression of LIGHT within the coeliac lesion would allow increased cell signalling via HVEM, which has been shown to be an important secondary signalling event for the full activation of T cells causing enhanced secretion of Th1 cytokines such as INF- γ , IL-2, TNF- α and GM-CSF (Harrop, 1998). HVEM signalling alone is enough to induce the INF- γ production by lamina propria T cells (Cohavy, 2004). Unlike Crohn's disease, the trigger for CD is known (gluten), and removal of this from the diet seems to cause a

reversal, at least in the case of HVEM, INF- γ and BTLA, of mRNA expression patterns to that of the control cohort.

The development of a Th1 response in CD does not seem to involve the main Th1 promoting cytokine, IL-12 (Nilsen, 1998). Increased levels of IL-18 and IFN- α , both of which promote Th1 cell differentiation, have been detected in coeliac tissue (Monteleone 2001; Salvati 2002). Interestingly, LIGHT mediation of a Th1 response is independent of IL-12 signalling (Brown, 2005). This may indicate that LIGHT expression could be an important factor for the development of a Th1 response in CD in place of IL-12 signalling. Cytokine upregulation in the lamina propria in response to gliadin is rapid. Using *in vitro* small intestine biopsy cultures incubated with gliadin, a significant increase in proinflammatory cytokines can be seen as early as 2-6 hours (Nilsen, 1998). As mentioned previously, CD4⁺ T cells that infiltrate the lamina propria in active CD are of a memory phenotype as characterised by the positive expression of CD45RO (Halastensen, 1990). LIGHT protein expression at the cell surface is very rapid on memory T cells showing a marked increase after 1-2 hours (Cohavy, 2004; Morel, 2003). Consequently, the rapid expression of LIGHT on gut homing T cells may facilitate the rapid increase in proinflammatory cytokines in response to gliadin.

BTLA can regulate T cell activation through its interactions with HVEM (Sedy, 2005, Gonzalez, 2005). This study shows that active CD patients, have significantly reduced levels of BTLA mRNA when compared to either the control or treated CD cohorts (Fig 3.24 C). Naïve T cells are first stimulated by the TCR engaging with a MHC-peptide complex on APCs. The fate of T cells is also dependent on delivery of a secondary signal,

which can be costimulatory or coinhibitory. Costimulatory signals allow clonal expansion of T cells and effective immune responses, the coinhibitory signals maintain T cell self-tolerance and prevent autoimmunity (Gonzalez, 2005). The balance of these two signals will determine the outcome of an immune response. With increased levels of LIGHT mRNA in active CD, along with reduced levels of BTLA, the balance between costimulation and coinhibition is greatly skewed in favour of an active T cell response. Furthermore, as HVEM levels are also decreased during active disease (Fig 3.21) will further facilitate the binding of LIGHT, as it has a higher affinity for it than BTLA, (Cheung, 2005). The sustained costimulation signals from LIGHT with little coinhibitory signal for BTLA this would lead to the strong proinflammatory response.

The expression of $LT\beta R$ is not transcriptionally regulated during inflammation of the small intestine in active CD (Fig 3.22). $LT\beta R$ can also act as a receptor for the heterotrimeric protein $LT\alpha 1\beta 2$ (Ware, 1995). To identify if changes small intestine in CD could be attributed to increase $LT\alpha 1\beta 2$ expression we measured the expression of $LT\beta$. This demonstrated that $LT\beta$ expression is unchanged in the coeliac lesion, as there is no difference between the control and untreated cohorts (Fig 3.24 B). LIGHT and $LT\alpha 1\beta 2$ are known to cooperate in lymphoid organogenesis and the development of lymphoid structures by signalling through $LT\beta R$ (Scheu, 2002; Wang, 2002). As $LT\beta$ expression is not elevated in untreated CD and that LIGHT is, would suggest that any alterations in coeliac lesion are due to additional signalling through $LT\beta R$ by LIGHT.

During active CD, there is recruitment of CD4⁺ T cells and B cells into the lamina propria (Sollid, 2000). The engagement of LIGHT with LT β R can help to create an environment suitable for the recruitment of lymphocytes into the lamina propria by upregulating several adhesion molecules and chemokines. Integrin family members are associated with the trafficking of lymphocytes to and maintaining them within immune effector sites. MAdCAM-1 specifically promotes α 4 β 7 integrin bearing lymphocytes to migrate to intestinal effector sites (Berlin, 1993). LIGHT-Tg mice showed increased levels of MAdCAM-1 as demonstrated by immunohistochemistry (Wang, 2004). Recombinant human LIGHT also stimulates increased expression of MAdCAM-1 (Wang, 2005). It has been recently reported that LIGHT expression in the small intestine is almost exclusively found on integrin β 7⁺ T cells (Cohavy, 2004). Therefore, LIGHT expressing T cells that are β 7⁺ can home to the gut, where they can interact with LT β R to further increase the expression of MAdCAM-1, which can cause increased levels of T and B lymphocytes to infiltrate the lamina propria.

Transgenic mice that overexpress LIGHT show increased apoptosis of intestinal epithelial cells (Wang, 2004). This increase in apoptosis could be mediated directly via LT β R (Rooney, 2000) or indirectly via the proapoptotic effect of cytokines secreted (INF- γ , TNF- α) by various cells in response to HVEM-LIGHT interactions (Harrop, 1998).

3.4.6 LIGHT, associated receptor and WG

WG is a rare condition characterised by the presence of autoantibodies (c-ANCA) directed towards PR3 an antibiotic protein expressed by activated neutrophils (Van der Woude, 1985). The disease seems to have two phases a localised phase where disease activity is restricted to the upper respiratory tract and a generalised phase where systemic disease occurs. It is speculated that early WG is characterised by a Th1 type cytokine profile with high levels of INF- γ in both granulomatous lesion and peripheral blood (Mueller, 2001). The major autoantibody c-ANCA is not often detected in the early stages of WG (Lamprecht, 2005). After a period of localised disease, generalised c-ANCA positive WG usually develops. At this time, there is a switch from Th1 cytokine expression to increased levels of Th2 cytokines such as IL-4 with little expression of INF- γ (Balding, 2001).

As LIGHT has strong Th1 inducing properties, it is tempting to speculate that the very low expression of LIGHT mRNA in much of the WG cohort is because of a switch from a Th1 to a Th2 profile. The low expression of INF- γ and the positive titres for c-ANCA would also indicate that our cohort had generalised disease. In hindsight it would have been worthwhile quantifying the levels of Th2 cytokines, namely IL-4, in these patients to identify if there was a negative correlation between them and LIGHT mRNA expression in peripheral blood. There was no altered expression of HVEM (Fig 3.11), LT β R (Fig 3.13) or DcR3 (Fig 3.12) between our WG and control cohorts. This may further indicate that these pathways do not significantly contribute to the pathogenesis of WG.

3.4.7 Conclusion

In summary, during this study we have gained knowledge about the use of real-time PCR for quantitative analysis and effectively applied this to investigating the expression of LIGHT and associated receptors in human autoimmune diseases. In doing so, we have provided evidence that increased expression of LIGHT and its associated receptors in SLE and CD and thereby confirming our hypothesis, that LIGHT overexpression may be involved in the pathogenesis of both diseases. Elevated levels of LIGHT promote a strong Th1 response, particularly INF- γ secretion. The role of INF- γ in the development of lupus nephritis has been well characterised. Hence, LIGHT could play a critical role in the pathogenesis of glomerulonephritis and may serve as a potential target for therapeutic intervention.

In CD, there are increased levels of LIGHT expressing cells in peripheral circulation and the lamina propria of patients with active disease. Increased LIGHT-HVEM signalling would promote Th1-type cytokines that are known to play a role in the pathogenesis of CD. Furthermore, increased LIGHT-LT β R signalling would enhance the upregulation of adhesion molecules and chemokines and cause immune cells to infiltrate the lamina propria, which is a feature of the coeliac mucosal lesion. Further research into the effects of LIGHT expression in the intestine may lead to the development for novel therapies for chronic inflammatory diseases.

Chapter 4

EXPRESSION OF SOLUBLE LIGHT PROTEIN IN AUTOIMMUNE/PROINFLAMMATORY DISEASES

4.1 INTRODUCTION

4.1.1 Soluble LIGHT

Many members of the TNFSF can be cleaved from the cell surface where they can act as soluble cytokines. The release of the soluble form allows modulation of systemic immune responses whereas the cell restricted forms will only effect the local environment. As described previously, there are three forms of the mature LIGHT protein; the cell membrane and intracellular forms are the products of pre-mRNA splicing (Morel, 2001). The third form is identical to the membrane form except it has been cleaved from the cell surface and is shorter by approximately 80 aa. This cleaved version of LIGHT is now free to act as a soluble cytokine.

The matrix metalloproteinases (MMPs) are a family of more than 24 enzymes (Pender, 2004). They are subdivided based on their primary substrate specificity such as collagen, gelatin, elastase and stromolysin. The natural endogenous inhibitors of MMPs are known as the tissue inhibitors of metalloproteinases (TIMPs). TIMPs form a 1:1 complex with MMPs and control the local activity of these enzymes in tissues. MMPs have been widely associated with the turnover, degradation and destruction of the extracellular matrix (ECM) (Parks, 2004). However, they can also function in the cleavage of cell surface ligands to release them as soluble cytokines. LIGHT and FasL show significant amino acid (31%) homology in their extracellular domains (Granger, 2001), a MMP cleavage site in FasL is also conserved in LIGHT between amino acids 81-84. The use of MMP inhibitors dramatically decreases the release of soluble LIGHT in to tissue culture supernatants

(Granger, 2001). This indicates that release of soluble LIGHT is due to the activity of an MMP. A specific MMP for this role has not yet been identified.

4.1.2 *In vitro* activity of soluble LIGHT

Several *in vitro* studies have shown that soluble LIGHT retains its biological activity. These studies have also demonstrated that LIGHT can modulate the activity of cells in both the innate and adaptive immune responses.

The addition of soluble LIGHT to T cells in conjunction with CD3 stimulation enhances T cell proliferation through HVEM signalling (Harrop, 1998). In addition, HVEM stimulation by soluble LIGHT enhances the production of proinflammatory cytokines such as INF- γ , GM-CSF and IL-2 by T cells (Tamada, 2000). Dendritic cell maturation is also enhanced by soluble LIGHT. In conjunction with CD40L, soluble LIGHT can costimulate the maturation of DC and significantly increase their ability to secrete IL-12 (Morel, 2001). IL-12 signalling through IL-12R is a critical factor in the induction of a Th1-type response (ref).

LT β R signalling can promote upregulation of adhesion molecules including VCAM-1 (Dejardin, 2002), ICAM-1 (Zhang, 2003) MAdCAM-1 (Wang, 2004). MAdCAM-1 plays an important role in the recruitment of inflammatory cells into the intestine. Soluble LIGHT directly upregulates the expression of MAdCAM-1 by engaging with LT β R (Wang, 2005).

A recent report demonstrated that soluble LIGHT enhances the bactericidal activity of monocytes and neutrophils (Heo, 2006). The addition to soluble LIGHT to monocytes and neutrophils at concentrations ranging from 1-100 ng/ml increased their ability to kill *Listeria monocytogenes* and *Staphylococcus aureus* cultures. This enhanced bactericidal activity was attributed to the ability of soluble LIGHT to enhance nitric oxide (NO) and reactive oxygen species (ROS) production by monocytes and neutrophils by interacting with HVEM. They also reported that soluble LIGHT could significantly enhance the production of the proinflammatory cytokines IL-8 and TNF- α (Heo, 2006). This was dose-dependent on soluble LIGHT concentrations and noticeable changes were identified at concentrations above 1ng/ml. Kim et. al., reported that there is a synergistic effect between INF- γ and soluble LIGHT to enhance the production of TNF- α and MMP-9 by macrophages that were isolated from the synovium of RA patients (Kim, 2005). Macrophages can also secrete other MMPs such as MMP-1 and -13 as well as TIMPs 1 and 2 in response to soluble LIGHT (Lee, 2004). Increased activity of MMPs has been reported in many human diseases including CD (Daum, 1999).

Soluble LIGHT also retains its ability to induce apoptosis of cells such as the HT-29 human colonic carcinoma cell line (Rooney, 2000). LIGHT mediated apoptosis is enhanced by INF- γ in a dose-dependent manner (Chen, 2000; Zhang, 2005).

4.1.3 Enzyme linked immunosorbent assay (ELISA)

ELISA assays have proved very useful for quantifying antigen in biological fluids and tissue culture supernatants. There are several approaches to how ELISA can be performed depending on the nature of the analyte (Carpenter, 1997). For the detection of autoantibodies in patient sera, for example, it is useful to coat the surface of the 96-well plate with the autoantigen, such as tTG in CD, and then sera from the patient is added to the well. If autoantibodies are present, they will bind to the antigen where they can be subsequently detected. The sandwich ELISA is another variation of the techniques and can be used to quantify (Fig 4.01). During this assay, two antibodies (capture and detection) that are specific for the target antigen are used. The capture antibody is coated on the surface of the plate, when test sample is added any specific antigen present will be bound by the antibody. Not all antibodies are suitable for sandwich ELISA as the capture and detection antibodies are required to detect different epitopes on the antigen to avoid competition for binding. The detection antibody is commonly labelled with biotin this facilitates the binding of avidin to the complex, which in turn can be conjugated to an enzyme. The most commonly used enzymes are horseradish peroxidase (HRP) and alkaline phosphatase (AP). HRP catalyses the oxidation of substrates by hydrogen peroxidase and AP catalyses the hydrolysis of phosphate groups from substrate molecules. HRP has become the enzyme of choice for most applications due to its superior specific activity, stability, low cost and availability of substrates. Commonly used substrates for HRP included o-phenylenediamine dihydrochloride (OPD) and 3, 3', 5, 5'-tetramethylbenzidine (TMB). TMB is the most commonly used substrate for HRP due to its high sensitivity of ~5.5 pg/well. The activity of HRP on TMB yields a blue colour which

when the enzyme reaction is stopped by the addition of sulphuric acid to the well, it is converted to a yellow product that can be spectrophotometrically detected at 450 nm. If recombinant proteins are used to generate a standard curve, this allows accurate quantification of soluble proteins in serum.

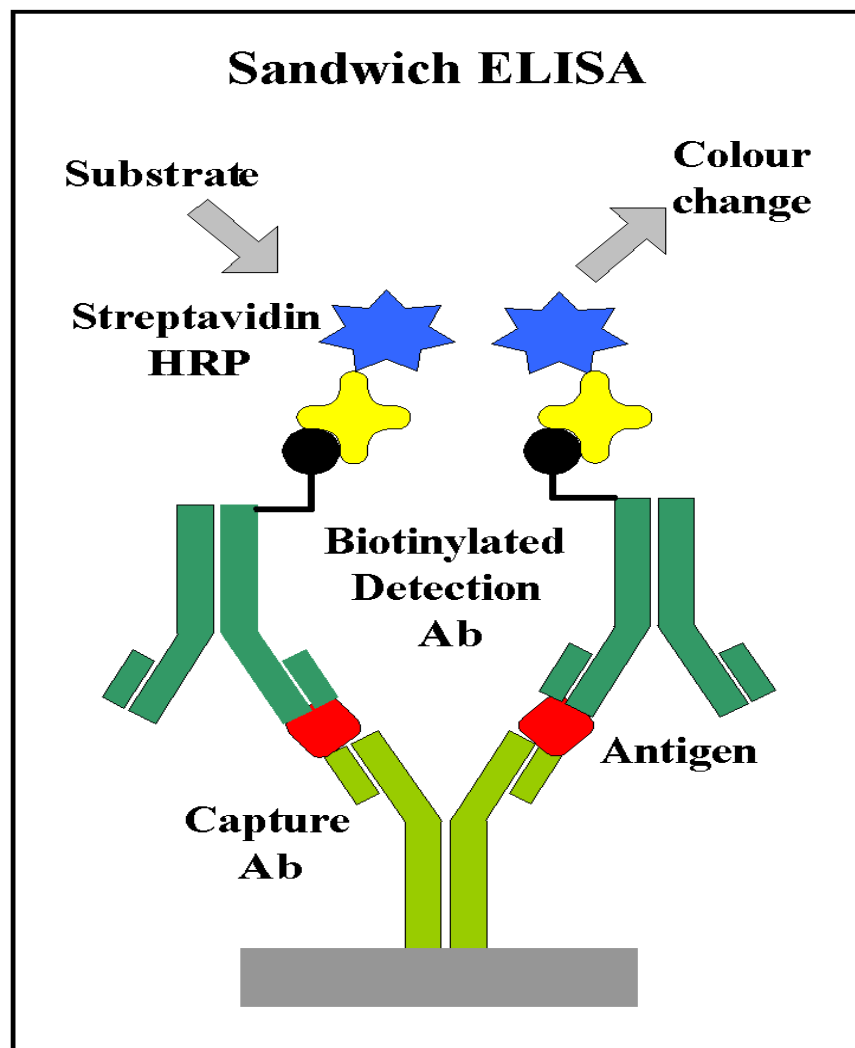


Fig 4.01 Format of a sandwich ELISA. Antibody (Ab); horseradish peroxidase (HRP).

4.1.4 Aim of this chapter

Many members of the TNF superfamily can be cleaved from the cell surface by proteases. These cleaved ligands have been shown to retain biological activity allowing them to ligate to their respective receptors. LIGHT is cleaved from the surface of the cell by members of the MMP family. The aim of this chapter is to identify if serum levels of soluble LIGHT are elevated in patients with CD and SLE using ELISA. As soluble LIGHT has been demonstrated to retain its biological activity, elevated levels would promote a strong proinflammatory response. This work will support our findings of our gene expression study and provide further evidence that LIGHT is involved in the pathogenesis of these diseases.

4.2 MATERIALS AND METHODS

4.2.1 Patient samples

Serum samples were collected from a control cohort (28), which consisted of people with no known autoimmune or inflammatory condition. Serum samples were also collected from patients with SLE (50), WG (30) and CD (32). Informed consent was obtained from all patients in accordance with both the Dublin Institute of Technology's ethics review board and St James's Hospital ethics review board.

4.2.2 Jurkat T cell stimulation

Jurkat cells were stimulated for the time-course assay as described in Methods 3.2.1. Cell culture supernatants were harvested, at timepoints from 0-48 hrs, and stored at -80°C pending analysis

4.2.3 ELISA for soluble LIGHT

The detection of soluble LIGHT was performed using a commercially available kit (R&D systems), the manufacturer's instructions were followed. Briefly, LIGHT capture antibody was reconstituted to $720\ \mu\text{g/ml}$ in sterile PBS. A 96-well plate was coated with $100\ \mu\text{l}$ of diluted capture antibody ($4\ \mu\text{g/ml}$) and incubated overnight at RT. Plates were washed 3 times using $400\ \mu\text{l}$ of wash buffer (0.05% tween in phosphate buffered saline (PBS) @ pH 7.2-7.4). After the last wash, any remaining buffer was removed by blotting on clean paper

towels. All non-specific binding sites on the plate were blocked using 300 µl of reagent diluent (1% BSA in PBS @ pH 7.2 – 7.4) for a minimum of 1 hr. Washing procedure was repeated as before. Recombinant human (rh) LIGHT standards were prepared in the range of 2000 pg/ml to 32.2 pg/ml in reagent diluent. Add 100 µl of rhLIGHT standards or sample in duplicate and incubate at RT for 2 hours. Washing procedure was repeated. Plates were coated with 100 µl of diluted detection antibody (100ng/ml) and incubated at RT for 2 hours. Washing procedure was repeated. Streptavidin-HRP stock was diluted in PBS (50 µl + 9950 µl PBS), 100 µl of this was then added to each well the plate was covered and incubated at RT for 20 mins. Avoid placing plate in direct light. Washing procedure was repeated. The substrate solution was prepared by mixing 5 mls of colour reagent A and 5 mls of colour reagent B. 100 µl of the substrate solution was added to each well and incubated at RT for 20 mins. 50 µl of stop solution (2N H₂SO₄) was then added to each well, the plate was then gently tapped to ensure adequate mixing. The optical density of each well was immediately determined using a microplate reader set to 450 nm. Absorbance measurements were also taken at 570 nm as recommended by the manufacturer, this corrects for any imperfections in the plastic of the plate.

4.2.4 Statistical analysis

Statistical analysis of the ELISA data was performed using the non-parametric Mann-Whitney U-test. P values were two-sided and significance was considered when P <0.05.

4.3 RESULTS

4.3.1 Evaluation of a suitable diluent for the LIGHT standards

During an ELISA, it is important to block all non-specific binding sites on the plastic surface of the 96-well plate. This helps to prevent non-specific binding of proteins during subsequent steps in the procedure, which reduces the background noise and improves the sensitivity of the assay.

Three different blocking solutions were prepared in PBS: 1% BSA, 20% fetal calf serum (FCS) and 1% BSA and 20% FCS. In addition to acting as a blocking solution, these reagents were also used to dilute the rhLIGHT stock to make the standards. The standard curves produced using each of the diluents were almost identical (Fig 4.02) with a linear range from 32 pg – 1000 pg per ml. This allowed accurate quantification of samples within this range. As a 1% BSA solution is the most economical of the three blocking solutions it was used for all subsequent experiments.

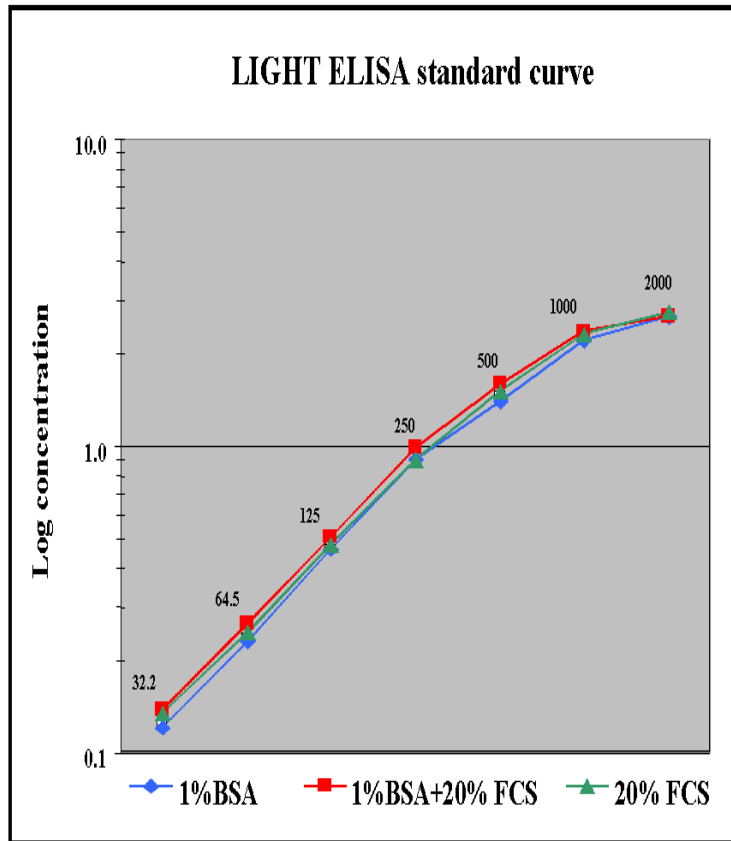


Fig 4.02 **LIGHT ELISA standard curve using three different diluents.** Values above each data point indicate the concentration of recombinant human LIGHT (rhLIGHT) in pg/ml.

4.3.2 Determination of the stability of soluble LIGHT

The detection of proteins using ELISA is dependent on the antibody being able to capture the protein. For this the epitope that the antibody recognises must be available. If any degradation of the protein, that may destroy this epitope, occurs during storage of the serum, then the data may be misinterpreted. As there was no information about the stability of sLIGHT we analysed 5 serum samples that were stored under two conditions: room temperature (~25°C) and refrigeration temp (~6°C). These two temperatures reflected the condition that patient serum samples, that we wished to use in this study, may have been subjected to. Serum samples were collected and an aliquot was immediately stored at –80°C (fresh frozen) and the remaining serum was left at either room or refrigeration temperature for up to 6 days at each time point an aliquot was taken and stored at –80°C. Samples were then analysed for levels of soluble LIGHT. At room temperature no significant change was seen at any of the time points when compared to the fresh frozen aliquot (Fig 4.03 A). The same pattern was demonstrated for the samples stored at refrigeration temperature (Fig 4.03 B). This showed that sLIGHT was stable in serum samples stored at room temperature for up to six days.

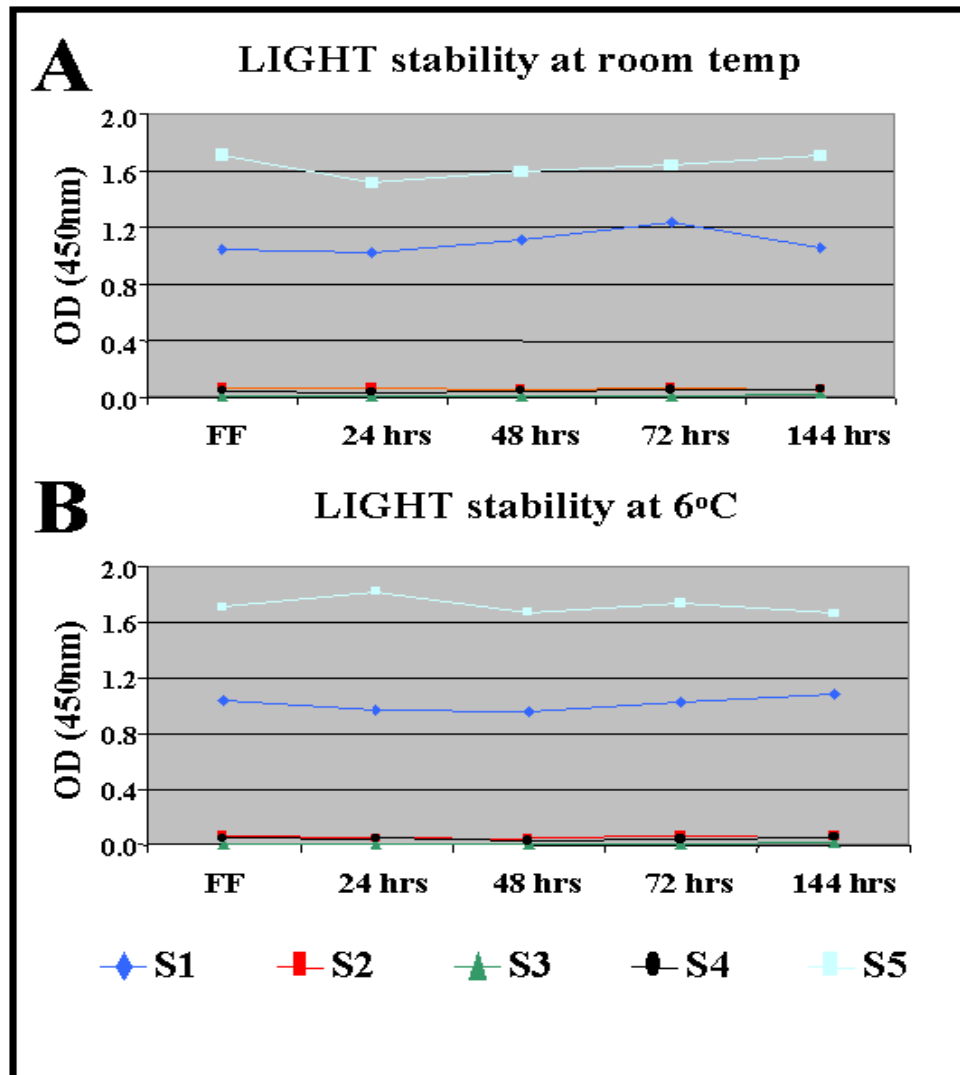


Fig 4.03 **Stability of soluble LIGHT in serum stored at room and refrigeration temperature.** Fresh frozen (FF). Panel A shows the stability of soluble LIGHT at room temperature ; Panel B shows the stability of soluble at 6°C.

4.3.4 Intra-assay and inter-assay variation

The level of intra- and inter-assay precision was also measured for both the recombinant standards and the sera samples. The average coefficient of variation (CV) for intra-assay analysis for the recombinant standards was 5.1% (range: 2.3-7.1), for inter-assay analysis this was 11.6% (range 5.8-17.1). A similar trend was seen for the sera samples, the CV for intra-assay analysis was 8.1% (range 6.1-10.2) and inter-assay 13% (range 11.3-14.9). These CVs are within the generally accepted variation for both intra and inter assay analysis (Carpenter, 1997).

4.3.5 Expression of soluble LIGHT from Jurkat T cells

To identify if LIGHT protein and mRNA levels correlate, we analysed the expression of sLIGHT in tissue culture supernatants collected from P/I stimulated Jurkat T cells over a period of 48 hrs (Fig 4.04). The mRNA expression results from the previous chapter are overlaid on Fig 4.04 to directly show the mRNA and protein levels in context with each other. The levels of soluble LIGHT were seen to steadily rise from 8 hrs post-stimulation up to 32 hrs at which point the increase began to plateau. After 48 hrs there was an approximate 7-fold increase in the level of soluble LIGHT present in the tissue culture supernatants.

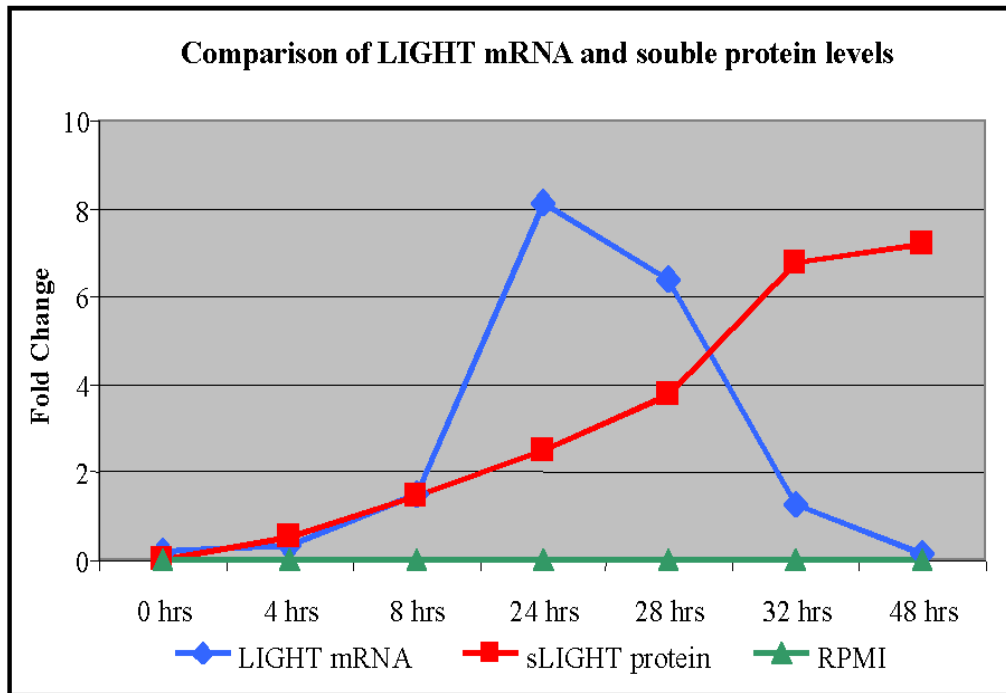


Fig 4.04 Kinetics of soluble LIGHT (sLIGHT) release from stimulated Jurkat T cells.

4.3.6 Analysis of patient samples for soluble LIGHT

Once the procedure for the ELISA was established, the analysis of the test sera could begin. Along with a control group, sera from SLE, CD and WG patients were also tested. All patients were positive for autoantibodies at the time of obtaining the serum sample. The SLE patients were ANA positive, the WG patients were c-ANCA positive and the CD patients were anti-tTG positive. Positive autoantibody titres were an indication that there was disease activity in the selected patients.

The results of the quantitative ELISA were converted from optical density (OD) units to pg/ml of soluble protein in the manner specified by the manufacturer (R&D systems). The manufacturer of the soluble LIGHT ELISA (R&D systems) had previously tested 60 control samples all of which were under 250 pg/ml. In our control group, the majority are clustered below 300 pg/ml, though three samples have levels greater than 1000 pg/ml (Fig 4.05). The percentage of samples undetectable in the manufacturers control group is 7% compared to our 10.7%. Therefore, with the exception of three outlying samples our controls compare very well to those tested by the manufacturer.

Following statistical analysis of the data, the SLE patients showed significantly higher levels of soluble LIGHT in their sera ($P = 0.033$). Conversely, the WG patients had significantly lower amounts of sLIGHT in their sera ($P = 0.012$) when compared to the control group. The CD patients were not deemed statistically different from the controls ($P = 0.172$). However, in this case the P value does not tell the whole story, as a large percentage (37.5%) of the CD patients tested had a high level of soluble LIGHT (>1000

pg/ml) in their sera compared to only 10 % of the controls (Table 4.01). This is comparable to the 40% of SLE patients that show levels greater than 1000 pg/ml. A large number of the WG patient failed to show expression of soluble LIGHT (43.3%) compared to only 10.7% of the controls

	Samples	Undetectable	>1000 pg/ml
	n	%	%
Controls	28	10.7	10.7
CD	32	3.1	37.5
WG	30	43.3	16.7
SLE	50	6.0	40.0

Table 4.01 **Percentage of patient cohort that had undetectable or strong positive soluble LIGHT levels.**

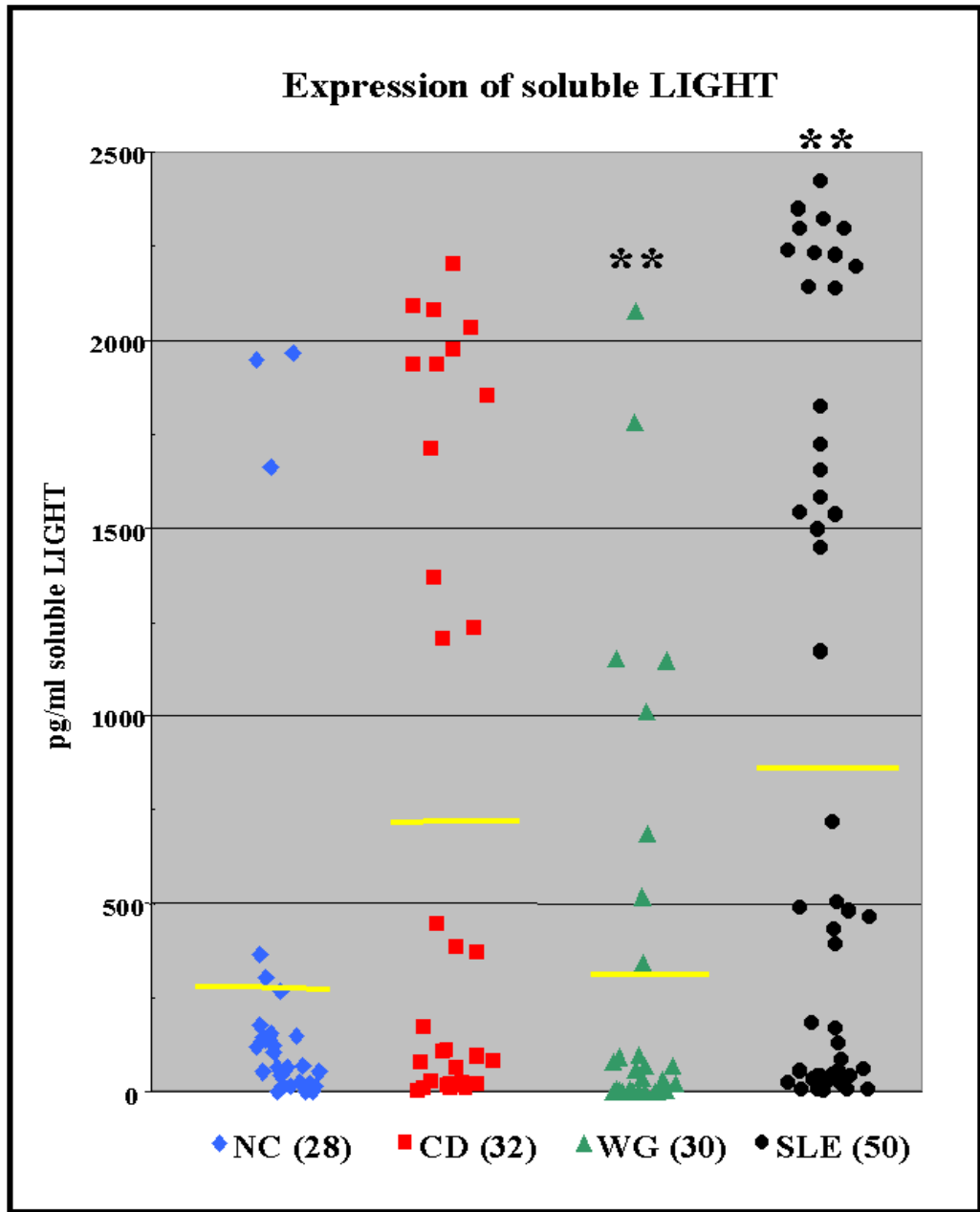


Fig 4.05 Soluble LIGHT levels in different patient groups. ** Indicates a group that is significantly different from the normal control. Horizontal lines indicate the mean of each group.

4.4 DISCUSSION

There are three forms of the LIGHT protein each is present within a different location, the cytosol, the cell membrane or the extracellular space. The cytosol and cell membrane associated forms of LIGHT are produced by alternative splicing (Granger, 2001). The third form of the protein is generated by proteolytic cleavage of the cell surface associated protein to release it as soluble LIGHT (Granger, 2001; Morel, 2000). While it has been speculated that this release of soluble LIGHT might be a method of downregulating the ligand (Granger, 2001), several studies have shown that it retains biological activity (Zhang, 2003; Zhang, 2004; Heo, 2005).

The aim of this study was to measure the levels of soluble LIGHT in the sera of CD, SLE and WG patients as well as a control cohort. Based on our findings that there is increased mRNA expression of LIGHT in both CD and SLE (chapter 3), we speculated that there would also be increased serum concentrations of soluble LIGHT in these two diseases. By demonstrating that increased mRNA expression is also reflected in elevated protein levels, this would provide further evidence that LIGHT may play a role in the pathogenesis of both CD and SLE. To measure the amount of soluble LIGHT present in the test sera a commercially available sandwich ELISA (R&D systems) was employed a commonly used method for quantifying antigen in biological fluids and cell culture medium.

As there was no information on the stability of soluble LIGHT our initial experiments set-out to demonstrate that the protein was stable for an extended period at both room and

refrigeration temperatures. These temperatures would reflect possible storage conditions that the serum samples may be exposed to. Five serum samples were tested in this experiment. Each sample showed similar levels of soluble LIGHT whether the aliquot was fresh frozen (-70°C at time of collection) or stored for up to 144 hrs at each of the temperatures (Fig 4.03). This ensured that any changes seen in the expression of soluble LIGHT would not be due to degradation of the protein, which may affect the epitopes recognised by the capture and detection antibodies used in the sandwich ELISA.

Jurkat T cell have been used extensively to elucidate many aspect of T cell activation and initiation of an immune response (Abraham, 2004). In this study, Jurkat T cells were used to demonstrate that increases in LIGHT mRNA corresponded with a similar fold increase in the release of soluble LIGHT. As demonstrated in chapter 3, P/I stimulation of Jurkat cells induces an 8-fold increase in the expression of LIGHT mRNA. By collecting the cell culture supernatants from these activated cells, it was possible to measure the release of soluble LIGHT using ELISA. The levels of LIGHT mRNA peak at ~ 24 hrs whereas the peak of soluble LIGHT protein occurs between 8-24 hrs later (Fig 4.04). This demonstrates that increases in LIGHT mRNA are also reflected in the release of soluble LIGHT from activated Jurkat T cells.

4.4.1 Soluble LIGHT and CD

CD is characterised by chronic inflammation that leads to severe destruction of the small intestine in response to gliadin ingestion by genetically susceptible individuals (Sollid, 2002). Activated CD4⁺ T cells in the lamina propria of the small intestine with a Th1 phenotype have been proposed to be central to the disease process (Schuppan, 2000). In chapter 3 it was demonstrated that patients with positive anti-tTG antibody titres have elevated levels of LIGHT mRNA expressing cells in peripheral circulation (Fig 3.17). Therefore, in this study serum samples were only selected if they had positive titres for anti-tTG antibodies indicating that there was disease activity, as these antibodies tend to disappear following the removal of gluten from the diet (Sulkanen, 1998).

Following soluble LIGHT quantification using the described ELISA protocol, a statistically significant difference between the control and CD cohorts was not observed ($P = 0.172$) (Fig 4.05). During *in vitro* stimulation studies using soluble LIGHT, noticeable changes in the levels of proinflammatory cytokines and adhesion molecules can be seen at concentrations of >1000 pg/ml (Zhang, 2003; Zhang, 2004; Heo, 2005). During this study, to identify strongly positive samples a cut-off value of >1000 pg/ml were used. When samples above the cut-off are considered, a large number of the CD cohort (37.5%) have high levels of soluble compared with only 10.7 % of the controls (Table 4.01). This result indicates that a considerable proportion of CD patients may have excessive soluble LIGHT in their serum, which could have significant implications for those patients.

CD has been linked to the development of secondary autoimmune diseases such as IDDM (Cronin, 1997), rheumatoid arthritis (Collin, 1994) and autoimmune hepatitis (Volta, 1998) to name but a few. The expression of LIGHT has also been demonstrated to play a role in the development of various autoimmune diseases including IDDM (Wang, 2001), RA (Kim, 2005) and autoimmune hepatitis (Anand, 2006) among others. Furthermore, chronically elevated levels of LIGHT in mice can cause a breakdown in self-tolerance that leads to systemic autoimmunity (Wang, 2001; Shiakh, 2001). CD patients are 10 times more likely to develop an autoimmune disease than the general population (Green, 2003). Sustained increases in soluble LIGHT concentrations could be one contributing factor to this phenomenon.

4.4.2 Soluble LIGHT and SLE

SLE is a prototypical autoimmune disease in which multiple organs can become inflamed and damaged. The major autoantibodies present in these patients are anti-nuclear antibodies (ANA) that are directed against various nuclear components including DNA. Increased levels of Th1 cytokines have been found in the serum of SLE patients, particularly those with renal involvement (Uhm, 2003). As soluble LIGHT retains its ability to induce a Th1 type response (Tamada, 2000), increased serum levels could have a major role to play in the pathogenesis of SLE.

The SLE patients analysed in this study showed significantly increased levels of soluble LIGHT ($P = 0.033$) in their sera when compared to the control cohort (Fig 4.05) when quantified using the aforementioned ELISA protocol. When the samples with concentrations above the cut-off value ($>1000\text{pg/ml}$) are considered, 40% of the SLE cohort showed high levels of soluble LIGHT present in their serum.

In vitro stimulation of T cells using soluble LIGHT causes significant increases in $\text{INF-}\gamma$ expression with little or no increases in Th2 cytokines (IL-4 or IL-10) (Tamada, 2000). $\text{INF-}\gamma$ plays a significant role in the development of lupus nephritis in both human (Akahoshi, 1999) and mouse studies (Schwartzing, 1998; Haas, 1998). Anti- $\text{INF-}\gamma$ treatment for the lupus prone NZB/NZW mouse prevents renal disease (Ozmen, 1995), whereas the administration of $\text{INF-}\gamma$ greatly accelerates its progression (Jacob, 1987). Likewise, knocking out the $\text{INF-}\gamma$ gene in two different models (MRL/lpr and NZB/NZW) protects them from the development of nephritis (Schwartzing, 1998; Haas, 1998). In humans, an increased ratio of Th1/Th2 cytokines ($\text{INF-}\gamma/\text{IL-4}$) is thought to promote lupus nephritis (Akahoshi, 1999). Lupus patients with glomerulonephritis have increased levels of Th1 cytokine producing cells present in their kidneys (Uhm, 2003), which correlate with histological analysis of disease activity (Masutani, 2001; Kikawada, 2003). In addition, $\text{INF-}\gamma$ levels secreted by PBMCs from SLE patients significantly correlate with disease activity scoring systems such as the systemic lupus activity measure (SLAM) (Viallard, 1999; Sturfelt, 1997). Transgenic mice that over-express $\text{INF-}\gamma$ have also been demonstrated to produce anti-DNA antibodies (Seery, 1997), which are believed to be critical for the development of renal disease. Given the role of the LIGHT-HVEM pathway in $\text{INF-}\gamma$ upregulation (Zhai, 1998) it is likely that the elevated levels of soluble LIGHT could contribute to the deterioration in the health of these patients.

LIGHT and INF- γ can work in synergy to increase TNF- α secretion by monocytes (Kim, 2005). The role of TNF- α in the pathogenesis of SLE is debated; some reports indicate that it may have a protective role (Dean, 2000; Manson, 2003), while others have shown that TNF- α can contribute to the inflammation seen in these individuals (Aringer, 2003). Several animal studies would also indicate that TNF- α participates in the development of lupus nephritis (Boswell, 1988; Yokohama, 1995; Tsai, 1995). NZB/NZW mice have high levels of TNF- α deposited in their kidneys, once nephritis is established (Brennan, 1989). A finding that has also been demonstrated in humans (Herrera-Esparza, 1998; Malide, 1995; Takemura, 1994). Furthermore, the level of TNF- α expression correlates with histological assessment of renal inflammation (Herrera-Esparza, 1998).

Given the effect that soluble LIGHT has on increasing both INF- γ and TNF- α among other proinflammatory molecules it is reasonable to assume that it could very well contribute significantly to the development of glomerulonephritis in these patients. Incidentally, about 40% of patients with SLE develop nephritis during the course of the disease (Cervera, 1993) a figure which is strikingly similar to the number of our test cohort that show highly elevated levels of soluble LIGHT.

4.4.3 Soluble LIGHT and WG

WG is an autoimmune disease characterised by granulomatous and vasculitic lesions. The disease usually presents as localised WG, in which granulomatous lesions are restricted to the upper airways, and progresses to generalised WG. Autoantibodies specific for PR3 are

detected in the vast majority of patients with generalised WG (Lamprecht, 2005). Granulomatous lesions in localised disease predominantly express Th1-type cytokines whereas a shift towards Th2-type cytokine expression is found in generalised disease (Mueller, 2000; Balding, 2001).

All WG serum samples included in this study were positive for autoantibodies directed against PR3. The results of this study showed a statistically significant lower expression of soluble LIGHT between the WG and control sera ($P = 0.012$). Furthermore, the WG cohort had a very high proportion (43%) of samples in which no soluble LIGHT could be detected (Table 4.01). This is a significantly higher proportion of samples with no detectable soluble LIGHT than either our controls (10.7%) or the controls tested by the manufacturer (7%). This finding provides further evidence that overexpression of LIGHT is not likely to participate in the pathogenesis of WG. The absence of soluble LIGHT in anti-PR3 positive WG patients would support the hypothesis of a skewed Th-2 cytokine profile in these patients.

4.4.4 Conclusion

To conclude, the aim of this chapter was to measure the levels of soluble LIGHT in our three test cohorts, which was achieved using a commercially available sandwich ELISA specific for soluble human LIGHT. The data generated in this study shows that soluble LIGHT is significantly elevated in the serum of SLE patients. Soluble LIGHT can induce a strong Th1-type response predominantly causing the secretion of large amounts of INF- γ . Increased INF- γ levels are well documented to play a role in the development of lupus nephritis in both human and murine studies. Hence, it is reasonable to suggest that increased soluble LIGHT levels may be a contributing factor to renal involvement in SLE.

A large proportion of the CD cohort showed elevated levels of soluble LIGHT in their serum despite the site of inflammation being localised to the small intestine. Constitutive expression of LIGHT in Tg-mice induces a breakdown of self-tolerance and leads the onset of autoimmune disease. An extremely high incidence of secondary autoimmune disease is found in patients diagnosed with CD. We speculate that patients with chronically elevated levels of soluble LIGHT in their serum may be more prone to developing some of the other autoimmune conditions that are associated with CD.

The WG patients showed significantly lower levels of soluble LIGHT compared with the controls. This results confirms that at least in our cohort of anti-PR3 autoantibody positive WG patients that LIGHT overexpression is not a contributing factor to disease

Chapter 5

GENERAL DISCUSSION

Since its discovery, LIGHT has proved to be an important secondary co-stimulatory molecule for the activation of T cells (Harrop, 1998; Tamada 2000). The co-stimulation signal caused by LIGHT-HVEM interactions induces a strong Th1 type response (Tamada, 2001; Wang, 2001). Additionally, roles in dendritic cell maturation (Morel, 2001), negative selection of thymocytes (Wang, 2002; Wang 2001) and secondary lymphoid organogenesis (Wang, 2002) have also been attributed to LIGHT. Evidence that LIGHT may play an important role in human disease came from two papers that specifically overexpressed LIGHT in T cells of mice (Wang, 2001; Shaihk, 2001). The mice generated in these studies developed profound inflammation of the intestine as well as severe glomerulonephritis and autoantibody production. The small intestinal inflammation seen in these transgenic mice resulted in villous atrophy, crypt hyperplasia and the loss of goblet cells (Shiahk, 2001). This destruction of the small intestinal structure, while not specific to CD alone, is similar to the gut lesion seen in human subjects with the disease (Marsh, 1992). The development of glomerulonephritis and the production of anti-DNA autoantibodies in LIGHT-Tg mice resembles manifestations seen in established models for SLE (Wang, 2001). From these two studies we speculated that upregulation of LIGHT may play a role in the development of CD or SLE in humans. Therefore, the overall aim of this thesis was to assess the expression of LIGHT and its associated receptors in these two immune-mediated diseases. We also included a cohort of WG patients in this study as it is characterised by the presence of multiple autoantibodies, vasculitis and glomerulonephritis (Langford, 1999). In order to obtain data on the expression of LIGHT in these diseases, Real-time quantitative RT-PCR methodologies were to be optimised.

Real-time PCR has emerged as a powerful technique for quantitative analysis (Bustin, 2000). While microarray technology is popular for monitoring the expression of many thousands of genes at a time, it is now common practice to validate these results using quantitative real-time PCR. Much of this is to do with the sensitivity, wide dynamic range and the adaptability of Real-time PCR technology for quantitative analysis (Logan, 2004). Before embarking on a logistically complex and expensive gene expression study it was felt that gaining hands-on experience with developing Real-time PCR assays, where the end results could be predetermined, would yield benefits in the long-term. To this end, two disease models were chosen to study various aspects of Real-time PCR assay design. In order to look at SNP detection we used cystic fibrosis as a model as it is a common genetic disease and, while over 1000 mutations (Tsui, 2003) have been associated with its development, as few as five of these account for ~90% of mutations seen in the Irish population (Scotet, 2003). The model chosen for quantitative analysis was the examination of PMP22 gene dosage in relation to two hereditary peripheral neuropathies: CMT1A and HNPP. These are traditionally very difficult conditions to diagnose at the molecular level due to the subtle differences between a normal and abnormal genotype. Therefore, this study provided a strong challenge to the capabilities of quantitative Real-time PCR analysis.

5.1 Review of results

The ultimate aim of chapter 2 was to explore the use of Real-time PCR as a methodology and to push its capabilities to the limit. In chapter 2.1, Real-time PCR was used to develop an assay to detect the five most common CFTR mutations in the Irish population. A previous study had compared Real-time PCR to traditional PCR techniques for detecting the delF508 mutation in CF, and had shown that it was as accurate and a much more rapid technique (Dempsey, 2002). Hence, we wanted to expand on this to produce a multiplex Real-time PCR that could detect the five most common CF mutations in Ireland. This would account for approximately 90% of mutant alleles present in the Irish population (Scotet, 2003). The initial approach was to develop the multiplex in a manner similar to other groups (Bestmann, 2002, Gundry, 2001, Bernard, 1998) by placing the hybridisation probes at the site of the mutation. Nonetheless, it was quickly realised that there would be significant problems with this technique as it did not allow us to differentiate more than one mutation per colour channel during melting curve analysis. To avoid these problems a novel approach to performing multiplex mutation detection on the LightCycler instrument was developed (Dempsey, 2004). This involved combining ARMS PCR (Newton, 1989) with Real-time melting curve analysis (Wittwer, 1997). Our approach proved to be quite successful, allowing easy discrimination of melting curve peaks that corresponded to particular CFTR genotypes (Figs 2.06-2.08). This assay also passed a blinded trial carried out in conjunction with the National Centre for Medical Genetics, Our Lady's Hospital for Sick Children. The use of Real-time PCR for CF mutation detection allows for a much faster turnaround time for genetic analysis. This is of particular importance for newborns that may have the potential for developing the disease. Newborn infants have healthy

sterile lungs (Wine, 1999), but they can quickly become colonised with bacteria that are pathogenic to CF patients such as *Staphylococcus aureus* (Hutchison, 1999) and *Pseudomonas aeruginosa* (Emerson, 2002). Early treatment of these infants can slow down the progression of lung colonisation and ultimately the progression of the disease (Starner, 2005). Therefore, it is vital that a diagnosis can be made as rapidly as possible. The use of Real-time PCR for mutation detection in newborns also has the advantage of requiring only small amounts of starting genomic DNA, as the technique is highly sensitive. If necessary, successful PCR analysis can be performed using only picogram quantities of starting template helping to reduce the amount of cells/blood that need to be donated for genetic analysis.

In chapter 2.2, Real-time quantitative PCR was used for gene dosage analysis in two hereditary peripheral neuropathies, CMT1A and HNPP. Gene dosage analysis using traditional techniques such as southern blotting (Lupski, 1991) can be time-consuming and require large amounts of high quality DNA. Real-time PCR a truly quantitative technique is sensitive, rapid and requires only small amounts of DNA (Logan, 2004) making it very suitable for gene dosage analysis. The PMP22 gene is contained within a 1.5 Mb region of chromosome 17p11.2. The gene can be duplicated leading to CMT1A (Lupski, 1991; Raeymaekers, 1991) or deleted and thus cause HNPP (Chance, 1993). Consequently, a normal individual will possess two copies of the PMP22 gene, CMT1A individuals will have three and a HNPP patient will have only a single copy. The quantification of such subtle changes would push Real-time PCR to the limits of its capabilities. In this study, relative quantification was used where β -globin acted as a reference that is present at two copies per genome. PMP22 copy numbers were then expressed as a ratio of β -globin. The

development of a multiplex PCR, that allowed the simultaneous quantification of both β -globin and PMP22 in the same capillary, was an important aspect of this study. Otherwise, the test sample would have to be added to two separate PCRs, therefore creating the potential for error to be introduced into the assay. However, the generation of both amplicons in the same PCR would mean that extensive optimisation was required so that the PCR efficiencies were similar. If this were not so it could potentially lead to over/under estimation of the PMP22 ratio. Once the quantitative multiplex was optimised and shown to be reproducible, we tested a number of samples for PMP22 copy numbers. The results generated were similar to the findings of other groups (Thiel, 2003; Choi, 2005). Normal controls had a ratio of PMP22 to β -globin of approximately 1, CMT1A had a ratio of >1.4 and HNPP had a ratio of <0.55 . All normal control samples tested fell within a range of 0.8 – 1.2 showing a clear division between normal and pathogenic ratios (Fig 2.15).

During these two studies, model diseases (CF, CMT and HNPP) were used to generate a better understanding of how to effectively use Real-time PCR as a tool in molecular biology. A lot of knowledge about was gained about the general design and positioning of hybridisation probes for the development of a successful real-time PCR assay. Steps were made to improve the multiplexing capabilities of real-time mutation detection (Dempsey, 2003). We also demonstrated that Real-time PCR is a very sensitive technique capable of discriminating between samples that differed by as little as 1.5 fold change. This work gave us a good foundation when designing primers and hybridisation probe pairs for the gene expression work performed in chapter 3. It also demonstrated the power of Real-time PCR as a quantitative tool for detecting even the subtlest alterations in copy number.

The aim of chapter 3 was to utilise real-time PCR to achieve the ultimate aim of the thesis: to analyse the expression of LIGHT and its associated receptors in human immune-mediated diseases. In this chapter, we successfully developed Real-time RT-PCR protocols allowing us to quantify changes in mRNA expression profiles.

The reciprocal expression of LIGHT and HVEM on activated T cells had been previously characterised using semi-quantitative RT-PCR (Granger, 2001). Therefore, we used Jurkat cells stimulated in a timecourse with P/I to verify the reciprocal expression of LIGHT and HVEM upon T cell activation (Figs 3.07 & 3.08) using our Real-time PCR protocols. These results showed that deltaLIGHT follows a similar pattern to that of LIGHT upregulation in these cells (Fig 3.07). To our knowledge, this is the first time this has been demonstrated. The success of these initial studies allowed us to progress to the collection of samples from patients. Over 90 samples were obtained for the first part of this study: to characterise the mRNA expression profile of LIGHT and its receptors in PBLs isolated from our test cohorts (CD, SLE and WG patients).

Subsequent Real-time RT-PCR analysis revealed that LIGHT mRNA is elevated in CD PBLs when compared to healthy controls (Fig 3.17). It has been previously reported that PBLs isolated from active CD express increased levels of mRNA for Th1-cytokines (Lahat, 1999). From previous studies on Crohn's disease, it is highly likely that these LIGHT⁺ T cells have had previous antigen exposure (CD45RO⁺) and secrete INF- γ (Cohavy, 2005). LIGHT-Tg mice have revealed that increased LIGHT on peripheral T cells can lead to the breakdown of peripheral tolerance leading to the development of autoimmunity (Wang, 2001). The exposure of coeliacs to gluten as indicated by anti-tTG positivity can increase

the number of T cells that express LIGHT in the periphery. In a similar manner, as occurs in LIGHT-Tg mice, long-term exposure to gluten could cause a breakdown in self-tolerance. The expression of HVEM is normally regulated (reciprocal expression to that of LIGHT) in PBLs from CD patients (Fig 3.11). The mRNA copy numbers for LT β R (Fig 3.13) and DcR3 (Fig 3.12) did not vary from that of the control cohort.

In chapter 3 it was also demonstrated that LIGHT and its associated receptors may contribute in the pathogenesis of SLE. The expression of LIGHT and deltaLIGHT mRNA was elevated in PBMCs isolated from SLE patients (Fig 3.19). Furthermore, the levels of both LIGHT and deltaLIGHT mRNA strongly correlated with the increased levels of INF- γ mRNA seen in our patients (Fig 3.16). The levels of mRNA for LIGHT's three receptors (HVEM, DcR3 and LT β R) were also identified as being significantly elevated in our cohort of SLE patients (Figs 3.11 & 3.15), indicating, that there is a profound dysregulation of these signalling pathways in SLE.

One of the more interesting results generated in this thesis was the significant elevation of HVEM in PBLs isolated from SLE patients. It was initially thought that this might indicate that HVEM mRNA was not regulated as normal in these patients. However, upon further investigation it seems that the reciprocal expression of HVEM and LIGHT is maintained in PBMCs and the overexpression of HVEM is within cells of the granulocyte population (Fig 3.18). HVEM is expressed by neutrophils, (Kwon, 2003) making it is tempting to speculate that the increased expression is on this cell type. The addition of soluble LIGHT, at concentration of >1000 pg/ml, to neutrophils causes the release NO and ROS as well as TNF- α and IL-8 (Heo, 2006), all of which have been implicated in the pathogenesis of

lupus nephritis (Blount, 1994; Nathan, 1997; Rovin, 2002; Aringer, 2003). SLE patients may express high levels of HVEM on their neutrophils, in conjunction with high levels of soluble LIGHT (>1000 pg/ml) in their serum (Fig 4.05), suggesting that the LIGHT-HVEM pathway might be of particular importance in the development of glomerulonephritis, one of the most serious manifestations of SLE.

Elevated levels of soluble HVEM have been identified in the serum of SLE patients (Jung, 2003). However, the authors did not speculate as to the biological significance of increased soluble HVEM. Both LIGHT and BTLA need to be considered when assessing the potential role of soluble HVEM in SLE pathogenesis. LIGHT is capable of reverse signalling by interacting with solid phase DcR3-Fc protein (Shi, 2002; Wan, 2002), which serves to further enhance Th1 responses. It might be possible that soluble HVEM could also function in this manner by cross-linking LIGHT on the surface of T cells. Nevertheless, it could be just as likely that soluble HVEM can block cell membrane bound HVEM from interacting with LIGHT or BTLA. The interaction of HVEM and BTLA transmits co-inhibitory signals into T cells (Sedy, 2005; Gonzalez, 2005). Anergic T cells have been reported to express high levels of BTLA (Hurchla, 2005). If soluble HVEM acted as a decoy ligand for BTLA this may have the effect of preventing co-inhibitory signals being transduced into T cells and therefore increasing the likelihood of uncontrolled T cell activation. While it can be equally argued that soluble HVEM can block LIGHT co-stimulation of T cells and maturation of DC, by switching off the BTLA-HVEM circuit other co-stimulatory circuits could induce activation of T cells that should by right be anergic. T cells from HVEM knockout mice show hyper-responsiveness during *in vitro*

stimulation (Wang, 2005), which indicates to the importance of the BTLA-HVEM interactions in maintaining balance between stimulation and inhibition.

In chapter 3 the expression of DcR3 mRNA was also examined in PBLs isolated from our test cohorts. The gene expression analysis showed that DcR3 expression was unaltered in both CD and WG, although a significant increase was identified in the SLE cohort (Fig 3.15) confirming a previous study (Otsuki, 2000). The biological role of DcR3 is quite complex as it acts as a soluble receptor for LIGHT (Yu, 1999), FasL (Pitti, 1998) and TL1A (Migone, 2002). In addition, it has been speculated that it may have other unidentified ligands (Yang, 2005). DcR3 has been typically associated with anti-apoptotic activities by blocking the function of its three ligands (Yu, 1999; Roth, 2001; Migone, 2002).

The commonly used knockout mice MRLlpr/lpr (Fas) and gld/gld (FasL) spontaneously develop a lupus-like disease (Watanabe, 1992; Takahashi, 1994). *In vitro* studies have shown that Fas-FasL is critical for activation induced cell death (AICD) a mechanism used to delete lymphocytes in peripheral circulation at the end of an immune response (Ashkenazi, 1999). T cells from SLE patients have been shown to resist AICD (Lu, 2004). A potential mechanism for this resistance could be the increased presence of DcR3, which can interfere with the activity of Fas (Roth, 2001).

However, DcR3 can also modulate the activity of many cells. DcR3 increases monocyte adhesion to endothelial cells by upregulating ICAM-1 and VCAM-1 expression (Yang, 2005). It can also modulate the maturation of dendritic cells so that they favour the

production of Th2 type cytokines (Hsu, 2002). Furthermore, *in vitro* DcR3 has been shown to induce reverse signalling via LIGHT to enhance the secretion of Th1 cytokines (Wan, 2002). DcR3 can be partially cleaved *in vivo* by proteolysis to produce two functional fragments that have different activities against FasL and LIGHT (Wroblewski, 2003). The cleaved fragment of DcR3 (amino acids 1-218) does not bind to FasL but retains its ability to bind to LIGHT. This may explain the wide range of functions that DcR3 seems to display. While the full biological significance of DcR3 expression is still to be elucidated, this study shows that further investigation into its altered expression in SLE is warranted, particularly into the source and levels of the different DcR3 fragments, their effects on AICD and the effects they have on different cytokine profiles secreted by DC and T cells.

Real-time PCR analysis of the WG cohort shows that LIGHT and its associated receptors do not show a dysregulated profile. No significant changes were seen in the levels of mRNA for LIGHT, any of its receptors or INF- γ when compared to the control cohort. All patients used in the study were positive for c-ANCA, indicating they may have progressed to generalised WG, which seems to be dominated by a Th2-type cytokine profile, (the lack of INF- γ mRNA expression would support this).

The second part of this chapter was the examination of mRNA expression in the lamina propria of intestinal biopsies collected from patients with active CD. The results from this study showed that LIGHT was elevated in the gut lesion during active CD when compared to controls. These results are similar to those seen in Crohn's disease, another chronic inflammatory disease of the gastrointestinal tract, where LIGHT is elevated in sites of inflammation (Cohavy, 2005; Wang, 2005). The LIGHT-HVEM pathway promotes a

strong Th1 response independent of CD-28 of IL-12 signalling (Brown, 2005). It is well recognised that CD is characterised by increases in Th1 cytokines. Both INF- γ and IL-2 mRNA and protein have been previously reported to be elevated in CD (Nilsen, 1998; Lahat, 1999). Our data also confirms this as both are significantly elevated in our active CD cohort (Fig 3.25).

LT β R also acts as a receptor of LIGHT (Mauri, 1998; Zhai, 1998; Harrop; 1998), it has a different expression pattern to that of HVEM (Zhai, 1998) and is thought to function as a communication link between T cells and stromal cells (Gommerman, 2003). Our results show that LT β R mRNA is not upregulated during active CD (Fig 3.22). Besides LIGHT, LT β R can also bind LT β when it forms a heterotrimer with LT α (Ware, 1995). To identify if LT β could be responsible of some of the dysregulated immune response in CD we analysed the levels of its mRNA and showed that it was not upregulated during active CD. This suggests that any function LT β R plays in the pathogenesis of CD is mostly like not to involve increased signalling via interactions with LT β . However, as LIGHT expression is increased in the active CD it is highly probable that any increases in LT β R activity is due to LIGHT. T cells that mediate an inflammatory response must first migrate from sensitisation areas to sites where they may exert their function. This migration is dependent of the expression of tissue-specific adhesion molecules and chemokine gradients (Brandtzaeg, 2001; Butcher, 1996). Infiltration of the lamina propria by large number of immune cells is a feature of the coeliac lesion (Sollid, 2000; Marsh, 1992). Signalling through LT β R by LIGHT would serve to increase the expression of various adhesion molecules and chemokines (Dejardin, 2002; Zhang, 2003; Wang, 2004), which would direct a large number of cells towards the intestinal mucosa.

Increased apoptosis of enterocytes is one contributing factor to the villus atrophy seen in CD (Moss, 1996). Transgenic mice that overexpress LIGHT show increased apoptosis of intestinal epithelial cells (Wang, 2004). LIGHT can directly cause apoptosis via LT β R (Rooney, 2000), particularly if the cells have been exposed to INF- γ (Zhang, 2004; Chung, 2004). As both LIGHT (Fig 3.19) and INF- γ (Fig 3.23) (Nilsen, 1998; Lahat, 1999) are upregulated in active CD, it is feasible that the LIGHT-LT β R pathway could directly contribute to apoptosis of enterocytes.

From our quantitative analysis, it seems that BTLA is strongly down-regulated in the lamina propria in untreated CD (Fig 3.25). This molecule functions to attenuate lymphocyte activity by acting as a co-inhibitory molecule (Watanabe, 2003) and it has just been recently linked to the LIGHT-HVEM pathway (Sedy, 2005; Gonzalez, 2005). It is speculated that if BTLA and LIGHT are expressed on the same cell then the binding of HVEM to both results in a cancellation of any positive signals from LIGHT (Croft, 2005). As LIGHT is upregulated in active CD, the lack of BTLA expression in the gut lesion would allow LIGHT-signalling activity through HVEM to predominate. This would further enhance the activation of T cells, upregulation of Th1 cytokines, immune cell infiltration to the lamina propria and result in profound inflammation and damage to the surrounding tissue.

In chapter 4, we investigated the levels of soluble LIGHT protein in the serum of patients with CD, SLE or WG using ELISA. Soluble LIGHT is generated from the cleavage of cell surface LIGHT to release the extracellular portion (Granger, 2001) and can effectively

promote a Th1 type response (Tamada, 2000). Using P/I stimulated Jurkat T cells as a model, it was established that upregulation of LIGHT mRNA correlated with a similar fold increase in soluble LIGHT levels in the tissue culture supernatants (Fig 4.04). Subsequent analysis of patient samples provided further proof that LIGHT could be an important factor in the pathogenesis of CD and SLE as a large percentage of both cohorts had elevated levels of soluble LIGHT in their serum (Fig 4.05 & Table 4.01).

As LIGHT mRNA and INF- γ mRNA levels correlate (Fig 3.16) in SLE, it is also likely that the protein levels correlate. We speculate that increased soluble LIGHT may play a role in lupus nephritis by promoting INF- γ upregulation. This important Th1 cytokine is known to function in the development of renal disease in SLE (Akahoshi, 1999; Schwarting, 1998; Haas, 1998). Soluble LIGHT can also induce monocytes and neutrophils to secrete a wide range of proinflammatory molecules including TNF- α , IL-8, NO and ROS (Kim, 2005; Heo, 2006) all of which can cause renal damage (Blount, 1994; Nathan, 1997; Rovin, 2002; Aringer, 2003).

There is a high incidence of secondary autoimmune disease associated with CD (Green, 2003). LIGHT-Tg mice, whilst having severe inflammation of the intestine, also develop many symptoms of autoimmune diseases (Wang, 2001; Shaikh, 2001). Many of the autoimmune diseases have been associated with LIGHT's activity, including IDDM (Wang, 2001), RA (Kim, 2005) and autoimmune hepatitis (Anand, 2006). Interestingly, many of the same autoimmune conditions are associated with CD (Alaedini, 2005). We speculate that chronic exposure to gliadin, the triggering antigen for CD, could serve to keep LIGHT at elevated levels and over a period of time this could lead to a breakdown of self-tolerance

and result in secondary autoimmune diseases. However, in order to show this a long term study would need to be performed using coeliac patients, which could be a direction for future work.

The WG cohort had a number of patients who expressed lower amounts of soluble LIGHT than the controls (Fig 4.05). The evidence from our study would indicate that LIGHT and associated receptors are not involved in the pathogenesis of WG, at least to the point there is not increased levels of soluble LIGHT in their serum or there are no increases in circulating cells that express high levels of LIGHT mRNA. As all of our WG patients were positive for ANCA directed against PR3 this suggests that their disease had progressed to the generalised form (Lamprecht, 2005). Generalised WG is characterised by a switch from a Th1 to a Th2 cytokine profile (Mueller, 2000; Balding, 2001). This could be one explanation for the low levels of soluble LIGHT in this cohort as it is typically seen as a Th1 promoting cytokine. In hindsight, Th2 cytokine protein levels should have been measured in these patients to provide proof of this.

5.2 Treatment of human disease by targeting LIGHT

The treatment of CD with a GFD provides a satisfactory therapy for the majority of patients. However, some patients fail to respond to this treatment and are deemed to have refractory CD. It has been reported that refractory CD has a prevalence of 7-8% within the CD population (O'Mahony, 1996). As there is strong evidence of a link between CD and malignancies of the gastrointestinal tract (Catassi, 2002; Green, 2001; O'Farrelly, 1986),

there is a necessity to provide these patients with alternative treatment. The use of immunosuppressants in these refractory patients has had mixed results, with reports of patients responding to the treatment but later succumbing to opportunistic infections (Vaidya, 1999).

Anti-TNF therapy is commonly used in the treatment of autoimmune conditions such as rheumatoid arthritis (Elliott, 1993) and Crohn's disease (Targan, 1997) and has been used to treat refractory CD patients (James, 2005). The most common TNF- α antagonists used are a murine/human chimeric monoclonal antibody (infliximab) and a soluble TNF- α receptor fused to the Fc portion of human IgG1 (etanercept). There are some drawbacks to the use of anti-TNF therapy. A number of reports have shown the treatment with infliximab or etanercept can cause new-onset SLE (Mohan, 2002; Hanauer, 2002; Shakoor, 2002) and neurological disease resembling multiple sclerosis (Mohan, 2001). Anti-TNF- α therapy has been avoided in SLE because of this despite the increase of the cytokine in these patients (Aringer, 2002; Gabay, 1997).

The research of others has demonstrated that LIGHT may be useful as an alternative target for the treatment of Th1 associated diseases. Murine models of IBD (Wang, 2005) and IDDM (Wang, 2001) have been successfully treated by administering the chimeric LT β R-Ig protein, an antagonist of the LIGHT- LT β R pathways. Our research shows that LIGHT is upregulated in both CD and SLE. In addition, a recently published study looking at genes expressed by CD4⁺ T cells in individuals with severe SLE has also demonstrated that LIGHT is upregulated during active disease (Deng, 2005). Although treatment of CD patients with anti-LIGHT therapy would be extreme it could prove useful in the treatment

of severe refractory disease. In the case of patients with SLE, where anti-TNF therapy is avoided in their treatment, anti-LIGHT therapy could prove to be an effective method of downregulating their uncontrolled T cell response. As INF- γ is strongly associated with lupus nephritis, anti-LIGHT therapy could be of particular use in patients with renal involvement.

It has been demonstrated that forced expression of LIGHT within tumours causes the influx of immune cells and elimination of the tumour (Yu, 2004). Not only is the local tumour destroyed but memory tumour-antigen specific CD8⁺ T cells were generated that cleared tumours at other sites in the body. This is another exciting facet of LIGHT's function as a therapeutic agent. However, it does warn that manipulation of LIGHT could also have some serious side effects such as the development of malignancy. Specific targeting of HVEM and/or LT β R with monoclonal antibodies may be a better route for potential therapies rather than completely blocking LIGHT altogether with chimeric recombinant proteins. As LIGHT has diverse roles to play in both the adaptive and innate immune response, completely switching it off could result in opportunistic infections and possibly malignancy in the long term. By specifically targeting either HVEM or LT β R, this would allow for the fine-tuning of the activity of LIGHT in the treatment of disease. Nevertheless, a much greater understanding of how LIGHT functions within different environments of the body is needed before the step to treating humans with anti-LIGHT therapy can be made.

5.3 Future work

As the scope of this thesis has been quite broad and from the results generated there are a number of possible avenues for further research. Our results have demonstrated that LIGHT mRNA expression is elevated in the lamina propria of patients with active CD. Therefore, analysing protein levels would provide further evidence as to the potential involvement of LIGHT in the pathogenesis of CD. This could be done using immunohistochemistry, a technique that can be used to quantify as well as localise antigen in tissue sections. It is also possible to culture duodenal biopsies for up to 48 hrs in an organ culture system (Nilsen, 1998). The addition of gliadin to biopsies from treated CD patients induces rapid changes in the expression of proinflammatory cytokines (Nilsen, 1998). Using a combination of quantitative Real-time PCR, immunohistochemistry and ELISA it would then be possible to analyse the expression of LIGHT in these biopsies in response to gliadin. Mouse models of IBD have been treated using a soluble LT β R-Fc chimeric protein (Wang, 2005; An, 2005). A study in which biopsies from treated CD patients were incubated with gliadin and where LIGHT's expression was blocked, using LT β R-Fc/HVEM-Fc, would allow cytokine profiles and any morphological changes that are a function of LIGHT expression to be identified. This study would further define the role of LIGHT in the pathogenesis of CD.

Elevated levels of LIGHT have also been identified in IBD, particularly Crohn's disease (Cohavy, 2004). Interestingly a susceptibility locus of IBD (Rioux, 2000) overlaps with the region of Chr 19 in which the gene for LIGHT is located (Granger, 2001). Similarly, susceptibility loci for SLE (Lindqvist, 2000) and CD (van Belzen, 2003) have been

localised to this area. While the promoter region of LIGHT has been characterised, no study to date has been performed to identify polymorphisms that may effect its expression. Polymorphisms have been characterised for several cytokines, including TNF- α (Wilson, 1992; D'Alfonso, 1994), which effects the expression of their mRNA and can contribute to the development of autoimmune diseases (Nath, 2004; Dean, 2000). Therefore, it is a possibility that LIGHT mRNA expression could be altered due to the presence of SNPs within the promoter region. Particular genotypes may lead to higher or longer sustained peak levels of LIGHT, which could be a risk factor for a wide range of human diseases. Further characterisation of the promoter region and identification of possible SNPs leading to altered expression would be useful in the assessment of LIGHT's role in the development of autoimmunity.

We have revealed that deltaLIGHT is upregulated, with similar kinetics to that of LIGHT, in activated Jurkat T cells (Fig 3.07). Little is known about deltaLIGHT other than it is held intracellularly (Morel, 2001). Our results demonstrate that it is upregulated in SLE (Figs 3.10 & 3.15) therefore it may play a role in the development of autoimmunity. The commonly used method to elucidate the function of a gene is to create a knockout model and examine the phenotype of the animal. However, small interfering RNAs (siRNAs) have emerged as a useful technology for knocking out specific mRNAs (Shi, 2003; Dykxhoorn, 2003). The use of siRNAs would have the advantage of allowing the expression of specific splice variants of an mRNA to be eliminated and thereby allowing its specific function to be elucidated. Separately targeting LIGHT and deltaLIGHT using siRNAs would determine the function of each during the activation and proliferation of T cells.

Our initial finding of lower expression levels of BTLA mRNA in the lamina propria of CD patients warrants further investigation. The discovery that BTLA is linked to the LIGHT-HVEM pathway is a very recent discovery (Sedy, 2005; Gonzalez, 2005). As a result, we did not get to thoroughly investigate its expression patterns during this thesis. BTLA has been demonstrated to be highly polymorphic in mice (Hurchla, 2005). Given the importance of BTLA in maintaining a balance between T cell activation and the induction of anergy (Watanabe, 2003), any genetic factor that predisposes to its underexpression would allow self-reactive T cells to escape anergy, and thereby facilitate the induction of autoimmune diseases. Further investigation into LIGHT-HVEM-BTLA crosstalk would yield information as to how these molecules effect T cell activation and the induction of anergy.

To formally prove our hypothesis that HVEM mRNA is overexpressed in neutrophils it would be necessary to selectively isolate different cell populations in SLE patients and analyse their mRNA expression patterns. It may be possible to investigate if neutrophils constitutively express higher amounts of HVEM in SLE or if it is upregulated in response to neutrophil activation. A recent report would suggest that HVEM is not upregulated on the surface as neutrophils become activated (Kim, 2005), which may indicate that the increased expression of HVEM in SLE patients is constitutive. PR3 is normally contained in the cytosol, but following neutrophil activation, by cytokines such as TNF- α , it is translocated to the cell surface (Reumaux, 2004). It has been reported that constitutive expression of PR3 on the surface of resting neutrophils is genetically predetermined (Schrieber, 2003) and is a risk factor for WG development. In a similar manner, surface expression of HVEM may be altered due to potential polymorphisms in its promoter

region. If HVEM is constitutively expressed at higher levels on neutrophils in SLE patients this would provide further evidence that targeting the LIGHT-HVEM pathway could be a potential therapeutic approach.

There are several animal models, including the NZB/NZW and MRL/lpr mice, which show similar disease manifestations to that of human SLE. These mice have been used extensively to establish the role of proinflammatory cytokines in SLE (Boswell, 1988; Ozmen, 1995; Schwarting, 1998). To test the hypothesis that LIGHT plays a significant role in the development of lupus nephritis, recombinant proteins, such as LT β R-Ig or HVEM-Ig, which block LIGHT signalling (Wang, 2001; Wang, 2005; An, 2005) could be administered to these mice and disease activity monitored. If LIGHT plays a significant role in the pathogenesis of SLE, particularly lupus nephritis, the administration of blocking proteins would at least delay the onset of disease in these animals. This would be a key step in identifying if anti-LIGHT therapy could be used in the treatment of SLE.

5.4 Conclusion

In summary, the aim of this thesis was to characterise the expression of LIGHT and its associated receptors in human immune-mediated diseases. Using a combination of Real-time RT-PCR and sandwich ELISA methodologies we have successfully achieved this goal. The work of this thesis has provided strong evidence that LIGHT and its associated receptors may play an important role in the pathogenesis of both SLE and CD and less so in WG. LIGHT mRNA expression is elevated in both the peripheral blood and lamina propria of active CD patients. A large number of our CD cohort also had high levels of soluble LIGHT present in their serum. LIGHT can enhance the proliferation of Th1 T cells that can in turn secrete large amounts of INF- γ and IL-2 among other proinflammatory cytokines. LIGHT can also participate in the maturation of DC, and in doing so, cause them to be strong activators of CD8⁺ CTL responses. Increased amounts of INF- γ as well as high levels of active CTLs can bring about the apoptosis of enterocytes and induce the destruction of the villous leading to the formation of the characteristic CD lesion.

In SLE, there is a more profound dysregulation of LIGHT and its associated receptors. Increased levels of LIGHT can stimulate secretion of INF- γ , which is well known to contribute to the pathogenesis of SLE, particularly renal disease. A significant elevation in the serum levels of soluble LIGHT was also identified in SLE. Furthermore, elevated levels of all three receptors for LIGHT were identified in the peripheral blood of our SLE patients. We have revealed that HVEM is strongly elevated on granulocytes, possibly neutrophils, although this still needs to be formally proved. Triggering of the HVEM-LIGHT pathway on these cells induces the release of NO and ROS as well as TNF- α and

IL-8 all of which are speculated to play a role in lupus nephritis. Therefore, increased levels of LIGHT in SLE patients may contribute to the development of lupus nephritis in a number of ways.

Targeting of LIGHT effector pathways could be a potential treatment for both SLE and refractory CD. Further research into LIGHT will lead to a better understanding of the development of Th1 mediated diseases and it should lead to the development of new therapies for chronic inflammatory and systemic autoimmune diseases.

References

- Aarskog NK, Vedeler CA. Real-time quantitative polymerase chain reaction. A new method that detects both the peripheral myelin protein 22 duplication in Charcot- Marie-Tooth type 1A disease and the peripheral myelin protein 22 deletion in hereditary neuropathy with liability to pressure palsies. *Hum Genet* 2000; 107: 494-498.
- Abi Rached L, McDermott MF, Pontarotti P. The MHC big bang. *Immunol Rev* 1999; 167: 33-49.
- Abraham RT, Weiss A. Jurkat T cells and the development of the T-cell receptor signalling paradigm. *Nat Rev Immunol* 2004; 4: 301-308.
- Abramson SB, Amin AR, Clancy RM, Attur M. The role of nitric oxide in tissue destruction. *Best Prac Res Clin Rheum* 2001; 15: 831-845.
- Aeschlimann D, Paulsson M. Transglutaminases: protein cross-linking enzymes in tissues and body fluids. *Thromb Haemost* 1994; 71: 402-415.
- Agostoni E, Gobessi S, Brancolini C, Schneider C. Identification and characterisation of a new member of the gas3/PMP22 gene family in *C. elegans*. *Genes* 1999; 234: 267-274.
- Ahmed S, Ihara K, Kanemitsu S, Nakashima H, Otsuka T, Tsuzuka K, Takeuchi T, Hara T. Association of CTLA-4 but not CD28 gene polymorphisms with systemic lupus erythematosus in the Japanese population. *Rheumatology (Oxford)* 2001; 40: 662-667.
- Akadegawa K, Ishikawa S, Sato T, Suzuki J, Yurino H, Kitabatake M, Ito T, Kuriyama T, Matsushima K. Breakdown of mucosal immunity in the gut and resultant systemic sensitization by oral antigens in a murine model for systemic lupus erythematosus. *J Immunol* 2005; 174: 5499-506.
- Akane A, Matsubra K, Nakamura H, Takahashi S, Kimura K. Identification of the heme compound copurified with deoxyribonucleic acid (DNA) from blood stains, a major inhibitor of polymerase chain reaction (PCR) amplification. *J Forensic Sci* 1994; 34:362-372.
- Al Soud WA, Radstrom P. Capacity of nine thermostable DNA polymerases to mediate DNA amplification in the presence of PCR-inhibiting samples. *Appl Environ Microbiol* 1998; 64: 3748-3753.
- Anand S, Wang P, Yoshimura K, Choi IH, Hilliard A, Chen YH et al. Essential role of TNF family molecule LIGHT as a cytokine in the pathogenesis of hepatitis. *J Clin Invest* 2006; 116: 1045-51.
- Aringer M, Feierl E, Steiner G, Stummvoli GH, Hofler E, Steiner CW, Radda I, Smolden JS, Graninger WB. Increased bioactive TNF in human systemic lupus nerythematosus: associations with cell death. *Lupus* 2002; 11: 102-108.
- Aringer M, Smolen JS. Complex cytokine effects in a complex autoimmune disease: tumour necrosis factor in systemic lupus erythematosus. *Arthritis Res Ther* 2003, 5: 172-177.
- Ashkenazi A. Targeting death and decoy receptors of the tumour-necrosis factor superfamily. *Nat Rev Cancer* 2002; 2: 420-30.
- Aslanidis C, Nauck M, Schmitz G. High-speed prothrombin GA20210 and methylenetetrahydrofolate reductase CT677 mutation detection using Real-time fluorescence PCR and melting curves. *Biotechniques* 1999; 27: 234-238.
- Bach JF. Insulin-dependent diabetes mellitus as an autoimmune disease. *Endocr Rev* 1994; 15: 516-542.
- Badano JL, Inoue K, Katsanis N, Lupski JR. New polymorphic short tandem repeats for PCR-based Charcot-Marie-Tooth disease type 1A duplication diagnosis. *Clin Chem* 2001; 47: 838-843.
- Baechner D, Liehr T, Hameister H, Altenberger H, Grehel H, Suter U, Rautenstrauss B. Widespread expression of the peripheral myelin protein-22 gene (PMP22) in neural and non-neural tissues during murine development. *J Neurosci Res* 1995; 42: 733-741.
- Bai C, Connolly B, Metzker ML, Hilliard CA, Liu X, Sandig V, Soderman A, Galloway SM, Liu Q, Austin CP, Caskey CT. Overexpression of M68/DcR3 in human gastrointestinal tract tumors independent of gene amplification and its location in a four-gene cluster. *Proc Natl Acad Sci U S A* 2000; 97: 1230-5.
- Balding CE, Howie AJ, Drake-Lee AB, Savage COS. Th2 dominance in nasal mucosa in patients with Wegener's granulomatosis. *Clin Exp Immunol* 2001; 125: 332-339.
- Ball TB, Plummer FA, HayGlass KT. Improved mRNA quantitation in LightCycler RT-PCR. *Int Arch Allergy Immunol* 2003; 130: 82-6.

- Bamias G, Martin C, 3rd, Marini M, Hoang S, Mishina M, Ross WG, Sachedina MA, Friel CM, Mize J, Bickston SJ, Pizarro TT, Wei P, Cominelli F. Expression, localization, and functional activity of TL1A, a novel Th1-polarizing cytokine in inflammatory bowel disease. *J Immunol* 2003; 171: 4868-74.
- Banchereau J, Steinman RM. Dendritic cells and the control of immunity. *Nature* 1998; 392: 245-251.
- Banks TA, Rouse BT, Kerley MK, Blair PJ, Godfrey VL, Kuklin NA, Bouley DM, Thomas J, Kanagat S, Mucenski ML. Lymphotoxin-alpha –deficient mice: effects on secondary lymphoid organ development and humoral immune responsiveness. *J Immunol* 1995; 155: 1685-1693.
- Barroso I, Banito B, Garci-Jimenez C, Hernandez A, Obregon MJ, Santisteban P. Norepinephrine, tri-iodothyronine and insulin upregulate glyceraldehyde-3-phosphate dehydrogenase mRNA during brown-adipocyte differentiation. *Eur J Endocrin* 1999; 141: 169-179.
- Beg AA, Baltimore D. An essential role for NF- κ B in preventing TNF- α -induced cell death. *Science* 1996; 274: 782-784.
- Bell C, Haite N. Genetic aspects of Charcot-Marie-Tooth disease. *Arch Dis Child* 1998; 78: 296-300
- Belmont HM, Levartovsky D, Goel, Amin A, Giorna R, Rediske J, Skovron ML, Abramson SB. Increased nitric oxide production accompanied by the upregulation of inducible nitric oxide synthase in vascular endothelium from patients with systemic lupus erythematosus. *Arth Rheum* 1997; 40: 1810-1816.
- Bennett L, Palucka AK, Arce E, Cantrell V, Borvak J, Banchereau J, Pascual V. Interferon and granulopoiesis in systemic lupus erythematosus blood. *J Ex Med* 2003; 197: 711-723.
- Bennett SR, Carbone FR, Karamalis F, Flavell RA, Miller JF, Heath WR. Help for cytotoxic-T cell responses is mediated by CD40 signalling. *Nature* 1998; 393: 478-479.
- Berden JHM. Lupus nephritis: consequences of disturbed removal of apoptotic cells? *Ned J Med* 2003; 61: 233-238.
- Berlin C, Berg EL, Briskin MJ, Andrew DP, Kilshaw PJ, Holzmann B, Weismann IL, Hamann A, Butcher EC. Alpha 4 Beta 7 integrin mediates lymphocyte attachment to the mucosal vascular addressing MAdCAM-1. *Cell* 1993; 74: 185:195.
- Bernard P, Reiser A, Pritham G. Mutation detection by fluorescent hybridisation probe melting curves in “Rapid cycle real-time PCR methods and applications”. Edition Eds. Meuer S, Witter C, Nakagawara K. Springer, Berlin. 2001: 11-19.
- Bernard PS, Ajioka RS, Kushner JP, Wittwer CT. Homogeneous multiplex genotyping of haemochromatosis mutations with fluorescent hybridization probes. *Am J Pathol* 1998; 153:1055-1061.
- Bernard PS, Ajioka RS, Kushner JP, Wittwer CT. Homogeneous multiplex genotyping of haemochromatosis mutations with fluorescent hybridization probes. *Am J Pathol* 1998; 153: 1055-61.
- Bernard PS, Pritham GH, Wittwer CT. Colour multiplexing hybridisation probes using the apolipoprotein E locus as a model system for genotyping. *Analytical Biochemistry* 1999; 273: 221-228.
- Bestmann L, Helmy N, Garofalo F, Demirtas A, Vonderschmitt D, Maly FE. LightCycler PCR for the polymorphisms –308 and –238 in the TNF alpha gene and for the TNFB1/B2 polymorphism in the LT alpha gene in “Rapid cycle real-time PCR methods and applications: Genetics and Oncology”. Edition Eds. Dietmaier W, Witter C, Sivasubramanian N. Springer, Berlin. 2002: 95–106.
- Beutler E, Gelart T, Kulh W. Interference of heparin with the polymerase chain reaction. *Biotechniques* 1990; 9: 166.
- Bird TB. 2004. Charcot-Marie-Tooth Hereditary neuropathy overview. <http://www.geneclinics.org>.
- Birouk N, Gouider R, Le Guern E, Gugenheim M, Tardieu S, Maisonobe T, Le Forestier N, Agid Y, Brice A, Bouche P. Charcot-Marie-Tooth disease type 1A with 17p11.2 duplication:clinical and electrophysiological phenotype study and factors influencing disease severity in 119 cases. *Brain* 1997; 120: 813-823.

- Blair IP, Kennerson ML, Nicholson GA. Detection of Charcot-Marie-Tooth type 1A duplication by the polymerase chain reaction. *Clin Chem* 1995; 4: 1105-1108.
- Blair PJ, Riley JL, Harlan DM, Abe R, Tadaki DK, Hoffmann SC, White L, Francomano T, Perfetto SJ, Kirk AD, June CH. CD40 ligand (CD154) triggers a short-term CD4 (+) T cell activation response that results in secretion of immunomodulatory cytokines and apoptosis. *J Exp Med* 2000; 191: 651-60.
- Blount S, Lunec J, Griffiths H, Herbert K, Isenberg D. *Immunol Lett* 1994; 41: 135-138.
- Bobik A, Kalinina N. Tumor necrosis factor receptor and ligand superfamily family members TNFRSF14 and LIGHT: new players in human atherogenesis. *Arterioscler Thromb Vasc Biol* 2001; 21: 1873-5.
- Boerkoel CF, Takashima H, Garcia CA, Olney RK, Johnson J, Berry K, Russo P, Kennedy S, Teebi AS, Scavina M, Williams LL, Mancias P, Butler IJ, Krajewski K, Shy M, Lupski JR. Charcot-Marie-Tooth disease and related neuropathies: mutation distribution and genotype-phenotype correlation. *Ann Neurol* 2002; 51: 190-201.
- Boerkoel CF, Takashima H, Stankiewicz P, Garcia CA, Leber SM, Rhee-Morris L, Lupski JR. Periaxin mutations cause recessive Dejerine-Sottas neuropathy. *Am J Hum Genet* 2001; 68: 325-333
- Bort S, Nelis E, Timmerman V, Sevilla T, Cruz-Martinez F, et al. Mutational analysis of the MPZ, PMP22 and Cx32 genes in patients of Spanish ancestry with Charcot-Marie-Tooth disease and hereditary neuropathy with liability to pressure palsies. *Hum Genet* 1997; 99: 746-754.
- Boswell JM, Yui MA, Burt DW, Kelley VE. Increased tumour necrosis factor and IL-1beta gene expression in the kidneys of mice with lupus nephritis. *J Immunol* 1988; 144: 3050-3054.
- Botto M, Dell'Agnola C, Bygrave AE, Thompson EM, Cook HT, Petry F, Loos M, Pandolfi PP, Walport MJ. Homozygous C1q deficiency causes glomerulonephritis associated with multiple apoptotic bodies. *Nature Genet* 1998; 19: 56-59.
- Bouma G, Strober W. The immunological and genetic basis of inflammatory bowel disease. *Nat Rev Immunol* 2003; 3: 521-33.
- Bradbury J. Neutrophil elastase inhibitors for cystic fibrosis. *DDT* 2001; 6; 441-442.
- Brancolini C, Edomi P, Marzinotto S, Schneider C. Exposure at the cell surface is required for gas3/PMP22 To regulate both cell death and cell spreading: implication for the Charcot-Marie-Tooth type 1A and Dejerine-Sottas diseases. *Mol Biol Cell* 2000; 11: 2901-2914.
- Braud VM, Allan DS, O'Callaghan CA, Soderstrom K, D'Andrea A, Ogg GS, Lazetic S, Young NT, Bell JI, Phillips JH, Lanier LL, McMichael AJ. HLA-E binds to natural killer cell receptors CD94/NKG2A, B and C. *Nature* 1998; 391: 795-799.
- Brechtbuehl K, Whalley SA, Dusheiko GM, Saunders NA. A rapid real-time quantitative polymerase chain reaction for hepatitis B virus. *J Virol Methods* 2001; 93: 105-113.
- Brooks EM, Sheflin LG, Spaulding SW. Secondary structure in the 3' UTR of EGF and the choice of reverse transcriptases affect the detection of message diversity by RT-PCR. *Biotechniques* 1995; 19: 806-815.
- Brown GR, Lee EL, El-Hayek J, Kintner K, Luck C. IL-12-independent LIGHT signaling enhances MHC class II disparate CD4+ T cell alloproliferation, IFN-gamma responses, and intestinal graft-versus-host disease. *J Immunol* 2005; 174: 4688-95.
- Bruewer M, Luegering A, Kucharzik T, Parkos CA, Madara JL, Hopkins AM, Nusrat A. Proinflammatory cytokines disrupt epithelial barrier function by apoptosis-independent mechanisms. *J Immunol* 2003; 171: 6164-72.
- Burggraf S, Malik N, Schumacher E, Olgemöller B. Rapid screening for five major Cystic Fibrosis mutations by melting peak analysis using fluorogenic hybridisation probes. In: Dietmaier W, Wittwer C, Sivasubramanian N, eds. *Rapid cycle real-time PCR Methods and applications (Genetics and Oncology)*. Springer, 2002: 47-56.
- Bustin SA, Gyselman VG, Williams NS, Dorudi S. Detection of cytokeratins 19/20 and guanylyl cyclase C in peripheral blood of colorectal cancer patients. *B J Cancer* 1999; 79: 1813-1820.
- Bustin SA, Nolan T. Analysis of mRNA expression by Real-time PCR. In *Real-time PCR: An essential guide*. Eds Edwards K, Logan J, Saunders N. Horizon bioscience United Kingdom 2004 31-70.

- Bustin SA. Absolute quantification of mRNA using real-time reverse transcription polymerase chain reaction assays. *J Mol Endocrinol* 2000; 25: 169-93.
- Butcher EC, Williams M, Youngman K, Rott L, Briskin M. Lymphocyte trafficking and regional immunity. *Adv Immunol* 1999; 72: 209-253.
- Caamano J, Hunter CA. NF- κ B family of transcription factors: central regulators on innate and adaptive immune functions. *Clin Microbiol Rev* 2002; 15: 414-429.
- Cale JM, Millican DS, Itoh H, Magness RR, Bird IM. Pregnancy induces and increase in the expression of glyceraldehyde-3-phosphate dehydrogenase in uterine artery endothelial cells. *J Soc Gyn Invest* 1997; 4: 284-292.
- Calvani N, Tucci M, Richards HB, Tartaglia P, Silvestris F. Th1 cytokines in the pathogenesis of lupus nephritis: The role of IL-18. *Autoimmunity Rev* 2005; 4: 542-548.
- Cannons JL, Bertram EM, Watts TH. Cutting edge: profound defect in T cell responses in TNF receptor-associated factor 2 dominant negative mice. *J Immunol* 2002; 169: 2828-31.
- Caradoso FDC, Jankovic J. Hereditary motor-sensory neuropathy and movement disorders. *Muscle Nerve* 1993; 16: 904-910.
- Carpenter AB. Enzyme-linked Immunoassays. In *Manual of clinical laboratory immunology* 5th Ed. Rose N, Conway de Macario E, Folds J, et al (Eds) ASM Press, Washington DC 1997; 5-29.
- Carroll MC. The complement system in regulation of adaptive immunity. *Nat Immunol* 2004; 5: 981-6.
- Carter GT, Abresch RT, Fowler WM, et al. Hereditary motor and sensory neuropathy, types I and II. *Am J Phys Med Rehabil* 1995; 74: S140-149.
- Carter GT, Jensen MP, Galer BS, Kraft GH, Crabtree LD, Beardsley RM, Abresch RT, Bird TD. Neuropathic pain in Charcot-Marie-Tooth disease. *Arch Phys Med Rehabil* 1998; 79:1560-1564.
- Cascicola-Rosen LA, Anhalt G, Rosen A. Autoantigen targets in systemic lupus erythematosus are clustered in two populations of surface structures on apoptotic keratinocytes. *J Ex Med* 1994; 179: 1317-1370.
- Casciola-Rosen L, Rosen A, Petri M, Schliessel M. Surface blebs on apoptotic cells are sites of enhanced procoagulant activity: Implications for coagulation events and antigenic spread in systemic lupus erythematosus. *PNAS* 1996; 93: 1624-1629.
- Castellano R, Van Lint C, Peri V, Veithen E, Morel Y, Costello R, Olive D, Collette Y. Mechanisms regulating expression of the tumor necrosis factor-related light gene. Role of calcium-signaling pathway in the transcriptional control. *J Biol Chem* 2002; 277: 42841-51.
- Cataldo F, Marino V, Ventura A, Bottaro G, Corazza GR. Prevalence and clinical features of selective immunoglobulin A deficiency in coeliac disease: an Italian multicentre study. Italian society of Paediatric Gastroenterology and Hepatology (SIGEP) and "Club del Tenue" Working groups on coeliac disease. *Gut* 1998; 42: 362-365.
- Catassi C, Bearzi I, Holmes GK. Association of celiac disease and intestinal lymphomas and other cancers. *Gastroenterology* 2005; 128: S79-86.
- Catassi C, Fabiani E, Corrao G, Barbato M, De Renzo A, Carella AM, Gabrielli A, Leoni P, et al. Risk of non-Hodgkin lymphoma in celiac disease. *JAMA* 2002; 287: 1413-1419.
- Cellier C, Patey N, Mauvieux L, Jabri B, Delabesse E, Cervoni JP, Burtin ML, Guy-Grand D, et al. Abnormal intestinal intraepithelial lymphocytes in refractory sprue. *Gastroenterology* 1998; 114: 471-481.
- Cerf-Bensussan N, Cuenod-Jabri B, Guy-Grand D. In: *Coeliac disease. Proceedings of the seventh international symposium on coeliac disease.* Maki M, Collin P, Visakorpi JK (eds). Coeliac Disease Study Group, Tampere Finland; 1997: 291-301.
- Cervera R, Khamashta MA, Font J, Sebastiani GD, Gil A, Lavilla P, et al. Systemic lupus erythematosus: clinical and immunologic patterns of disease expression in a cohort of 1000 patients. The European working party on systemic lupus erythematosus. *Medicine* 1993; 72: 113-124.
- Chance PF, Abbas N, Lensch MW, Pentao L, Roa BB, Patel PI, et al. Two autosomal dominant neuropathies result from reciprocal DNA deletion/deletion of a region on chromosome 17. *Hum Mol Gent* 1994; 3: 223-228.

- Chance PF, Alderson MF, Leppig KA, Lensch MW, Matsunami N, Smith B, Swanson PD, Odelberg SJ, Distèche CM, Bird TD. DNA deletion associated with hereditary neuropathy with liability to pressure palsies. *Cell* 1993; 72: 143-151
- Chao CC, Yam WC, Lin-Chao S. Coordinated induction of two unrelated glucose-regulated protein genes by a calcium ionophore: human Bip/GRP78 and GAPDH. *Biochem Biophys Res Commun* 1990; 171:431-438.
- Chaplin DD, Fu Y. Cytokine regulation of secondary lymphoid organ development. *Curr Opin Immunol* 1998; 10: 289-97.
- Charcot JM, Marie P. Sur une forme particuliere d'atrophie musculaire progressive souvent familiale debutant par les pieds et les jambes et atteignant plus tard les mains. *Rev Med* 1886; 6: 97-138.
- Chatila T, Silverman L, Miller R, Geha R. Mechanisms of T cell activation by the calcium ionophore ionomycin. *J Immunol* 1989; 143: 1283-1289.
- Chen J, Zhang L, Kim S. Quantification and detection of DcR3, a decoy receptor in TNFR family. *J Immunol Methods* 2004; 285: 63-70.
- Chen MC, Hsu TL, Luh TY, Hsieh SL. Overexpression of bcl-2 enhances LIGHT- and interferon-gamma-mediated apoptosis in Hep3BT2 cells. *J Biol Chem* 2000; 275: 38794-801.
- Chen NJ, Huang MW, Hsieh SL. Enhanced secretion of IFN-gamma by activated Th1 cells occurs via reverse signaling through TNF-related activation-induced cytokine. *J Immunol* 2001; 166: 270-6.
- Chiochia G, Smith KA. Highly sensitive method to detect mRNAs in individual cells by direct RT-PCR using Tth DNA polymerase. *Biotechniques* 1997; 22: 312-318.
- Choi JR, Lee WH, Sunwoo IN, Lee E, Lee C, Lim JB. Effectiveness of Real-time quantitative PCR compared to repeat PCR for the diagnosis of Charcot-Marie-Tooth type 1A and hereditary liability to pressure palsies. *Yonsei Med J* 2005; 46: 347-352.
- Chung JY, Park YC, Ye H, Wu H. All TRAFs are not created equal: common and distinct molecular mechanisms of TRAF-mediated signal transduction. *J Cell Sci* 2002; 115: 679-88.
- Chung Y-H, Chao Y, Hsieh S-L, Lin W-W. Mechanism of LIGHT/Interferon- γ induced cell death in HT-29 cells. *J Cell Biochem* 2004; 93: 1188-1202.
- Ciccocioppo R, Di Satatino A, Corazza GR. The immune recognition of gluten in coeliac disease. *Clin Exp Immunol* 2005; 140: 408-416.
- Ciclitira PJ. Recent advances in coeliac disease. *Clin Med* 2003; 3: 166-9.
- Clegg RM. Fluorescence resonance energy transfer and nucleic acids. In: *Methods in enzymology*. Lilley DMJ, Dahlber JE, Eds. Academic Press, NY. 1992; 211: 353-388.
- Clemente MG, De Virgiliis S, Kang JS, Macatagney R, Musu MP, Di Pierro MR, Drago S, Congia M, Fasano A. Early effects of gliadin on enterocyte intracellular signalling involved in intestinal barrier function. *Gut*; 52: 218-223.
- Cohavy O, Zhou J, Granger S, Ware CF, Targan SR. LIGHT expression by mucosal T cell may regulate INF- γ expression in the intestine. *J Immunol* 2004; 173: 251-258.
- Cohavy O, Zhou J, Ware CF, Targan SR. LIGHT is constitutively expressed on T and NK cells in the human gut and can be induced by CD2-mediated signaling. *J Immunol* 2005; 174: 646-653.
- Collette Y, Gilles A, Pontarotti P, Olive D. A co-evolution perspective of the TNFSF and TNFRSF families in the immune system. *Trends Immunol* 2003; 24: 387-94.
- Collin P, Kaukinen K, Vogelsang H, Korponay-Szabo I, Sommer R, Schreier E, Volta U, Granito A, Veronesi L, Mascart F, et al. Antiendomysial and antihuman recombinant tissue transglutaminase antibodies in the diagnosis of coeliac disease: a biopsy-proven European multicentre study. *Eur J Gastroenterol Hepatol* 2005; 17: 85-91.
- Collin P, Reunala T, Pullala E, Laippala P, Keyrilainen O, Pasternack A. Coeliac disease-associated disorders and survival. *Gut* 1994; 35: 1215-1218.
- Collins F. Cystic fibrosis: molecular biology and therapeutic implications. *Science* 1992; 256: 774-779.
- Compaan DM, Gonzalez LV, Tom I, Loyet KM, Eaton D, Hymowitz SG. Attenuating lymphocyte activity: the crystal structure of the BTLA-HVEM complex. *J Bio Chem* 2005; 280: 39553-39561.

- Cone RW, Hobson AC, Huang ML. Coamplified positive control detects inhibition of polymerase chain reactions. *J Clin Microbiol* 1992; 30: 3185-3189.
- Cope AP. Studies of T-cell activation in chronic inflammation. *Arthritis Res* 2002; 4 Suppl 3: S197-211.
- Cotch MF, Fauci AS, Hoffman GS. HLA typing in patients with Wegener's granulomatosis. *Ann Inter Med* 1995; 122: 635-638.
- Creusot RJ, Mitchison NA. How DCs control cross-regulation between lymphocytes. *Trends Immunol* 2004; 25: 126-31.
- Crispin JC, Vargas MI, Alcocer-Varela J. Immunoregulatory T cells in autoimmunity. *Autoimmun Rev* 2004; 3: 45-51.
- Croft M. Co-stimulatory members of the TNFR family: keys to effective T-cell immunity? *Nat Rev Immunol* 2003; 3: 609-20.
- Croft M. The evolving crosstalk between co-stimulatory and co-inhibitory receptors: HVEM-BTLA. *Trends Immunol* 2005; 26: 292-4.
- Csernok E, Ernst M, Schmitt W, Bainton DF, Gross WL. Activated neutrophils express PR3 on their plasma membrane in vitro and in vivo. *Clin Exp Immunol* 1994; 95: 244-250.
- Csiszar A, Nagy GY, Gergely P, Pozsonyi T, Pocsik E. Increased interferon-gamma (INF- γ), IL-10 and decreased IL-4 mRNA expression in peripheral blood mononuclear cells (PBMC) from patients with systemic lupus erythematosus (SLE). *Clin Exp Immunol* 2000; 122: 464-470.
- Dairaghi DJ, Soo KS, Oldham ER, Premack BA, Kitamura T, Bacon KB, Schall TJ. RANTES-induced T cell activation correlates with CD3 expression. *J Immunol* 1998; 160: 426-33.
- Daum S, Bauer U, Foss HD, Schuppan D, Stein H, Riecken EO, Ullrich R. Increase expression of mRNA for matrix metalloproteinases-1 and -3 and tissue inhibitor of metalloproteinases-1 in intestinal biopsy specimens from patients with coeliac disease. *Gut* 1999; 44: 17-25.
- Davidson A, Diamond B. Autoimmune diseases. *N Engl J Med* 2001; 345: 340-50.
- Davies EJ, Snowdon N, Haillarby MC, Carthy D, Grennan DM, Thompson W, Ollier WE. Mannose-binding protein gene polymorphisms in systemic lupus erythematosus. *Arthritis Rheum* 1995; 38: 110-114.
- Davies JC, Geddes DM, Alton EW. Prospects for gene therapy for cystic fibrosis. *Mol Med Today* 1998; 4: 292-9.
- Dean GS, Tyrrell-Price J, Crawley E, Isenberg DA. Cytokines and systemic lupus erythematosus. *Ann Rheum Dis* 2000; 59: 243-251.
- Deem RL, Shanahan F, Targan SR. Triggered human mucosal T cell release tumour necrosis factor- α and interferon- γ which kill human colonic epithelial cells. *Clin Exp Immunol* 1991; 83: 79-84.
- Degli-Esposti MA, Davis-Smith T, Din WS, Smolak PJ, Goodwin RG, Smith CA. Activation of the lymphotoxin beta receptor by cross-linking induces chemokine production and growth arrest in A375 melanoma cells. *J Immunol* 1997; 58: 1756-1762.
- Dejardin E, Droin NM, Delhase M, Haas E, Cao Y, Makris C, Li ZW, Karin M, Ware CF, Green DR. The Lymphotoxin-beta receptor induces different patterns of gene expression via two NF-kappaB pathways. *Immunity* 2002; 17: 525-535.
- Dempsey E, Barton DE, Ryan F. Detection of Five common *CFTR* mutations by Rapid-Cycle Real-Time Amplification Refractory Mutation System PCR. *Clin Chem* 2004; 50: 773-775.
- Dempsey E, Ryan F. Genetic testing for cystic fibrosis. *The Irish Scientist* 2002: 106.
- Dempsey PW, Doyle SE, He JQ, Cheng G. The signaling adaptors and pathways activated by TNF superfamily. *Cytokine Growth Factor Rev* 2003; 14: 193-209.
- Devidas S, Guggino WB. The cystic fibrosis transmembrane conductance regulator and ATP. *Curr Opin Cell Biol* 1997; 9: 547-552.
- Dewar D, Pereira SP, Ciclitira PJ. The pathogenesis of coeliac disease. *Int J Biochem Cell Biol* 2004; 36: 17-24.
- Dewar DH, Ciclitira PJ. Clinical features and diagnosis of celiac disease. *Gastroenterology* 2005; 128: S19-24.

- Dieterich W, Ehnis T, Bauer M, Donner P, Volta U, Riecken E, Schuppan D. Identification of tissue transglutaminase as the autoantigen of celiac disease. *Nat Med* 1997; 3: 797-801.
- Digass AU, Podolsky DK. Cytokine modulation of intestinal epithelial cells restitution: central role of transforming growth factor beta. *Gastroenterology* 1993; 105: 1323-1332.
- Dijkstra HM, Scheepers RH, Oost WW, Stegeman CA, van der Pol WL, Slutier WJ, Kallenberg CG, van de Winkel JG, Tervaert JW. Fc gamma receptor polymorphisms in Wegener's granulomatosis: risk factors for disease relapse. *Arthritis Rheum* 1999; 42: 1823-1827.
- DiSant'Agnese PA. Exocrine gland dysfunction in cystic fibrosis of the pancreas. *Acta Paediatr Stockh* 1953; 46: 51
- Duggan JM. Coeliac disease: the great imitator. *Med J Aust* 2004; 180: 524-6.
- D'Urso D, Prior R, Greiner-Petter R, Gabreels-Festen AA, Muller HW. Overloaded endoplasmic reticulum-Golgi compartments, a possible pathomechanism of peripheral neuropathies caused by mutations of the peripheral myelin protein PMP22. *J Neurosci* 1998; 18: 731-740.
- Dutton RW, Bradley LM, Swain SL. T cell memory. *Ann Rev Immunol* 1998; 16: 201-235.
- Dyck PJ, Chance P, Lebo RV, et al. Hereditary motor and sensory neuropathies. In Dyck PJ, Thomas PK, Griffin JW, Low PA, Poduslo JF (Eds). *Peripheral neuropathy*. 3rd ed Philadelphia: WB Saunders; 1993: 1094-1136.
- Dyck PJ, O'Brien PC, Konsanke JL, Gillen DA, Karnes JL. A 4,2, and 1 stepping algorithm for quick and accurate estimation of cutaneous sensation threshold. *Neurology* 1993; 43: 1508-1512.
- Dykxhoorn DM, Novina CD, Sharp PA. Killing the messenger: Short RNAs that silence gene expression. *Nat Rev Mol Cell Biol* 2003; 4: 457-467.
- Ebert EC. Interleukin 15 is a potent stimulant of intraepithelial lymphocytes. *Gastroenterology* 1998; 115: 1439-1445.
- Edberg JC, Wainstein E, Wu J, Csernok E, Sneller MC, Hoffman GS, Keystone EC, Gross WL, Kimberly RP. Analysis of Fc gamma RII gene polymorphisms in Wegener's granulomatosis. *Exp Clin Immunogenet* 1997; 14: 183-195.
- Edwards KJ, Logan JM. Mutation detection by Real-time PCR. In *Real-time PCR: An essential guide*. Eds Edwards K, Logan J, Saunders N. Horizon bioscience, United Kingdom 2004; 31-70.
- Elkon KB, Sutherland DC, Rees AJ, Hughes GRV, Batchelor JR. HLA frequencies in systemic vasculitis. Increase in HLA-DR2 in Wegener's granulomatosis. *Arthritis Rheum* 1983; 26: 102-105.
- Emerson J, Rosenfeld M, McNamara S, Ramsey B, Gibson RL. *Pseudomonas aeruginosa* and other predictors of mortality and morbidity in young children with cystic fibrosis. *Pediatr Pulmonol* 2002; 34: 91-100.
- Esnault VL, Audrain MA, Sesboue R. Alpha-1-antitrypsin phenotyping in ANCA-associated diseases: one of several arguments for protease/anti-protease imbalance in systemic vasculitis. *Exp Clin Immunogenet* 1997; 14: 206-213.
- Esparza J, Vilardell C, Calvo J, Juan M, Vives J, Urbano-Marquez A, Yague J, Cid MC. Fibronectin upregulates gelatinase B (MMP-9) and induces coordinated expression of gelatinase A (MMP-2) and its activator MT1-MMP (MMP-14) by human T lymphocyte cell lines. A process repressed through RAS/MAP kinase signaling pathways. *Blood* 1999; 94: 2754-66.
- Esposito C, Paparo F, Caputo I, Rossi M, Maglio M, Sblattero D, Not T, Porta R, Auricchio S, Marzari R, Troncone R. Anti-tissue transglutaminase antibodies from coeliac patients inhibit transglutaminase activity both in vitro and in situ. *Gut* 2002; 51: 177-181.
- Fabbretti E, Edomi P, Brancolini C, Schneider C. Apoptotic phenotype induced by overexpression of wild-type gas3/PMP22: its relation to the demyelinating peripheral neuropathy CMT1A. *Genes Dev* 1995; 9: 1846-1856.
- Falchuk ZM, Strober W. Gluten-sensitive enteropathy: synthesis of anti-gliadin antibody in vitro. *Gut* 1974; 15: 947-952.
- Falk RJ, Jennette JC. Anti-neutrophil cytoplasmic autoantibodies with specificity for myeloperoxidase in patients with system vasculitis and idiopathic necrotising and crescentic glomerulonephritis. *N Eng J Med*. 1988; 318: 1615-1657.
- Farrell RJ, Kelly CP. Celiac sprue. *N Engl J Med* 2002; 346: 180-8.

- Farrell RJ, Kelly CP. Diagnosis of celiac sprue. *Am J Gastroenterol* 2001; 96: 3237-46.
- Fasano A, Not T, Wang W, Uzzau S, Berti I, Tomassini A, Goldblum SE. Zonulin, a newly discovered modulator of intestinal permeability and its expression in coeliac disease. *Lancet*, 2000; 355: 1518-1519.
- Fathman CG, Soares L, Chan SM, Utz PJ. An array of possibilities for the study of autoimmunity. *Nature* 2005; 435: 605-11.
- Fauci AS, Haynes BF, Katz P, Wolff SM. Wegener's granulomatosis: prospective clinical and therapeutic experience with 85 patients for 21 years. *Ann Intern Med* 1983; 116: 488-494.
- Fava RA, Notidis E, Hunt J, Szanya V, Ratcliffe N, Ngam-Ek A, De Fougereolles AR, Sprague A, Browning JL. A role for the lymphotoxin/LIGHT axis in the pathogenesis of murine collagen-induced arthritis. *J Immunol* 2003; 171: 115-26.
- Fehinger TA, Caligiuri MA. Interleukin 15: biology and relevance to human disease. *Blood* 2001; 97: 14-32.
- Feighery C, Weir DG, Whealan A, Willoughby R, Youngprapakorn S, Lynch S, O'Morain C, McEneaney P, O'Farrelly C. Diagnosis of gluten-sensitive enteropathy: is exclusive reliance on histology appropriate? *Eur J Gastroenterol Hepatol* 1998; 10: 919-925.
- Feighery C. Fortnightly review: coeliac disease. *Bmj* 1999; 319: 236-9.
- Feldmann M, Steinman L. Design of effective immunotherapy for human autoimmunity. *Nature* 2005; 435: 612-9.
- Ferrie RM, Schwarz MJ, Robertson NH, Vaudin S, Super M, Malone G, Little S. Development, Multiplexing and Application of ARMS Tests for Common Mutations in the CFTR Gene. *Am J Hum Genet* 1992; 51: 251-262.
- Ferrie RM, Schwarz MJ, Robertson NH, Vaudin S, Super M, Malone G, Little S. Development, Multiplexing and Application of ARMS Tests for Common Mutations in the CFTR Gene. *Am J Hum Genet* 1992; 51: 251-262.
- Ferry B, Antrobus P, Huzicka I, Farrel A, Lane A, Chapel H. Intercellular cytokine expression in whole blood preparations from normals and patients with atopic dermatitis. *Clin Exp Immunol* 1997; 110: 410-417.
- Filaci G, et al. Impairment of CD8+ T suppressor cell function in patients with active systemic lupus erythematosus. *J Immunol* 2001; 166: 6452-6457.
- Fink L, Seeger W, Ermert L, Hanze J, Stahl U, Grimminger F, Kummer W Bohle RM. Real-time quantitative RT-PCR after laser-assisted cell picking. *Nat Med* 1998; 4: 1329-1333.
- Fischer FR, Luo Y, Luo M, Santambrogio L, Dorf ME. RANTES-induced chemokine cascade in dendritic cells. *J Immunol* 2001; 167: 1637-43.
- Force WR, Cheung TC, Ware CF. Dominant negative mutants of TRAF3 reveal an important role for the coiled coil domains in cell death signalling by the lymphotoxin-beta receptor. *J Biol Chem* 1997; 272: 30835-30840.
- Forster R, Schubel A, Breitfeld D, Kremmer E, Renner-Muller I, Wolf E, Lipp M. CCR7 coordinates the primary immune response by establishing functional microenvironments in secondary lymphoid organs. *Cell* 1999; 99: 23-33.
- Foy CA, Parkes HC. Emerging homogeneous DNA-based technologies in the clinical laboratory. *Clin Chem* 2001; 47: 990-1000.
- Franzoso G, Zazzeroni F, Papa S. JNK: a killer on a transcriptional leash. *Cell Death Differ* 2003; 10: 13-5.
- Freeman GJ, Boussiotis VA, Anumathan A, Bernstein GM, Ke XY, Rennert PD, Gray GS, Gribben JG, Nadler LM. B7-1 and B7-2 do not deliver identical costimulatory signals, since B7-2 but not B7-1 preferentially costimulates the initial production of IL-4. *Immunity* 1995; 2: 523-531.
- Freeman WM, Walker SJ, Vrana KE. Quantitative RT-PCR: pitfalls and potential. *Biotechniques* 1999; 26: 112-22, 124-5.
- Fronhoffs S, Totzke G, Stier S, Wernert N, Rothe M, Bruning T, Koch B, Sachinidis A, Vetter H, Ko Y. A method for the rapid construction of cRNA standard curves in quantitative real-time reverse transcription polymerase chain reaction. *Mol Cell Probes* 2002; 16: 99-110.

- Fu XY, Chaplin DD. Development and maturation of secondary lymphoid tissues. *Annu Rev Immunol* 1999; 17:399-433.
- Futterer A, Mink K, Luz A, Kosco-Vilbois MH, Pfeffer K. The lymphotoxin β receptor controls organogenesis and affinity maturation in peripheral lymphoid tissues. *Immunity* 1998; 9: 59-70.
- Gabay C, Cakir N, Moral F, Roux-Lombard P, Meyer O, Dayer JM, Vischer T, Yazici H, Guerne PA. Circulating levels of tumour necrosis factor soluble receptors in systemic lupus erythematosus are significantly higher than in other rheumatic diseases and correlate with disease activity. *J Rheumatol* 1997; 24: 303-308.
- Gabriel JM, Erne B, Pareyson D, Sghirlanzoni A, Taroni F, Steck AJ. Gene dosage effects in hereditary peripheral neuropathy. Expression of peripheral myelin protein 22 in Charcot-Marie-Tooth disease type 1A and hereditary neuropathy with liability to pressure palsies nerve biopsies. *Neurology* 1997; 49: 1635-1640.
- Gaffney PM, Ortmann WA, Selby SA, Shark KB, Ockenden TC, Rohlf KE, Walgrave NL, Boyum WP, Malmgren ML, Miller ME, Kearns GM, Messner RP, King RA, Rich SS, Behrens TW. Genome screening in human systemic lupus erythematosus: results from a second Minnesota cohort and combined analyses of 187 sib-pair families. *Am J Hum Genet* 2000; 66: 547-556.
- Gale L, Wimalaratna H, Brotodiharjo A, Duggan JM. Down syndrome is strongly associated with coeliac disease. *Gut* 1997; 40: 492-496.
- Garcia CA. A clinical review of Charcot-Marie-Tooth. *Ann N Y Acad Sci* 1999; 883: 69-76.
- Garside P, Mowat AM, Khoruts A. Oral tolerance in disease. *Gut* 1999; 44: 137-42.
- Gaur U, Aggarwal BB. Regulation of proliferation, survival and apoptosis by members of the TNF superfamily. *Biochem Pharmacol* 2003; 66: 1403-8.
- Geddes D, Alton E. Cystic fibrosis clinical trials. *Advanced Drug Delivery Reviews* 1998; 30: 205-217.
- Gelfand DH. Taq DNA polymerase. In PCR theory, principles and application to DNA amplification. Erlich HA (Ed) PCR Technology. Stockton Press, NY 1989; 17-22.
- Gencik M, Muller S, Borgmann S, Fricke H. Proteinase 3 gene polymorphisms and Wegener's granulomatosis. *Kidney Int* 2000; 58: 2473-2477.
- Gentle A, Anastasopoulos F, McBrien NA. High-resolution semi-quantitative real-time PCR without the use of a standard curve. *Biotechniques* 2001; 31: 502, 504-6, 508.
- Gertsch J, Guttinger M, Sticher O, Heilmann J. Relative quantification of mRNA levels in Jurkat T cells with RT-real time-PCR (RT-rt-PCR): new possibilities for the screening of anti-inflammatory and cytotoxic compounds. *Pharm Res* 2002; 19: 1236-43.
- Gibson LE, Cooke RE. A test for concentration of electrolytes in sweat in cystic fibrosis of the pancreas utilizing pilocarpine by iontophoresis. *Pediatrics* 1959; 23: 545-549.
- Gill RM, Ni J, Hunt JS. Differential expression of LIGHT and its receptors in human placental villi and amniochorion membranes. *Am J Pathol* 2002; 161: 2011-7.
- Gingeras TR, Higuchi R, Kricka LJ, Lo YM, Wittwer CT. Fifty years of molecular (DNA/RNA) diagnostics. *Clin Chem* 2005; 51: 661-71.
- Ginzinger DG. Gene quantification using real-time quantitative PCR: an emerging technology hits the mainstream. *Exp Hematol* 2002; 30: 503-12.
- Giscombe R, Grunewald J, Nityanand S, Lefvert AK. T cell receptor (TCR) V gene usage in patients with systemic necrotising vasculitis. *Clin Exp Immunol* 1995; 101: 213-218.
- Giulietti A, Overbergh L, Valckx D, Decallonne B, Bouillon R, Mathieu C. An overview of real-time quantitative PCR: applications to quantify cytokine gene expression. *Methods* 2001; 25: 386-401.
- Glaab W, Skopek TR. A novel assay for allelic discrimination that combines the fluorogenic 5' nuclease polymerase chain reaction (TaqMan®) and mismatch amplification mutation assay. *Mutat Res* 1999; 430: 1-12.
- Goblet C, Prost E, Whalen RG. One-step amplification of transcripts in total RNA using the polymerase chain reaction. *Nucleic Acids Res* 1989; 17: 2144-2149.

- Godfrey TE, Kim SH, Chavira M, Ruff DW, Warren RS, Gray JW, Jensen RH. Quantitative mRNA expression analysis from formalin-fixed, paraffin-embedded tissues using 5' nuclease quantitative reverse transcription- polymerase chain reaction. *J Mol Diag* 2000; 2: 84-91.
- Goetzl EJ, Banda MJ, Leppert D. Matrix metalloproteinases in immunity. *J Immunol* 1996; 156: 1-4.
- Gommerman JL, Browning JL. Lymphotoxin/light, lymphoid microenvironments and autoimmune disease. *Nat Rev Immunol* 2003; 3: 642-55.
- Gommerman JL, Giza K, Perper S, Sizing I, Ngam-Ek A, Nickerson-Nutter C, Browning JL. A role for surface lymphotoxin in experimental autoimmune encephalomyelitis independent of LIGHT. *J Clin Invest* 2003; 112: 755-67.
- Gommerman JL. A role for the lymphotoxin/LIGHT pathway in T cell mediated autoimmunity and infectious diseases. *Clin Appl Immunol Rev* 2004; 4: 367-393.
- Goodnow CC, Sprent J, de St Groth BF, Vinuesa CG. Cellular and genetic mechanisms of self-tolerance and autoimmunity. *Nature* 2005; 435: 590-7.
- Goronzy JJ, Weyand CM. Rheumatoid arthritis. *Immunol Rev* 2005; 204: 55-73.
- Granger SW, Butrovich KD, Houshmand P, Edwards WR, Ware CF. Genomic characterization of LIGHT reveals linkage to an immune response locus on chromosome 19p13.3 and distinct isoforms generated by alternate splicing or proteolysis. *J Immunol* 2001; 167: 5122-8.
- Granger SW, Rickert S. LIGHT-HVEM signaling and the regulation of T cell-mediated immunity. *Cytokine Growth Factor Rev* 2003; 14: 289-96.
- Granger SW, Ware CF. Turning on LIGHT. *J Clin Invest* 2001; 108: 1741-2.
- Greco L, Romino R, Coto I, Di Cosmo N, Percopo S, Maglio M, Paparo F, Gasperi V, Limongelli MG, Cotichini R, D'Agate C, Tinto N, Sacchetti L, Tosi R, Stazi MA. The first large population based twin study of coeliac disease. *Gut* 2002; 50: 624-628.
- Green PH, Jabri B. Coeliac disease. *Lancet* 2003; 362: 383-91.
- Green PHR, Stavropoulos SN, Panagi SG, Goldstein SL, McMahon DJ, Absan H, Neugut AI. Characteristics of adults celiac disease in the USA: results of national survey. *Am J Gastroenterol* 2001; 96: 126-131.
- Gundry C. Fluorescent hybridisation probe detection of the delF508 cystic fibrosis allele of the LightCycler in "Rapid cycle real-time PCR methods and applications". Edition Eds. Meuer S, Witter C, Nakagawara K. Springer, Berlin. 2001: 111 – 117.
- Gundry CN, Wittwer, CT. Sybr Green 1 analysis of the trinucleotide repeat responsible for Huntington's disease in "Rapid cycle real-time PCR methods and applications: Genetics and Oncology". Edition Eds. Dietmaier W, Witter C, Sivasubramanian N. Springer, Berlin. 2002: 57–63.
- Guo Z, Wang J, Meng L, Wu Q, Kim O, Hart J, He G, Zhou P, Thistlethwaite JR, Jr., Alegre ML, Fu YX, Newell KA. Cutting edge: membrane lymphotoxin regulates CD8(+) T cell-mediated intestinal allograft rejection. *J Immunol* 2001; 167: 4796-800.
- Gupta S. Molecular signaling in death receptor and mitochondrial pathways of apoptosis. *Int J Oncol* 2003; 22: 15-20.
- Haas C, Ryffel B, Le Hir M. INF-gamma receptor deletion prevents autoantibody production and glomerulonephritis in lupus-prone (NZB X NZW)F1 mice. *J Immunol* 1998; 160: 3708-3713.
- Hadida F, Vieillard V, Mollet L, Clark-Lewis I, Baggiolini M, Debre P. Cutting edge: RANTES regulates Fas ligand expression and killing by HIV-specific CD8 cytotoxic T cells. *J Immunol* 1999; 163: 1105-9.
- Halastensen TS, Brandzaeg P. Activated T lymphocytes in the coeliac lesion: non-proliferative activation (CD25) of CD4+ α/β cells in the lamina propria but proliferation (Ki-67) of the α/β and γ/δ cells in the epithelium. *Eur J Immunol* 1993; 23: 505-510.
- Halastensen TS, Farstad IN, Scott H, Fausa I, Brandtzaeg P. Intraepithelial TCR α/β + lymphocytes express CD45RO more often than the TCR γ/δ + counterparts in coeliac disease. *Immunology* 1990; 71: 460-466.
- Halttunen T, Marttinen A, Rantala I, Kainulainen H, Maki M. Fibroblasts and transforming growth factor beta induce organization and differentiation of T84 human epithelial cells. *Gastroenterology* 1996; 111: 1252-1262.

- Hamalainen HK, Tubman JC, Vikman S, Kyrola T, Ylikoski E, Warrington JA, Lahesmaa R. Identification and validation of endogenous reference genes for expression profiling of T helper cell differentiation by quantitative real-time RT-PCR. *Anal Biochem* 2001; 299: 63-70.
- Haney C, Snipes GJ, Shooter EM, Suter U, Garcia C, Griffin JW, Trapp BD. Ultrastructural distribution of PMP22 in Charcot-Marie-Tooth disease type 1A. *J Neuropathol Exp Neurol* 1996; 55: 290-299.
- Harding AE. From the syndrome of Charcot, Marie and Tooth to disorders of peripheral myelin proteins. *Brains* 1995; 118: 809-818.
- Harper L, Savage COS. Pathogenesis of ANCA-associated systemic vasculitis. *J Pathol* 2000; 190: 349-359.
- Harrop JA, McDonnell PC, Brigham-Burke M, Lyn SD, Minton J, Tan KB, Dede K, Spampinato J, Silverman C, Hensley P, DiPrinzio R, Emery JG, Deen K, Eichman C, Chabot-Fletcher M, Truneh A, Young PR. Herpesvirus entry mediator ligand (HVEM-L), a novel ligand for HVEM/TR2, stimulates proliferation of T cells and inhibits HT29 cell growth. *J Biol Chem* 1998; 273: 27548-56.
- Harrop JA, Reddy M, Dede K, Brigham-Burke M, Lyn S, Tan KB, Silverman C, Eichman C, DiPrinzio R, Spampinato J, Porter T, Holmes S, Young PR, Truneh A. Antibodies to TR2 (herpesvirus entry mediator), a new member of the TNF receptor superfamily, block T cell proliferation, expression of activation markers, and production of cytokines. *J Immunol* 1998; 161: 1786-94.
- Hashimoto JG, Beadles-Bohling AS, Wiren KM. Comparison of RiboGreen and 18S rRNA quantitation for normalizing real-time RT-PCR expression analysis. *Biotechniques* 2004; 36: 54-6, 58-60.
- Hauer J, Puschner S, Ramakrishnan P, Simon U, Bongers M, Federle C, Engelmann H. TNF receptor (TNFR)-associated factor (TRAF) 3 serves as an inhibitor of TRAF2/5-mediated activation of the noncanonical NF-kappaB pathway by TRAF-binding TNFRs. *Proc Natl Acad Sci U S A* 2005; 102: 2874-9.
- Haupt A, Schols L, Przuntek H, Epplen Jt. Polymorphisms in the PMP-22 gene region (17p11.2-12) are crucial for simplified diagnosis of duplication/deletions. *Hum Genet* 1997; 99: 688-691.
- Hausch F, Shan L, Santiago NA, Gray GM, Khosla C. Intestinal digestive resistance of immunodominant gliadin peptides. *Am J Physiol Gastro Liver Physiol* 2002; 283: 996-1003.
- Herrera-Esparza R, Barbosa-Cisneros O, Villalobos-Hurtado R, Avalos-Diaz E. Renal expression of IL-6 and TNF- α genes in lupus nephritis. *Lupus* 1998; 7: 154-158.
- Higuchi R, Dollinger G, Walsh PS, Griffith R. Simultaneous amplification and detection of specific DNA sequences. *Biotechnology* 1992; 10: 413-417.
- Higuchi R, Fockler C, Dollinger G, Watson R. Kinetic PCR analysis: real-time monitoring of DNA amplification reactions. *Biotechnology* 1993; 11:1026-1030.
- Hill ID. What are the sensitivity and specificity of serologic tests for celiac disease? Do sensitivity and specificity vary in different populations? *Gastroenterology* 2005; 128: S25-32.
- Hjelmstrom P, Fjell J, Nakagawa T, Sacca R, Cuff CA, Ruddle NH. Lymphoid tissue homing chemokines are expressed in chronic inflammation. *Am J Pathol* 2000; 156: 1133-1138.
- Hoffenberg EJ. Should all children be screened for celiac disease? *Gastroenterology* 2005; 128: S98-103.
- Hoffman GS, Kerr GS, Leavitt RY, Hallahan CW, Lebovics RS, Travis WD, Rottem M, Faci AS. Wegener's granulomatosis: and analysis of 158 patients. *Ann Intern Med* 1992; 116: 488-498.
- Hoffman RW. T cells in the pathogenesis of systemic lupus erythematosus. *Clin Immunol* 2004; 113: 4-13
- Hogan PG, Chen L, Nardone J, Rao A. Transcriptional regulation by calcium, calcineurin, and NFAT. *Genes Dev* 2003; 17: 2205-2232.
- Holmes GKT. Non-malignant complications of coeliac disease. *Acta Paediatr Suppl* 1996; 412: 68-75.
- Hoogendijk JE, De Visser M, Bolhusi PA, Hart AA, Ongerboer de Visser BW. Hereditary motor and sensory neuropathy type 1:clinical and neurographical features of the 17p duplication subtype. *Muscle Nerve* 1994; 17: 787-800.

- Horiuchi T, Nishizaka, Yasunga S, Higuchi M, Tsukamoto H, Hayashi K, Nagasawa K. Association of Fas/Apo-1 gene polymorphism with systemic lupus erythematosus in Japanese. *Rheumatology (Oxford)* 1999; 38: 516-520.
- Hsu H, Solovyev I, Colombero A, Elliott R, Kelley M, Boyle WJ. ATAR, a novel tumor necrosis factor receptor family member, signals through TRAF2 and TRAF5. *J Biol Chem* 1997; 272: 13471-4.
- Hsu TL, Chang YC, Chen SJ, Liu YJ, Chiu AW, Chio CC, Chen L, Hsieh SL. Modulation of dendritic cell differentiation and maturation by decoy receptor 3. *J Immunol* 2002; 168: 4846-53.
- Huang D, Zhou Y, Hoffman GS. Pathogenesis: immunogenetic factors. *Best Prac Res Clin Rheum* 2001; 15: 239-258.
- Hurchla MA, Sedy JR, Gavrieli M, Drake CG, Murphy TL, Murphy KM. B and T lymphocyte attenuator exhibits structural and expression polymorphisms and is highly induced in anergic CD4+ T cells. *J Immunol* 2005; 174: 3377-85.
- Hutchison ML, Govan JR. Pathogenicity of microbes associated with cystic fibrosis. *Microbes Infect* 1999; 1: 1005-1014.
- Hutchison ML, Govan JR. Pathogenicity of microbes associated with cystic fibrosis. *Microbes and Infection* 1999; 1: 1005-1014.
- Huxley C, Passage E, Manson A, et al. Construction of a mouse model of Charcot-Marie-Tooth disease type 1A by pronuclear injection of human YAC DNA. *Hum Mol Genet* 1996; 5: 563-569.
- Huxley C, Passage E, Robertson AM, Youl B, Huston S, Manson A, Saberan-Djoniedi D, Figarella-Branger D, et al. Correlation between varying levels of PMP22 expression and the degree of demyelination and reduction in nerve conduction velocities in transgenic mice. *Hum Mol Genet* 1998; 7: 449-458.
- Iijima T, Minami Y, Nakamura N, Onizuka M, Morishita Y, Inadome Y, Noguchi M. MMP-2 activation and stepwise progression of pulmonary adenocarcinoma: analysis of MMP-2 and MMP-9 with gelatin zymography. *Pathol Int* 2004; 54: 295-301.
- Iltanen S, Collin P, Korpela M, Holm K, Partanen J, Polvi A, Maki M. Celiac disease and markers of celiac disease latency in patients with primary Sjogren's syndrome. *Am J Gastroenterol* 1999; 94: 1042-1046.
- Ionasescu VV. Charcot-Marie-Tooth neuropathies: from clinical description to molecular genetics. *Muscle Nerve* 1995; 18: 267-275.
- Isakov N, Altman A. Protein Kinase C θ in T cell activation. *Ann Rev Immunol* 2002; 20: 761-794.
- Ishtani R, Sunaga K, Tanaka M, Aishita H, Chuang DM. Overexpression of glyceraldehyde-3-phosphate dehydrogenase is involved in low K⁺-induced apoptosis but not necrosis of cultured cerebellar granule cells. *Mol Phram* 1997; 51: 542-550.
- Jabri B, Patey-Mariaud De Serre N, Cellier C, Evans K, Gache C, Carvalho C, Mougenot JF, Allez M, et al. Selective expansion of intraepithelial lymphocytes expressing the HLA-E specific natural killer receptor CD94 in celiac disease. *Gastroenterology* 2000; 118: 867-879.
- Jacob CO, van der Meide PH, McDevitt HO. In vivo treatment of (NZB X NZW) F1 lupus-like nephritis with monoclonal antibody to gamma interferon. *J Ex Med* 1987; 166: 798-803.
- Jagiello P, Gross WL, Epplen JT. Complex genetics of Wegener granulomatosis. *Autoimmun Rev* 2005; 4: 42-47.
- James SP. Prototypic disorders of gastrointestinal mucosal immune function: Celiac disease and Crohn's disease. *J Allergy Clin Immunol* 2005; 115: 25-30.
- Janatuinen EK, Kemppainen TA, Julkunen RJK, Kosma VM, Mäki M, Heikkinen M, Uusitupa MIJ. No harm from five-year ingestion of oats in coeliac disease. *Gut* 2002; 50: 332-335.
- Jayne DR, Weetman AP, Lockwood CM. IgG subclass distribution of autoantibodies to neutrophil cytoplasmic antigens in systemic vasculitis. *Clin Exp Immunol* 1991; 84: 476-481.
- Jentsch TJ. Chloride channels: a molecular perspective. *Curr Opin Neurobiol* 1996; 6: 303-10.
- Jung HW, La SJ, Kim JY, Heo SK, Wang S, Kim KK, Lee KM, Cho HR, Lee HW, Kwon B, Kim BS, Kwon BS. High levels of soluble herpes virus entry mediator in sera of patients with allergic and autoimmune diseases. *Exp Mol Med* 2003; 35: 501-8.

- Kagnoff MF. Celiac disease pathogenesis: the plot thickens. *Gastroenterology* 2002; 123: 939-43.
- Kagnoff MF. Overview and pathogenesis of celiac disease. *Gastroenterology* 2005; 128: S10-8.
- Kamholz J, Menichella D, Jani A, Garbern J, Lewis RA, Krajewski KM, Lilien J, Scherer SS, Shy ME. Charcot-Marie-Tooth disease type 1: molecular pathogenesis to gene therapy. *Brain* 2000;123(Pt 2):222-233.
- Kamholz J, Menichella D, Jani A, Garbern J, Lewis RA, Krajewski KM, Lilien J, Scherer SS, Shy ME. Charcot-Marie-Tooth disease type 1: molecular pathogenesis to gene therapy. *Brain* 2000; 123: 222-233.
- Karin M, Greten FR. NF- κ B: Linking inflammation and immunity to cancer development and progression. *Nat Rev Immunol* 2005; 5: 749-759.
- Karin M, Lin A. NF- κ B at the crossroads of life and death. *Nat Immunol* 2002; 3: 221-227.
- Karin M. The regulation of AP-1 activity by mitogen-activated protein kinases. *J Bio Chem* 1995; 270: 16483-16486.
- Karsai A, Muller S, Platz S, Hauser MT. Evaluation of a homemade SYBR green I reaction mixture for real-time PCR quantification of gene expression. *Biotechniques* 2002; 32: 790-2, 794-6.
- Kasahara M. The chromosomal duplication model of the major histocompatibility complex. *Immunol Rev* 1999; 167: 17-32.
- Kashii Y, Giorda R, Herberman RB, Whiteside TL, Vujanovic NL. Constitutive expression and role of the TNF family ligands in apoptotic killing of tumor cells by human NK cells. *J Immunol* 1999; 163: 5358-66.
- Kashork CD, Lupski JR, Shaffer LG. Prenatal diagnosis of Charcot-Marie-Tooth disease type 1A by interphase fluorescence in situ hybridisation. *Prenat Diagn* 1999; 19: 446-449.
- Kaufmann SH. γ/δ and other unconventional T lymphocytes: what do they see and what do they do? *Proc Natl Acad Sci U S A* 1996; 93: 2272-9.
- Kawai S, Yokosuka O, Kanda T, Imazeki F, Maru Y, Saisho H. Quantification of hepatitis C virus by TaqMan PCR: comparison with HCV amplicon monitor assay. *J Med Virol* 1999; 58: 121-126.
- Kerem B, Rommens JM, Buchanan JA, Markiewicz D, Cox TK, Chakravarti A, Buchwald M, Tsui LC. Identification of the cystic fibrosis gene: genetic analysis. *Science* 1989; 245: 1073-80.
- Kertula TO, Hallstrom O, Maki M. Phenotypical characterisation of peripheral blood T cells in patients with coeliac disease: elevation of antigen-primed CD45RO+ T lymphocytes. *Immunol* 1995; 86: 104-109.
- Kilmartin C, Lynch S, Abuzakouk M, Weiser H, Feighery C. Avenin Fails to induce a Th1 response in coeliac tissue following in vitro culture. *Gut* 2003; 52: 47-52.
- Kim C-H, Quarsten H, Bergsten E, Khosla C, Sollid LM. Structural basis for HLA-DQ2 mediated presentation of gluten epitopes in celiac disease. *Proc Natl Acad Sci USA* 2004; 101: 4175-4179.
- Kim S, Fotiadu A, Kotoula V. Increased expression of soluble decoy receptor 3 in acutely inflamed intestinal epithelia. *Clin Immunol* 2005; 115: 286-94.
- Kim SW, Lee KS, Jin HS, Lee TM, Koo SK, Lee YJ, Jung SC. Rapid detection of duplication/deletion of the PMP22 gene in patients with Charcot-Marie-Tooth type 1A and hereditary neuropathy with liability to pressure palsies by Real-time quantitative PCR using Sybr Green 1 dye. *J Korean Med Sci* 2003; 18: 727-732.
- Kim TG, Kim KY, Lee SH, Cho CS, Park SH, Choi HB, Han H, Kim DJ. Systemic lupus erythematosus with nephritis is TNFB*2 homozygote in the Korean population. *Hum Immunol* 1996; 46: 10-17.
- Kim W-J, Kang Y-J, Koh E-M, Ahn K-S, Cha H-S, Lee W-H. LIGHT is involved in the pathogenesis of rheumatoid arthritis by inducing the expression of proinflammatory cytokines and MMP-9 in macrophages. *J Immunol* 2005; 114: 272-279.
- Kim YS, Nedospasov SA, Liu ZG. TRAF2 plays a key, nonredundant role in LIGHT-lymphotoxin beta receptor signaling. *Mol Cell Biol* 2005; 25: 2130-7.

- King W, Brooks C, Holder R, Hughes P, Adu D, Savage C. T lymphocyte responses to anti-neutrophil cytoplasmic autoantibody (ANCA) antigens are present in patients with ANCA-associated systemic vasculitis and persist during disease remission. *Clin Exp Immunol* 1994; 112: 539-546.
- Kishimoto H, Sprent J. The thymus and negative selection. *Immunol Res* 2000; 21: 315-324.
- Kishimoto H, Sprent J. Several different cell surface molecules control negative selection of medullary thymocytes. *J Exp Med* 1999; 190: 65-73.
- Kiyosawa H, Lensch MW, Chance PF. Analysis of the CMT1A-REP repeat: mapping crossover breakpoints in CMT1A and HNPP. *Hum Mol Genet* 1995; 4: 2327-2334.
- Kleinle S, Tabiti K, Gallati S. Limitations of melting curve analysis using Sybr Green 1 – fragment differentiation and mutation detection in the CFTR-gene. In: Dietmaier W, Wittwer C, Sivasubramanian N, eds. *Rapid cycle real-time PCR Methods and applications (Genetics and Oncology)*. Springer, 2002:47-56.
- Kleinle S, Tabiti K, Gallati S. Limitations of melting curve analysis using Sybr Green 1 – fragment differentiation and mutation detection in the CFTR gene. In: Dietmaier W, Wittwer C, Sivasubramanian N, eds. *Rapid cycle Real-time PCR Methods and applications (Genetics and Oncology)*. Springer, 2002:47-56.
- Kleppe K, Ohtsuka E, Kleppe R, Molineux I, Khorana HG. Studies on polynucleotides. Repair replications of short synthetic DNA's as catalysed by DNA polymerises. *J Mol Biol* 1971; 56: 341-361.
- Kleppe K, Ohtsuka E, Kleppe R, Molineux I, Khorana HG. Studies on polynucleotides. Repair replications of short synthetic DNA's as catalysed by DNA polymerases. *J Mol Biol*; 1971: 341-361.
- Koni PA, Sacca R, Lawton P, Browning JL, Ruddle NH, Flavell RA. Distinct roles in lymphoid organogenesis for Lymphotoxin α and β revealed in lymphotoxin β -deficient mice. *Immunity* 1997; 6: 491-500.
- Krajewski KM, Lewis RA, Fuerst DR, Turansky C, Hinderer SR, Garbern J, Kamholz J, Shy ME. Neurological dysfunction and axonal degeneration in Charcot-Marie-Tooth disease type 1A. *Brain* 2000; 12: 1516-1527.
- Kratz A, Campos-Neto A, Hanson MS, Ruddle NH. Chronic inflammation caused by lymphotoxin is lymphoid neogenesis. *J Exp Med* 1996; 183: 1461-72.
- Kronenberg M, Rudensky A. Regulation of immunity by self-reactive T cells. *Nature* 2005; 435: 598-604.
- Kuai J, Nickbarg E, Wooters J, Qiu Y, Wang J, Lin LL. Endogenous association of TRAF2, TRAF3, cIAP1, and Smac with lymphotoxin beta receptor reveals a novel mechanism of apoptosis. *J Biol Chem* 2003; 278: 14363-9.
- Kuchroo VK, Das MP, Brown JA, Ranger AM, Zamvil SS, Sobel RA, weiner HL, Nabavi N, Glimcher LH. B7-1 and B7-2 costimulatory molecules activate differentially the Th1/Th2 developmental pathways: application to autoimmune disease therapy. *Cell* 1995; 80: 707-712.
- Kupper C. Dietary guidelines and implementation for celiac disease. *Gastroenterology* 2005; 128: S121-7.
- Kuprash DV, Alimzhanov MB, Tumanov AV, Anderson AO, Pfeffer K, Nedospasov SA. TNF and lymphotoxin beta cooperate in the maintenance of secondary lymphoid tissue microarchitecture but not in the development of lymph nodes. *J Immunol* 1999; 163: 6575-80.
- Kwok S, Kellogg DE, McKinney N, Spasic D, Goda L, Levenson C et al. Effects of primer-template mismatches on the polymerase chain reaction: human immunodeficiency virus type 1 model studies. *Nucleic Acids Res* 1990; 18: 999-1005.
- Kwok S, Kellogg DE, McKinney N, Spasic D, Goda L, Levenson C et al. Effects of primer-template mismatches on the polymerase chain reaction: human immunodeficiency virus type 1 model studies. *Nucleic Acids Res* 1990; 18: 999-1005.
- Kwon B, Kim BS, Cho HR, Park JE, Kwon BS. Involvement of tumor necrosis factor receptor superfamily (TNFRSF) members in the pathogenesis of inflammatory diseases. *Exp Mol Med* 2003; 35: 8-16.

- Kwon BS, Tan KB, Ni J, Oh KO, Lee ZH, Kim KK, Kim YJ, Wang S, Gentz R, Yu GL, Harrop J, Lyn SD, Silverman C, Porter TG, Truneh A, Young PR. A newly identified member of the tumor necrosis factor receptor superfamily with a wide tissue distribution and involvement in lymphocyte activation. *J Biol Chem* 1997; 272: 14272-6.
- Kyriakis JM, Avruch J. Sounding the alarm: protein kinase cascade activated by stress and inflammation. *J Bio Chem* 1996; 271: 24313-24316.
- Lacki JK, Leszczynski P, Kelemen J, Muller W, Mackiewicz SH. Cytokine concentration in serum of lupus erythematosus patients: the effect on acute phase response. *J Med* 1997; 28: 99-107.
- Lahat N, Shapiro S, Karban A, Gerstein R, Kinarty A, Lerner A. Cytokine profile in coeliac disease. *Scand J Immunol* 1999; 49: 441-6.
- Lama J, Ware CF. Human immunodeficiency virus type 1 Nef mediates sustained membrane expression of tumor necrosis factor and the related cytokine LIGHT on activated T cells. *J Virol* 2000; 74: 9396-402.
- Lamprecht P. Off balance: T cells in antineutrophil cytoplasmic antibody (ANCA)-associated vasculitides. *Clin Exp Immunol* 2005; 141: 201-210.
- Landt O. Selection of hybridisation probes for real-time quantification and genetic analysis in "Rapid cycle real-time PCR methods and applications". Edition Eds. Meuer S, Witter C, Nakagawara K. Springer, Berlin. 2001: 35-41.
- Langford CA, Hoffman GS. Rare diseases 3: Wegener's granulomatosis. *Thorax* 1999; 54: 629-637.
- Laxminarayana D, et al. Diminished levels of protein kinase A RI alpha and RI beta transcripts and proteins in systemic lupus erythematosus T lymphocytes. *J Immunol* 1999; 162: 5639-5648.
- Lay MJ, Wittwer CT. Real-time fluorescence genotyping of Factor V Leiden during rapid-cycle PCR. *Clin Chem* 1997; 43: 2262-2267.
- Le Douarin NM, Dupin E. Cell lineage analysis in neural crest ontogeny. *J Neurobiol* 1993; 24: 146-161
- Lee MA, Squirrell DJ, Leslie DL, Brown T. Homogeneous fluorescent chemistries for Real-time PCR in Real-time PCR: An essential guide. Eds Edwards K, Logan J, Saunders N. Horizon bioscience United Kingdom 2004 31-70.
- Lee WH, Kim SH, Lee Y, Lee BB, Kwon B, Song H, Kwon BS, Park JE. Tumor necrosis factor receptor superfamily 14 is involved in atherogenesis by inducing proinflammatory cytokines and matrix metalloproteinases. *Arterioscler Thromb Vasc Biol* 2001; 21: 2004-10.
- LeGuern E, Gouider R, Ravise N, Lopes J, Tardieu S, Gugenheim M, Abbas N, Bouche P, Agid Y, Brice A. A de novo case of hereditary neuropathy with liability to pressure palsies (HNPP) of maternal origin: a new mechanism for deletion in 17p11.2? *Hum Mol Genet* 1996; 5: 103-106.
- Lehmann U, Kreipe H. Real-time PCR analysis of DNA and RNA extracted from formalin-fixed and paraffin-embedded biopsies. *Methods* 2001; 25: 409-18.
- Lenssen PP, Gabreels-Festen AA, Valentijn LJ, Jongen PJ, van Beersum SE, van Engelen BG, van Wensen PJ, Bolhuis PA, Gabreels FJ, Mariman EC. Hereditary neuropathy with liability to pressure palsies. Phenotypic differences between patients with the common deletion and a PMP22 frame shift mutation. *Brain* 1998; 121: 1451-1458.
- Li J, Krajewski K, Lewis RA, Shy ME. Loss-of-function phenotype of hereditary neuropathy with liability to pressure palsies. *Muscle Nerve* 2004; 29: 205-210.
- Li Q, Verma IM. NF- κ B regulation in the immune system. *Nat Rev Immunol* 2002; 2: 725-734.
- Lindqvist AK, Steinsson K, Johanneson B, Kristjansdottir H, Arnasson A, Grondal G, Jonasson I, Magnusson V, Sturfelt G, Truedsson L, Svenungsson E, Lundberg I, Terwilliger JD, Gyllensten UB, Alarcon-Riquelme, ME. A susceptibility locus for human systemic lupus erythematosus (hSLE1) on chromosome 2q. *J Autoimmun* 2000; 14: 169-178.
- Lipsky PE. Systemic lupus erythematosus: an autoimmune disease of B cell hyperactivity. *Nat Immunol* 2001; 2: 764-766.
- Liu C-M, and Hermann TE. Characterisation of ionomycin as a calcium ionophore. *J Biol Chem* 1978; 253: 5892-5894.
- Liu MF, Wang LL, Wu CR. Decreased CD4+CD25+ T cells in the peripheral blood of patients with systemic lupus erythematosus. *Scand J Immunol*. 2004; 59: 198-202.

- Locksley RM, Killeen N, Lenardo MJ. The TNF and TNF receptor superfamilies: integrating mammalian biology. *Cell* 2001; 104: 487-501.
- Lopes J, Ravise N, Vandenberghe A, Palau F, Ionasescu V, Mayer M, Levy N, Wood N, et al. Fine mapping of de novo CMT1A and HNPP rearrangements within CMT1A-REPs evidences two distinct sex-dependent mechanisms and candidate sequences involved in recombination. *Hum Mol Genet* 1998; 7: 141-148.
- Lopes J, Tardieu S, Silander K, Blair I, Vandenberghe A, Palau F, Ruberg M, Brice A, LeGuern E. Homologous DNA exchanges in humans can be explained by the yeast double-strand break repair model: a study of 17p11.2 rearrangements associated with CMT1A and HNPP. *Hum Mol Genet* 1999; 12: 2285-2292.
- Lopes J, Vandenberghe A, Tardieu S, Ionasescu V, Levy N, Wood N, Tachi N, Bouche P, Latour P, Brice A, LeGuern E. Sex-dependent rearrangements resulting in CMT1A and HNPP. *Nature Genet* 1997; 17: 136-137.
- Lopez AJ. Alternative splicing of pre-mRNA: developmental consequences and mechanisms of regulation. *Ann Rev Genet* 1998; 32: 279-305.
- Lu L, Zhang L, Yi Y, Kang H-K, Datta SK. Human lupus T cells resist inactivation and escape death by upregulating COX-2. *Nat Med* 2004; 1-5.
- Ludviksson B, Sneller M, Chua K, et al. Active Wegener's granulomatosis is associated with HLA-DR⁺CD4⁺ T cells exhibiting an unbalanced Th1-type T cell cytokine pattern: reversal by IL-10. *J Immunol* 1998; 160: 3602-3609.
- Lundqvist C, Melgar S, Yeung MM, Hammarstrom S, Hammarstrom ML. Intraepithelial lymphocytes in human gut have lytic potential and a cytokine profile that suggest T helper I and cytotoxic functions. *J Immunol* 1996; 157: 1926-1934.
- Lupberger J, Kreuzer KA, Baskaynak G, Peters UR, le Coutre P, Schmidt CA. Quantitative analysis of beta-actin, beta-2-microglobulin and porphobilinogen deaminase mRNA and their comparison as control transcripts for RT-PCR. *Mol Cell Probes* 2002; 16: 25-30.
- Lupski JR, de Oca-Luna RM, Slaugenhaupt S, Pentao L, Guzzetta V, Trask BJ, Saucedo-Cardenas O, Barker DF, Killian JM, Garcia CA, et al. DNA duplication associated with Charcot-Marie-Tooth disease type 1A. *Cell* 1991; 66: 219-232.
- Lupski JR, Wise CA, Kuwano A, Pentao L, Parker JT, Glase DG, et al. Gene dosage is a mechanism for Charcot-Marie-Tooth disease type 1A. *Nat Genet* 1992; 1: 29-33.
- MacDonald TT, Monteleone G. IL-12 and Th1 immune responses in human Peyer's patches. *Trends Immunol* 2001; 22: 244-7.
- Macdonald TT, Monteleone G. Immunity, inflammation, and allergy in the gut. *Science* 2005; 307: 1920-5.
- Mackay F, Kalled SL. TNF ligands and receptors in autoimmunity: an update. *Curr Opin Immunol* 2002; 14: 783-90.
- Mackay IM, Arden KE, Nitsche A. Real-time PCR in virology. *Nucleic Acids Res* 2002; 30: 1292-305.
- Magyar JP, Martini R, Ruelicke T, Aguzzi A, Adlkofer K, Dembic Z, Zielasek J, Toyka KV, Suter U. Impaired differentiation of Schwann cells in transgenic mice with increased PMP22 gene dosage. *J Neurosci* 1996; 16: 5351-5360.
- Mahr A, Guillevin L, Poissonnet M, Ayme S. Prevalences of polyarteritis nodosa, microscopic polyangiitis, Wegener's granulomatosis, and Churg-Strauss syndrome in a French urban multiethnic population in 2000: a capture-recapture estimate. *Arthritis Rheum* 2004; 51: 92-99.
- Maiuri L, Ciacci C, Auricchio S, Brown V, Quarantino S, Londei M. Interleukin 15 mediates epithelial changes in coeliac disease. *Gastroenterology* 2000; 119: 996-1006.
- Maiuri L, Ciacci C, Ricciardelli I, Vacca L, Raia V, Auricchio S, Picard J, Osman M, Quarantino S, Londei M. Association between innate response to gliadin and activation of pathogenic T cells in coeliac disease. *Lancet* 2003; 362: 30-7.
- Maiuri L, Ciacci C, Vacca L, Ricciardelli I, Auricchio S, Quarantino S, Londei M. IL-15 drives the specific migration of CD94⁺ and TCR γ/δ ⁺ intraepithelial lymphocytes in organ cultures of treated coeliac disease patients. *Am J Gastroenterol* 2001; 96: 150-156.

- Makowski GS, Ramsby ML. Calibrating gelatin zymograms with human gelatinase standards. *Anal Biochem* 1996; 236: 353-6.
- Makowski GS, Ramsby ML. Concentrations of circulating matrix metalloproteinase 9 inversely correlate with autoimmune antibodies to double stranded DNA: implications for monitoring disease activity in systemic lupus erythematosus. *Mol Pathol* 2003; 56: 244-7.
- Malec M, Soderqvist M, Sirsjo A, MacNamara B, Lewin N, Sjoberg J, Bjorkholm M, Porwit-MacDonald A. Real-time polymerase chain reaction determination of cytokine mRNA expression profiles in Hodgkin's lymphoma. *Haematologica* 2004; 89: 679-85.
- Malide D, Russo P, Bendayan M. Presence of tumour necrosis factor alpha and interleukin-6 in renal mesangial cells of lupus nephritis patients. *Hum Pathol* 1995; 26: 558-564.
- Mallet F, Oriol G, Mary C, Verrier B, Mandrand B. Continuous RT-PCR using AMV-RT and Taq DNA polymerase characterisation and comparison to uncoupled procedures. *Biotechniques* 1995; 18: 678-687.
- Manfredi A, Rovere P, Galati G, Heltai S, Bozzolo E, Soldini L, Davoust J, Balestrieri G, Tincani A, Sabbadini MG. Apoptotic cell clearance in systemic lupus erythematosus. Opsonisation by anti-phospholipid antibodies. *Arthritis Rheum* 1998; 41: 205-214.
- Mannhalter C, Koizar D, Mitterbauer G. Evaluation of RNA isolation methods and reference genes for RT-PCR analyses of rare target RNA. *Clin Chem Lab Med* 2000; 38: 171-7.
- Manson JJ, Isenberg DA. The pathogenesis of systemic lupus erythematosus. *Ned J Med* 2003; 61: 343-346.
- Mansur NR, Meyer-Siegler K, Wurzer JC, Sirover MA. Cell cycle regulation of the glyceraldehyde-3-phosphate dehydrogenase/uracil DNA glycosylase gene in normal human cells. *Nuc Acid Res* 1993; 21: 993-998.
- Mariadason JM, Nicholas C, L'Italien KE, Zhuang M, Smartt HJ, Heerdt BG, Yang W, Corner GA, Wilson AJ, Klampfer L, Arango D, Augenlicht LH. Gene expression profiling of intestinal epithelial cell maturation along the crypt-villus axis. *Gastroenterology* 2005; 128: 1081-8.
- Mariman ECM, Gabreels-Festen AA, van Beersum SE, Valentijn LJ, Baas F, Bolhuis PA, et al. Prevalence of the 1.5 Mb 17p deletion in families with hereditary neuropathy with liability to pressure palsies. *Ann Neurol* 1994; 36: 650-655.
- Marsh MN. Gluten, major histocompatibility complex, and the small intestine. A molecular and immunobiologic approach to the spectrum of gluten sensitivity ('celiac sprue'). *Gastroenterology* 1992; 102: 330-54.
- Marsters SA, Ayres TM, Skubatch M, Gray CL, Rothe M, Ashkenazi A. Herpesvirus entry mediator, a member of the tumor necrosis factor receptor (TNFR) family, interacts with members of the TNFR-associated factor family and activates the transcription factors NF-kappaB and AP-1. *J Biol Chem* 1997; 272: 14029-32.
- Martin CA, Panja A. Cytokine regulation of human intestinal primary epithelial cell susceptibility to Fas-mediated apoptosis. *Am J Physiol Gastrointest Liver Physiol* 2002; 282: G92-G104.
- Martin-Pagola A, Perez-Nanclares G, Ortiz L, Vitoria JC, Hualde I, Zaballa R, Preciado E, Castano L, Bilbao JR. MICA response to gliadin in intestinal mucosa from coeliac patients. *Immunogenetics* 2004; 56: 549-554.
- Masopust D, Vezys V, Marzo AL, Lefrancois L. Preferential localization of effector memory cells in nonlymphoid tissue. *Science* 2001; 291: 2413-2417.
- Mateu E, Calafel F, Ramos MD, Casals T, Bertanpetit J. Can a place of origin of the main cystic fibrosis mutation be identified? *Am J Hum Genet.* 2002; 70: 257-264.
- Matsui H, Grubb BR, Tarran R, Randell SH, Gatzky JT, Davis CW, et al. Evidence for periciliary liquid layer depletion, not abnormal ion composition, in the pathogenesis of cystic fibrosis airways disease. *Cell* 1998; 95: 1005-1015.
- Matsui H, Hikichi Y, Tsuji I, Yamada T, Shintani Y. LIGHT, a member of the tumor necrosis factor ligand superfamily, prevents tumor necrosis factor-alpha-mediated human primary hepatocyte apoptosis, but not Fas-mediated apoptosis. *J Biol Chem* 2002; 277: 50054-61.

- Matsunami N, Smith B, Ballard L, Lensch MW, Robertson M, Albertsen H, Hanemann CO, Muller HW, Bird TD, White R, Chance PF. Peripheral myelin protein-22 gene maps in the duplication in chromosome 17p11.2 associated with Charcot-Marie-Tooth 1A. *Nature Genet* 1992; 1: 176-179.
- Mauri DN, Ebner R, Montgomery RI, Kochel KD, Cheung TC, Yu GL, Ruben S, Murphy M, Eisenberg RJ, Cohen GH, Spear PG, Ware CF. LIGHT, a new member of the TNF superfamily, and lymphotoxin alpha are ligands for herpesvirus entry mediator. *Immunity* 1998; 8: 21-30.
- McCawley LJ, Matrisian LM. Matrix metalloproteinases: they're not just for matrix anymore! *Curr Opin Cell Biol* 2001; 13: 534-40.
- McDevitt H, Munson S, Ettinger R, Wu A. Multiple roles for tumor necrosis factor-alpha and lymphotoxin alpha/beta in immunity and autoimmunity. *Arthritis Res* 2002; 4 Suppl 3: S141-52.
- McKay DM, Baird AW. Cytokine regulation of epithelial permeability and ion transport. *Gut* 1999; 44: 283-9.
- McManus R, Kelleher D. Celiac disease: the villain unmasked? *N Engl J Med* 2003; 348: 2573-4.
- McPherson M, Moller P. PCR - the basics from background to bench. BIOS Scientific Publishers Ltd, Oxford. 2000: 1 – 83 and 249 – 251.
- McQuaid S, Joyce C, Ward A et al. The Irish Cystic Fibrosis data base – year 2000 update. *J Med Genet* 2000; 37 sp6.17.
- Mearin ML, Koning F. Tissue transglutaminase: master regulator of celiac disease? *J Pediatr Gastroenterol Nutr* 2003; 36: 9-11.
- Mehra R, Quismorio FP, Strassmann G, Stimmler MM, Horwitz DA, Kitridou RC, Gauderman WJ, Morrison J, Brautbar C, Jacob CO. Synergistic effects between IL-10 and bcl-2 genotypes in determining susceptibility to systemic lupus erythematosus. *Arthritis Rheum* 1998; 41: 596-602.
- Meier CR, Sturkenboom MC, Cohen AS, et al. Postmenopausal oestrogen replacement therapy and the risk of developing systemic lupus erythematosus or discoid lupus. *J Rheumatol* 1998; 25: 1515-1519.
- Mok CC, Lau CS. Pathogenesis of systemic lupus erythematosus. *J Clin Pathol* 2003; 56: 481-490.
- Molberg Ø, McAdam SN, Korner R, Quarsten H, Kristiansen C, Madsen L, Fugger L, Scott H, Roepstorff P, Lundin KEA, Sjoström H, Sollid L. Tissue transglutaminase selectively modifies gliadin peptides that are recognized by gut-derived T cell. *Nat Med* 1998; 4: 713-717.
- Molberg Ø, McAdam SN, Lundin KEA, Kristiansen C, Arentz-Hansen H, Kett K, Sollid LM. T cells from celiac disease lesions recognize gliadin epitopes deamidated in situ by endogenous tissue transglutaminase. *Eur J Immunol* 2001; 31: 1317-1323.
- Mondino A, Khoruts A, Jenkins MK. The anatomy of T-cell activation and tolerance. *Proc Natl Acad Sci U S A* 1996; 93: 2245-52.
- Monks CR, Kupfer H, Tamir I, Barlow A, Kupfer A. Selective modulation of protein kinase C during T-cell activation. *Nature* 1997; 385: 83-86.
- Monteleone M, Pender SL, Alstead E, Hauer AC, Lionetti P, McKense C, MacDonald TT. Role of interferon- α in promoting T helper cell type 1 responses in the small intestine in coeliac disease. *Gut* 2001; 48: 425-429.
- Montgomery RI, Warner MS, Lum BJ, Spear PG. Herpes simplex virus-1 entry into cells mediated by a novel member of the TNF/NGF receptor family. *Cell* 1996; 87: 427-436.
- Morel Y, Schiano de Colella JM, Harrop J, Deen KC, Holmes SD, Wattam TA, Khandekar SS, Truneh A, Sweet RW, Gastaut JA, Olive D, Costello RT. Reciprocal expression of the TNF family receptor herpes virus entry mediator and its ligand LIGHT on activated T cells: LIGHT down-regulates its own receptor. *J Immunol* 2000; 165: 4397-404.
- Morel Y, Truneh A, Sweet RW, Olive D, Costello RT. The TNF superfamily members LIGHT and CD154 (CD40 ligand) costimulate induction of dendritic cell maturation and elicit specific CTL activity. *J Immunol* 2001; 167: 2479-86.
- Morrison TM, Weiss JJ, Wittwer CT. Quantification of low-copy transcripts by continuous SYBR green I monitoring during amplification. *Biotechniques* 1998; 24: 954-962.
- Mortarini R, Scarito A, Nonaka D, Zanon M, Bersani I, Montaldi E, Pennacchioli E, Patuzzo R, Santinami M, Anichini A. Constitutive expression and costimulatory function of LIGHT/TNFSF14 on human melanoma cells and melanoma-derived microvesicles. *Cancer Res* 2005; 65: 3428-36.

- Moss SF, Attia L, Scholes JV, Ealters JR, Holt PR. Increased small intestinal apoptosis in coeliac disease. *Gut* 1996; 39: 811-817.
- Mossmann TR, Coffman RL. TH1 and TH2 cells: different patterns of lymphokine secretion lead to different functional properties. *Annu Rev Immunol* 1989; 7: 145-173.
- Mowat AM. Anatomical basis of tolerance and immunity to intestinal antigens. *Nat Rev Immunol* 2003; 3: 331-41.
- Mueller A, Trabandt A, Gloeckner-Hofmann K, Seitzer U, Csernok E, Schonermarck U, Feller AC, Gross WL. Localized Wegener's granulomatosis: predominance of CD26 and IFN-gamma expression. *J Pathol* 2000; 192: 113-20.
- Mulder AH, Heeringa C, Brouwer E, Limburg PC, Kallenberg CG. Activation of granulocytes by anti-neutrophil cytoplasmic antibodies (ANCA): a FcγRII-dependent process. *Clin Exp Immunol* 1994; 98: 270-278.
- Muller PY, Janovjak H, Miserez AR, Dobbie Z. Processing of gene expression data generated by quantitative real-time RT-PCR. *Biotechniques* 2002; 32: 1372-4, 1376, 1378-9.
- Mullis KB, Faloona FA. Specific synthesis of DNA in vitro via a polymerase catalysed chain reaction. *Meth Enzymol* 1987; 155: 335-350.
- Myers TW, Galfand DH. Reverse transcription and DNA amplification by *Thermophilus* DNA polymerase. *Biochemistry* 1991; 30: 7661-7666.
- Naef R, Suter U. Impaired intracellular trafficking is a common disease mechanism of PMP22 point mutations in peripheral neuropathies. *Neurobiol Dis* 1999; 6: 1-14.
- Nakano H, Oshima H, Chung W, Williams-Abbott L, Ware CF, Yagita H, Okumura K. TRAF5, an activator of NF-κB and putative signal transducer for the lymphotoxin-beta receptor. *J Biol Chem* 1996; 271: 14661-4.
- Naruse S, Kitagawa M, Ishiguro H. Molecular understanding of chronic pancreatitis: a perspective on the future. *Mol Med Today* 1999; 5: 493-499.
- Nath SK, Kilpatrick J, Harley JB. Genetics of human systemic lupus erythematosus the emerging picture. *Curr Opin Immunol* 2004; 16: 794-800.
- Nath SK, Namjou B, Hutchings D, Garriott CP, Pongratz C, Guthridge J, James JA. Systemic lupus erythematosus (SLE) and chromosome 16: confirmation of linkage to 16q12-13 and evidence for genetic heterogeneity. *Europ J Hum Genet* 2004; 12: 668-672.
- Nathan C. Perspectives series: nitric oxide and nitric oxide synthases. Inducible nitric oxide synthase: what difference does it make? *J Clin Invest* 1997; 100: 2417-2423.
- Newton AC. Regulation of protein kinase C. *Curr Opin Cell Biol* 1997; 9: 161-167.
- Newton CR, Graham A, Heptinstall LE, Powell SJ, Summers C, Kalsheker N, Smith JC, Markham AF. Analysis of any point mutation in DNA. The amplification refractory mutation system (ARMS). *Nucleic Acids Res* 1989; 17: 2503-2516.
- Newton CR, Graham A, Heptinstall LE, Powell SJ, Summers C, Kalsheker N et al. Analysis of any point mutation in DNA. The amplification refractory mutation system (ARMS). *Nucleic Acids Res* 1989; 17: 2503-16.
- Nilsen EM, Gjertsen HA, Jensen K, Brandtzaeg P, Lundin KEA. Gluten activation of peripheral blood T cells induces a Th0-like cytokine pattern in both coeliac patients and controls. *Clin Exp Immunol* 1996; 103: 295-303.
- Nilsen EM, Jahnsen FL, Lundin KEA, Johansen FE, Fausa O, Sollid LM, Jahnsen J, Scott H, Brandtzaeg P. Gluten induces an intestinal cytokine response strongly dominated by interferon-γ in patients with coeliac disease. *Gastroenterology* 1998; 115: 551-563.
- Nilsen EM, Lundin KEA, Krajci P, Scott H, Sollid LM, Brandtzaeg P. Gluten specific, HLA-DQ restricted T cells from coeliac mucosa produce cytokines with Th1 or Th0 profile dominated by interferon gamma. *Gut* 1995; 37: 766-776.
- Notterpek L, Ryan MC, Tobler AR, Shooter EM. PMP22 accumulation in aggresomes: implications for CMT1A pathology. *Neurobiol Dis* 1999; 6: 450-460.

- Nunes I, Gleizes P-E, Metz C, Rifkin D. Latent transforming growth factor- β binding domains involved in activation and transglutaminase-dependent cross-linking of latent transforming growth factor- β . *J Cell Biol* 1997; 136: 1151-1163.
- Oda K, Miura H, Shibasaki H, Endo C, Kakigi R, Kuroda Y, Tanaka K. Hereditary pressure-sensitive neuropathy: demonstration of 'tomacula' in motor nerve fibers. *J Neurol Sci* 1990; 98: 139-148.
- Ohashi PS. T-cell signalling and autoimmunity: molecular mechanisms of disease. *Nat Rev Immunol* 2002; 2: 427-38.
- Oishi Y, Sumida T, Sakamoto A, Kita Y, Kurasawa K, Nawata Y, Takabayashi H, Yoshida S, Taniguchi M, Saito Y, Iwamoto I. Selective reduction and recovery of invariant $V\alpha 24J\alpha Q$ T cell receptor T cells in correlation with disease activity in patients with systemic lupus erythematosus. *J Rheumatol* 2001; 28: 275-283.
- Okayama H, Curiel DT, Brantly ML, Holmes MD, Crystal RG. Rapid, nonradioactive detection of mutations in the human genome by allele-specific amplification. *J Lab Clin Med* 1989; 114: 105-13.
- O'Shea JJ, Ma A, Lipsky P. Cytokines and autoimmunity. *Nat Rev Immunol* 2002; 2: 37-45.
- Otsuki T, Tomokuni A, Sakaguchi H, Aikoh T, Matsuki T, Isozaki Y, Hyodoh F, Ueki H, Kusaka M, Kita S, Ueki A. Over-expression of the decoy receptor 3 (DcR3) gene in peripheral blood mononuclear cells (PBMC) derived from silicosis patients. *Clin Exp Immunol* 2000; 119: 323-7.
- Ozmen L, Roman D, Fountoulakis M, Schmid G, Ryffel B, Garotta G. Experimental therapy of systemic lupus erythematosus: the treatment of NZB/W mice with mouse soluble interferon-gamma receptor inhibits the onset of glomerulonephritis. *Eur J Immunol* 1995; 25: 6-12.
- Page DM. Cutting edge: thymic selection and autoreactivity are regulated by multiple coreceptors involved in T cell activation. *J Immunol* 1999; 163: 3577-81.
- Pakala SV, Ilic A, Chen L, Sarvetnick N. TNF-alpha receptor 1 (p55) on islets is necessary for the expression of LIGHT on diabetogenic T cells. *Clin Immunol* 2001; 100: 198-207.
- Palau F, Lofgren A, De Jonghe P, Bort S, Nelis E, Sevilla T, Martin JJ, Vilchez J, Prieto F, van Broeckhoven C. Origin of the de novo duplication in Charcot-Marie-Tooth disease type 1A: unequal nonsister chromatid exchange during spermatogenesis. *Hum Mol Genet* 1993; 2: 2031-2035.
- Pall AA, Savage COS. Mechanisms of endothelial cell injury in vasculitis. *Springer Semin Immunopathol* 1994; 16: 23-27.
- Papadopoulos GK, Wijmenga C, Koning F. Interplay between genetics and the environment in the development of celiac disease: perspectives for a healthy life. *J Clin Invest* 2001; 108: 1261-6.
- Papiha SS, Murty GE, Ad'Hia A, Mains BT, Venning M. Association of Wegener's granulomatosis with HLA antigens and other genetic markers. *Ann Rheum Dis* 1992; 51: 246-248.
- Pareek S, Suter U, Snipes GJ, Welcher A, Shooter EM, Murphy RA. Detection and processing of peripheral myelin protein PMP22 in cultured Schwann cells. *J Biol Chem* 1993; 268: 10372-10379
- Pareek SL, Notterpek L, Snipes GJ, Naef R, Sossin W, Lalibrete J, Lacampo S, Suter U, Shooter EM, Murphy RA. Neurons promote the translocation of peripheral myelin protein 22 into myelin. *J Neurosci* 1997; 17: 7754-7762.
- Parks WC, Wilson CL, Lopez-Boado YS. Matrix metalloproteinases as modulators of inflammation and innate immunity. *Nat Rev Immunol* 2004; 4: 617-29.
- Parren PW, Warmerdam PA, Boeije, LC, Arts J, Westerdaal NA, Vlug A, Capel PJ, Aarden LA, van de Winkel JG. On the interaction of IgG subclasses with the low affinity Fc gamma RIIa (CD32) on human monocytes, neutrophils and platelets. Analysis of functional polymorphism to human IgG2. *J Clin Invest* 1992; 90:1537-1546.
- Patel PI, Lupski JR. Charcot-Marie-Tooth disease: a new paradigm for the mechanism of inherited disease. *Trends Genet* 1994; 10: 128-133
- Patel PI, Roa BB, Welcher AA, Schoener-Scott R, Trask BJ, Pentao L, Snipes GJ, Garcia CA, Francke U, Shooter EM, Lupski JR, Suter U. The gene for the peripheral myelin protein PMP-22 is a candidate for Charcot-Marie-Tooth disease type 1A. *Nature Genet* 1992; 1: 159-165.
- Peirson SN, Butler JN, Foster RG. Experimental validation of novel and conventional approaches to quantitative real-time PCR data analysis. *Nucleic Acids Res* 2003; 31: e73.

- Pender SL, Tickle SP, Docherty AJ, Howie D, Wathen NC, McDonald TT. A major role for matrix metalloproteinases in T cell injury in the gut. *J Immunol* 1997; 158: 1582-1590.
- Pender SLF, McDonald TT. Matrix metalloproteinases and the gut – new roles for old enzymes. *Curr Opin Pharm* 2004; 4: 546-550.
- Peng SL, Moslehi J, Craft J. Roles of interferon- γ and interleukin-4 in murine lupus. *J Clin Invest* 1997; 99:1936-1946.
- Pentao L, Wise CA, Chinault AC, Patel PI, Lupski JR. Charcot-Marie-Tooth type 1A duplication appears to arise from recombination at repeat sequences flanking the 1.5 Mb monomer unit. *Nature Genet* 1992; 2: 292-300.
- Perea J, Robertson A, Tomachova T, Muddle J, King RHM, Ponsford S, Thomas PK, Huxley C. Induced myelination and demyelination in a conditional mouse model of Charcot-Marie-Tooth disease type 1A. *Hum Molec Genet* 2001; 10: 1007-1018.
- Perez-Romero P, Perez A, Capul A, Montgomery R, Fuller AO. Herpes simplex virus entry mediator associates in infected cells in a complex with viral proteins gD and at least gH. *J Virol* 2005; 79: 4540-4.
- Pfaffl M, Hageleit, M. Validities of mRNA quantification using recombinant RNA and recombinant DNA external calibration curves in Real-time RT-PCR. *Biotech Letters* 2001; 23: 275-282.
- Pfaffl M. 2005. <http://www.genequantification.de>
- Pfaffl MW. A new mathematical model for relative quantification in real-time RT-PCR. *Nucleic Acids Res* 2001; 29: e45.
- Pfeffer K. Biological functions of tumor necrosis factor cytokines and their receptors. *Cytokine Growth Factor Rev* 2003; 14: 185-91.
- Picarelli A, Maiuri L, Frate A, Greco M, Auricchio S, Londei M. Production of antiendomysial antibodies after in vitro gliadin challenge of small intestinal biopsy samples from patients with coeliac disease. *Lancet* 1996; 348: 1065-1067.
- Pitti RM, Marsters SA, Lawrence DA, Roy M, Kischkel FC, Dowd P, Huang A, Donahue CJ, Sherwood SW, Baldwin DT, Godowski PJ, Wood WI, Gurney AL, Hillan KJ, Cohen RL, Goddard AD, Botstein D, Ashkenazi A. Genomic amplification of a decoy receptor for Fas ligand in lung and colon cancer. *Nature* 1998; 396: 699-703.
- Poddar SK, Sawyer MH, Conner JD. Effect of inhibitors in clinical specimens on Taq and Tth polymerase-based PCR amplification of influenza A virus. *J Med Microbiol* 1998; 47: 1131-1135.
- Popa ER, Stegeman CA, Kallenberg CGM, Cohen Tervaert JW. Staphylococcus aureus and Wegener's granulomatosis. *Arthritis Res* 2002; 4: 77-79.
- Poropat RA, Nicholson GA. Determination of gene dosage at the PMP22 and androgen receptor loci by quantitative PCR (comments) *Clin Chem* 1998; 44: 724-730.
- Pravica V, Perrey C, Stevens A, Lee JH, Hutchinson IV. A single nucleotide polymorphism in the first intron of the human IFN-gamma gene: absolute correlation with a polymorphic CA microsatellite marker of high IFN-gamma production. *Hum Immunol* 2000; 61: 863-866.
- Prokunia L, Catillejo-lopez C, Oberg F, Gunnarsson I, Berg L, Magnusson V, Brookes AJ, Tentler D, Kristjansdottir H, Grondal G, et al. A regulatory polymorphism in PDCD1 is associated with susceptibility to systemic lupus erythematosus in humans. *Nat Genet* 2002; 32: 666-669.
- Quarsten H, Molberg Ø, Fugger L, McAdam SM, Sollid LM. HLA-binding and T cell recognition of a tissue transglutaminase modified gliadin epitope. *Eur J Immunol* 1999; 29: 2506-2514.
- Quinlivan M, Dempsey E, Ryan F, Arkins S, Cullinane A. Real-time reverse transcription PCR for detection and quantitative analysis of equine influenza virus. *J Clin Micro* 2005; 43: 5055-5057.
- Radonic A, Thulke S, Mackay IM, Landt O, Siegert W, Nitsche A. Guideline to reference gene selection for quantitative real-time PCR. *Biochem Biophys Res Commun* 2004; 313: 856-62.
- Raeymaekers P, Timmerman V, De Jonghe P, Swerts L, Gheuens J, Martin JJ, et al. Localisation of the mutation in an extended family with Charcot-Marie-Tooth neuropathy (HMSN 1). *Am J Hum Genet* 1989; 45: 953-958.
- Raeymaekers P, Timmerman V, Nelis E, De Jonghe P, Hoogendijk JE, Baas F, Barker DF, Martin JJ, De Visser M, Bolhuis PA, et al. Duplication in chromosome 17p11.2 in Charcot-Marie-Tooth

neuropathy type 1a (CMT 1a). The HMSN Collaborative Research Group. *Neuromuscul Disord* 1991; 1:93-97.

- Raman K, Mohan C. Genetic underpinnings of autoimmunity--lessons from studies in arthritis, diabetes, lupus and multiple sclerosis. *Curr Opin Immunol* 2003; 15: 651-9.
- Rao A, Luo C, Hogan PG. Transcription factors of the NFAT family: regulation and function. *Annu. Rev. Immunol.* 1997; 15: 707-747.
- Rasmussen R. Quantification on the LightCycler. In Meuer S, Wittwer C, Nakagawara K, (eds). *Rapid Cycler Real-time PCR: Methods and applications.* Springer Press, Heidelberg, 21-34.
- Ravetch JV, Bolland S. IgG Fc receptors. *Annu Rev Immunol* 200; 19: 275-290.
- Ravik-Glavac M, Glavac D, Dean D. Sensitivity of single-stranded conformation polymorphism and heteroduplex method for mutation detection in the cystic fibrosis gene. *Hum Mol Genet* 1994; 3: 801-807.
- Ravik-Glavac M, Glavac D, Dean D. Sensitivity of single-stranded conformation polymorphism and heteroduplex method for mutation detection in the cystic fibrosis gene. *Hum Mol Genet* 1994; 3: 801-807.
- Reddy MM, Light MJ, Quinton PM. Activation of the epithelial Na⁺ channel (ENaC) requires CFTR Cl⁻ channel function. *Nature* 1999; 402: 301-304.
- Reich K, Mossner R, Konig IR, Westphal G, Ziegler A, Neumann C. Promoter polymorphisms of the genes encoding tumor necrosis factor-alpha and interleukin-1beta are associated with different subtypes of psoriasis characterized by early and late disease onset. *J Invest Dermatol* 2002; 118:155-163.
- Reinecker H, MacDermott R, Mirau S, Dignass A, Podolsky DK. Intestinal epithelial cells both express and respond to interleukin-15. *Gastroenterology* 1996; 111: 1706-1713.
- Reiter LT, Murakami T, Koeuth T, Pentao L, Muzny DM, Gibbs RA, Lupski JR. A recombination hotspot responsible for two inherited peripheral neuropathies is located near a mariner transposon-like element. *Nature Genet* 1996; 12: 288-297.
- Reumaux D, Duthilleul P, Roos D. Pathogenesis of diseases associated with antineutrophil cytoplasm autoantibodies. *Hum Immuno* 2004; 65: 1-12
- Rewers M. Epidemiology of celiac disease: what are the prevalence, incidence, and progression of celiac disease? *Gastroenterology* 2005; 128: S47-51.
- Rimoldi M, Chieppa M, Salucci V, Avogadri F, Sonzogni A, Sampietro GM, Nespoli A, Viale G, Allavena P, Rescigno M. Intestinal immune homeostasis is regulated by the crosstalk between epithelial cells and dendritic cells. *Nat Immunol* 2005; 6: 507-14.
- Riordan JR, Rommens JM, Kerem B, Alon N, Rozmahel R, Grzelczak Z, Zielenski J, Lok S, Plavsic N, Chou JL, et al. Identification of the cystic fibrosis gene: cloning and characterization of complementary DNA. *Science* 1989; 245: 1066-73.
- Rioux JD, Abbas AK. Paths to understanding the genetic basis of autoimmune disease. *Nature* 2005; 435: 584-9.
- Ripple MO, Wilding G. Alteration of glyceraldehyde-3-phosphate dehydrogenase activity and messenger RNA content by androgen in human prostate carcinoma cell. *Cancer Res* 1995; 55: 4234-4236.
- Ririe KM, Rasmussen RP, Wittwer CT. Product differentiation by analysis of DNA melting curves during the polymerase chain reaction. *Analytical Biochemistry* 1997; 245: 154-160.
- Roa BB, Garcia CA, Suter U, Kulpa DA, Wise CA, Mueller J, Welcher AA, Snipes GJ, Shooter EM, Patel PI, et al. Charcot-Marie-Tooth disease type 1A. Association with a spontaneous point mutation in the PMP22 gene. *N Engl J Med* 1993; 329: 96-101.
- Roberts AI, Lee L, Schwartz E, Groh V, Spies T, Ebert EC, Jabri B. NKG2D receptors induced by IL-15 costimulate CD28-negative effector CTL in the tissue microenvironment. *J Immunol* 2001; 167: 5527-5530.
- Rolny P, Sigurjonsdottir HA, Remotti H, Nilsson LA, Ascher H, Tlaskalova-Hogenove H, Tuckova L. Role of immunosuppressive therapy in refractory sprue-like disease. *Am J Gastroenterol* 1999; 94: 219-225.

- Rommens JM, Iannuzzi MC, Kerem B, Drumm ML, Melmer G, Dean M, Rozmahel R, Cole JL, Kennedy D, Hidaka N, et al. Identification of the cystic fibrosis gene: chromosome walking and jumping. *Science* 1989; 245: 1059-65.
- Ronnblom L, Alm GV. Systemic lupus and the type 1 interferon system. *Arthritis Res Ther* 2002; 5: 68-75.
- Rooney IA, Butrovich KD, Glass AA, Borboroglu S, Benedict CA, Whitbeck JC, Cohen GH, Eisenberg RJ, Ware CF. The lymphotoxin-beta receptor is necessary and sufficient for LIGHT-mediated apoptosis of tumor cells. *J Biol Chem* 2000; 275: 14307-15.
- Rostom A, Dube C, Cranney A, Saloojee N, Sy R, Garritty C, Sampson M, Zhang L, Yazdi F, Mamaladze V, Pan I, MacNeil J, Mack D, Patel D, Moher D. The diagnostic accuracy of serologic tests for celiac disease: a systematic review. *Gastroenterology* 2005; 128: S38-46.
- Rovin BH, Lu L, Zhang X. A novel IL-8 polymorphism is associated with severe systemic lupus nephritis. *Kid Inter* 2002; 62: 261-267.
- Rowe SM, Miller S, Sorscher EJ. Cystic fibrosis. *N Engl J Med* 2005; 352: 1992-2001.
- Ruedl C, Kopf M, Bachmann MF. CD8(+) T cells mediate CD40-independent maturation of dendritic cells in vivo. *J Exp Med* 1999; 189: 1875-84.
- Ruemmele FM, Russo P, Beaulieu J, Dionne S, Levy E, Lentze MJ, Seidman EG. Susceptibility to FAS-induced apoptosis in human non-tumoral enterocytes: role of costimulatory factors. *J Cell Physiol* 1999; 181: 45-54.
- Ruiz-Irastorza G, Khamashta MA, Castellino G, Hughes GR. Systemic lupus erythematosus. *Lancet* 2001; 357: 1027-32.
- Ruiz-Ponte C, Loidi L, Vega A, Carracedo A, Barros F. Rapid real-time fluorescent PCR gene dosage test for the diagnosis of DNA duplications and deletions. *Clin Chem* 2000; 46: 1574-1582.
- Ryan BM, Kelleher D. Refractory celiac disease. *Gastroenterology* 2000; 119: 243-51.
- Saiki RK, Gelfand DH, Stoffel S, Scharf SJ, Higuchi R, Horn GT, Mullis KB, Erlich HA. Primer-directed enzymatic amplification of DNA with a thermostable DNA polymerase. *Science* 1988; 239: 487-491.
- Saiki RK, Scharf S, Faloona F, Mullis KB, Horn GT, Erlich HA, Arnheim N. Enzymatic amplification of beta-globin genomic sequences and restriction site analysis for diagnosis of sickle cell anemia. *Science* 1985; 230: 1350-1354.
- Saito M, Hayashi Y, Suzuki T, Tanaka H, Hozumi I, Tsuji S. Linkage mapping of the gene for Charcot-Marie-Tooth disease type 2 to chromosome 1p (CMT2A) and the clinical features of CMT2A. *Neurology* 1997; 49:1630-1635.
- Sallusto F, Lenig D, Forster R, Lipp M, Lanzavecchia A. Two subsets of memory T lymphocytes with distinct homing potentials and effector functions. *Nature* 1999; 401: 708-712.
- Salmon JE, Edberg JC, Brogle NL, Kimberley RP. Allelic polymorphisms of human Fc gamma receptor IIA and Fc gamma receptor IIIB. Independent mechanisms for differences in human phagocyte function. *J Clin Invest* 1992; 89:1274-1281.
- Salmon JE, Millard S, Schachter LA, Arnette FC, Ginzler EM, Gourley MF, Ramsey-Goldman R, Peterson MG, Kimberly RP. Fc gamma RIIA alleles are heritable risk factors for lupus nephritis in African Americans. *J Clin Invest* 1996; 97: 1348-1354.
- Salmon, JE, Millard SS, Brogle NL, Kimberly RP. Fc gamma receptor IIIb enhances Fc gamma receptor IIa function in an oxidant-dependent and allele-sensitive manner. *J Clin Invest* 1995; 95: 2877-2885.
- Salomonsson S, Larsson P, Tengner P, Mellquist E, Hjelmstrom P, Wahren-Herlenius M. Expression of the B cell-attracting chemokine CXCL13 in the target organ and autoantibody production in ectopic lymphoid tissue in the chronic inflammatory disease Sjogren's syndrome. *Scand J Immunol* 2002; 55: 336-342.
- Salvati VM, MacDonald TT, Bajaj-Elliott M, Borelli M, Staiano A, Auricchio S, Troncone R, Monteleone M. Interleukin 18 and associated markers of T helper cell type 1 activity in coeliac disease. *Gut* 2002; 50: 186-190.
- Sanchez-Guerrero J, Karlson EW, Liang MH. Past use of oral contraceptive and the risk of developing systemic lupus erythematosus. *Arthritis Rheum* 1997; 40: 804-808.

- Sanchez-Guerrero J, Liang MH, Karlson EW, Hunter DJ, Colditz GA. Postmenopausal estrogen therapy and the risk of developing systemic lupus erythematosus. *Ann Intern Med* 1995; 122: 430-430.
- Sancho S, Young P, Suter U. Regulation of Schwann cell proliferation and apoptosis in PMP22-deficient mice and mouse models of Charcot-Marie-Tooth disease type 1A. *Brain* 2001; 124: 2177-2187.
- Sanders JS, Stegman CA, Kallenberg CG. The Th1 and Th2 paradigm in ANCA-associated vasculitis. *Kidney Blood Press Res* 2003; 26: 215-220.
- Sarrias MR, Whitbeck JC, Rooney I, Ware CF, Eisenberg RJ, Cohen GH, Lambris JD. The three HveA receptor ligands, gD, LT-alpha and LIGHT bind to distinct sites on HveA. *Mol Immunol* 2000; 37: 665-73.
- Sasso EH, Silverman GJ, Mannik M. Human IgM molecules that bind staphylococcal protein A contain VHIII heavy chains. *J Immunol* 1989; 142: 2778-2783.
- Sauer CG, Kappeler A, Spath M, Kaden JJ, Michel MS, Mayer D, Bleyl U, Grobholz R. Expression and activity of matrix metalloproteinases-2 and -9 in serum, core needle biopsies and tissue specimens of prostate cancer patients. *Virchows Arch* 2004.
- Saunders NA. Quantitative Real-time PCR in Real-time PCR: An essential guide. Eds Edwards K, Logan J, Saunders N. Horizon bioscience United Kingdom 2004 103-123.
- Savage CO, Harper L, Adu D. Primary systemic vasculitis. *Lancet* 1997; 349: 553-8.
- Savage COS, Gaskin G, Pusey CD, Pearson JD. Anti-neutrophil cytoplasm antibodies (ANCA) can recognise vascular endothelial cell-bound ANCA-associated autoantigens. *J Exp Nephrol* 1993; 1: 190-195.
- Savill J, Smith J, Ren Y, Sarraf C, Abbott F, Rees A. Glomerular mesangial cells and inflammatory macrophages ingest neutrophils undergoing apoptosis. *Kidney Int* 1992; 42: 924-936.
- Scherer SS. The biology and pathobiology of Schwann cells. *Curr Opin Neurol* 1997; 10: 386-397.
- Scheu S, Alferink J, Potzel T, Barchet W, Kalinke U, Pfeffer K. Targeted disruption of LIGHT causes defects in costimulatory T cell activation and reveals cooperation with lymphotoxin beta in mesenteric lymph node genesis. *J Exp Med* 2002; 195: 1613-24.
- Schiemann B, Gommerman JL, Vora K, Cachero TG, Shulga-Morskaya S, Dobles M, Frew E, Scott ML. An essential role for BAFF in the normal development of B cells through a BCMA-independent pathway. *Science* 2001; 293: 2111-2114.
- Schlesier M, Kaspar T, Gutfleisch J, Wolff-Vorbeck G, Peter HH. Activated CD4⁺ and CD8⁺ T-cell subsets in Wegener's granulomatosis. *Rheumatol Int* 1995; 14: 213-19.
- Schneider K, Potter KG, Ware CF. Lymphotoxin and LIGHT signaling pathways and target genes. *Immunol Rev* 2004; 202: 49-66.
- Schneider P, Holler N, Bodmer JL, Hahne M, Frei K, Fontana A, Tschopp J. Conversion of membrane-bound Fas(CD95) ligand to its soluble form is associated with downregulation of its proapoptotic activity and loss of liver toxicity. *J Exp Med* 1998; 187: 1205-13.
- Schoenberger SP, Toes RE, van der Voort EI, Offringa R, Melief CJ. T-cell help for cytotoxic T lymphocytes is mediated by CD40-CD40L interactions. *Nature* 1998; 393: 480-486.
- Schuppan D, Esslinger B, Dietrich W. Innate immunity and coeliac disease. *Lancet* 2003; 362: 3-4.
- Schuppan D. Current concepts of coeliac disease pathogenesis. *Gastroenterology* 2000; 119: 234-242.
- Schur PH. Genetics of Systemic Lupus Erythematosus. *Lupus* 1995; 4: 425-437.
- Schütz E, Von Ahsen N. Spreadsheet software for thermodynamic melting point prediction of oligonucleotide hybridization with and without mismatches. *Biotechniques* 1999; 27: 1218-1222.
- Schwarting A, Wada T, Kinoshita K, Tesch G, Kelley VR. Interferon-gamma receptor signalling is essential for the initiation, acceleration and destruction of autoimmune kidney disease in MRL-Fas(lpr) mice. *J Immunol* 1998; 161: 494-503.
- Scotet V, Barton DE, Watson JB, Audrezet MP, McDevitt T, McQuaid S, et al. Comparison of the CFTR mutation spectrum in three cohorts of patients of Celtic origin from Brittany (France) and Ireland. *Hum Mutat* 2003; 22:105-111.

- Scott BB, Goodall A, Stephenson P, Jenkins D. Small intestinal plasma cells in coeliac disease. *Gut* 1984; 25: 41-46.
- Sebzda E, Mariathasan S, Ohteki T, Jones R, Bachmann MF, Ohashi PS. Selection of the T cell repertoire. *Annu Rev Immunol* 1999; 17: 829-857.
- Seder RA, Ahmed R. Similarities and differences in CD4+ and CD8+ effector and memory T cell generation. *Nat Immunol* 2003; 4: 835-42.
- Sedy JR, Gavrieli M, Potter KG, Hurchla MA, Lindsley RC, Hildner K, Scheu S, Pfeffer K, Ware CF, Murphy TL, Murphy KM. B and T lymphocyte attenuator regulates T cell activation through interaction with herpesvirus entry mediator. *Nat Immunol* 2005; 6: 90-8.
- Seery JP, Carroll JM, Cattel V, Watt FM. Antinuclear autoantibodies and lupus nephritis in transgenic mice expressing interferon gamma in the epidermis. *J Ex Med* 1997; 186: 1451-1459.
- Sereda M, Griffiths I, Puhlhofer A, Stewart H, Rossner MJ, Zimmerman F, et al. A transgenic rat model of Charcot-Marie-Tooth disease. *Neuron* 1996; 16: 1049-1060.
- Shaffer LG, Kennedy GM, Spikes AS, Lupski JR. Diagnosis of CMT1A duplications and HNPP deletions by interphase FISH: implications for testing in the cytogenetics laboratory. *Am J Med Genet* 1997; 69: 325-331.
- Shai R, Quismorio FP, Li L, Kwon OJ, Morrison J, Wallace DJ, Neuwelt CM, Brautbar C, Gauderman WJ, Jacob CO. Genome-wide screen for systemic lupus erythematosus susceptibility genes in multiplex families. *Hum Molec Genet* 1999; 8: 639-644.
- Shaikh RB, Santee S, Granger SW, Butrovich K, Cheung T, Kronenberg M, Cheroutre H, Ware CF. Constitutive expression of LIGHT on T cells leads to lymphocyte activation, inflammation, and tissue destruction. *J Immunol* 2001; 167: 6330-7.
- Shan L, Molberg Ø, Parrot I, Hausch F, Filiz F, Gray GM, Sollid LM, Khosla C. Structural basis for gluten intolerance in celiac sprue. *Science* 2002; 297: 2257-2279.
- Sher KS, Jayanthi V, Probert CSJ, Stewert CR, Mayberry JF. Infertility, obstetric and gynaecological problems in coeliac disease. *Dig Dis* 1994; 12: 186-190.
- Shi F, Ljunggren HG, Sarvetnick N. Innate immunity and autoimmunity: from self-protection to self-destruction. *Trends Immunol* 2001; 22: 97-101.
- Shi G, Luo H, Wan X, Salcedo TW, Zhang J, Wu J. Mouse T cells receive costimulatory signals from LIGHT, a TNF family member. *Blood* 2002; 100: 3279-86.
- Shi G, Mao J, Yu G, Zhang J, Wu J. Tumor vaccine based on cell surface expression of DcR3/TR6. *J Immunol* 2005; 174: 4727-35.
- Shi G, Wu Y, Zhang J, Wu J. Death decoy receptor TR6/DcR3 inhibits T cell chemotaxis in vitro and in vivo. *J Immunol* 2003; 171: 3407-14.
- Shi Y. Mammalian RNAi for the masses. *Trends in Genetics* 2003; 19: 9-12
- Shimokawa Ki K, Katayama M, Matsuda Y, Takahashi H, Hara I, Sato H, Kaneko S. Matrix metalloproteinase (MMP)-2 and MMP-9 activities in human seminal plasma. *Mol Hum Reprod* 2002; 8: 32-6.
- Shlomchik MJ, Craft JE, Mamula MJ. From T and B and back again: positive feedback in systemic autoimmune disease. *Nat Rev Immuno* 2001; 1: 147-153.
- Sibia J, Benlagha K, Vanhille P, Ronco P, Brouet JC, Mariette X. Structural analysis of human antibodies to proteinase 3 from patients with Wegener granulomatosis. *J Immunol* 1997; 159: 712-719.
- Singh RR, Yang J. CD1d-reactive NKT cells inhibit autoreactive B cells. *Arthritis Rheum* 2004; 40: S589.
- Simpson D, Crosby RM, Skopek TR. A method for specific cloning and sequencing of human hprt cDNA for mutation analysis. *Biochem Biophys Res Commun* 1988; 151: 487-492.
- Slamon DJ, Clark GM, Wong SG, Levin WJ, Ullrich A, McGuire WL. Human breast cancer: correlation of relapse and survival with amplification of the HER-2/neu oncogene. *Science* 1987; 235: 177-1
- Smith C, Andreacos E, Crawley JB, Brennan FM, Feldmann M, Foxwell BM. NF-kappaB-inducing kinase is dispensable for activation of NF-kappaB in inflammatory settings but essential for

lymphotoxin beta receptor activation of NF-kappaB in primary human fibroblasts. *J Immunol* 2001; 167: 5895-903.

- Smith JJ, Travis SM, Greenberg EP, Welsh MJ. Cystic fibrosis airway epithelia fail to kill bacteria because of abnormal airway surface fluid. *Cell* 1996; 85: 229-236.
- Snipes GJ, Orfali W, Fraser A, Dickson K, Colby J. The anatomy and cell biology of peripheral myelin protein-22. *Ann N Y Acad Sci* 1999;883:143-151.
- Snipes GJ, Suter U, Welcher AA, Shooter EM. Characterisation of a novel peripheral nervous system myelin protein (PMP-22, SR-13). *J Cell Biol* 1992; 117: 225-238.
- Sollid LM. Coeliac disease: dissecting a complex inflammatory disorder. *Nat Rev Immunol* 2002; 2: 647-55.
- Sollid LM. Molecular basis of celiac disease. *Annu Rev Immunol* 2000; 18: 53-81.
- Sommer SS, Cassady JD, Sobell JL, Bottema CD. A novel method for detecting point mutations or polymorphisms and its application to population screening for carriers of phenylketonuria. *Mayo Clin Proc* 1989; 64: 1361-72.
- Sommer SS, Cassady JD, Sobell JL, Bottema CD. A novel method for detecting point mutations or polymorphisms and its application to population screening for carriers of phenylketonuria. *Mayo Clin Proc* 1989; 64: 1361-72.
- Sommer SS, Groszbaach AR, Bottema CD. PCR amplification of specific alleles (PASA) is a general method for rapidly detecting known single-base changes. *Biotechniques* 1992; 12: 82-87.
- Spahn TW, Kucharzik T. Modulating the intestinal immune system: the role of lymphotoxin and GALT organs. *Gut* 2005; 53: 456-465.
- Spiegelmark M, Elzouki A, Weislander J, Eriksson S. The PiZ gene of α_1 -antitrypsin as a determinant of outcome in PR3-ANCA-positive vasculitis. *Kidney Int* 1995; 48: 844-850.
- Spreyer P, Kuhn G, Hanemann CO, Gillen C, Schaal H, Kuhn R, Lemke G, Muller HW. Axon-regulated expression of a Schwann cell transcript that is homologous to a "growth arrest-specific" gene. *EMBO J* 1991; 10: 3661-3668.
- Spriewald BM, Witzke O, Wassmuth R, Wenzel RR, Arnold M-L, Philipp T, Kalden JR. Distinct tumour necrosis factor α , interferon γ , interleukin 10, and cytotoxic T cell antigen 4 gene polymorphisms in disease occurrence and end stage renal disease in Wegener's granulomatosis. *Ann Rheum Dis* 2005; 64: 457-461.
- Stegeman CA, Cohen Tervert JW, Sluiter WJ, Manson WL, de Jong PE, Kallenberg CGM. Association of chronic nasal carriage of *S. aureus* and higher relapse rates in Wegener's granulomatosis. *Ann Int Med* 1994; 120: 12-17.
- Stopfer P, Obermeier F, Dunger N, Falk W, Farkas S, Janotta M, Moller A, Mannel DN, Hehlhans T. Blocking lymphotoxin-beta receptor activation diminishes inflammation via reduced mucosal addressin cell adhesion molecule-1 (MAdCAM-1) expression and leucocyte margination in chronic DSS-induced colitis. *Clin Exp Immunol* 2004; 136: 21-9.
- Street VA, Goldy JD, Golden AS, Tempel BL, Bird TD, Chance PF. Mapping of Charcot-Marie-Tooth Disease Type 1C to Chromosome 16p Identifies a Novel Locus for Demyelinating Neuropathies. *Am J Hum Genet* 2002; 70: 244-250.
- Stroanch EA, Clark C, Bell C, Logren A, McKay NG, Timmerman V, Van Broeckhoven C, Haites NE. Novel PCR based diagnostic tools for Charcot-Marie-Tooth type 1A and hereditary neuropathy with liability to pressure palsies. *J Peripher Nerv Syst* 1999; 4: 117-122.
- Sturfelt G, Roux-Lombard P, Wolheim FA, Dayer JM. Low levels of interleukin-1 receptor antagonist coincide with kidney involvement in systemic lupus erythematosus. *Br J Rheumatol* 1997; 36: 1283-1289.
- Sulkanen S, Halttunen T, Laurila K, Kolho KL, et al. Tissue transglutaminase autoantibody enzyme-linked immunosorbent assay in detecting celiac disease. *Gastroenterology* 1998; 115: 1322-1328.
- Sun Z, Arendt CW, Ellmeler W, Schaeffer EM, Sunshine MJ, Gandhl L, Annes J, Petrzilka, Kupfer A, Schwartzberg PL, Littman DR. PKC θ is required for TCR induced NF κ B activation in mature but not immature T lymphocytes. *Nature* 2000; 404: 402-408.

- Suter U, Snipes GJ, Schoener-Scott R, Welcher AA, Pareek S, Lupski JR, Murphy RA, Shooter EM, Patel PI. Regulation of tissue specific expression of alternative peripheral myelin protein 22 (PMP22) gene transcripts by two promoters. *J Biol Chem* 1994; 269: 25795-25808
- Sutton IJ, Mocroft AP, Lindley VH, Barber RM, Bryon RJ, Winer JB, MacDonald F. Application of multiplex ligation-dependent probe analysis to define a small deletion encompassing PMP22 exons 4 and 5 in hereditary neuropathy with liability to pressure palsies. *Neuromuscul Disord* 2004; 14: 804-809.
- Suzuki I, Fink PJ. Maximal proliferation of cytotoxic T lymphocytes requires reverse signaling through Fas ligand. *J Exp Med* 1998; 187: 123-8.
- Suzuki I, Martin S, Boursalian TE, Beers C, Fink PJ. Fas ligand costimulates the in vivo proliferation of CD8+ T cells. *J Immunol* 2000; 165: 5537-43.
- Sykes M, Nikolic B. Treatment of severe autoimmune disease by stem-cell transplantation. *Nature* 2005; 435: 620-7.
- Syvanen AC. Accessing genetic variation: genotyping single nucleotide polymorphisms. *Nat Rev Genet* 2001; 2: 930-42.
- Takahashi E, Takeda O, Himoro M, Nanao K, Takada G, Hayasaka, K. Localization of PMP-22 gene (candidate gene for the Charcot-Marie-Tooth disease 1A) to band 17p11.2 by direct R-banding fluorescence in situ hybridization. *Jpn. J. Hum Genet* 1992; 37: 303-306.
- Takahashi T, Tanaka M, Brannan CI, Copeland NG et al. Generalised lymphoproliferative disease in mice, caused by a point mutation in the Fas ligand. *Cell* 1994; 76: 969-976.
- Takemura S, Braun A, Crowson C, Kurtin PJ, Cofield RH, O'Fallon WM, Goronzy JJ, Weyand CM. Lymphoid neogenesis in rheumatoid synovitis. *J Immunol* 2001; 167: 1072-1080.
- Takemura T, Yohioka K, Murakami K, Akano N, Okada M, Aya M, Maki S. Cellular localisation of inflammatory cytokines in human glomerulonephritis. *Virchows Arch* 1994; 424: 459-464.
- Tamada K, Ni J, Zhu G, Fiscella M, Teng B, van Deursen JM, Chen L. Cutting edge: selective impairment of CD8+ T cell function in mice lacking the TNF superfamily member LIGHT. *J Immunol* 2002; 168: 4832-5.
- Tamada K, Shimozaki K, Chapoval AI, Zhai Y, Su J, Chen SF, Hsieh SL, Nagata S, Ni J, Chen L. LIGHT, a TNF-like molecule, costimulates T cell proliferation and is required for dendritic cell-mediated allogeneic T cell response. *J Immunol* 2000; 164: 4105-10.
- Tamada K, Shimozaki K, Chapoval AI, Zhu G, Sica G, Flies D, Boone T, Hsu H, Fu YX, Nagata S, Ni J, Chen L. Modulation of T-cell-mediated immunity in tumor and graft-versus-host disease models through the LIGHT co-stimulatory pathway. *Nat Med* 2000; 6: 283-9.
- Tamada K, Tamura H, Flies D, Fu YX, Celis E, Pease LR, Blazar BR, Chen L. Blockade of LIGHT/LTbeta and CD40 signaling induces allospecific T cell anergy, preventing graft-versus-host disease. *J Clin Invest* 2002; 109: 549-57.
- Thellin O, Zorzi W, Lakaye B, De Borman B, Coumans B, Hennen G, Grisar T, Igout A, Heinen E. Housekeeping genes as internal standards: use and limits. *J Biotechnol* 1999; 75: 291-5.
- Thiel CT, Kraus C, Rauch A, Ekici AB, Rautenstrauss B, Reis A. A new quantitative PCR multiplex assay for rapid analysis of chromosome 17p11.2-12 duplications and deletions leading to HMSN/HNPP. *Eur J Hum Genet* 2003; 11: 170-178.
- Thomas PK, Marques W, Davis MB, Sweeney MG, King RH, Bradley JL, Muddle JR, Tyson J, Malcolm S, Harding AE. The phenotypic manifestations of chromosome 17p11.2 duplication. *Brain* 1997; 120: 465-478.
- Thomas PK. Overview of Charcot-Marie-Tooth disease type 1A. *Ann N Y Acad Sci* 1999; 883: 1-5.
- Timmerman V, Nelis E, Van Hul W, Nieuwenhuijsen BW, Chen KL, Wang S, Othman KB, Cullen B, et al. The peripheral myelin protein gene PMP-22 is contained within the Charcot-Marie-Tooth disease type 1A duplication. *Nature Genet* 1992; 1: 171-175.
- Tolba KA, Bowers WJ, Eling DJ, Casey AE, Kipps TJ, Federoff HJ, Rosenblatt JD. HSV amplicon-mediated delivery of LIGHT enhances the antigen-presenting capacity of chronic lymphocytic leukemia. *Mol Ther* 2002; 6: 455-63.
- Tooth HH. The peroneal type of progressive muscular atrophy. London Lewis HK; 1886.

- Topilski I, Flaishon L, Naveh Y, Harmelin A, Levo Y, Shacher I. The anti-inflammatory effects of 1, 24-dihydroxyvitamin D3 on Th2 cells in vivo are due in part to integrin-mediated T lymphocyte homing. *Eur J Immunol* 2004; 34: 1068-107.
- Trysberg E, Blennow K, Zachrisson O, Tarkowski A. Intrathecal levels of matrix metalloproteinases in systemic lupus erythematosus with central nervous system engagement. *Arthritis Res Ther.* 2004; 6:551-556.
- Tsao BP, Cantor RM, Kalunian KC, Chen CJ, Badsha H, Singh R, Wallace DJ, Kitridou RC, Chen S, Shen N, Song YW, Isenberg DA, Yu CL, Hahn BH, Rotter JI. Evidence for linkage of a candidate chromosome 1 region to human systemic lupus erythematosus. *J Clin Invest* 1997; 99: 725-731.
- Tsao BP. The genetics of human lupus. In Dubois' *Lupus Erythematosus*. Wallace DJ, Hahn BH, eds. Lippincott, Williams & Wilkins 2002; 97-120.
- Tsao BP. The genetics of human systemic lupus erythematosus. *Trends Immunol* 2003; 24: 595-602.
- Tsokos GC, Kammer GM. Molecular aberrations in human systemic lupus erythematosus. *Mol Med Today* 2000; 6: 418-24.
- Tsui LC. 2003. Cystic Fibrosis Mutation Database. <http://www.genet.sickkids.on.ca>
- Tumanov AV, Kuprash DV, Nedospasov SA. The role of lymphotoxin in development and maintenance of secondary lymphoid tissues. *Cytokine Growth Factor Rev* 2003; 14: 275-88.
- Tyagi S, Bratu DP, Kramer FR. Multicolour molecular beacons for allele discrimination. *Nat Biotechnol* 1998; 16: 49-53.
- Tyagi S, Marras S, Kramer FR. Molecular beacons: probes that fluoresce upon hybridisation. *Nat Biotechnol* 1996; 14: 303-308.
- Tyson J, Ellis D, Fairbrother U, King RHM, Muntoni F, Jacobs J, et al. Hereditary demyelinating neuropathy of infancy: a genetically complex syndrome. *Brain* 1997; 120: 47-63.
- Utz PJ, Anderson P. Posttranslational protein modifications, apoptosis and the bypass of tolerance to autoantigens. *Arthritis Rheum* 1998; 41:1152
- Vaidya A, Bolanos J, Berkelhammer C. Azathioprine in refractory sprue. *Am J Gastroenterol* 1999; 94: 1967-1969.
- Valentijn LJ, Baas F, Wolterman RA, Hoogendijk JE van der Bosch N, Zorn I, et al. Identical point mutations of PMP-22 in Trembler-J mouse and Charcot-Marie-Tooth disease type 1a. *Nat Genet* 1992b; 2: 288-291.
- Valentijn LN, Bolhuis PA, Zorn I, Hoogendijk JE, van den Bosch N, Hensels GW, et al. The peripheral myelin gene PMP-22/GAS-3 is duplicated in Charcot-Marie-Tooth disease type 1a. *Nat Genet* 1992a; 1: 166-170.
- Vallat JM, Sindou P, Preux PM, Tabaraud F, Milor AM, Couratier P, LeGuern E, Brice A. Ultrastructural PMP22 expression in inherited demyelinating neuropathies. *Ann Neurol* 1996; 39: 813-817.
- Van der Woude FJ, Rasmussen N, Lobatto S, Wiik A, Permin H, van Es LA, van der Giessen M, van der Hem GK, The TH. Autoantibodies to neutrophils and monocytes: a new tool for the diagnosis and a marker of disease activity in Wegener's granulomatosis. *Lancet* 1985: 425-429.
- Van der Woude FJ, van Es LA, Daha MR. The role of the c-ANCA antigen in the pathogenesis of Wegener's granulomatosis. A hypothesis based on both humoral and cellular mechanisms. *Neth J Med* 1990; 36: 169-173.
- Van Kooten C, Banchereau J. Function of CD40 on B cells, dendritic cells and other cells. *Curr Opin Immunol* 1997; 9: 330-338.
- Van Parijs L, Abbas AK. Role of Fas-mediated cell death in the regulation of immune responses. *Curr Opin Immunol* 1996; 8: 355-61.
- Van Parijs L, Biuckians A, Abbas AK. Functional roles of Fas and Bcl-2-regulated apoptosis of T lymphocytes. *J Immunol* 1998; 160: 2065-71.
- VanArsdale TL, VanArsdale SL, Force WR, Walter BN, Mosialos G, Kieff E, Reed JC, Ware CF. Lymphotoxin-beta receptor signaling complex: role of tumor necrosis factor receptor-associated factor 3 recruitment in cell death and activation of nuclear factor kappaB. *Proc Natl Acad Sci U S A* 1997; 94: 2460-5.

- Vance J. The many faces of Charcot-Marie-Tooth disease. *Arch Neurol* 2000; 57: 638-640.
- Vance JM, Nicholson GA, Yamaoka LH, Stajich J, Stewart CS, Speer MC, Hung WY, Roses AD, Barker D, Pericak-Vance MA. Linkage of Charcot-Marie-Tooth neuropathy type 1a to chromosome 17. *Exp Neurol* 1989; 104:186-189.
- Vandenbroucke, II, Vandesompele J, Paepe AD, Messiaen L. Quantification of splice variants using real-time PCR. *Nucleic Acids Res* 2001; 29: E68-8.
- Vandesompele J, De Preter K, Pattyn F, Poppe B, Van Roy N, De Paepe A, Speleman F. Accurate normalization of real-time quantitative RT-PCR data by geometric averaging of multiple internal control genes. *Genome Biol* 2002; 3: RESEARCH0034.
- VanEyndhoven WG, Gamper CJ, Cho E, Mackus WJ, Lederman S. TRAF-3 mRNA splice-deletion variants encode isoforms that induce NF-kappaB activation. *Mol Immunol* 1999; 36: 647-658.
- Varaganam M, Adu D, Taylor CM, Micheal J, Richards N, Neuberger J, Thompson RA. Endothelium MPO-anti-MPO interactions in vasculitis. *Nephrol Dial Transplant* 1992; 7: 1077-1081.
- Varani J, Ginsburg I, Schuger L, Gibbs DF, Bromberg J, Johnson KJ, Ryan US, Ward PA. Endothelial cell killing by neutrophils: synergistic interaction of oxygen products and proteases. *Am J Pathol* 1989; 135: 435-438.
- Vassilopoulos D, Kovacs B, Tsokos GC. TCR/CD3 complex-mediated signal transduction pathway in T cells and cell lines from patients with systemic lupus erythematosus. *J Immunol* 1995; 155: 2269-2281.
- Venter JC, Adams MD, Myers EW, Li PW, Mural RJ, Sutton GG, Smith HO, Yandell M, et al. The sequence of the human genome. *Science* 2001; 291: 1304-1351.
- Ventura A, Magazzu G, Greco L. Duration and exposure to gluten and risk for autoimmune disorders in patients with coeliac disease. SIGEP Study group for autoimmune disorders in coeliac disease. *Gastroenterology* 1999; 117: 297-303.
- Verhagen WIM, Gabreels-Festen AA, van Wensen PJ, Joosten EM, Vingerhoets HM, Gabreels FJ, et al. Hereditary neuropathy with liability to pressure palsies: a clinical, electroneurophysiological and morphological study. *J Neurol Sci* 1993; 116: 176-184.
- Viallard JF, Pellegrin JL, Ranchin V, Schaeverbeke T, Dehais J, Longy-Boursier M, et al. Th1 and Th2 cytokine production by peripheral blood mononuclear cells (PBMC) from patients with systemic lupus erythematosus. *Clin Exp Immunol* 1999; 115: 189-195.
- Visakorpi JK. Changing features of coeliac disease. In: Coeliac disease. Proceedings of the seventh international symposium on coeliac disease. Maki M, Collin P, Visakorpi JK (eds). Coeliac Disease Study Group, Tampere Finland; 1997: 1-8.
- Von Ahsen N, Oellerich M, Armstrong VW, Schütz E. Application of a Thermodynamic Nearest-Neighbor Model to Estimate Nucleic Acid Stability and Optimize Probe Design: Prediction of Melting Points of Multiple Mutations of Apolipoprotein B-3500 and Factor V with a Hybridization Probe Genotyping Assay on the LightCycler. *Clin Chem* 1999; 45: 2094-2101.
- Von Ahsen N, Oellerich M, Armstrong VW, Schütz E. Application of a Thermodynamic Nearest-Neighbor Model to Estimate Nucleic Acid Stability and Optimize Probe Design: Prediction of Melting Points of Multiple Mutations of Apolipoprotein B-3500 and Factor V with a Hybridization Probe Genotyping Assay on the LightCycler. *Clin Chem* 1999; 45: 2094-2101.
- Von Andrian UH, Mackay CR. T-cell function and migration. Two sides of the same coin. *N Engl J Med* 2000; 343: 1020-1034.
- von Herrath MG, Harrison LC. Antigen-induced regulatory T cells in autoimmunity. *Nat Rev Immunol* 2003; 3: 223-32.
- Voon DC, Subrata LS, Karimi M, Ulgiati D, Abraham LJ. TNF and phorbol esters induce lymphotoxin-beta expression through distinct pathways involving Ets and NF-kappaB family members. *J Immunol* 2004; 172: 4332-41.
- Vreiling H, Simons JW, van Zeeland AA. Nucleotide sequence determination of point mutations at the mouse HPRT locus using *in vitro* amplification of HPRT mRNA sequences. *Mutat Res* 1988; 198: 107-113.

- Wallach D, Varfolomeev EE, Malinin NL, Goltsev YV, Kovalenko AV, Boldin MP. Tumor necrosis factor receptor and Fas signaling mechanisms. *Annu Rev Immunol* 1999; 17: 331-67.
- Wan X, Zhang J, Luo H, Shi G, Kapnik E, Kim S, Kanakaraj P, Wu J. A TNF family member LIGHT transduces costimulatory signals into human T cells. *J Immunol* 2002; 169: 6813-21.
- Wang J, Anders RA, Wang Y, Turner JR, Abraham C, Pfeffer K, Fu YX. The critical role of LIGHT in promoting intestinal inflammation and Crohn's disease. *J Immunol* 2005; 174: 8173-8182.
- Wang J, Anders RA, Wu Q, Peng D, Cho JH, Sun Y, Karaliukas R, Kang HS, Turner JR, Fu YX. Dysregulated LIGHT expression on T cells mediates intestinal inflammation and contributes to IgA nephropathy. *J Clin Invest* 2004; 113: 826-35.
- Wang J, Chun T, Lo JC, Wu Q, Wang Y, Foster A, Roca K, Chen M, Tamada K, Chen L, Wang CR, Fu YX. The critical role of LIGHT, a TNF family member, in T cell development. *J Immunol* 2001; 167: 5099-105.
- Wang J, Foster A, Chin R, Yu p, Sun Y, Wang Y Pfeffer K, Fu YX. The complementation of lymphotoxin deficiency with LIGHT, a newly discovered TNF family member, for the restoration of secondary lymphoid structure and function. *Eur J Immunol* 2002; 32: 1969-1979.
- Wang J, Fu YX. LIGHT (a cellular ligand for herpes virus entry mediator and lymphotoxin receptor)-mediated thymocyte deletion is dependent on the interaction between TCR and MHC/self-peptide. *J Immunol* 2003; 170: 3986-93.
- Wang J, Fu YX. Tumor necrosis factor family members and inflammatory bowel disease. *Immunol Rev* 2005; 204: 144-55.
- Wang J, Lo JC, Foster A, Yu P, Chen HM, Wang Y, Tamada K, Chen L, Fu YX. The regulation of T cell homeostasis and autoimmunity by T cell-derived LIGHT. *J Clin Invest* 2001; 108: 1771-80.
- Wang Y, Subudhi SK, Anders RA, Lo J, Sun Y, Blink S, Wang J, Liu X, Mink K, Grandi D, Pfeffer K, Fu YX. The role of herpesvirus entry mediator as a negative regulator of T cell-mediated responses. *J Clin Invest* 2005; 115: 711-7.
- Ware CF, VanArsdale TL, Crowe PD, Browning JL. The ligands and receptors of the lymphotoxin system. *Curr Top Microbiol Immunol* 1995; 198: 175-218.
- Ware CF. The TNF superfamily. *Cytokine Growth Factor Rev* 2003; 14: 181-4.
- Ware CF. Network communications: Lymphotoxins, LIGHT and TNF. *Annu Rev Immunol* 2005; 23: 787-819.
- Ware RE, Hart MK, Haynes BF. Induction of T cell CD7 gene transcription by nonmitogenic ionomycin-induced transmembrane calcium flux. *J Immunol* 1991; 147: 2787-2794.
- Watanabe-Fukunaga R, Brannan CI, Copeland NG et al Lymphoproliferation disorder in mice explained by defects in Fas antigen that mediates apoptosis. *Nature* 1992; 356: 314-317.
- Webster H de F. Development of peripheral nerve fibers. In Dyck PJ, Thomas PK, Griffin JW, Low PA, Poduslo JF (Eds). *Peripheral neuropathy*. 3rd ed Philadelphia: WB Saunders; 1993: 243-266.
- Weinberg JB, Granger DL, Pisetsky DS, Seldin MF, Misukonis MA, Mason SN, Pippen AM, Ruiz P, Wood ER, Gilkeson GS. The role of nitric oxide in the pathogenesis of spontaneous murine autoimmune disease. Increased nitric oxide production and nitric oxide synthase expression in MRL-lpr/lpr mice and reduction of spontaneous glomerulonephritis and arthritis by orally administered NG-monomethyl-L-arginine. *J Ex Med* 1994; 179: 651-660.
- Welcher AA, Suter U, De Leon M, Snipes JG, Shooter EM. A myelin protein is encoded by the homologue of a growth arrest-specific gene. *Proc Natl Acad Sci USA* 1991; 88: 7195-7199.
- Weyand CM, Kurtin PJ, Goronzy JJ. Ectopic lymphoid organogenesis, a fast track for autoimmunity. *Am J Pathol* 2001; 159: 787-793.
- Whelan JA, Russell NB, Whelan MA. A method for the absolute quantification of cDNA using real-time PCR. *J Immunol Methods* 2003; 278: 261-9.
- Whitbeck JC, Peng C, Lou H, Xu R, Willis SH, Ponce de Leon M, Peng T, Nicola AV, Montgomery RI, Warner MS, Soulika AM, Spruce LA, Moore WT, Lambris JD, Spear PG, Cohen GH, Eisenberg RJ. Glycoprotein D of herpes simplex virus (HSV) binds directly to HVEM, a member of the tumor necrosis factor receptor superfamily and a mediator of HSV entry. *J Virol* 1997; 71: 6083-93.
- Wiik A. What you should know about PR3-ANCA. An introduction. *Arthritis Res* 2000; 2: 252-4.

- Wilson AG, di Giovine FS, Blakemore AI, Duff GW. Single base polymorphism in the human tumour necrosis factor alpha (TNF alpha) gene detectable by NcoI restriction of PCR product. *Hum Mol Genet* 1992; 1: 353-353.
- Wilson AG, Gordon C, di Giovine FS, de Vries N, van de Putte LB, Emery P, Duff GW. A genetic association between systemic lupus erythematosus and tumour necrosis alpha. *Eur J Immunol* 1994; 24: 191-195.
- Wilson IG. Inhibition and facilitation of nucleic acid amplification. *Appl Environ Microbiol* 1997; 63: 3741-3751.
- Wine JJ. Cystic fibrosis: How do CFTR mutations cause cystic fibrosis? *Curr Biol* 1995; 5: 1357-1359.
- Wine JJ. Cystic fibrosis: the bicarbonate before chloride hypothesis. *Curr Biol* 2001; 11: R463-R466.
- Wine JJ. The genesis of cystic fibrosis lung disease. *J Clin Invest* 1999; 103: 309-312.
- Witko-Sarsat V, Lesavre P, Lopez S, Bessou G, Hieblot C, Prum B, Noel LH, Guillevin L, Sermet-Gaudelus I, et al. A large subset of neutrophils expressing membrane proteinase 3 is a risk factor for vasculitis and rheumatic arthritis. *J Am Soc Nephrol* 1999; 10: 1224-1233.
- Wittwer C, Ririe K, Andrew R, David D, Gundry R, Balis U. The LightCycler™: A microvolume multisample fluorimeter with rapid temperature control. *BioTechniques* 1997; 22: 176-181.
- Wittwer CT, Herrmann MG, Moss AA, Rasmussen RP. Continuous fluorescence monitoring of rapid cycle DNA amplification. *Biotechniques* 1997; 22: 130-138.
- Wittwer CT, Reed GH, Gundry CN, Vandersteen JG, Pryor RJ. High resolution genotyping by amplicon melting analysis using LCGreen. *Clin Chem* 2003; 49: 853-860.
- Wroblewski VJ, Witcher DR, Becker GW, Davis KA, Dou S, Micanovic R, Newton CM, Noblitt TW, Richardson JM, Song HY, Hale JE. Decoy receptor 3 (DcR3) is proteolytically processed to a metabolic fragment having differential activities against Fas ligand and LIGHT. *Biochem Pharmacol* 2003; 65: 657-67.
- Wu DY, Ugozzoli L, Pal BK, Qian J, Wallace RB. The effect of temperature and oligonucleotide primer length on the specificity and efficiency of amplification by the polymerase chain reaction. *DNA and Cell Biology* 1991; 10: 233-238.
- Wu DY, Ugozzoli L, Pal BK, Wallace RB. Allele-specific enzymatic amplification of beta-globin genomic DNA for diagnosis of sickle cell anemia. *Proc Natl Acad Sci USA* 1989; 86: 2757-60.
- Wu J, Edberg JC, Redecha BP, Bansa L V, Guyre PM, Coleman K, Salmon JE, Kimberly RP. A novel polymorphism of Fc gamma IIIa (CD16) alters receptor function and predisposes to autoimmune diseases. *J Clin Invest* 1997; 100: 1059-1070.
- Wu J, Metz C, Xu X, Abe R, Gibson AW, Edberg JC, Cooke J, Xie F, Cooper GS, Kimberly RP. A novel polymorphic CAAT/enhancer-binding protein beta element in the FasL gene promoter alter Fas ligand expression: a candidate background gene in African American systemic lupus erythematosus patients. *J Immunol* 2003; 170: 132-138.
- Wu Q, Wang Y, Wang J, Hedgeman EO, Browning JL, Fu YX. The requirement of membrane lymphotoxin for the presence of dendritic cells in lymphoid tissues. *J Exp Med* 1999; 190: 629-38.
- Wu Y, Han B, Sheng H, Lin M, Moore PA, Zhang J, Wu J. Clinical significance of detecting elevated serum DcR3/TR6/M68 in malignant tumor patients. *Int J Cancer* 2003; 105: 724-32.
- Wulf P, Bernhardt RR, Suter U. Characterization of peripheral myelin protein 22 in zebrafish (zPMP22) suggests an early role in the development of the peripheral nervous system. *J Neurosci Res* 1999; 57: 467-478.
- Yang CR, Hsieh SL, Ho FM, Lin WW. Decoy receptor 3 increases monocyte adhesion to endothelial cells via NF-kappa B-dependent up-regulation of intercellular adhesion molecule-1, VCAM-1, and IL-8 expression. *J Immunol* 2005; 174: 1647-56.
- Yang J, Ketritz R, Falk R, Jennette J, Gaido M. Apoptosis of endothelial cells induced by neutrophil serine proteases proteinase 3 and elastase. *Am J Pathol* 1996; 149: 1617-1626.
- Yang JQ, Saxena V, Xu H, Van Kaer L, Wang CR, Singh RR. Repeated α -galactosylceramide administration results in expansion of NK T cells and alleviates inflammatory dermatitis in MRL-lpr/lpr mice. *J Immunol* 2003; 171: 4439-4446.

- Ye Q, Fraser CC, Gao W, Wang L, Busfield SJ, Wang C, Qiu Y, Coyle AJ, Gutierrez-Ramos JC, Hancock WW. Modulation of LIGHT-HVEM costimulation prolongs cardiac allograft survival. *J Exp Med* 2002; 195: 795-800.
- Yi ES, Colby TV. Wegener's granulomatosis. *Semin Diagn Pathol* 2001; 18(1): 34-46.
- Yndestad A, Damas JK, Geir Eiken H, Holm T, Haug T, Simonsen S, Froland SS, Gullestad L, Aukrust P. Increased gene expression of tumor necrosis factor superfamily ligands in peripheral blood mononuclear cells during chronic heart failure. *Cardiovasc Res* 2002; 54: 175-82.
- Young P, Stogbauer F, Wiebusch H, Lofgren A, Timmerman V, Van Broeckhoven C, Ringelstein EB, Assmann G, Funke H. PCR-based strategy for the diagnosis of hereditary neuropathy with liability to pressure palsies and Charcot-Marie-Tooth disease type 1A. *Neurology* 1998; 50: 760-763.
- Young P, Wiebusch H, Stögbauer F, Ringelstein B, Assmann G, Funke H. A novel frameshift mutation in PMP22 accounts for hereditary neuropathy with liability to pressure palsies. *Neurology* 1997; 48: 450-452.
- Yu KY, Kwon B, Ni J, Zhai Y, Ebner R, Kwon BS. A newly identified member of tumor necrosis factor receptor superfamily (TR6) suppresses LIGHT-mediated apoptosis. *J Biol Chem* 1999; 274: 13733-6.
- Yu P, Lee Y, Liu W, Chin RK, Wang J, Wang Y, Schietinger A, Philip M, Schreiber H, Fu YX. Priming of naive T cells inside tumors leads to eradication of established tumors. *Nat Immunol* 2004; 5: 141-9.
- Zhai Y, Guo R, Hsu TL, Yu GL, Ni J, Kwon BS, Jiang GW, Lu J, Tan J, Ugustus M, Carter K, Rojas L, Zhu F, Lincoln C, Endress G, Xing L, Wang S, Oh KO, Gentz R, Ruben S, Lippman ME, Hsieh SL, Yang D. LIGHT, a novel ligand for lymphotoxin beta receptor and TR2/HVEM induces apoptosis and suppresses in vivo tumor formation via gene transfer. *J Clin Invest* 1998; 102: 1142-51.
- Zhang J, Roschke V, Baker KP, Wang Z, Alarcon GS, Fessler BJ, Bastian H, Kimberly RP, Zhou T. Cutting edge: a role for B lymphocyte stimulator in systemic lupus erythematosus. *J Immunol* 2001; 166: 6-10.
- Zhang J, Salcedo TW, Wan X, Ullrich S, Hu B, Gregorio T, Feng P, Qi S, Chen H, Cho YH, Li Y, Moore PA, Wu J. Modulation of T-cell responses to alloantigens by TR6/DcR3. *J Clin Invest* 2001; 107: 1459-68.
- Zhang M, Guo R, Zhai Y, Fu XY, Yang D. Light stimulates IFN γ -mediated intercellular adhesion molecule-1 upregulation of cancer cells. *Hum Immunol* 2003; 64: 416-26.
- Zhang MC, Liu HP, Demchik LL, Zhai YF, Yang da J. LIGHT sensitizes IFN- γ -mediated apoptosis of HT-29 human carcinoma cells through both death receptor and mitochondria pathways. *Cell Res* 2004; 14: 117-24.
- Zhong H, Simons JW. Direct comparison of GAPDH, beta-actin, cyclophilin and 28S rRNA as internal standards for quantifying RNA levels under hypoxia. *Biochem Biophys Res Commun* 1999; 259: 523-526.
- Zimmer KP, Naim H, Weber P, Ellis HJ, Ciclitira PJ. Targeting of gliadin peptides, CD8 α/β -TCR and γ/δ -TCR to Golgi complexes and vacuoles within celiac disease enterocytes. *J Exp Biol* 1998; 12: 1349-1357.
- Zimmerman GA, Prescott SM, McIntyre TM. Endothelial cell interactions with granulocytes: tethering and signaling molecules. *Immunol Today* 1992; 13: 93-100.
- Zimmermann B, Holzgreve W, Wenzel F, Hahn S. Novel Real-time quantitative PCR test for Trisomy 21. *Clin Chem* 2002; 48: 362-363.
- Zoidl G, Blass-Kampmann S, D'Urso D, Schmalenbach C, Muller HW. Retroviral-mediated gene transfer of the peripheral myelin protein PMP22 in Schwann cells: modulation of cell growth. *EMBO J* 1995; 14: 1122-1128.
- Zoidl G, D'Urso D, Blass-Kampmann S, Schmalenbach C, Kuhn R, Muller HW. Influence of elevated expression of rat wild-type PMP22 and its mutant PMP22 Trembler on cell growth of NIH3T3 fibroblasts. *Cell Tissue Res* 1997; 287: 459-470.
- Zone JJ. Skin manifestations of celiac disease. *Gastroenterology* 2005; 128: S87-91.

- Zucker S, Cao J, Chen WT. Critical appraisal of the use of matrix metalloproteinase inhibitors in cancer treatment. *Oncogene* 2000; 19: 6642-6650.

Appendices

Appendix I

Preparation of 10% Acrylamide gel for analysis of the sizing PCR products

Clean glass plate with 70% ethanol solution. Arrange the rubber gasket around the ridge of one plate and place the flat plate on top of it. Arrange the gasket as necessary to give a watertight seal. Use bulldog clips to hold the plates together. Pour distilled water in between the plates to check for leaks. If there are no leaks, empty out the water and leave on tissue to drain.

Prepare 10 mls of 10% Acrylamide solution as follows:

40% acylamide (19:1)	2.5 ml
TBE 10X	1.0 ml
H ₂ O	6.5 ml
APS (10%)	200 µl
TEMED	40 µl

Fresh 10% ammonium persulfate (APS) should be made daily using distilled H₂O. This is double the amount of TEMED and APS normally used, but it is necessary for proper well formation in the mini ATTO gel system. Mix well and pour into the gel template, insert the comb to make wells for loading sample. Allow the gel to set for approximately 20 minutes. When the gel is set, remove the comb, bulldog clips and the gasket. Place the gel, which is still encased by the glass plates into the electrophoresis box. The ridged plate should face inwards and another plate should be arranged similarly on the other side. Pour running buffer (1X TBE) in between the two plates and allow the wells of the gel to fill up. Pour running buffer in to the chamber outside of the plates, check for air bubbles underneath the gels, as these will distort the DNA bands as they move through the gel. Prepare samples to run on gel by adding 5µl of PCR, 5µl H₂O and 2µl 6X loading buffer to a tube. Spin the

contents down in a microfuge and load all 12 μ l into one of wells. Place the lid on the box, connect to the power supply, run the gel at 150 volts for approximately 3.5 hours (until the xylene cyanol has just run off the bottom of the gel). When the dye front reaches the base of the gel, turn off the power supply and disconnect the leads. Remove the gel plate from the tanks and separate the glass plates with the end of a spatula. With a scalpel carefully cut the gel free from the ridged plate and place it in a 10 μ g/ml ethidium bromide solution for 10-20 minutes. The ethidium bromide will bind to the DNA and can be visualised under UV light. Use a transilluminator to visualise the DNA bands and photograph.

Publications related to this thesis

- **Eugene Dempsey**, David E. Barton, and Fergus Ryan. Detection of Five common *CFTR* mutations by Rapid-Cycle Real-Time Amplification Refractory Mutation System PCR. *Clin Chem* 2004; 50: 773-775.
- **Eugene Dempsey** and Fergus Ryan. Genetic testing for cystic fibrosis. *The Irish Scientist* 2002: 106.
- **Eugene Dempsey**, Mohamed Abuzakouk, Fergus Ryan, Con Feighery, Sara Lynch. Quantification of LIGHT and Herpes Virus Entry Mediator (HVEM) mRNA expression in patients with autoimmune and proinflammatory conditions using real-time quantitative PCR. *Clin Invest Med* 2004; 27, T7.110, p19B.

Other relevant publications

- Michelle Quinlivan, **Eugene Dempsey**, Fergus Ryan, Sean Arkins, Ann Culinane. Real-time RT-PCR for the detection and quantitative analysis of equine influenza virus. *J Clin Microbiol* 2005; 43: 5055-5057.

Oral and Poster Presentations

- Quantification of LIGHT and Herpes Virus Entry Mediator (HVEM) mRNA expression in patients with autoimmune and proinflammatory conditions using real-time quantitative PCR.

Poster presented at the 12th International Congress of Immunology and 4th Annual conference of FOCIS, Montreal, 2004.

- Detection of Five common *CFTR* mutations by Rapid-Cycle Real-Time Amplification Refractory Mutation System PCR.

Presented at the Academy of Medical Laboratory Sciences annual conference 2003.
Received award for oral presentation.